

Quantifying the effect of air particle pollution mitigation by dry deposition in Chinese residential areas

A THESIS SUBMITTED TO THE WELSH SCHOOL OF
ARCHITECTURE, CARDIFF UNIVERSITY

IN PARTIAL FULFILMENT OF THE REQUIREMENTS FOR THE DEGREE OF
DOCTOR OF PHILOSOPHY

BY
LIKUN YANG

JULY 2021

Acknowledgment

First and foremost, I am deeply grateful to my supervisors Prof. Phillip Jones and Dr Yangang Xing for their invaluable advice, continuous support and patience during my PhD study. Dr Yangang Xing has guided me since the beginning of my study with his immense knowledge.

And Prof. Phillip Jones guided me to the end with plentiful experience. Both of them encouraged me in all the time of my academic research and daily life. I would also like to thank Huw Jenkins for his technical support on my study. I would like to extend my sincere thanks to the research management team in WSA. It is their kind help and support that have made my study and life in the UK a great time. Moreover, I would like to offer my special thanks to my parents, whom without this would have not been possible. I also appreciate my husband. Without his understanding and encouragement in the past few years, it would be impossible for me to complete my study.

Abstract

Air pollution has increased in the last decade all around the world, especially in developing countries, such as in China. A series of control policies, laws, and regulations were enacted by the Chinese government. However, particulate matters are still the main type air pollution in northern China. Air pollution, such as $PM_{2.5}$ and PM_{10} , impacts human health and well-being, ecosystem health, and the climate. Urban green infrastructure is pointed out as a nature-based method to improve air quality. Air pollution can be reduced by urban green infrastructure in many ways. For instance, urban tree can act as vegetation barriers to prevent the penetration of pollutants into certain areas. They can also removal pollutants from the atmosphere by dry deposition process on the tree canopy. However, most dry deposition studies focus on a city scale. Therefore, this study aims to explore optimization of urban green plans for air quality improvement in the mid-scale residential area. Based on a literature review of the development of dry deposition studies and the application in urban planning and design, the commonly used models of green spaces effect have limited consideration of the impact of wind speed and tree species and lack focus on mid-scale areas. So, this study develops a green planning model to estimate the effect of urban vegetations on particulate matter pollution mitigation by dry deposition. This model contains two parts, which are a CFD model (ENVI-met) and a SD model (Vensim PLE). The model setup and boundary conditions are described in three steps, which are 1) identification of land types by local microclimate zones; 2) collection of meteorological and air quality data; 3) calculation of air pollution removal. This model is validated by a comparison that is made between monitored particle pollutant concentration data and simulated concentration results of the model in the study area in Taiyuan, China. Then, this green planning model is applied in a mid-scale residential area to explore optimum green plans of this area. The results are analyzed and discussed to propose an optimum green plan, which is to have 14% - 25% green cover with evergreen leaf trees that are planted in the locations with higher wind speeds. Finally, this thesis summarizes the contributions of the urban planning model and the findings of the simulation results, as well as the direction of future study.

List of Tables

Table 2-1 Measurements of leaf area index by biome in various studies.....	34
Table 2-2 Influence of wind direction on traffic-emitted PM _{2.5} concentration with 5m/s wind speed, without urban background concentrations. Wind direction is the angle of the street in the study (Jeanjean et al. 2017).	37
Table 2-3 Annual air quality improvement by the reduction of pollutants for three different vegetation covers during 2000–2001 in Santiago (Escobedo, Nowak 2009).	41
Table 3-1. Mean dry deposition velocity with different wind speeds on three urban surfaces (Roupsard et al. 2013).....	50
Table 3-2 References list of modelling applications of dry deposition in urban planning researches.	61
Table 3-3 Summary of average dry deposition velocities (cm/s) of PM _{2.5} based on different wind speeds from the literature per unit of leaf area (Hirabayashi et al. 2015).....	66
Table 4-1 Contents of variables in the dry deposition model described by the equations and their input data.	83
Table 5-1 Meteorological data (wind speed, humidity, and temperature) collected from the compact-H zone and open-H zone.	97
Table 5-2 Dylos monitored data of PM ₁₀ concentration(μg/m ³) from the compact-H zone, open-H zone, and Kang Le Road over 30 minutes. The table shows the monitored PM ₁₀ concentration data per minute.....	98
Table 5-3 Dylos monitored data of PM _{2.5} concentration(μg/m ³) from compact-H zone, open-H zone, and Kang Le Road over 30 minutes. The table shows monitored PM _{2.5} concentration data per minute.	101
Table 5-4 Input data of leaf areas in compact-H and open-H zones for simulation.	105
Table 5-5 Monitored and simulated PM ₁₀ concentration in compact-H zone and open-H zone over 30 minutes, and the percentage difference between monitored and simulated PM ₁₀ concentrations.....	108
Table 5-6 Monitored and simulated PM _{2.5} concentration in compact-H zone and open-H zone over 30 minutes, and the percentage difference between the monitored and simulated PM _{2.5} concentrations.....	110
Table 6-1. Meteorological data and PM ₁₀ concentrations monitored in the study area.....	118
Table 6-2 Variables and constants of input data for each scenario.	121
Table 6-3 Input data for scenario 1 simulation.....	123
Table 6-4 Meteorological boundary conditions for ENVI-met simulation	124
Table 6-5 Average PM ₁₀ concentration (μg/m ³) in the study area and Total amount of PM ₁₀ removal by different green levels (μg) in 10 hours.	125
Table 6-6 Input data for scenario 2 simulation.....	129
Table 6-7 Total amount of PM ₁₀ removal in the study area with different source pollution concentrations for 10 hours.	129
Table 6-8 Simulated wind speeds (m/s) in the four chosen location.....	133
Table 6-9 Input data for scenario 3 simulation.....	134
Table 6-10 Total amount of PM ₁₀ removal (10 ⁻⁵ μg) by a tree that planted in the four chosen locations.....	134
Table 6-11 Input data for scenario 4 simulation.....	137
Table 6-12 Monthly PM ₁₀ concentration (μg/m ³) and total amount of PM ₁₀ (μg) in Taiyuan city in 2017.....	137

Table 6-13 Leaf area index by tree species (Asner et al. 2003) and their acronyms.....	140
Table 6-14 Input data for scenario 5 simulation.....	141
Table 6-15 Average PM ₁₀ concentration /in the study and total amount of PM ₁₀ estimated based on different tree species.	141
APPENDIX 5-6 Simulated PM _{2.5} concentration(µg/m ³) in compact-H zone and open-H zone over 30 minutes. The shows the simulated PM ₁₀ concentration data at a 15 second frequency.	185

List of Figueres

Figure 1-1 Distribution of Chinese industry in 1999 (left) and 2011 (right)(China 2015).12

Figure 1-2 Regions in China (Created by the author)13

Figure 1-3 Transformation of territory and cities from the Qin Empire (210B.C.) to the Qing Dynasty (1820's)(Nguyen1310 2006).14

Figure 1-4 Proportion of the population exposed to a PM_{2.5} concentration of 10 µg/m³ (D. Zhang et al. 2014).16

Figure 1-5 Taiyuan pollution levels: days in 2019 at different PM_{2.5} concentration levels.....17

Figure 1-6 Taiyuan pollution levels: days in 2019 at different PM₁₀ concentration levels.17

Figure 1-7 Research outline and structure.21

Figure 3-1 Electrical analogy for the dry deposition (Giardina, Buffa 2018).52

Figure 3-2 The new method for the parametrization of the deposition velocity for particles (Giardina, Buffa 2018).55

Figure 4-1 A generic framework of the green planning model and its data flow.76

Figure 4-2 A spaces model (downward side) of a mid-scale residential area based on the satellite image (upward side) in Taiyuan by ENVI-met.78

Figure 4-3 Abridged definitions of the local climate zones (Stewart, Oke 2012). LCZs 1–9 correspond to Oke’s (2004) urban climate zones.79

Figure 4-4 Schematic of the dry deposition process based on the differential equations in the Vensim workplace.86

Figure 4-5 Equation editor window shows the variables of the dry deposition velocity equation.87

Figure 4-6 Graphs of the box variable ‘Concentration at zone level’ and its related variables.88

Figure 5-1 Basic process and data flow of the integrated green planning model validation..93

Figure 5-2. Districts in the city of Taiyuan94

Figure 5-3 Classification of satellite images in Taiyuan City based on building types: compact high-rise (top part of the map) and open high-rise (bottom part of the map) (source: map.baidu.com)95

Figure 5-4 Line graphs of monitored data of PM₁₀ concentration(µg/m³) from the (a)compact-H zone, (b) open-H zone, and (c)Kang Le Road over 30 minutes.....100

Figure 5-5 Line graphs of monitored data of PM_{2.5} concentration(µg/m³) from the (a)compact-H zone, (b) open-H zone, and (c)Kang Le Road over 30 minutes.....104

Figure 5-6 Satellite images of compact-H zone (a) and open-H zone (b).105

Figure 5-7 Line graphs of simulated PM₁₀ concentration(µg/m³) in (a)compact-H zone and (b)open-H zone over 30 minutes.107

Figure 5-8 Line graphs of simulated PM_{2.5} concentration(µg/m³) in (a)compact-H zone and (b)open-H zone over 30 minutes108

Figure 5-9 Monitored and simulated PM₁₀ concentration in (a) compact-H zone and (b) Open-H zone.109

Figure 5-10 Monitored and simulated PM_{2.5} concentration in (a) compact-H zone and (b) Open-H zone.111

Figure 5-11 Average concentration of PM_{2.5} and PM₁₀ by (a)monitoring and (b)simulation in compact-H zone and open-H zone.....112

Figure 6-1 Satellite image of the study area in Taiyuan City. (Sourced from Baidu Map)118

Figure 6-2 Line graphs of (a) monitored wind speeds (m/s) and (b) PM₁₀ concentration (µg/m³) in the study area from 8:00 to 18:00.120

Figure 6-3 Average wind speed simulated by ENVI-met based on different green levels. ...123

Figure 6-4 Maps of the study area in the ENVI-met interface showing (a) 7%, (b) 14%, (c) 25%, (d) 50%, (e) 100% of land covered by trees.124

Figure 6-5 Total PM₁₀ removal by different percentages of land covered by trees in a 10-hour simulation.125

Figure 6-6 Increased PM₁₀ removal between different green cover levels.126

Figure 6-7 The rising rate of PM₁₀ removal by different percentages of land cover by trees.126

Figure 6-8 PM₁₀ concentrations estimated by the dry deposition model in Vension PLE based on different percentages of green cover for 10 hours.127

Figure 6-9 Different levels of source PM₁₀ concentration in the study area after 10-hour dry deposition process by trees.130

Figure 6-10 Total PM₁₀ removal at different source pollution concentration levels.130

Figure 6-11 The rising rate of PM₁₀ removal across different source pollution concentration levels.131

Figure 6-12 Four locations in the study area with different wind speeds.133

Figure 6-13 Total PM₁₀ removal (10⁻⁵ µg) in the four locations.135

Figure 6-14 Rising rate of PM₁₀ removal (10⁻⁵ µg) under different wind speeds in the study area.135

Figure 6-15 Monthly (a) source pollution concentration (µg/m³), (b) PM₁₀ concentration (µg/m³), and (c) total amount of PM₁₀ (µg) in Taiyuan city in 2017.139

Figure 6-16 (a) PM₁₀ concentration and (b) total amount of PM₁₀ of different tree species.143

List of equations

(3-1).....	51
(3-2).....	52
(3-3).....	52
(3-4).....	52
(3-5).....	53
(3-6).....	53
(3-7).....	53
(3-8).....	53
(3-9).....	54
(3-10).....	54
(3-11).....	54
(3-12).....	55
(3-13).....	55
(3-14).....	55
(3-15).....	55
(3-16).....	56
(3-17).....	56
(3-18).....	56
(3-19).....	56
(3-20).....	56
(3-21).....	58
(3-22).....	59
(3-23).....	60
(3-24).....	66
(5-1).....	96
(5-2).....	105
(6-1).....	122

Table of Contents

CHAPTER 1. INTRODUCTION.....	11
1.1. BACKGROUND	12
1.1.1. <i>Development of Chinese industry.....</i>	12
1.1.2. <i>Regions in China</i>	12
1.1.3. <i>Air pollution in the world.....</i>	14
1.1.4. <i>Particle Pollutants in China</i>	15
1.1.5. <i>Modelling air pollution mitigation by urban green infrastructure</i>	18
1.2. RESEARCH AIM AND OBJECTIVES	19
1.3. THESIS OUTLINE.....	20
1.4. RESEARCH SCOPE AND FOCUS.....	23
1.4.1. <i>Scope</i>	23
1.4.2. <i>Focus</i>	24
CHAPTER 2. A SUSTAINABLE SOLUTION OF URBAN PLANNING FOR IMPROVING AIR QUALITY – LITERATURE REVIEW.....	25
2.1. INTRODUCTION	26
2.2. ECOSYSTEM SERVICE AND SUSTAINABLE URBAN PLANNING.....	26
2.3. GREEN FACTORS.....	29
2.3.1. <i>Biotope Area Factor</i>	30
2.3.2. <i>Seattle Green Factor.....</i>	30
2.3.3. <i>Malmo Green Factor</i>	31
2.3.4. <i>Green plot ratio and leaf area index</i>	32
2.4. URBAN GREEN INFRASTRUCTURES BENEFIT ON AIR POLLUTION MITIGATION.....	34
2.4.1. <i>Aerodynamic effects by green infrastructures at street level</i>	35
2.4.2. <i>Urban vegetation barrier</i>	38
2.4.3. <i>Air pollution mitigation by deposition.....</i>	39
2.4.4. <i>Other benefits of green infrastructures.....</i>	41
2.5. CONCLUSION.....	43
CHAPTER 3. MITIGATION OF PARTICLE AIR POLLUTION BY URBAN GREEN SPACES – DRY DEPOSITION	45
3.1. INTRODUCTION.....	47
3.2. PARTICLE AIR POLLUTION	48
3.3. DRY DEPOSITION	49
3.3.1. <i>Development of dry deposition velocity models.....</i>	51
3.3.2. <i>Modelling applications of dry deposition in urban planning research</i>	57
3.3.3. <i>Dry deposition velocity used to quantify pollutants removal.....</i>	58
3.3.4. <i>Combination of dry deposition model and other atmospheric simulation models</i>	60
3.3.5. <i>UFORE and EMEP MSC-W model</i>	65
3.4. CONCLUSION.....	67
CHAPTER 4. A GREEN PLANNING MODEL TO IMPROVING AIR QUALITY IN MID-SCALE URBAN RESIDENTIAL AREAS – MODEL SETUP	70
4.1. INTRODUCTION.....	72
4.2. FRAMEWORK OF THE GREEN PLANNING MODEL	73
4.2.1. <i>Vensim.....</i>	74
4.2.2. <i>ENVI-met</i>	75
4.3. APPLICATION OF THE INTEGRATED SIMULATION MODEL.....	77
4.3.1. <i>Step 1: Identification of land types by local microclimate zones.....</i>	77
4.3.2. <i>Step 2: Collection of meteorological and air quality data</i>	80
4.3.3. <i>Step 3: Calculation of air pollution removal.....</i>	81
4.4. CONCLUSION.....	89

CHAPTER 5. COMPARISON BETWEEN FIELD MEASUREMENT AND SIMULATION – MODEL VALIDATION	91
5.1. INTRODUCTION	92
5.2. REVIEW OF ENVIRONMENTAL MODEL VALIDATION METHODS	92
5.3. OBTAINING REAL WORLD DATA — PM2.5 AND PM10 CONCENTRATION MONITORING	94
5.3.1. <i>Zone selection and classification</i>	94
5.3.2. <i>Real-world data monitoring</i>	95
5.4. COMPARISON OF SIMULATED AND REAL DATA	104
5.4.1. <i>Simulation</i>	104
5.4.2. <i>Comparison of real-world data and simulated results</i>	108
5.5. CONCLUSION	114
CHAPTER 6. DEVELOPMENT OF OPTIMUM URBAN GREEN PLANS FOR AIR QUALITY IMPROVEMENT IN MID-SCALE URBAN RESIDENTIAL AREAS — SIMULATION AND DISCUSSION	115
6.1. INTRODUCTION	116
6.2. THE STUDY AREA	117
6.3. SCENARIO DEVELOPMENT	121
6.3.1. <i>Scenario 1 – Green cover levels</i>	122
6.3.2. <i>Scenario 2 – Source pollution concentrations</i>	128
6.3.3. <i>Scenario 3 – Locations</i>	132
6.3.4. <i>Scenario 4 – Monthly particle pollutants removal</i>	136
6.3.5. <i>Scenario 5 – Tree species</i>	140
6.4. CONCLUSION	145
CHAPTER 7. CONCLUSIONS AND RECOMMENDATIONS FOR FUTURE RESEARCH	148
7.1. INTRODUCTION	149
7.2. LITERATURE REVIEW	149
7.2.1. <i>Air quality improvement by urban green spaces</i>	149
7.2.2. <i>Particle pollution mitigation by dry deposition</i>	151
7.3. THE INTEGRATED GREEN PLANNING MODEL	153
7.3.1. <i>Model validation</i>	153
7.3.2. <i>Application of the green planning model</i>	154
7.4. CONTRIBUTION	157
7.5. LIMITATION OF THE GREEN PLANNING MODEL	158
7.6. FUTURE RESEARCH	159
REFERENCE	161
APPENDIX 5-5 SIMULATED PM10 CONCENTRATION($\mu\text{G}/\text{M}^3$) IN COMPACT-H ZONE AND OPEN-H ZONE OVER 30 MINUTES. THE TABLE SHOWS THE SIMULATED PM10 CONCENTRATION DATA AT A 15 SECOND FREQUENCY	181
APPENDIX 5-6 SIMULATED PM2.5 CONCENTRATION($\mu\text{G}/\text{M}^3$) IN COMPACT-H ZONE AND OPEN-H ZONE OVER 30 MINUTES. THE SHOWS THE SIMULATED PM10 CONCENTRATION DATA AT A 15 SECOND FREQUENCY	185
APPENDIX 1 – SCENARIO 1 OUTPUT DATA OF PM ₁₀ CONCENTRATION IN THE STUDY AREA	189
APPENDIX 2 – SCENARIO 2 OUTPUT DATA OF PM ₁₀ REMOVAL IN THE STUDY AREA	192
APPENDIX 3.1 – SCENARIO 3 OUTPUT DATA OF PM ₁₀ REMOVAL IN THE STUDY AREA	194
APPENDIX 3.2 – SCENARIO 3 OUTPUT DATA OF WIND SPEEDS IN THE STUDY AREA FROM 8:00 TO 18:00	197
APPENDIX 4.1 – SCENARIO 4 INPUT DATA OF PM ₁₀ CONCENTRATION IN TAIYUAN IN 2017 FROM THE LOCAL WEATHER STATION	203
APPENDIX 4.2 – SCENARIO 4 OUTPUT DATA OF PM ₁₀ CONCENTRATION IN THE STUDY AREA	204
APPENDIX 5 – SCENARIO 5 OUTPUT DATA OF PM ₁₀ CONCENTRATION IN THE STUDY AREA	206

Chapter 1. Introduction

1.1. Background

1.1.1. Development of Chinese industry

Industry has always been the backbone of the economy and the dominant energy user and carbon emitter in China. The First Five-Year Plan (1953-57) stated that the aim was to convert China, step by step, from a backward agricultural country into an advanced and socialist industrial state. The first principle of the Plan was that “there should be a rapid growth of heavy industry through the development of the capital goods industries”, which lay the foundation for Chinese industry. In 1958, the Chinese government produced 270 million tons of coal, even greater than that of the United Kingdom. By 1936, the year prior to the outbreak of the Sino- Japanese War, the production of coal in China and Manchuria had reached an estimated level of 35 million tons. As time went on, Chinese industry became more varied. In 2008, it provided over 42% of output in the national economy, in addition to accounting for about 50% gains in GDP and a 37% rise in employment opportunities. According to the National Bureau of Statistics of the People’s Republic of China, until 2004, the industrial companies were increased to 2.3 million. Also, as seen from the Distribution of Chinese industry, the number of factories has rapidly increased in the past decade (see Figure 1-1).

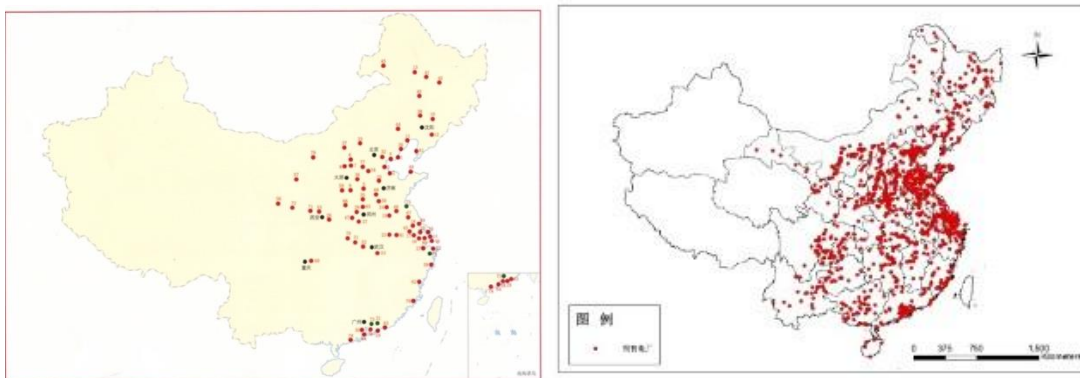


Figure 1-1 Distribution of Chinese industry in 1999 (left) and 2011 (right)(China 2015).

1.1.2. Regions in China

China is situated in the Middle East of Asia and on the West shore of the Pacific Ocean. The National territory area is about 9,597,000 square kilometres. China started to divide its

regions during the Zhou dynasty (256 B.C.). From the Qin dynasty (221 B.C.), the policy of division was used formally in ancient China. Over thousands of years, the territory of ancient China has changed a lot, but the form of division has been retained until now. As can be seen in Figure 2 below, the whole Qin Empire was divided into three parts by landform. As time went on, these three regions were developed and grew to some new regions. After the People's Republic of China was founded, all these regions were slightly regrouped because of politics and economics and so they became seven different regions, namely the North, Northeast, Northwest, East, South Central, and Southwest. The North, East, and South Central Regions have the longest history and largest population in the whole country and so most of the industry is in this area. However, because of the difference in geography, the type and form of industry varies among the three regions. As a result, their environmental issues are diverse. Hence, they all have their own policies to deal with pollution problems.



Figure 1-2 Regions in China (Created by the author)

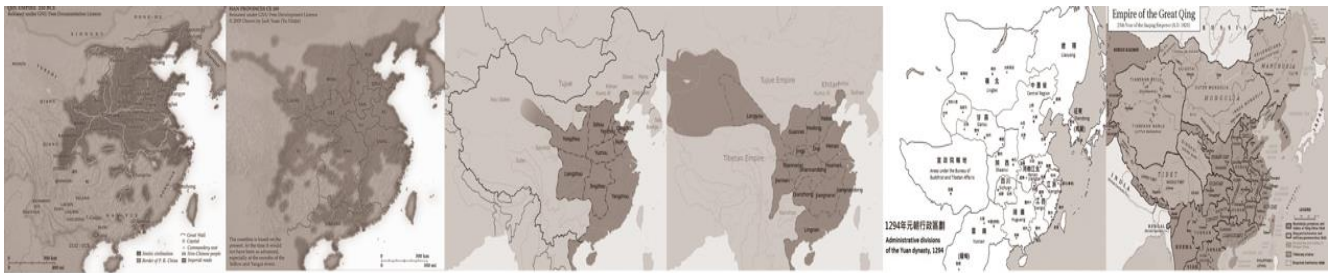


Figure 1-3 Transformation of territory and cities from the Qin Empire (210B.C.) to the Qing Dynasty (1820's)(Nguyen1310 2006).

Most of China's industrial companies have developed in the North, East, and South-Central regions of China, and they cause a lot of pollution, especially carbon dioxide emissions. However, influences from CO2 emissions are various in different regions due to differences in the climate and geography of these areas. This project will focus on the North Region, which hosts around 1/3 of China's total population. The North Region is in the Yellow River Valley and was once the centre of ancient China. This area is considered the cradle of ancient Chinese civilization. Many years ago, the valley's topography served as a plentiful water resource all year around, which provided a perfect environment for farming. Therefore, this area has always been the military, political, and cultural centre of China. However, the valley topography that once helped to develop this area is now the cause of severe regional pollution. The terrain in the North Region is low-lying and surrounded by mountains, therefore the pollutants are not easily dispersed. Meanwhile, factories in this area are clustered, which means a mass of contaminants have been discharged but they are also unable to escape the area. Therefore, these pollutants have increasingly amassed in the North Region for a long time and are causing more serious environmental problems than in other regions. Also, since the increasing development of the mining industry in this area, the water resources that used to be abundant have been overused and polluted.

1.1.3. Air pollution in the world

The attitude towards air pollution in the industrialised world has changed in the last several decades. The number of urban dwellers has increased more than four times since the 1960s, meanwhile global energy consumption has grown nearly five times. Sulphur dioxide, from

the usage of fossil fuels in heat and power production, was the main urban pollution after World War II, but by starting to use clean energy, such as wind power, solar and hydro power, this problem has been partly solved (Shafik 1994). The disaster that pushed forward the development of air pollution legislation and abatement was 'the Great Smog' in London in December 1952. Due to the heavy demand for heating in that cold winter, up to 1000 tonnes of smoke particles, 370 tonnes of sulphur dioxide and 140 tonnes of hydrochloric acid were discharged in London (Fenger 2009; Bharadwaj et al. 2016). This caused over 4000 people died. After this, the number of monitoring stations were increased and the Clean Air Act was enacted in 1956. The attention towards the emission of sulphur dioxide not only rose in the UK, but also in Europe (Fenger 2009). In the United States, the levels of air pollution were dramatically risen until the end of the Second World War, as the increased industrial production during the war (Sullivan et al. 2018). After that, the air pollution legislation and monitoring were developed by the Environmental Protection Agency in the US. Nowadays, many developing countries, such as China, are facing the increasing air pollution. But unlike the problems that Europe and the US had 50 years ago, with the development of industrialised urban areas and the growing levels of traffic, nitrogen oxides and volatile organic compounds have become the main source of urban air pollution. The volatile organic compounds were measured as atmospheric particles and classified as PM₁₀ and PM_{2.5} since 1990 (Fenger 2009). PMs are mainly emitted from industrial emissions, road traffic and construction works. They can cause haze, and pose harmful effects to human health. Epidemiological studies (Hoek et al. 2013; Sun et al. 2016) pointed out that particle pollutants have a significant impact on respiratory and cardio-pulmonary diseases and the daily mortality. They can damage the brain and cardiovascular system of mammals, impact body temperature, and lead to lung function decline (Guo et al. 2012; Rice et al. 2015). PM_{2.5} is even more hazardous than PM₁₀, as the smaller size of PM_{2.5} allows it to reach deeper into the human body.

1.1.4. Particle Pollutants in China

Fast industrial development usually accompanies mass energy consumption. The issue of air pollution was first observed in the 1970s in China. The emissions of sulphur dioxide and total suspended particulates from industry were the main problems. Then in the 1990s, the

number of vehicles on roads rapidly increased in medium and large cities. In Taiyuan, which is in North Region, the number of vehicles increased 10 times from 1990 to 2012. The traffic emission in China is much higher than in developed countries. In 2009, the energy consumption by the industry accounted for a dominant share of over 70% of China's total energy consumption, and about 90% of China's total air pollution emissions came from industry activities and urban traffic (Zhang 2019; Xu, Zhang 2020). Rapidly increasing industrial development and urban traffic have already caused that the concentrations of nitrogen oxides and particulates are especially high. Since 2000, more than 92% of people in China were exposed to PM_{2.5} concentration over 10 µg/m³ (D. Zhang et al. 2014) (see Figure 1-4). In 2012, this number increased to 98% of population in China, on the contrary, it decreased to 21% and 16% in the UK and in the US, respectively.

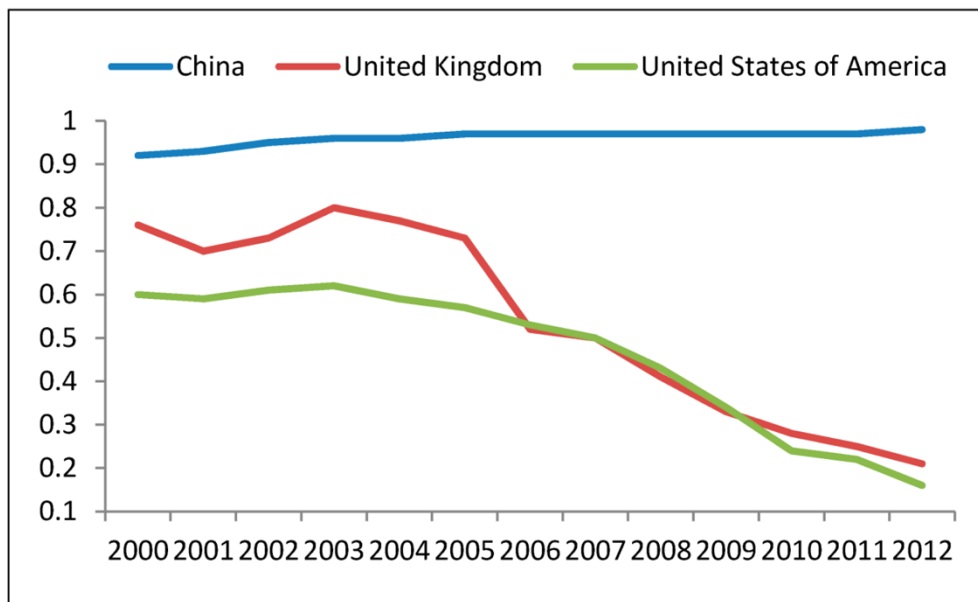


Figure 1-4 Proportion of the population exposed to a PM_{2.5} concentration of 10 µg/m³ (D. Zhang et al. 2014).

Due to the damage of air pollution on human health and global climate change, it has led to great public concern (Wang et al. 2019; Liu et al. 2020). To reduce air pollution, a series of control polices, laws, and regulations were enacted by the government (Wang et al. 2008). However, the haze episodes still occurred in the heating seasons in many northern Chinese cities. For instance, when the record-breaking heavy smog hit Beijing and large areas of North China in early 2013, during which the monthly average particle pollution concentration reached to 160 µg/m³ and affected around 1.3 million km² and 800 million

people (Huang et al. 2015), media concern over environmental quality reached a peak. Now, particulate matters are founded to be the primary pollution of urban areas in north China (China CSR Map 2015). In Taiyuan, only in 77 days of the year were monitored the PM₁₀ concentration under 50 µg/m³, which is the max value of WHO health guideline (WHO 2006) (see Figure 1-5). And only 22 days in 2019 had PM_{2.5} concentration under 50 µg/m³ (Sthjt.shanxi.gov.cn 2017) (see Figure 1-6). More half time of the year, residents in Taiyuan were exposed to PM₁₀ and PM_{2.5} over 50 µg/m³.

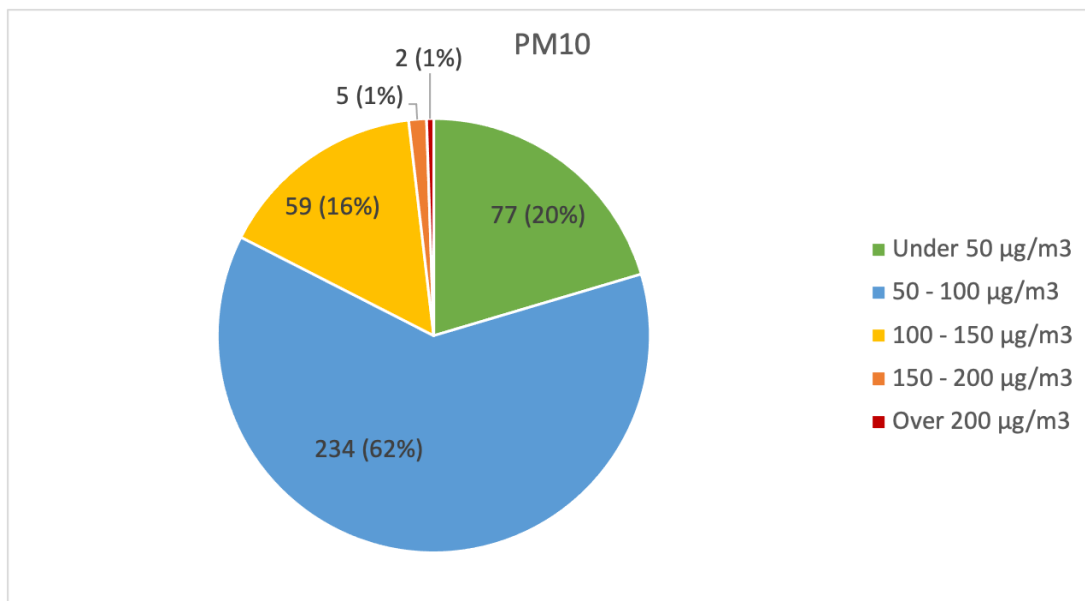


Figure 1-5 Taiyuan pollution levels: days in 2019 at different PM₁₀ concentration levels.

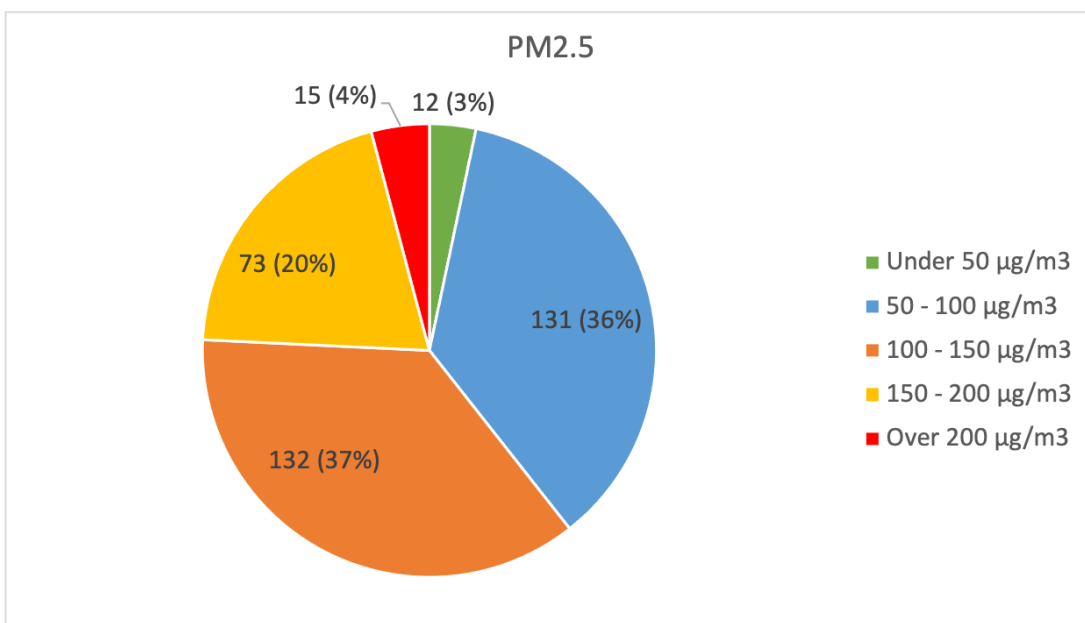


Figure 1-6 Taiyuan pollution levels: days in 2019 at different PM_{2.5} concentration levels.

Another source of PMs in China is cooking. It has been identified as main source for indoor PMs, and through ventilation system, cooking also discharges PMs to outdoors (Zhao et al. 2019). Studies (Hung et al. 2007; Wang et al. 2014) pointed out that the development of lung cancer in non-smoking Chinese women is associated with cooking oil fumes and some traditional Chinese cooking methods. These methods usually cook food over 200 °C, which will generate fine particulate matter and carcinogens, such as polycyclic aromatic hydrocarbons (He et al. 2004). The polycyclic aromatic hydrocarbons can easily attach to fine particles and cause more damage to human health than gaseous phase polycyclic aromatic hydrocarbons (Zhu et al. 2009). Chinese cooking can produce larger amount of particles with polycyclic aromatic hydrocarbons than Western cooking style (Chen et al. 2007). Considering the high density of population in most residential areas in China, cooking emissions have a considerable influence on urban air quality. For the residential areas near roads, both particle pollutants from traffic and cooking emissions would cause that the residents expose in high pollution concentration. Therefore, particle pollution mitigation has becoming increasingly significant for sustainable urban development and human well-being in China, especially in the near-road residential areas.

1.1.5. Modelling air pollution mitigation by urban green infrastructure

The concept of green infrastructure was first developed from two books of strategic landscape planning, which are Design with Nature (McHarg 1969) and Landscape Planning: Introduction to Theory and Practice (Crosby, Hackett 1972). Through 30 years development, green infrastructure was defined as (Communities 2005),

'Green infrastructure is a network of multifunctional greenspace provided across the defined area. It is set within, and contributes to, a high quality natural and built environment and is required to deliver liveability for existing and new communities.'

Green infrastructure includes urban trees, private and public gardens, parks, urban forest and urban agricultural spaces (Benedict, MacMahon 2002). It brings new purposes to green spaces, which urban green spaces need to be formalised as a coherent object of planning to

contribute to the urban sustainable development. Green infrastructures have positive effects on improving urban environment and human well-being, including air pollution mitigation, climate change reduction, flood control, and reducing heat island effect. In terms of air pollution mitigation, the filtration of polluted air is often studied, but the dilution of pollution concentration by dry deposition is less discussed. Many studies (Liu et al. 2017; Yang et al. 2004; Binkowski, Shankar 1995; Liu, Mo, et al. 2016) that are related with particle dry deposition attempted to estimate the economic benefits in large scale, such as city or regional levels. More specifically, particles and gas molecules in the atmosphere can be deposited when they pass close a surface, which is the dry deposition process. Due to the various factors and complex process of dry deposition, the air pollutant removal by vegetations is usually estimated by models (Escobedo, Nowak 2009; Alonso et al. 2011; Baró et al. 2014; Kim et al. 2014), but they rarely compared with field measurement (Morani et al. 2014; Guidolotti et al. 2016). The most common used models are EMEP/MSC-W model in Europe and UFORE in the US. They have limitations on applying at street or tree level (Simpson et al. 2012). Hence, it is necessary to develop a green planning model for mid-scale (from one hundred to several thousand square meters) residential area. So that will be able to estimate particle pollutant removal by trees through dry deposition to formalise green spaces as part of urban sustainable development.

1.2. Research aim and objectives

The aim of this research conducted is to explore optimization of urban green plans for particle pollutants mitigation in the mid-scale residential area. This work will develop a green planning model to estimate the effect of urban trees on particulate matter pollution removal by urban green spaces through dry deposition. This study will discuss to what

extent particle pollution concentration, green spaces, and wind speed can affect the efficiency of the dry deposition process on the tree canopy.

The objectives of this research are:

- Literature review on urban green infrastructure and how it can removal air pollution from the urban environment; and an investigation of the dry deposition process on absorbing particle pollution by vegetation canopy and current green spaces effect models.
- Development of a green planning model that estimates the amount of particle pollution mitigation in mid-scale residential areas.
- Validation of the model with the comparison of real-world data and simulation results.
- Application of the model to determine the optimum green plan for the study area (Taiyuan, China) by quantifying pollution mitigation based on various levels of pollution concentration, green cover, and wind speed.

1.3. Thesis Outline

The outline of research is presented in Figure 1-7, and the thesis structure is also illustrated in this diagram.

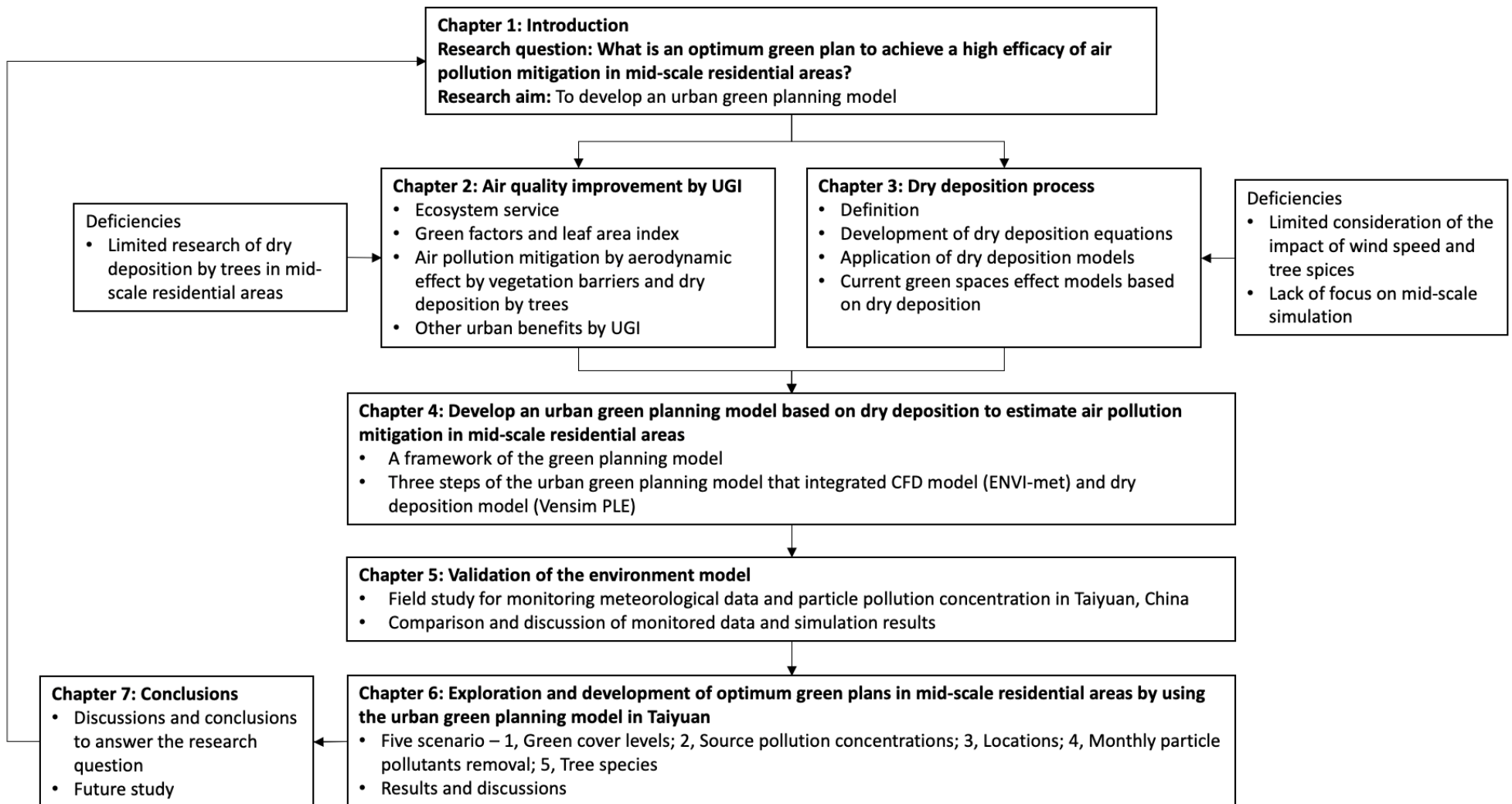


Figure 1-7 Research outline and structure.

The literature review of air pollution mitigation by urban green infrastructure is in chapter two, after this introduction. This section aims to introduce the concepts of 'ecosystem service' and 'green factors' to understand that green spaces planning and design is a nature-based method to improve urban air quality. It also points out the limitations of previous studies. The main limitations are the lack of research on particle pollution mitigation by dry deposition through trees in the mid-scale residential areas. Chapter 3 is the literature review of the dry deposition process on the vegetation canopy. It reviews the development of dry deposition studies and the application in urban planning and design. The limitations are pointed out by reviewing and discussing two commonly used models of green spaces effects. They are UFORE and EMEP MSC-W models, which have limited consideration of the impact of wind speed and tree species and lack focus on mid-scale areas.

The development of a green planning model is in chapter 4. A framework and data flow of this model are introduced first. This model contains two parts, which are a CFD model (ENVI-met) and a SD model (Vensim PLE). The model setup and boundary conditions are described in three steps, which are 1) identification of land types by local microclimate zones; 2) collection of meteorological and air quality data; 3) calculation of air pollution removal.

The model validation is in chapter 5. This chapter compares and discusses the real-world data and simulated results from the second part of the green planning model in the study area in Taiyuan, China. A field study was undertaken to monitor the PM_{2.5} and PM₁₀ concentration, and meteorological data, such as temperature, relative humidity, and wind speed.

Application of the green planning model in Taiyuan is discussed in chapter 6. This section aims to explore the optimum green plans for air quality improvement in the mid-scale study area. To achieve this, five scenarios, which are different percentages of green cover, level of source pollution concentration, locations with different wind speeds, monthly pollution concentration and wind speed, and various tree species, are investigated. The total amount of particle pollution removal is calculated for each scenario using the proposed model. The results are analyzed and discussed to propose an optimum green plan for the study area to

achieve a high efficiency of air pollution mitigation by dry deposition. The following chapter 7 is the final conclusion. It summarizes the contributions of the urban planning model and the findings of the simulation results, as well as the direction of future study. The findings are able to answer the research question, which is: 'what is an optimum green plan to achieve a high efficiency of air pollution mitigation in mid-scale residential areas?' The suggestions for future research based on this study are concluded at the end.

1.4. Research Scope and Focus

1.4.1. Scope

Air quality can be improved by many ways such as, source pollution control (Li et al. 2020), photocatalysis (Gómez et al. 2021), natural ventilation and vegetation barriers (Balczó et al. 2009; Abhijith et al. 2017), and dry deposition (Liu et al. 2017). Moreover, multiple benefits can be brought by urban green spaces, such as, removal of air pollutants by aerodynamic effects and the dry deposition process (Escobedo, Nowak 2009; Fantozzi et al. 2015; Janhäll 2015; Nowak 2006; Yin et al. 2011), reducing the urban heat island effect (Chen et al. 2014), noise pollution mitigation (Salmond et al. 2016), and improving the health and well-being of urban residents (Dean et al. 2011; Nowak et al. 2014). Each of these improvements is important for urban sustainability and human well-being. However, to interrelate all of them would cause many dimensional complexities and could not be handled in one single research project. Therefore, the scope of this research is defined more narrowly. It aims to develop urban green planning strategy to improve air quality by dry deposition of vegetation canopy in mid-scale residential areas. In other words, this research mainly concentrates on analysing the air pollution that is removed by only the dry deposition process on the surface of the vegetation canopy. In addition, due to the high particle pollution concentration in many Chinese cities, particle pollution mitigation by green spaces is the main benefit to be covered in this research. Third, to contribute to the existing

knowledge, mid-scale residential areas, which are defined as those with an area from one hundred to several thousand square meters, are concentrated on in this research, as there are limited studies and green planning models at this scale.

1.4.2. Focus

This research develops a green planning model to quantify the air pollution mitigation by trees in the mid-scale residential area. For the setup and application of the model, the focus of the model is identified. This model focuses on estimating the amount of PM_{2.5} and PM₁₀ removal by urban trees in a mid-scale residential area. Hence, first, the size of study area is from one hundred to several thousands square meters and contains mainly residential buildings. Second, the field study centres on monitoring particle pollution concentration. Third, the leaf area that is simulated in the model is mainly from trees, as trees are the most common vegetation in the residential areas in Taiyuan.

Chapter 2. A sustainable solution of urban planning for improving air quality – Literature review

2.1. Introduction

Air pollution has become a significant problem in China that impacts human health and well-being, ecosystem health, and the climate. Urban green infrastructure, such as trees and shrubs, are a nature-based method of improving air quality by directly removing air pollutants, altering local microclimates, and lowering building energy use (Chameides et al. 1988). Proactively planning green infrastructure would help urban development, nature conservation, and public health promotion (Tzoulas et al. 2007). The concept of urban green infrastructure has been discussed widely (Sandström 2002; Xing et al. 2018; Xing et al. 2017), with these discussions including all natural, semi-natural, and artificial networks of multifunctional ecological systems with the urban areas surrounded and in-between. There are many facets of urban green infrastructure, including great quality and quantity of urban green spaces (Rudlin, Falk 1999; Tzoulas et al. 2007), its multifunctionality, and its interconnection with the habitats (Walmsley 2006; Sandström 2002). This chapter will introduce green factors as the integration between green space and the outskirts of urban areas, and the relationship between human activity and nature linked by ecosystem services. Then, the green plot ratio will be reviewed to build a link between urban vegetation and environmental benefits. Finally, effects of green infrastructure on improving air quality will be discussed to clarify the role of deposition in pollutants removal.

2.2. Ecosystem service and sustainable urban planning

Ecosystem service valuation is playing an essential role in guiding future human activity for win-win opportunities with the environment (Farber et al. 2002). The term 'ecosystem service' in urban planning means the benefits that humankind receives from the activities of natural world (Harrison, Hester 2010). From clean air to food supply, our well-being heavily relies on multiple ecosystem services. Since the Millennium Ecosystem Assessment (MA) was published, ecosystem services have been rapidly developed and widely used for sustainable urban planning (Charles et al. 2020; Schirpke et al. 2014; Ash et al. 2010; Matos

et al. 2019). MA classifies ecosystem services into four categories, which are supporting, regulating, provisioning, and cultural (Harrison, Hester 2010). Discussion of the balance between environmental processes and socio-economic systems has received an increasing level of attention with the growth of ecosystem services. Urban green spaces provide various ecosystem services to the city, such as air purification, climate change mitigation, noise reduction, and they improve health and well-being of the urban population (Baró et al. 2014). Ecosystem service valuation can provide a guide to sustainably planning the relationship between society and the surrounding nature. More specifically, it presents general and essential links between green spaces, urban environment, and human activities. This research uses these links to quantify the benefits that are brought by vegetations.

In general, the term 'valuation' means the contribution of an action or object to user-specified goals, objectives, or conditions. However, it has been given additional disciplines in economic and ecological concepts. Farber (2002) highlighted various points in economic history that indicate there is no single element that can be used for economic value, but a combination of labour, cost, and preferences. This observation may help in part to guide ecosystem services assessment, but there is no need to over-study them. In terms of ecological concepts, usually natural scientists talk about causal relationships between different parts of a system by using the concept of value, such as the value of particular tree species in controlling soil erosion in a high slope area (Farber et al. 2002). Moreover, the idea of 'co-evolution' (Ehrlich, Raven 1964) in a whole group of interacting species could be expanded to show the 'value' of natural ecosystems and their components in terms of their contribution to human survival (Farber et al. 2002).

In addition, the contradiction between economic and ecological values has been indicated, because humans are only one of many species in an ecosystem. The value of our activities may be significantly different from the values of other ecosystem characteristics or the maintenance (health) of the ecosystem itself (Farber et al. 2002). People have different opinions about balancing and integrating economic and ecological values. Some people think ecosystems should be valued to fit into economic concepts, but others argue from ecological angles. Farber (2002) suggested the exchange value of ecosystem services should be traded in normal markets. Many techniques for valuing ecosystem services have been

developed to quantify the value of nature, which are not only by market prices but also by 'what a society would be willing and able to pay for a service or what it would be willing to accept to forego that service' (Hanemann 1991). On the other side, ecosystem services assessment aims to provide a more sustainable ecosystem for human benefit (Häyhä, Franzese 2014). More specifically, natural capital acts on ecosystems to impact the relationship between ecological and socio-economic systems.

Häyhä & Franzese (2014) also discussed different economic and ecological approaches, and proposed a conceptual framework to integrate environmental accounting and ecosystem services assessment. Three approaches of Evaluating ecosystems and their services were given. The first of these approaches is considering the thermodynamic and systems features of ecosystems. Socio-economic systems are embedded in and dependent on the ecological ecosystems that are characterized by non-equilibrium and irreversible phenomena (Folke et al. 2011). For instance, a healthy ecosystem could serve its structure and functions while generating several ecosystem services vital for human well-being (Costanza 2012a). The second is considering the ecological theory of value and assessment methods. Ecosystem health and integrity are the foundation of regulating, provisioning, and cultural ecosystem services. Accordingly, work capacity and regenerative capacity are used as a measure of life-supporting capacity of natural capital (Häyhä, Franzese 2014). The third approach is the economic theory of value and valuation methods. Market prices could be used to value ecosystem services to help to make decisions on how to use natural capital and ecosystem services in the presence of tradeoffs or when a conversion between different types of capital is involved (Farber et al. 2002). Häyhä & Franzese (2014) proposed a framework to show the costs, benefits, and impacts of ecosystem services and how they could help to improve a healthy ecosystem to maintain the sustainability of the socio-economic system. Baró et al. (2014) quantified the contribution of ecosystem services by urban forests through a dry deposition model. The results showed the forests regulated ecosystem services by providing substantial benefits in terms of air pollution mitigation. Moreover, urban pollution mitigation by green infrastructures needed to be coordinated with local policies, land, and building types.

In summary, ecosystem services present multiple benefits from the nature to human society. For sustainably acquiring the benefits, valuation of current ecosystem services and management of future ecosystem services are important for urban planning. Urban green space as a big part of the natural world provides many contributions in terms of ecosystem services, such as air pollution reduction and improving human well-being, which can guide the sustainable development of urban areas by quantifying the benefits from vegetations. Different approaches of ecosystem services valuation have been explored and developed over the years based on various economic and ecological backgrounds (Häyhä, Franzese 2014; Baró et al. 2014; Costanza 2012b; Folke et al. 2011; Charles et al. 2020). It is clear that the concepts and techniques of ecosystem services valuation cannot be described by a single set. Rather, it requires conceptual pluralism and additional details based on various scenarios to be adapted in different urban environments and scales. Green factors are planning tools that focus on green infrastructure development and evaluation around buildings on community scales.

2.3. Green factors

The question 'how much green space should a city have' has been asked since the 1920s, but slight discussions only started in the 1930s (Harnik 2010). In fact, the idea of urban green spaces became more important and popular after World War II. Harnik (2010) defined and classified different kinds of urban green spaces and their size, facilities, and distance from the city, and argued for a standard number of green spaces, facilities, and programs in a city. Various green factors were developed and applied for urban planning to improve urban green spaces efficiently. The green plot ratio (GPR) was introduced by Ong (2003) as a greenery metric based on leaf area index (LAI) for sustainable urban planning. It emphasized the importance of plants to the benefits of climate modification, carbon sequestration, smog mitigation, dry deposition of PM particulates, improvement in the quality of life, increased value of landed properties, decreased rainwater runoff, and protection against floods (Akbari et al., 2001). For this study, GPR will be utilised to assist green planning tool that aims to improve quality in urban communities (Lane 2019; van Houdt et al. 2011), which are defined on a scale of approximately one hundred to one hundred thousand

square meters. More specifically, LAI can act as a variable value in the model to show how different levels of urban green spaces affect air quality.

2.3.1. Biotope Area Factor

Many researchers suppose that landscape design is playing a significant role in fields of ecology and biology (Barnett, 2008, Handel et al., 2013, Hobbs, 1997), which asks strategies that could measure the ecological effectiveness of different types of urban green spaces (Kohsaka, 2010 and Mori and Christodoulou, 2012). In some European cities, the Biotope Area Factor (BAF) has been used as a guideline to manage urban landscapes sustainably (Finlay, 2010). The BAF shows the ratio of the ecologically effective surface area (areas covered by green vegetation and/or permeable to rainwater) to the total land area under consideration (Farrugia et al., 2013). This landscape requirement applies to development in the city centre (Beilin.de). Also, it intends to measure high quality urban green areas with respect to the ecosystem, protection of biotopes and species, the appearance of the landscape, and recreational use (Beilin.de.). The BAF presents a new understanding of green vegetation coverage, which includes not only simply knowing the amount of land covered by vegetation, but also obtaining a more accurate description of ecologically effective urban green spaces. Moreover, rainwater, which takes up a significant part of the BAF, is a valuable measurement of biotopes. Therefore, the BAF is good at more practically evaluating urban landscapes in a way that shows ecological values.

2.3.2. Seattle Green Factor

The Seattle Green Factor (SGF), which is derived from BAF, is a score-based code requirement to improve the quantity and quality of urban landscapes in new developments (Torgelson, 2016). The aim of SGF is to help new buildings fit into the surroundings, buffer incompatible uses, regulate privacy and screening, decrease headlight glare, and create a pleasant urban environment. Moreover, this rule could monitor urban landscapes to facilitate the bringing about of ecological benefits, such as reducing stormwater runoff, improving air and water quality, decreasing the urban heat island effect, improving energy efficiency, and providing wildlife habitats (Sugimura, 2015). Comparing with BAF, SGF is more scientific and logical, and is able to assess continuity urban landscapes. For instance, it

has been designed to allow the development of different projects, which means it has a high degree of flexibility when improving ecological and aesthetic qualities of urban landscapes (Hirst et al, 2008). Also, many elements have been included in SGF as guidance for ecological purposes, such as soils, bioretention facilities, planted areas, trees, green roofs, green walls, water features, and permeable paving. Each of those elements are given weighted according to their functional benefits and possible environmental impacts (Hirst et al, 2008). With the development of general measurements of BAF, SGF describes the urban landscape effectiveness in more details.

2.3.3. Malmo Green Factor

The Malmo Green Factor has been designed and used in an international housing exposition called 'The Sustainable City of Tomorrow' (Bo01), which was held in Malmo in 2001 (Kruuse, 2011). Malmo is one of main industrial cities in Sweden with developed traffic systems. However, with the evolution of modern industrial technology and the degradation of the eco-environment, the city needs to make some changes, which means it has many parallels with Taiyuan City. The aim of Bo01 is to promote eco and social sustainability and show a practical example of 'Sustainable City of Tomorrow' theme. For achieving this purpose with effect, green and blue infrastructures have been asked to make an important contribution to the character of the public space (Bo01, 2000). The landscape architect responsible for the green and blue aspects of Bo01 realised that the housing blocks' courtyards needed special schemes to prevent them becoming grey and visually boring surfaces. The objective of creating new, high-quality green space resulted in a breakthrough when the City Council agreed to use a 'Green Space Factor' and a 'Green Points System' to achieve at least a specified minimum level of greenery, and special green and blue qualities for the courtyards (Kruuse,2011). This Green Space Factor, which was adapted from the BAF, is applied to the whole building lot, taking into account both the building areas and the open space (Kruuse,2011). Different from BAF and SGF, the Malmo Green Factor adds in a new idea — Green Points — into the Green Space Factor (GSF) to achieve certain additional qualities. One of the main reasons is the limitation of GSF, which means it does not contain the full quality of the green cover. Developers are asked to choose 10 of 35 Green Points and given

detail plans among them. This is calculated to aid biodiversity, improve the architectural qualities, and help with stormwater management (Kruuse,2011).

To compare those cities with the research area of this study (Taiyuan), the weather conditions in north China are inclement. In Taiyuan City, the warmest month of the year is July, with an average temperature of 24.8 °C and a maximum of 30.0 °C; January has the lowest average temperature of the year, which is -6.4 °C, with a minimum of -10.0 °C. However, the climate in Seattle and Malmo is different. The average temperature of Seattle ranges from 18.1°C in summer to 4.3°C in winter, whereas in Malmo the averages are 16.7°C in summer and 0.0°C in winter (CLIMATE-DATA.ORG). Therefore, the requirements for plants in each of these places would be different. For example, the plants need to be short, with shallow roots and a high transplant survival rate. These plants could have a long greening period and good landscape effect. In addition, the plants must be tolerant to wind, cold, and drought weather conditions (W. Ji et al, 2005). These requirements are different from Seattle's. In SGF, planted areas include groundcover plants, green roofs, and walls specially designed for residential areas. BAF brings a new view of evaluating urban green space, which not only simply calculates the area of land that is covered by vegetation but assesses it with ecological and sustainable ideas. Developing that, SGF is a more detailed index that helps to create efficient green spaces around buildings. In Bo01, GSF helps to build urban green and blue infrastructure in Malmo to encourage more people to live there and draw more visitors in to travel around the area. For further development, Green Points have been added for sustainable biodiversity based on the local environment situation. All of these green ratio methods are useful and have their own advantages.

2.3.4. Green plot ratio and leaf area index

Green spaces play a significant role in the planning of sustainable cities. Plants are useful for improving cities in three ways: environmentally, aesthetically, and recreationally (Attwell 2000). A common greenery metric is important for sharing and comparing the experience of different projects, which can also provide guidance for new projects. Ong (2003) presented the Green Plot Ratio (GPR), which is able to link environmental benefits and land cover. Different from green factors such as BAF, SGF, and MGF, which are based primarily on the

configurations of land and buildings, the GPR is more focused on green spaces, such as lawns, shrubs, and trees. Therefore, a biological parameter of greenery is introduced to quantify green planning metrics — leaf area index (LAI). LAI is commonly used in the biological sciences for setting up mathematical models, monitoring the ecological health of natural ecosystems, and predicting the metabolic processes of plants. Hence, LAI is an essential tool for modelling ecological processes of green spaces as well as predicting the subsequent ecosystem responses (Asner et al. 2003; Jonckheere et al. 2004; Leonenko et al. 2013; Liu et al. 2012; Ong 2003).

The Leaf Area Index (LAI), as a dimensionless variable, is defined as the total one-sided area of photosynthetic tissue per unit ground surface area (Watson 1947; Jonckheere et al. 2004). The definition may change depending on the various leaf shapes and technique of measurement. For instance, both sides of broad leaf trees have the same surface area, yet for coniferous trees there is no clear one-side area (CHEN, BLACK 1992). It is important to understand that these different definitions can cause very different results between LAI calculations. In GPR, LAI is simply defined as the ratio of leaves to ground cover. There are two main methods of LAI measurement, which are destructive and direct methods, and non-destructive and indirect methods (Ong 2003). Direct methods require the calculation of the average area of leaves from trees physically and then to build a stand. It is the most accurate method but extremely time consuming. Indirect methods infer leaf area from other observational variables such as the level of light transmittance through the plant canopy and remote sensing measurements of Earth's albedo (Jonckheere et al. 2004; Ong 2003). These methods are generally faster for covering larger sample areas. Compared with direct methods, indirect methods have become more important and widely used (Olivas et al. 2013; Kalácska et al. 2004; le Maire et al. 2008; Liu et al. 2012; Leonenko et al. 2013).

Researchers (J. M. O. Scurlock et al. 2001) summarised global LAI data to help in determining the corresponding LAI of urban green planning. Table 2-1 lists the measurements of the LAI for some common biomes that are commonly planted in north China, as measured by (J. M. O. Scurlock et al. 2001) and other studies. As we can see, LAI of deciduous needleleaf and broadleaf trees are quite similar in most of studies. Liu et al.'s (2012) study showed different for evergreen broadleaf and needleleaf trees as the

measured LAIs are from mixed forests. In this research, J. M. O. Scurlock et al.'s (2001) data are used as benchmark values.

Table 2-1 Measurements of leaf area index by biome in various studies.

LAI				Reference
Deciduous broadleaf	Evergreen broadleaf	Deciduous needleleaf	Evergreen needleleaf	
2.6	4.8	4.6	5.5	(J M O Scurlock et al. 2001)
2.6	4.8	4.6	5.5	(Ong 2003)
2.6	4.8	4.6	5.5	(Asner et al. 2003)
	0.2 – 4.2	0 – 5.0	0.8 – 10.4	(Leonenko et al. 2013)
2.5	6.1	2.5	2.5	(Liu et al. 2012)
	4.5	3.1	5.5	(Garrigues et al. 2008)
2.6				(Xianfeng et al. 2010)
6.3				(le Maire et al. 2008)
	2.5			(Kalácska et al. 2004)

2.4. Urban green infrastructures benefit on air pollution mitigation

More than half of the global population lives in cities (United Nations 2014), while air pollution in urban areas is becoming a major health concern. Vehicle exhaust and industrial emissions are the main cause of low air quality in many cities worldwide (Kumar et al. 2016; Tzoulas et al. 2007). Vehicles in urban environments mainly emit particulate matters (PM10 and PM2.5) and some gaseous pollutants such as nitrogen oxides and carbon monoxide (Donaldson et al. 2001; Vardoulakis et al. 2003). Green infrastructure in urban environments, such as trees, vegetation barriers, green walls, and green roofs, are

considered to be sustainable urban planning solutions for removing air pollution (Salmond et al. 2016). These types of green infrastructure have been proven to impact urban dispersion patterns and help to remove air pollutants by aerodynamic effects and dry deposition process (Escobedo, Nowak 2009; Fantozzi et al. 2015; Janhäll 2015; Nowak 2006; Yin et al. 2011). Green infrastructure also helps with reducing the urban heat island effect (Chen et al. 2014), noise pollution mitigation (Salmond et al. 2016), and improving the health and well-being of urban residents (Dean et al. 2011; Nowak et al. 2014).

2.4.1. Aerodynamic effects by green infrastructures at street level

The ideas of urban vegetation improving air quality have always been controversial. Some studies indicated that urban vegetation can increase the pollution concentration specially at a street level. Amorim et al. (2013) assessed the level of CO pollutant removal by roadside trees in Portugal. By using computational fluid dynamics (CFD) models to simulate the aerodynamic effects of the trees in relation to the wind field, the CO concentration was found to be higher under the tree canopy compared to the atmosphere above the roof-level. However, when the capacity of ventilation and dispersion increased, the CO concentration dropped in the area. It was therefore suggested that the aerodynamic properties of the trees is important for planning optimal green areas for comfort and health purposes. Buccolieri et al. (2011) compared air pollution concentrations in street canyons with different aspect ratios of the canyons and wind direction. They investigated the effect of street trees on air flow and pollution dispersion. Their study found that trees would increase the pollutant concentration by affecting the flow and dispersion of traffic exhaust fumes. However, inclined wind direction decreased pollution concentration. Gromke and Ruck (2007) discussed the effects of crown diameter, crown permeability, crown height, and tree spacing on natural ventilation and pollution concentration. Increasing crown diameters causes higher concentration, while increasing tree spacing leads to a decrease in concentration. Wider tree spacing results in better air quality as vortices generated by atmospheric overflow can remove more air pollution. Hofman et al. (2016) analysed the influences of tree crown characteristics on the PM10 distribution inside urban street

canyons by using ENVI-met. It was found that the aerodynamic effect of the trees influences the street PM₁₀ concentration, with denser tree crowns leading to lower wind speeds and higher pollution concentrations. Wania et al. (2012) examined the impact of different levels of vegetation cover and different street sizes on the dispersion of particles in urban streets by using ENVI-met. Generally, vegetation was found to reduce wind speed, which inhibits ventilation of the canyon, thus increasing particle concentrations. This is due to the trees disrupting the flow field to the canyon at crown-height. The study found that increasing the height-to-width ratio of the canyon would improve the ventilation and reduce the pollution concentration. As we can see, the existing literature have found the negative impacts of trees on air quality, mainly because denser vegetation leads to higher air pollution concentrations by decreasing street ventilation. However, the ventilation could be improved by increasing the space between trees, choosing plants with a low-density crown, and improving height to width ratio of the street.

Some studies have claimed that street pollution concentration is mainly dependant on aerodynamic effects of winds. For instance, Vos et al. (2013) investigated the effects of different urban vegetation on air quality improvement by ENVI-met. They found that street vegetation leads to higher pollutant concentration rather than improving air quality, because they reduce ventilation. Their study also shows that the negative aerodynamic effect is much stronger than the pollutant mitigation capacity of vegetation. Jeanjean et al. (2017) assessed the impacts of trees on the dispersion of NO_x and PM_{2.5} emissions. They concluded the same as Vos et al. (2013) — the aerodynamic effects on pollutant concentration dominate over the dry deposition by trees. The deposition effects are found to be around four times lower than the aerodynamic effects. As Table 2-2 shows, for perpendicular wind directions, trees do not improve air pollution removal. For parallel wind directions, it is observed that the aerodynamic effects of trees decrease street pollutant concentrations, and tree deposition also reaches the highest in both the summer and autumn. In addition, based on dry deposition data presented in this study (see Table 2-2), it is important to note that tree deposition acts less with wind directions, even the pollution removal amount of dry deposition is much less than the aerodynamic effects. The dry deposition is a consistent process that only needs vegetation and pollution to occur.

Moreover, ENVI-met, as a CFD based environment software, has been used in many studies (Vos et al. 2013; Wania et al. 2012; Hofman et al. 2016) to investigate the impacts of vegetation on street.

Table 2-2 Influence of wind direction on traffic-emitted PM_{2.5} concentration with 5m/s wind speed, without urban background concentrations. Wind direction is the angle of the street in the study (Jeanjean et al. 2017).

Wind direction (°)	Aerodynamic effect of trees (µg/m ³)		Tree deposition (µg/m ³)	
	Spring and Autumn	Summer	Spring and Autumn	Summer
0	0.8	0.3	-0.2	-0.2
30	1.6	1.7	-0.4	-0.5
60	-1.0	-0.8	-0.2	-0.3
90	1.8	2.1	0.0	0.0
120	0.3	0.8	0.0	0.0
150	6.3	0.4	-0.3	0.0
180	7.6	11.7	-0.5	-0.7
195	2.6	3.8	-0.4	-0.7
210	6.6	4.8	-0.3	-0.4
240	-3.1	-2.9	-0.3	-0.4
255	-3.2	-2.7	-0.4	-0.5
270	1.6	2.1	-0.2	-0.3
300	2.4	2.5	-0.3	-0.4

2.4.2. Urban vegetation barrier

As vegetation significantly affects road ventilation, urban infrastructure can also serve as roadside barriers to reduce pollution. Brantley et al. (2014) compared measured data from each side of the roadside tree stand to determine the effects of vegetation barriers on air pollutant concentration. Their results showed that the time of day and wind direction dramatically affected the pollution concentration behind the tree stand. Their study found that pollution was reduced by up to 22% from the road during downwind and parallel wind phases, which a mature tree stand located on the roadside can improve air pollution from traffic. Hagler et al. (2012) measured ultrafine particle (UFP) concentrations on a main road and at a location near the road to analyse if a tree stand is a practical strategy for reducing air pollution concentration along populated traffic corridors. In general, lower concentrations were measured behind the vegetation barrier than on the road. Moreover, denser tree spacing and a higher leaf area index led to a lower concentration behind the tree stand. Lin et al. (2016) assessed the effects of deciduous and coniferous vegetation, as road barriers, on pollutant transport and tree deposition in summer and winter. Their study found a reduction in concentration of up to 60% with full foliage of vegetation, and no concentration change before and after the deciduous barrier in winter. This highlights the importance of the tree crown on reducing air pollution. Tong et al. (2016) investigated how the characteristics of vegetation barriers affected pollution levels. They recommended two design options to reduce roadside air pollution by decreasing pollution transport and deposition, which are wide vegetation barrier with a high Leaf Area Density, and a combination of vegetation and solid barriers.

In general, tree stands reduce traffic emissions by dispersion and deposition. Effects of dispersion depend on leaf area density, vegetation barrier width, oblique wind speed, and barrier height and distance from roadway. The deposition on the other hand depends on tree crown density and the presence of vegetation.

2.4.3. Air pollution mitigation by deposition

The studies discussed so far mainly focused on near-road areas with lower levels of vegetation, so dispersion has been accounted for the main part of air pollutants mitigation. However, this doesn't mean that deposition is not important for improving urban air quality. Janhäll (2015) reviewed two physical effects of vegetation on air quality improvement, deposition, and dispersion. This study concluded that higher air pollution concentrations increased deposition. In near-road areas, high density vegetation increased pollutants in street canyons, while low tree spacing close to pollution sources can improve air quality by increasing deposition. Also, denser tree crowns can offer larger deposition surfaces for better pollutant filtration. Beckett (2000) support the notion that that deposition on trees can remove significant amounts of particulate matter from urban atmospheres. Trees with lower leaf density, larger size, and bigger leaf area can capture more PM pollution. Moreover, medium size trees with higher canopy density also remove pollution effectively. In addition, the deposition process that reviewed and discussed in this paper is mainly dry deposition. Another way of removing air pollution from atmosphere is wet deposition. Wet deposition refers to the process of rain or snow scavenging (Tai et al. 2017). In this process, pollutants is generally serving as cloud-condensation nuclei, or captured by cloud water, or removed by raindrops as they fall (Chate et al. 2003). However, this research focuses on removing air pollution by the vegetation surfaces, which is mainly dry deposition.

The estimates of air pollution mitigation by tree deposition can clearly show how much pollutant has been removed annually. Escobedo and Nowak (2009) studied air pollution removal by urban forests through tree deposition in Santiago, Chile. They found that areas with higher vegetation cover removed more air pollution (see Table 2-3). Nowak also found that urban vegetation can improve local and regional air quality by removing air pollution through dry deposition in other cities and countries. For example, in the United States, annual air pollution is estimated to total 711,000 metric tons (Nowak et al. 2006). Nowak (2006) found that the total amount of air pollution (CO, NO₂, O₃, PM₁₀ and SO₂) removed globally in 2000, which the range of air pollution mitigation by tree deposition was from 8 metric tons a year in Fuenlabrada, Spain, to over 1500 metric tons in Atlanta and New York. In China, Yang et al. (2004) reported that urban forests in Beijing removed 1261.4 tons of pollutants by tree deposition from the air in 2002, and the most reduced pollutant was

PM10, having been reduced by 772 tons. Jim and Chen (2008) assessed dry deposition removal of air pollution by urban vegetation in Guangzhou, China, finding an annual removal of 312.03 tons of SO₂, NO₂, and total suspended particulates. More pollutants were removed by recreational land use as it has a higher green cover area and in winter as higher pollution concentration. Yin et al. (2011) found that urban parks with trees and shrubs can remove traffic pollutants such as SO₂, NO₂, and total suspended particles by deposition in Shanghai. In total, urban vegetation reduced 9.1% of total suspended particles, 5.3% of SO₂, and 2.6% of NO₂.

Other green infrastructures, such as green roofs and green walls, have also been found to have an impact on air pollution levels. Viecco et al. (2018) quantified the effects of green roofs and green walls on air pollution mitigation in high level PM concentration areas. By comparing nine vegetation species commonly used in green walls and green roofs in Chile, they showed a significant amount of PM was deposited on the vegetation and different species had large differences in the amount of PM dry deposition. Yang et al. (2008) evaluated the air pollution removal by green roofs and reported that green roofs could reduce air pollution in Chicago, contributing to 675 kg of air pollutants removal. O₃ was the most removed air pollutant by green roofs. The use of green roofs is recommended in areas where is shortage of land resources.

To sum up, by reviewing pollution removal, ambient pollution concentrations, and urban forest cover, a basis of most urban forest effects on air quality improvement seems to be high level of green cover, proportion of evergreen tree and leaf area. In addition, green roofs and green walls also contribute to improving air quality. Even though the removal amount is much less than that of urban forests, they still can be used as an alternative approach for cities with limited land available for planting trees (Yang et al. 2008). The Urban Forest Effects (UFORE) model, as a computational model, was developed by Nowak (Nowak, Crane 1998; Nowak et al. 2002) to estimate air pollution mitigation, ecosystem services, and the benefits urban forest. In UFORE, PM deposition depends on the leaf area index as the deposition velocity is assumed to be a specific value for the calculation. In terms of mid-scale urban areas, it seems that there is a lack of consideration of aerodynamic effects and pollution concentration of deposition activity in the existing literature.

Table 2-3 Annual air quality improvement by the reduction of pollutants for three different vegetation covers during 2000–2001 in Santiago (Escobedo, Nowak 2009).

Vegetation cover	Average air quality improvement (%)				
	PM10	O3	SO2	CO	NO2
26%	1.6	0.5	0.5	0.006	0.4
14%	0.7	0.2	0.2	0.003	0.2
12%	0.6	0.4	0.1	0.003	N/A

2.4.4. Other benefits of green infrastructures

Urban green infrastructures can not only reduce air pollution but also provide other benefits such as improving health and well-being of urban population, reducing noise pollution, mitigating the urban heat island effect, and climate change mitigation. Epidemiological studies have proven that green spaces provide a positive influence on the longevity of urban citizens (Tanaka et al. 1996; Takano et al. 2002). Powe and Willis (2004) assessed tree deposition effects on reducing air pollution, deaths, and hospital admissions caused by air pollution in Britain. Their results showed that air pollution reduced by urban woodland led to a decrease in the number of deaths (5 to 7 people) and hospital admissions (4 to 6 people). Maas et al.'s (2009) study found a lower prevalence of heart disease and diabetes in areas with more green spaces in the Netherlands. A similar relationship was found in Minnesota by Dengel et al. (2009), where fewer cases of cardiovascular disease and diabetes were found in greener areas. Moreover, the perceived general health impacted by quality of green spaces that less poor health reported with higher satisfaction of green land in their living area (Agyemang et al. 2007; Putrik et al. 2015; van Dillen et al. 2012). Mental health is also related to levels of urban vegetation and distance to a park. By analysing the self-reported health of over 10,000 people and green spaces in their living environment in the Netherlands, de Vries et al. (2003) found that people reported fewer symptoms and have better perception of their physical and mental health. Another survey (Stigsdotter et al. 2010) in Denmark supported the notion that the relationship between urban green

spaces and health is significant. Moreover, less stress and better health was reported amongst people who lived a shorter distance away from a green space. Sturm, Cohen (2014) found that living further away from an urban park would lead to lower mental health. In terms of green space and mortality, studies (Mitchell, Popham 2008; Mitchell et al. 2011; Villeneuve et al. 2012; Coutts et al. 2010) showed lower mortality rates are present presented in areas with more green spaces.

Alongside air pollution, noise pollution also decreases the quality of the urban living environment as it associated with annoyance, self-reported sleep disturbance, and hypertension (Jarup et al. 2008). Urban trees can play a significant role in reducing noise pollution by altering the noise soundscape. For example, trees can generate rustling of leaves in response to wind and attract bird and other wildlife sounds, which are all better than road traffic noise (Salmond et al. 2016). More studies (Papafotiou et al. 2004; Lam et al. 2005; Maleki, Hosseini 2011; Pathak et al. 2011) have attested the effects of urban vegetation on reducing noise levels. Bucur (2006) suggested that high density trees and shrubs can improve noise level reduction. Increasing urbanization would intensify the urban heat island effect, which may cause heat waves and extra energy consumption. Urban vegetation, such as parks and green roofs, can reduce the heat island effect by shading buildings and cooling the ambient air (Luber, McGeehin 2008; Alexandri, Jones 2008; Ahmed Memon et al. 2008; Bowler et al. 2010; Wong, Lau 2013). They can also reduce the cooling energy demand, and thus reduce greenhouse gas emissions, which helps mitigate climate change (Susca et al. 2011; Xu et al. 2012; Smith et al. 2012).

The studies discussed above prove that the quantity and quality of green spaces in a living environment are closely related with general health and mortality, noise pollution reduction, and mitigating both the urban heat island effect and climate change. These findings show the importance of green infrastructure in sustainable urban planning.

2.5. Conclusion

With increasing air pollution in cities, urban green spaces have been put forward as a sustainable solution for urban planning that can improve air quality and the living environment. This chapter presents a review of the effects of urban green spaces on developing sustainable cities and clarifies the social, economic, and environmental benefits of vegetation, especially their contribution to improving air quality. The concept of ecosystem services has been introduced to present a significant link between a city and its urban green spaces. Then, the valuation can quantify the benefits that are brought about by various types of green infrastructures, and subsequently guide urban plans for constructing better living environments. Due to the complexity of urban areas and the diversity of ecosystems, models of ecosystem service valuation need to be designed based on land types and scales, culture, and society. Green factors as greenery tools not only describe and identify biological elements in building environments, but also present the ecological and social impacts of different elements. More specifically, it narrows down the ecosystem services to a community scale and provides more details for green planning with the impact of land and building types. However, from BAF to MGF, land and building types plays a more dominant role in the valuation process than green spaces, so more consideration of vegetation is needed to develop a more effective green planning tool in this research. The green plot ratio (GPR) was developed based on the leaf area index (LAI) and applied to urban planning to improve urban green spaces efficiently. LAI, as a biological parameter, is commonly used to understand the ecological process of green spaces, such as air pollution reduction by deposition and dispersion.

A large body of evidence reviewed in this chapter indicates that green infrastructure can provide a range of ecosystem services to urban residents, such as air pollution mitigation, health and well-being improvements, and noise pollution and climate change reduction. Moreover, green spaces are closely connected with general health and mortality. Urban trees can reduce air pollution in many ways. For example, they can intercept atmospheric particles with their large leaf surface, onto which deposition of such particles may take place. Thus, the trees can act as vegetation barriers to prevent the penetration of pollutants

into certain areas. Air pollution mitigation is mostly associated with dispersion and deposition. Some studies (Jeanjean et al. 2017; Vos et al. 2013) found that decreasing dispersion by vegetation barriers could remove more pollutants than dry deposition on leaf surfaces. Dispersion is mainly impacted by aerodynamic effects while deposition is more dependent on the tree characteristics, such as crown density and the presence of vegetation and pollution concentration. In terms of controllability, urban green planning could have a strong impact on tree deposition levels because dispersion occurs with most of wind directions and speeds, which are difficult to control through a city plan. Although dry deposition by vegetation has been studied over many years, it still has not received as much attention as dispersion. Most dry deposition studies focus on a city scale, and studies on a street scale mainly discuss dispersion, which relies on different wind systems. Deposition through trees is a continuous process that is less subject to the effects of wind. Deposition is able to remove air pollutants continuously in areas that have higher pollution concentrations where it is difficult to build large vegetation barriers, such as the near-road living environment. Therefore, a special tool for green planning on the community scale would be a practical way to improve the air quality. In conclusion, urban green spaces have positive and significant influences on the urban living environment. It is important to investigate optimum green plans for bringing better air quality to specific urban areas. To achieve this aim, a model that can evaluate air pollution mitigation by deposition processes is needed. The next chapter will review the effect of dry deposition of urban vegetation on reducing particle pollution, and discuss the development and application of dry deposition models in urban areas.

Chapter 3. Mitigation of particle air pollution by urban green spaces – dry deposition

Notations

F	Deposition flux
C	Concentration
v_d	Dry deposition velocity
v_s	Settling velocity
R_a	Aerodynamic resistance
R_s	Vegetation surface resistance
K_p	Eddy diffusivity
d	Displacement height
z	Different height above the canopy
$U(h)$	Flow velocity at height (h)
ε	Location-independent collection efficiency
α	Aerodynamic extinction coefficient
r_a	Aerodynamic resistance
r_b	Quasi-laminar sublayer resistance
d_p	Particle diameter
g	Gravitational acceleration
ρ_p	Particle density
ρ_a	Air density
μ_a	Air dynamic viscosity
C_c	Cunningham factor
λ_a	Mean free path of air
$r(z)$	Total resistance to the transport
L	Monin-Obukov length
A	Empirical constant
u_*	Friction velocity based on the intensity of atmospheric turbulence
z_o	Surface roughness
k	Von Karman constant
c_p	Heat at constant pressure
T	Average temperature in surface layer

H	Sensible heat
r_{db}	Resistance of Brownian diffusion impact
ν_a	Air kinematic viscosity
K_B	Boltzmann constant
T_a	Absolute temperature
r_{ii}	Inertial impact
S_t	Stokes number
r_{ti}	Turbulent impact
τ	Particle relaxation time for particles

3.1. Introduction

Urban green spaces have become an important solution for sustainable urban planning as they can provide multiple environmental and social benefits. One of the environmental benefits of trees is to reduce air pollution (McPherson et al. 1994). There are mainly two ways that trees reduce air pollution: dispersion and dry deposition. Especially in the absence of rainfall events, dry deposition is the main transfer pathway of particles and gaseous pollutants from the air to the surface (Roupsard et al. 2013). Positive effects of green spaces on filtration air pollution have often been studied, but dilution of polluted air needs more attention. A few reviews have been done regarding the reduction of particle air pollution through dry deposition (Litschike, Kuttler 2008; Petroff et al. 2008; Janhäll 2015). Gaseous pollutants are adsorbed through leaf stomata, and airborne particles are intercepted and retained by the leaf surface, which is the dry deposition process (Beckett et al. 1995; Nowak et al. 2000; Nowak et al. 2006). Air particle pollution is one of the main pollutant sources in China, where the particle concentration is much higher than the WHO standard, the consequences of which are a deterioration of air quality and human wellbeing (Hou et al. 2018). This chapter discusses the physical impacts of urban vegetation on air quality from the perspective of dry deposition. That can contribute on the design of urban green planning based on air quality considerations. It also reviews the development of dry

deposition velocity expression since 1980s and the application of dry deposition in urban planning research. Two green spaces effect models that are commonly used are reviewed and discussed. Mainly particle air pollution is considered due to its significant health risks and high concentration in many Chinese cities, as well as its extra complications compared with gaseous pollutants.

3.2. Particle air pollution

With the increasing urban population, particulate matter (PM) has become one of the critical issues for human health. Particulate matter is divided to two types: fine particles and coarse particles. Fine particles (PM_{2.5}) are airborne particles with an aerodynamic diameter of less than 2.5 μm . PM_{2.5} is emitted from industry and road traffic. Coarse particles (PM₁₀) have an aerodynamic diameter between 2.5 and 10 μm , which mainly comes from road transport in the urban environment. Other human activities can also produce PM, such as mechanical grinding, windblown dust, sea spray, agriculture, construction, and quarrying activities (Charron, Harrison 2005). Traffic emissions are not only from engine exhaust, but also from non-exhaust vehicle emissions. For example, soil and dust on the road can be resuspended by the wind or due to the air turbulence induced by passing road traffic (Solazzo et al. 2007). PM can also be produced from the abrasion of brake and tyre components of motor vehicles (Thorpe et al. 2007). Harrison et al. (2001) found that the PM concentration from non-exhaust vehicle emissions is as much as that from exhaust emissions in London. Querol et al. (2004) support the idea that both types of exhaust increased by almost the same amount of PM emissions in many European cities. Moreover, coagulation would impact the particle mass and size, which means PM_{2.5} can increase to PM₁₀ by coagulation as potential contributors of coarse particles (Kassomenos et al. 2012). Hence, PM₁₀ will need more consideration in terms of air pollution reduction.

Epidemiological studies showed particle air pollution has directly affected the health of urban residents, causing cardiovascular and respiratory diseases, premature mortality, reduced birth weight, lung cancer, and inflammatory illnesses (Hoek et al. 2013; Sun et al. 2016). Brunekreef and Forsberg (2005) proved that both fine and coarse particles can cause negative health effects, and PM10 has a separate influence on respiratory morbidity. Since traffic emissions is one of the most important PM sources in the urban environment, pedestrians, cyclists, and near-road offices and houses would be significantly impacted. A Study from Pollution (2010) showed that exposure to traffic-related air pollution increased risks of asthma, impaired lung function, and increased cardiovascular mortality and morbidity. Hoek et al. (2002) studied that living near busy streets is associated chronic respiratory disease in children and mortality rates of elderly people. Medina-Ramón et al. (2008) concluded the mortality risk increased with decreasing distances to a major roadway or a bus route. Lipfert et al. (2006) argue that traffic-density is also closely associated with mortality. Trees are considered as one of the optimum ways to reduce particle air pollution, especially for the near-road living environment (Lin et al. 2016; Sgrigna et al. 2015).

3.3. Dry deposition

When particles and gas molecules in the atmosphere pass close to a surface, they can be deposited. Plants, which have a large surface area per unit volume, are able to provide higher activity of deposition compared with manufactured smooth surface in urban areas. Rousard et al. (2013) measured dry deposition velocities on urban surfaces, such as glass and cement facing, and grass with several wind speeds. Table 3-1 shows that the dry deposition velocity of sub-micrometre particles ($<1 \mu\text{m}$) on grass is faster than on glass and cement surfaces. Moreover, particle size significantly impacts deposition. Particles that are less than $0.1 \mu\text{m}$ are more like gas molecules and are hence deposited through diffusion. Particles that are between $1 - 10 \mu\text{m}$ affect on surfaces and force the air stream to bend. Particles that are bigger than $10 \mu\text{m}$ will fall to the ground by sedimentation (Hinds 1999). Two studies modelled dry deposition processes and calculated the air pollutant removal in

Guangzhou (Jim, Chen 2008) in south China, and in Beijing (Liu, Zhu, et al. 2016) in north China. They suggested that dry deposition velocity on vegetation is higher than on wetland and water surfaces. In China, there are more fine particles deposited in the winter and more coarse particles deposited in the spring.

Table 3-1. Mean dry deposition velocity with different wind speeds on three urban surfaces (Roupsard et al. 2013).

Dry deposition velocity ($\times 10^{-5}$ m/s)			
Wind speed (m/s)	Conventional glass	Cement facing	Grass
1.3	1.7	3.1	3.3
5.0	2.8	4.9	7.0
9.9	5.6	7.6	13.1

Plants remove gaseous pollutants, such as O_3 , SO_2 , and NO_2 , through leaf stomate absorption. When the pollutants are inside the leaf, they will diffuse into intercellular spaces, then react with inner leaf surface or be absorbed by water films (Nowak et al. 2014). For particle pollution, some of the particles can be absorbed but most of them are intercepted and retained on the leaf surface. Then, the captured particles usually have three destinations: first, they are resuspended to the atmosphere; second, they are washed off by rain; third, they drop to the ground with the leaves (Abhijith et al. 2017). In dry periods, a part of particles repeatedly intercepted and resuspended depended on wind speed. Darley (1971) found that accumulative pollutants on the leaf surface will influence photosynthesis and potentially impact pollution mitigation of plants. Particles washed off by precipitation can be dissolved and transferred to the soil. In general, plants can only temporarily retain particle pollutants, as they will eventually go back to the air or the ground. However, this research will focus on the deposition process that involves particles transferring from the atmosphere to the leaf surfaces.

Dry deposition on plants is usually represented as one-dimensional vertical deposition on a conspecific layer of vegetation in a forest or field. One-dimensional deposition can be divided into: 1) transport from free air to the surface, which does not depend on the physical and chemical characters of the pollution but the turbulent movements of air; 2) across the laminar layer adjacent to the surface, which is primarily associated with the molecular diffusion of gas, turbulent diffusion, and Brownian motion of particle pollutants; 3) processes relating to surface properties (Janhäll 2015; Giardina, Buffa 2018). In urban areas, the vegetation mainly includes single trees and bushes in living areas or in urban gardens and parks, or road-side trees and vegetation barriers. The deposition process of urban vegetation needs to be modelled in more detail. In many studies (Yang et al. 2004; Liu et al. 2017; Nowak et al. 2000; Yang et al. 2019; Yang et al. 2008; Liu, Mo, et al. 2016; Donato, Contini 2014; Yan et al. 2014; Rouspard et al. 2013), the process is described as a particle passing a single leaf surface instead of a whole forest. Dry deposition velocity is the key to studying and simulating the deposition process.

3.3.1. Development of dry deposition velocity models

The term 'dry deposition velocity' is generically used to describe meteorological models of removing air pollution from the air to surfaces. It has been used to calculate the amount of air pollution mitigation through urban green spaces. The deposition models have been developed over decades by discovering and describing the relationships of different resistances between pollutants and surfaces with increasing detail.

Dry deposition velocity (V_d) (m/s) of gases and particles were defined by Chamberlain in 1953 as the deposition flux (F) (gm^{-2}/s) divided by a pollutant concentration (C) (gm^{-3}) at a reference height (equation (3-1)).

$$v_d = \frac{F}{C} \quad (3-1)$$

Historically, the reference height for airborne concentration was around 1 – 1.5 m for land surfaces and 10 – 15 m for water surfaces (Sehmel 1980a), while more recent research tended to use the height of the tree crown level (Yang et al. 2004; Liu et al. 2017; Tong et al. 2016; Zhang et al. 2017).

Slinn (1982) developed a theoretical framework to present particle dry deposition on the vegetation canopy, which included most of the deposition processes such as gravitational

settling, impaction, particle rebound, interception, and Brownian diffusion (Zhang et al. 2001). These processes were expressed by the collective term 'resistance', or more specifically, aerodynamic resistance and surface resistance of vegetation. The dry deposition velocity expressed as:

$$v_d = v_s + \frac{1}{R_a + R_s} \quad (3-2)$$

where v_s is the settling velocity, R_a is the aerodynamic resistance, and R_s is the vegetation surface resistance. In Slinn's (1982) model, R_a is given by:

$$R_a = \int_{z_1}^{z_2} \frac{dz}{K_p} \quad (3-3)$$

where K_p is eddy diffusivity for particles, d is displacement height, z is the different height above the canopy. The expression for R_a in Zhang et al.'s (2001) model does not include the canopy height. The surface resistance (R_s) is impacted by the turbulent transport and particle collection of the vegetation canopy, which expressed as:

$$R_s = \frac{U(h)}{u_*^2} \left[1 + \frac{1 - \varepsilon}{\varepsilon + \sqrt{\varepsilon} \tanh(\alpha \sqrt{\varepsilon})} \right] \quad (3-4)$$

where U is mean flow velocity at height (h), u_* is friction velocity, ε is the location-independent collection efficiency, and α is the aerodynamic extinction coefficient.

Giardina and Buffa (2018) represented deposition phenomena by an electrical analogy as V_d is the overall resistance to mass transfer. Their study described the transfer factor between the air and the surface as resistances in circuits in parallel and series on Slinn's (1982) model (see in Figure 3-1).

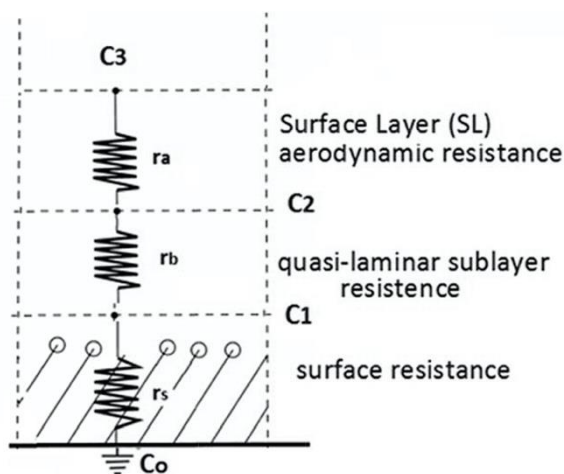


Figure 3-1 Electrical analogy for the dry deposition (Giardina, Buffa 2018).

For particle pollutants, with the influence of gravity, the resistances were defined as the reciprocal of the gravitational settling velocity (v_s) by (Slinn 1980; Hicks et al. 1987; Hanna et al. 1991; Seinfeld, Pandis 2006). Based on the assumption that r_a is 0, Seinfeld, Pandis (2006) expressed the relationship as:

$$F = \frac{C_3 - C_2}{r_a} + u_s c_2 = \frac{C_2 - C_1}{r_b} + v_s c_1 \quad (3-5)$$

where r_a is the aerodynamic resistance considering the turbulence phenomenon in the surface layer; r_b is the quasi-laminar sublayer resistance related to the diffusion phenomenon and the Brownian motion for particles. By resolving equation (3-5) and (3-1), v_d can be described as,

$$v_d = v_s + \frac{1}{r_a + r_b + r_a r_b v_s} \quad (3-6)$$

The settling velocity (v_s) increases with the particle diameter (d_p). When the diameter is less than 50 μm , v_s is calculated as:

$$v_s = \frac{d_p^2 g (\rho_p - \rho_a) C_c}{18 \mu_a} \quad (3-7)$$

where g is the gravitational acceleration, ρ_p is the particle density, ρ_a is air density, μ_a is the air dynamic viscosity, and C_c is the Cunningham factor (Seinfeld, Pandis 2006), which calculated as:

$$C_c = 1 + \frac{\lambda_a}{d_p} \left(2514 + 0.8 e^{-\frac{0.55 d_p}{\lambda_a}} \right) \quad (3-8)$$

where λ_a is mean free path of air. It is worth noting that the dependence of the dry deposition velocity on the particle diameter would increase the uncertainty of the simulation models. Although some studies (Davidson et al. 1982; Legg, Powell 1979; Wesely et al. 1985) claimed that the dry deposition velocity only changed slightly when the diameter range was between 1 μm to 10 μm , other research (Mammarella et al. 2011; Petroff et al. 2008; Gallagher et al. 1997) showed that the deposition velocity rises rapidly with the diameters larger than 1 μm . The changes are different for $\text{PM}_{2.5}$ and PM_{10} , with $\text{PM}_{2.5}$ showing a linear change with a difference of one order of magnitude. PM_{10} shows a non-linear change with the difference ranging from 10^{-2} cm/s to 10^{-1} cm/s (Petroff et al. 2008).

Venkatram, Pleim (1999) described that the dry deposition velocity of the particles mentioned above was missing the mass conservation equation, which means the turbulent transport and particle setting can be added in the vertical transport process. CSANADY (1973) described it as,

$$K_p \frac{dC}{dz} + v_s C = F \quad (3-9)$$

where K_p is the eddy diffusivity for the mass transfer of species with a concentration (C) , and v_s is the settling velocity evaluated from equation (3-7). Then, v_d can be integrated based on the equations above to give:

$$v_d = \frac{v_s}{1 - e^{-[r(z)v_s]}} \quad (3-10)$$

where $r(z)$ is the total resistance to the transport, which can be calculated as a function of d_p and height z .

Hinds (1999) believed that that aerodynamic resistance is generally smaller than the other types of resistances for particles less than 10 μm diameter, so the deposition velocity is higher than the settling velocity for PM_{10} and $\text{PM}_{2.5}$ (Petroff et al. 2008). Moreover, Janhäll (2015) reported that super-micrometre particles ($<1 \mu\text{m}$) have a higher deposition velocity with a larger size, while the velocity of sub-micrometre particles ($>1 \mu\text{m}$) declines with size. For particles less than 1 μm diameter, Vong (2010) suggested that the deposition velocity depended on the atmospheric stability of the boundary layer, which described as:

$$v_d = Av_s d_p \left[1 + \left(-\frac{300}{L} \right)^{\frac{2}{3}} \right] \quad (3-11)$$

where L is the Monin-Obukov length; A is the empirical constant, which is 0.63 for coniferous forest (Vong et al. 2010), 1.35 for broadleaf forest (Gallagher et al. 1997), and 0.2 for grass.

Giardina, Buffa (2018) proposed a new method to describe the dry deposition velocity of particles that are larger than 1 μm based on an electrical analogy. Wesely (1989) proposed a three distinct pathways of mass transfer for gaseous dry deposition model. Figure 3-2 shows the quasi-laminar sublayer resistance was presented by a parallel circuit, which r_{db} represented the effect of Brownian diffusion, r_{ii} was the simplex inertial impaction regime for particles, and series connection of r_{ti} and r_{ii} showed the mutual impact between the

inertial effect (r_{ii}) and the turbulent effect (r_{ti}). Based on this method, v_d can be described as,

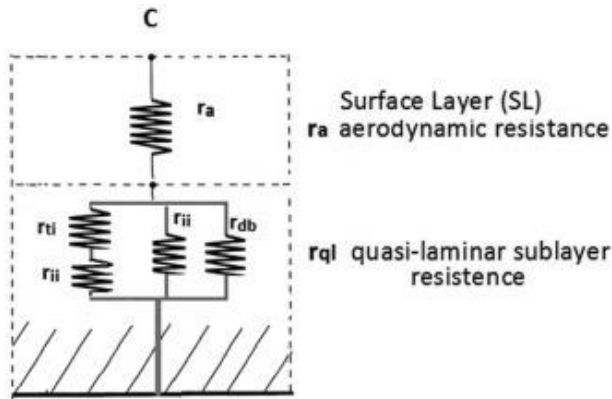


Figure 3-2 The new method for the parametrization of the deposition velocity for particles (Giardina, Buffa 2018).

In this method, by using the Monin–Obukhov similarity theory that has been often used in many dry deposition models (Wesely, Hicks 1977; Slinn et al. 1978; Voldner et al. 1986; Hanna et al. 1991; Maryon et al. 1996), r_a , r_{db} , r_{ii} and r_{ti} were evaluated as,

$$r_a = \frac{1}{ku_*} \left(\ln \frac{z}{z_o} - \Psi_h \right) \quad (3-12)$$

Where u_* is the friction velocity based on the intensity of atmospheric turbulence; z_o is the surface roughness, which (Giardina, Buffa 2018) proposed that the range of roughness for this model can be 0.03m to 6m; and k is the von Karman constant. Ψ_h can be calculated as (Brandt et al. 2002),

$$\Psi_h = -5 \frac{z}{L} \quad \text{when } \frac{z}{L} > 0 \quad (3-13)$$

$$\Psi_h = e \left\{ 0.598 + 0.39 \ln \left(-\frac{z}{L} \right) - 0.09 \left[\ln \left(-\frac{z}{L} \right) \right]^2 \right\} \quad \text{when } \frac{z}{L} < 0 \quad (3-14)$$

Where L is the Monin-Obukov length, calculated as,

$$L = \frac{u_*^3 c_p \rho T}{kgH} \quad (3-15)$$

Where c_p is the heat at constant pressure, T is the average temperature in surface layer, H is the sensible heat.

Resistance of Brownian diffusion impact r_{db} was evaluated as,

$$r_{db} = \frac{K_B T_a C_C}{u_* v_a 3\pi \mu_a d_p} \quad (3-16)$$

Where v_a is the air kinematic viscosity, K_B is the Boltzmann constant, T_a is the absolute temperature, μ_a is the air dynamic viscosity, C_C is the Cunningham factor.

The inertial impact r_{ii} was evaluated as,

$$r_{ii} = \frac{1}{u_* \left(\frac{S_t^2}{S_t^2 + 1} \right)} \quad (3-17)$$

S_t is the Stokes number, which was,

$$S_t = \frac{v_s u_*^2}{g v_a} \quad (3-18)$$

The turbulent impact r_{ti} was described as,

$$r_{ti} = \frac{1}{u_* m \left(\tau \frac{u_*^2}{v_a} \right)^n} \quad (3-19)$$

Which τ is the particle relaxation time for particles, constant n is 3 (Giardina, Buffa 2018).

So, based on the equations (3-12)(3-16)(3-17)(3-19), dry deposition velocity v_d can be calculated as,

$$v_d = \frac{v_s}{1 - e^{-\left\{ v_s \left[r_a + 1 / \left(\frac{1}{r_{db}} + \frac{1}{r_{ii}} + \frac{1}{r_{ii} + r_{ti}} \right) \right] \right\}}} \quad (3-20)$$

In dry deposition models, the vegetation surface plays an important role in absorbing particle pollutants, and it is closely associated with different types of resistances. Hence, describing their relationship with more realistic details would increase the veracity when estimating air pollution mitigation. Compared with Hinds's (1999) and Slinn's (1982) model, Giardina and Buffa (2018) considered more detailed and realistic aerodynamic resistances. A main improvement was the surface resistance along three pathways at the sublayer to the surface layer of the vegetation canopy. It represented Brownian diffusion motion and impaction phenomena by a parallel circuit instated of a whole series circuit, as turbulent diffusion and Brownian motion of particles were simultaneously acted on the quasi-laminar sublayer as well as interaction between each other. This model was consistent with the

physical behaviour exhibited by the particles during the deposition process. That would provide more precise results for studying and simulating the impacts of green spaces on air quality improvement. However, even though the new model improved the description of the laminar sublayer resistances, it is still unable to represent all of the extremely complex processes involved in pollution deposition. Hence, there is no internationally common standard for deposition velocity measurements because of the experimental uncertainty (Sehmel 1980a). The next section will discuss the measurements that have been made by different international laboratories.

3.3.2. Modelling applications of dry deposition in urban planning research

The last section reviewed the different modelling approaches of deposition velocity to discuss the developments on the resistances model that more accurately represent the relationship of turbulent diffusion and Brownian motion. This section will discuss the applications of dry deposition on vegetation for air pollution removal. In many sustainable urban environment studies (Sehmel 1980a; Slinn 1982; Baldocchi et al. 1987; Wesely et al. 1985; Cabaraban et al. 2013; Yang et al. 2004; Nowak 1994; Currie, Bass 2008; Hirabayashi et al. 2011; Zhang et al. 2016; Liu, Zhu, et al. 2016; Huang et al. 2016; Han et al. 2017), dry deposition has been used to calculate the effects of air pollutant mitigation by vegetation surfaces. More specifically, these studies mainly aim to develop urban green spaces by quantifying the dry deposition process, comparing different environment models, and evaluating various urban green infrastructures (see Table 3-2). Moreover, dry deposition can be applied into many other environmental models to evaluate different urban green plans and improve the living environment, such as UFORE, urban forest effects model (also known as i-Tree) (Hirabayashi et al. 2011), RANS, Reynolds-Averaged Navier-Stokes model (Ji, Zhao 2014), Regional Atmospheric Modeling System-Models-3 Community Multiscale Air Quality (RAMS-CMAQ) (Han et al. 2017), and the Chem nested-grid model (GEOS) (Zhang et al. 2012). This section will review the dry deposition models that were used in green planning research for various purposes in recent decades.

3.3.3. Dry deposition velocity used to quantify pollutants removal

One of the common ways of using dry deposition models in urban sustainable research is to quantify the pollution flux in certain areas. This could not only help to locate air quality issues but also to understand the effect of different green infrastructures or urban forms for improving air quality. Numerical simulations of dry deposition are able to provide the data for ecosystem services valuation, which means they can guide future urban planning for win-win opportunities between human activities and the environment (Farber et al. 2002).

For quantifying the effect of urban vegetation on air quality, many studies calculated the dry deposition flux based on a 'resistance' model (Slinn 1982; Zhang et al. 2001; Giardina, Buffa 2018). Huang et al. (2016) analysed seasonal and interannual changes on stomatal and non-stomatal dry deposition of ozone in Texas. They showed that the dry deposition velocity of ozone in the forests dropped during periods of drought. The deposition velocity was calculated as:

$$v_d = \frac{1}{R_a + R_b + R_c} \quad (3-21)$$

where R_a is aerodynamic resistance, R_b is quasi-laminar resistance, and R_c is overall canopy resistance. By using dry deposition model in 48 states of the USA, Nowak et al. (2006) estimated that there were 711,000 metric tons of air pollution (CO , NO_2 , O_3 , PM_{10}) mitigated by urban trees each year. They proposed that an urban vegetation canopy cover can be used as a feasible strategy for air quality improvement. Yang (2004) established characteristics of urban forests in Beijing by analysing satellite images and data from field surveys. They examined the effect on particle pollutants collection. Their analysis showed 1261.4 tons of pollutants were removed in one year. Their dry deposition velocity calculation was based on Slinn's (1982) model for resistances. Yang (2008) also used a dry deposition model of resistance to estimate air pollution (O_3 , NO_2 , SO_2 , PM_{10}) removal by green roofs in Chicago. 14% of the total amount of particle pollutants were found to have been removed. Similarly, the resistance expression of deposition velocity was used in Zhang et al.'s (2012) study to simulate nitrogen deposition in the US. As we can see from the above studies, R expressions were commonly used for simulations and analysis based on vegetation canopy surfaces. The reasons are that they describe a more complete deposition

process, focus on the relationship between pollutants and leaf surfaces, and cover more types of pollutants.

Another expression of dry deposition velocity was also used in some research. Liu (2016) and Zhang (2017) developed models to quantify particle dry deposition velocity and fluxes on different surfaces, such as urban forests, wetlands, and water areas. The studies showed that the forests had the highest deposition velocity among the three surfaces, and collected more coarse particles (PM_{10}) than fine particles ($PM_{2.5}$). Moreover, on the leaf level, water washing and scanning electron microscopy methods show that urban forests have a better capability of fine particle collection (Zhang et al. 2017). For the quantitative analysis of particle pollutant removal, the dry deposition velocity of vegetation canopy (v_d) was calculated in these studies as (Petroff et al. 2008; Liu, Zhu, et al. 2016):

$$v_d = v_s + V_{IN} + V_{IM} \quad (3-22)$$

where V_{IN} is the collection velocity associated with the interception process and V_{IM} is collection velocity associated with the impaction process, which is based on Slinn's (1982) and Zhang et al. (2001)'s model. The difference is that Slinn (1982) used resistances to express the whole deposition processes, but equation (3-22) mainly focuses on interception and impaction as Brownian diffusion and rebound had limited impact for their studies' aim (Liu, Zhu, et al. 2016; Zhang et al. 2017). Zhu et al. (2016) also calculated the dry deposition flux of particle pollutants on wetland surfaces. They concluded that dry deposition was higher at 10 m during dry periods and during the night time. Similar equations (Petroff et al. 2008) were used for deposition velocity calculation, which involved the gravitational settling speed based on the particle diameters, and the total transfer velocity in the constant-flux layer and dry deposition layer. The transformative expressions have been applied in researches with more specific aims, such as focusing on fine particles only (Zhang et al. 2017), and analysing water and wetland surfaces (Liu, Zhu, et al. 2016). Therefore, they did not need to consider the whole deposition process, but only a part of it. These studies also showed that the dry deposition models have a good level of adaptability.

3.3.4. Combination of dry deposition model and other atmospheric simulation models

Different atmospheric simulation models are used with dry deposition model to calculate the amount of air pollution on various scales and in various regions. The Regional Atmospheric Modelling System (RAMS) is a multipurpose numerical prediction model for simulating atmospheric circulations, which is commonly used for operational weather forecasting, air quality regulatory applications, and other related research (Cotton et al. 2003). The Community Multiscale Air Quality (CMAQ) modelling system was developed by the US Environmental Protection Agency (US EPA) for simulating multiple air quality situations on different scales (Carter 1999). Han et al. (2017) combined the two models to simulate dry deposition of reactive nitrogen (N) and quantify dry N deposition over China. The dry deposition velocity in RAMS-CMAQ was calculated as (Nenes et al. 1999; Binkowski, Shankar 1995; Tremback, Kessler 1985):

$$v_d = \frac{1}{r_a + r_b + r_c} \quad (3-23)$$

where r_a is the aerodynamic resistance, r_b is the quasi-laminar boundary layer resistance, and r_c is the canopy resistance. This is a simplified version of deposition velocity from Sehmel (1980)'s model, in which the settling velocity of nitrogen was not considered. By comparing the simulated dry N deposition fluxes and observations of ground-based networks and satellite monitoring, Han et al. (2017)'s study clearly presented the fluxes of N components in different regions in China, which were able to inform more targeted urban policies and solutions.

The dry deposition model can also be combined with the Reynolds-Averaged Navier-Stokes (RANS) model based on computational fluid dynamics (CFD). Ji and Zhao (2014)'s research developed a CFD model to simulate the two main effects of trees on distributions of particle pollutants around buildings, which are airflow reduction around the trees and dry deposition by turbulent diffusion. Although dry deposition velocity calculation was not discussed deeply in their study, they still discussed the potential of a more accurate numerical simulation of dry deposition flux by combination with a CFD model.

Table 3-2 References list of modelling applications of dry deposition in urban planning researches.

Reference	Location	Pollutants	Calculation methods	Calculation duration	Year Calculated	Type of UGI	Aim	Dry deposition efficiency
(Sehmel 1980a)		Particle and gas	DD			VC	Dev	
(Slinn 1982)		PM	DD, WT			VC	Dev, Qua	
(Balducchi et al. 1987)		O ₃	DD			VC	Dev, Qua	g
(Wesely 1989)	United States	SO ₂ , O ₃ , NO _x , HNO ₃	DD			VC	Qua	
(Nowak 1994)	Chicago	CO, NO ₂ , O ₃ , PM ₁₀ , SO ₂	DD			UF	Eva	
(Zhang et al. 2001)	North America	PM	DD			VC	Dev, Qua	
(Yang et al. 2004)	Beijing	NO ₂ , O ₃ , PM ₁₀ , SO ₂	DD	Y	2001-02	UF	Qua	

(Nowak et al. 2006)	United States	O3, PM10, NO2, SO2, CO	DD	Y	1994	UF	Qua, Eva	g
(Yang et al. 2008)	Chicago	NO2, O3, PM10, SO2	DD	Y		GR	Qua	
(Currie, Bass 2008)	Toronto	NO2, SO2, CO, PM10, O3	UFORE			GR, GW	Qua, Com	
(Northern Research Station 2009)	Mainly	All types of air pollution	DD			UF	Eva	
(Hirabayashi et al. 2011)	Baltimore	CO, NO2, O3, PM10, and SO2	DD ^{UFORE}				Qua, Ana	
(Zhang et al. 2012)	United States	Nitrogen (N)	DD	Y	2006-8	VC	Qua, Com	
(Ji, Zhao 2014)	China	PM	DF, RANS, CFD			UF	Eva	g
(Vet et al. 2014)	America, much of Asia, Africa, Oceania, polar regions,	Gaseous pollutants, mainly S&N	Dry deposition and wet deposition		2005-7		Pol, Com, O	

	all of the oceans							
(Huang et al. 2016)	Texas	ozone	DD	Y	2006 & 2011	UF	Qua, Eva	f
(Liu, Zhu, et al. 2016)	Beijing	PM	DD	Y	2014	UF, W	Com	
(Zhu et al. 2016)	Beijing	PM	DD			W	Eva	
(Zhang et al. 2017)	Beijing	PM _{2.5}	DD ^{ECT} , DD TM			UF, W	Qua, Com	
(Han et al. 2017)	Northeast China, North China	Nitrogen (N)	DD ^{RAMS-CMAQ}	Y	2010-14		Qua	f
(Giardina, Buffa 2018)		PM	DD TM	Y	2018		Qua	

¹. Calculation methods: DD, dry deposition; ECM, eddy correlation method; TM, multi-layer model; UFORE, urban forest effects model (i-Tree); WT, wind-tunnel; DF, drift flux model; RANS, Reynolds-Averaged Navier-Stokes model; RAMS-CMAQ, Regional Atmospheric Modeling System-Models-3 Community Multiscale Air Quality

². Aim of paper: Qua, quantification dry deposition process; Dev, development dry deposition model; Com, comparison with different environmental models; Eva, evaluation different UGI; Ana, sensitivity analysis; Pol, comparison of pollution factors; O, other

3. Type of UGI: VC, vegetative canopies; UF, urban forests or trees; GF, green roof; GW, green wall; W, wetland
4. Dry deposition efficiency: p, poor; f, fair; g, good

3.3.5. UFORE and EMEP MSC-W model

With the increasing awareness of environmental quality improvement in cities, investigation and quantification of the benefits of urban trees has been receiving more attention from academia. However, evaluation and estimation of the dry deposition efficiency of vegetation on particle pollutant removal is a complicated process, owing to many uncertain factors involved and multiple interactions between these factors. As discussed above, dry deposition models are often used for estimating pollution mitigation by plants (Sehmel 1980a; Slinn 1982; Baldocchi et al. 1987; Wesely et al. 1985; Cabaraban et al. 2013; Yang et al. 2004; Nowak 1994; Currie, Bass 2008; Hirabayashi et al. 2011; Zhang et al. 2016; Liu, Zhu, et al. 2016; Huang et al. 2016; Han et al. 2017). Two computer programs based on a deposition model have been developed and applied internationally for large regional areas and urban forests (Guidolotti et al. 2016), which are UFORE and EMEP MSC-W model.

The Urban Forest Effects (UFORE) model (also known as i-Tree) was developed by The United States Department of Agriculture (USDA) Forest Service in the late 90s (Guidolotti et al. 2016; Hirabayashi et al. 2012; Nowak, Crane 1998; Nowak et al. 2008). It aims to quantify urban forest structure and functions, which include four parts: anatomy of the urban forest, biogenic volatile organic compounds (VOCs) emissions, carbon storage and sequestration, and dry deposition of air pollution. UFORE-D calculates the hourly pollutant (O_3 , SO_2 , NO_2 , CO_x , PM) mitigation for urban and non-urban area (Nowak, Crane 1998). Four types of input data are needed for the UFORE-D model, which are field type, leaf areas, meteorological data, and pollution concentration. Leaf areas index that used in UFORE model are measured by sampling aerial photographs from Lovett (1994). With precise inputs in specific environmental conditions, this model is able to provide accurate outputs (Nowak et al. 2006). However, the calculation of particle deposition rates is oversimplified, as only leaf and bark areas are considered as the variables (Nowak et al. 2014).

The EMEP MSC-W model, developed by the European Monitoring and Evaluation Programme and the Meteorological Synthesizing Centre West, is a chemical transport model that is generally used for European air pollution policy assessments (Guidolotti et al. 2016). The EMEP MSC-W model assumes that particle dry deposition occurs on a uniform canopy

surface, which means leaf area and species are not considered (Simpson et al. 2012). The reason is that this model has mainly been used for regional and global scales. For providing a consistent description from regional to local scales (e.g. city level or street level), the EMEP MSC-W model has been downscaled to a 5 km grid based on the Gaussian plume modelling method (Rolstad Denby et al. 2020). However, Dore and Vidič (2012) suggested that the low quality and resolution of the inputs on smaller scales could limit the model accuracy. Hence, this model is not an appropriate tool for tree-level simulation.

These two models calculate PM deposition flux by different approaches. Dry deposition velocity of particles in UFORE has been estimated based on common tree species and various wind speeds to allow the model application at tree level. For instance, average deposition velocities of PM_{2.5} were summarised in Table 3-3 from literature (Beckett, Freer-Smith, Gail Taylor 2000; Freer-Smith et al. 2004; Pullman 2009). Then, the deposition velocity was adjusted by leaf area indices and calculated as:

$$v_d = v_{d,PM2.5} \times LAI \quad (3-24)$$

Table 3-3 Summary of average dry deposition velocities (cm/s) of PM_{2.5} based on different wind speeds from the literature per unit of leaf area (Hirabayashi et al. 2015).

Species	Wind speed (m/s)			
	1	3	6	10
Quercus petraea		0.83	1.76	
Alnus glutinosa		0.13	0.17	
Fraxinus excelsior		0.18	0.38	
Acer pseudoplatanus		0.04	0.20	
Psuedotsuga menziesii		1.27	1.60	
Eucalyptus globulus		0.02	0.03	
Ficus nitida		0.04	0.10	
Pinus nigra	0.13	1.15		28.05
Cupressocyparis x leylandii	0.08	0.76		12.20
Acer campestre	0.03	0.08		0.57
Sorbus intermedia	0.04	0.39		2.11

Populus deltoides	0.03	0.12	1.18
Pinus strobus	0.01		
Tsuga canadensis	0.02		
Tsuga japonica	0.01		
Picea abies	0.02		

The EMEP MSC-W model calculates the deposition velocity based on the multi-resistance model (Slinn 1982) by assuming that all particles are absorbed on a uniform vegetation surface. In this model, deposition velocity depends on air density, dynamic viscosity, the convective velocity scale of the Planetary Boundary Layer, and particle size (Scire et al. 2000). Moreover, the bounce-off of coarse particles is considered by both models. Guidolotti et al. (2016) quantified the amount of particle pollutant removal in the same area by both models, the results of which showed very similar trends for the pollution concentration. The different removal rates might be caused by the fact that the UFORE model included leaf area index but the EMEP MSC-W model did not.

3.4. Conclusion

Urban air quality improvement is one of the significant environmental benefits that is provided by green spaces in our cities. Particulate matter is one of the critical pollution issues endangering people's health. The surfaces of trees and other plants can absorb particle pollutants by the dry deposition process. To study the effect of dry deposition on air pollutant removal, an expression of deposition velocity is important.

The dry deposition velocity of different pollutants and surfaces has been studied and evaluated over many years. The theoretical framework to present particle dry deposition on a vegetation canopy had been developed by Slinn in 1982. Expressions based on

aerodynamic resistance and vegetation surface resistance were later introduced. In Slinn's (1982) model, gravitational settling, impaction, particle rebound, interception, and Brownian diffusion were expressed in equations as a whole dry deposition process. Over the years, this model has been developed with increasing detail to adapt it to various research purposes and apply it in conjunction with different meteorologic and dynamic models. In the latest development by Giardina and Buffa (2018), a parallel circuit analogy was used to describe the relationship between Brownian diffusion motion and impaction phenomena. Especially for particle pollutants, they occur individually in the quasi-laminar sublayer and interact together with aerodynamic resistance in the surface layer. This may improve the accuracy on quantifying the rate of particle pollutant mitigation. The numerical simulation of the dry deposition model in many studies reviewed in this chapter support a clear understanding of air quality improvement by vegetation and have guided green strategies for sustainable urban planning. In addition, the dry deposition model can be applied with atmospheric simulation models, such as CFD models, which can help to quantify pollution removal more precisely by including different effects of the atmosphere.

However, because the complex effects of the fluid dynamic process on deposition flux, and a lack of complete experimental data that can cover all possible scenarios, it is still a limited possibility to represent and simulate the dry deposition process by a single modeling approach. To increase the modelling accuracy, the deposition process needs to be calculated based on different situations. The existing models that have been reviewed in this chapter are only valid for specific conditions, such as for certain pollutant types or deposition surfaces. Hence, this research is focused on developing a dry deposition model to evaluate particle pollutant mitigation by urban trees in near-road communities. More specifically, this model will mainly simulate the rate of particle removal by the tree leaf surfaces in a certain area. Moreover, the most common used computer programs (UFORE and EMEP MSC-W model) that are based on the dry deposition model have their limitations. For instance, the UFORE model simply calculates particle removal based only on leaf area. The effects of trees on air flow and pollution concentration by times are not considered in this model. The EMEP MSC-W model uses Slinn's (1982) model to quantify pollutant removal, but includes more details in the deposition process. However, first, it does not consider different leaf area indexes by assuming a uniform canopy surface for the whole

simulation area. Second, this model mainly simulates pollutant removal on large scales (regional and global levels). In mid-scale scales (street or tree levels), it can only provide low accuracy results. Third, the outcomes rarely compared with field measurement.

To summa up, the UFORE model is lack of considerations of the air flow effects of on dry deposition velocity. The EMEP MSC-W model cannot estimate pollution removal at street or tree level and does not consider the effect of tree species on leaf areas. Moreover, they are lack of comparation with field measurements. This research will try to cover these deficiencies by providing a green planning model for mid-scale urban areas. This green planning model, which will be introduced in the following chapter, integrates an atmospheric simulation model and a dry deposition model to quantify particle pollution removal by current green plans or to predict the effect of future plans. To bring more considerations on the changes of air flows, the computational fluid dynamic model will be applied to simulated the changes of air flow caused by different tree densities and urban forms. Moreover, the leaf area will be added in the dry deposition model as one of the crucial variables, which can be modified by numbers and species of trees. In this study, the results of this model will be compared with field measurements in a mid-scale residential area.

Chapter 4. A green planning model to improving air quality in mid-scale urban residential areas – model setup

Notation

	The amount of PM_{10}	
Q	removed by a certain area of green space in a certain time period	g
L	The total leaf area	m^2
T	The time period	s
F	The pollutant flux	$g/m^2/s$
C	The concentration of the particle pollutant in the air at zone level	$\mu g/m^3$
V_d	The dry deposition velocity of PM_{10}	cm/s
R_a	The aerodynamic resistance	
$u(z)$	The wind speed at height z	m/s
u_*	The frictional velocity	m/s
k	The von Karman's constant	
d	The displacement length	m
z_0	The roughness length	
L	The Monin–Obukhov stability length	
ϕ_m	The dimensionless ϕ_m stability function for momentum	
X	The dimensionless factor	
R_b	The resistance of molecular scale diffusive transport at quasi-laminar boundary layer	
k	The von Karman constant	

S_c	The Schmidt number	
P_r	The Prandtl number	
V_g	The gravitational settling velocity	m/s
ρ	The density of particles	kg/m ³
d_p	The particle diameter	m
g	Gravitational acceleration	
θ	Dynamic viscosity coefficient of air	Pa*s = kg/m/s
C	Rectification of small particles	
λ	The mean free path of a moving particle	nm

4.1. Introduction

With the obvious quickening of urbanization, road traffic has become one of the main sources of air pollution (Fenger 2009). The largest pollution concentrations are usually monitored at the street level (Karttunen et al. 2020). This decreases the well-being not only for people who walk and cycling in the street, but also for residents who live in the near-road areas. Urban green spaces have been proposed as a solution in previous chapters to improve air quality by removing pollutants by dry deposition.

The question ‘what is an optimum green plan to efficiently improving air quality in mid-scale near-road residential areas?’ is asked in this research. The term ‘mid-scale’ means urban areas that from a hundred to several thousand square metres in size, especially the residential areas with busy traffic and high air pollution concentrations. To answer the question, a green planning model will be needed to simulate various plans and suggest an

appropriate plan. Dry deposition process has been studied and used to estimate the amount of pollution removal by vegetation surfaces over decades. The previous chapter discussed the applications of dry deposition in environmental studies and reviewed two commonly used urban green planning programs. The analysis highlighted research gaps around the methods of quantifying pollution mitigation in mid-scale urban areas. It was suggested that a numerical simulation model based on the integration of dry deposition model and atmospheric simulation model may be able to cover these gaps to a certain extent. In this integrated model, an atmospheric simulation model, such as a CFD model, can simulate the changes of air flow caused by different crown densities or urban forms. The dry deposition model set up based on the Slinn's (1982) 'resistance' model of the dry deposition velocity on the vegetation canopy. Moreover, the equations that describe turbulent diffusion and Brownian motion of particles at the sublayer are developed based on Giardina and Buffa's (2018) studies.

One key aim of this chapter is to develop an integrated model as a green planning model to estimate the effect of dry deposition on air quality improvement, and propose optimum green plans for mid-scale urban areas with high pollutant levels. First, a generic framework of this model will be introduced to present the integration of the atmospheric simulation model and dry deposition model. This framework will clarify the data flow in the model. Then, this chapter will present the method of applying the integrated simulation model following three steps, which are 1), identification of land types by local microclimate zones; 2), collection of meteorological and air quality data; 3), calculation of air pollution removal.

4.2. Framework of the green planning model

The purpose of developing a green planning model is to determine the optimum numbers of trees and locations to plant these trees and appropriate tree species in mid-scale residential area, so that more particle pollutants can be removed from the air to improve the urban

living environment. To make sure the model will serve this goal, a main part of the model must be to quantify the amount of particle pollution removed in a mid-scale urban area. Dry deposition models, which have been reviewed in chapter three, are used to calculate the PM pollutant mitigation by urban trees. Figure 4-1 shows the system dynamic (SD) model of dry deposition process integrated with the Fluid Dynamics model (CFD) model as a whole model for estimating particle pollution mitigation. The different plans differ in terms of aspects such as the size of green cover and different locations of plants and various tree types. Three main parts of this integrated simulation model are presented in order to explore an appropriate green plan for a mid-scale residential area by quantifying the amount of particle pollutants mitigation. Step one is identification of land types, which aims to have a general understanding of the study area that is going to be analysed by the model, such as building height and location, tree species and number, land types. Then a spaces model can be set up and be used for the CFD model. The second step is to collect meteorological data and PMs pollution concentration in the study area. The meteorological data will be used to set up the CFD model boundary, so it can predict air flows. The PMs concentration will be entered into the dry deposition SD model as source pollution to estimate particle pollutants mitigation by trees in the study area in step three. The software of SD model and CFD model are Vensim and ENVI-met, respectively.

4.2.1. Vensim

The system dynamic (SD) modelling, which is based on the non-linear causal thinking, has been used to convert the dry deposition system into a dynamic simulated model. This method was first presented by Forrester (1968) as a simulation method for object-oriented feedback. He suggested that users are able to acquire a better understanding of the dynamic behaviour over time by using SD model. More specifically, it can be used to understand strategic principles of complex dynamic systems for better description of dynamic behaviour (Abadi et al. 2015). It is able to provide the flexibility of reading and changing variables in the dynamic process, which can be used to evaluate different scenarios. Moreover, it has been presented that this method is specific for the detection system dynamics and drawing feedback process (Sternam 2002). Many physical systems, such as dry deposition process, are presented by differential equations that are time

related. Systems dynamics software can be used to model the differential equations of dry deposition process. Compared with other software (e.g., Sphinx SD, OptiSim, Systems Dynamics, Simile, etc.), Vensim PLE has the fewest restrictions in the free license, which is good for academic use in terms of ease of use, power, and versatility (Widmark 2012). The Vensim software, which can depict, simulate, analyse, and optimize dynamic systems, is used in this research (Wan et al. 2015; Z. Zhang et al. 2014; Chen, Gao 2011; Li et al. 2015). Therefore, in step three, a SD model that describes the dry deposition equations will be set up in Vensim PLE to estimate the amount of particle pollution removal in a certain time.

4.2.2. ENVI-met

Moreover, to simulate how various green plans would influence the local air flow, a Computational Fluid Dynamics model (CFD) is needed to simulate the wind speed for the dry deposition model. It is important to understand changes of air flow around buildings in various urban forms. This could help to optimise the location for plants to remove more air pollution. CFD has great potential for modelling air flow and pollutant dispersion around buildings. However, it is hard to predict air flow accurately due to the complex interaction between atmospheric flows and flows around buildings (Tominaga, Stathopoulos 2013). As Stathopoulos (2002) concluded in *Computational Wind Engineering (CWE)*: *"In spite of some interesting and visually impressive results produced with Computational Wind Engineering, the numerical wind tunnel is still virtual rather than real. Its potential however, is extremely high and its progress should be monitored carefully."* ENVI-met is a 3D computational fluid dynamics (CFD) model developed by Bruse and Fleer (1998). It is based on the Reynolds Averaged Navier-Stokes (RANS) equations, and has obstacle resolving in non-hydrostatic micro scale with advanced parameterizations for the simulation of interactions between urban surfaces, vegetation, and atmosphere (Hofman et al. 2016; Bruse, Fleer 1998). In other words, it is particularly good at simulating the effects of plants on the atmosphere in a built environment at the mid-scale urban environment. In this research, ENVI-met is used to present wind speed changes in research areas with various levels of vegetation. For example, ENVI-met can simulate wind speeds in a residential area with buildings and trees, which will provide wind speed data for the dry deposition model to simulate the PM concentration and pollutant removal resulting from different green plans.

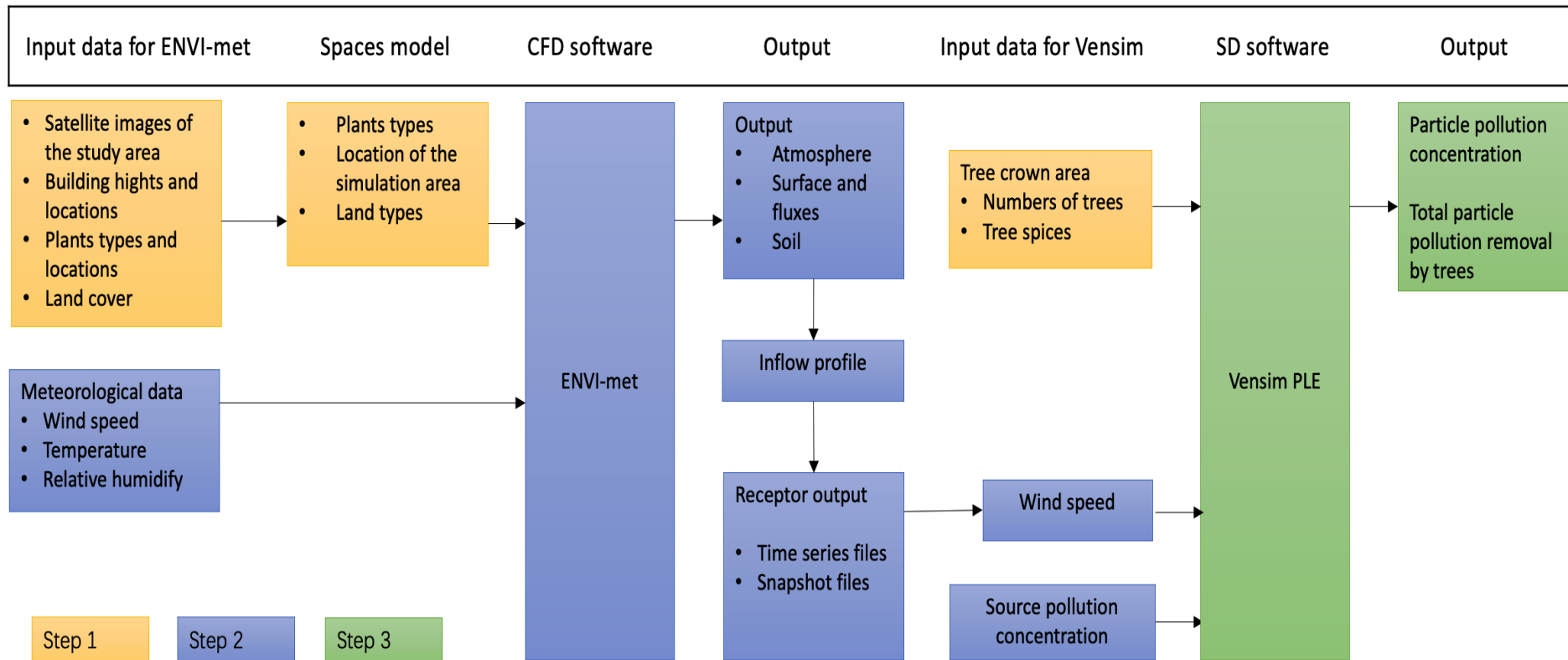


Figure 4-1 A generic framework of the green planning model and its data flow.

4.3. Application of the integrated simulation model

4.3.1. Step 1: Identification of land types by local microclimate zones

Understanding different urban forms is significant for developing optimum green plans for mid-scale urban environments. The size range of mid-scale urban areas is from hundreds of square meters to several square kilometres. Stewart (2011) presented “local climate zones (LCZ)” to classify urban types based on surface cover, structure, material, and human activity. Each LCZ considers different buildings sizes and distributions combined with different types of green covers in the land. It can be applied in this research to define land features effectively and thus develop an appropriate green plan for each selected zone. However, the LCZ is originally applied in urban heat island research so it also includes thermal differentiation parameters. This research will mainly focus on building types with different green covers, but because the thermal conditions have a limited impact on the dry deposition process (Sehmel 1980b). So, they will not be discussed in this study. There are two main LCZ types (see Figure 4-3): building types and land cover types. Building types (Oke, 2004) are described as building height, density, material, function, land cover, and green infrastructures, which are mainly used to analyse the study areas and to enter into the CFD model for with atmospheric simulation. Land cover types, which are complements to building types, introduced landscapes (no buildings) with different density of trees, green types, land covers (soil, sand, rock, desert, agriculture, water, and etc), and land faction.

Satellite imagery and field surveys will be needed to identify zone types and to set up the CDF model in ENVI-met. Satellite images can be found from lbsyun.baidu.com for China or Google Earth for other countries. Such images clearly show the distribution of buildings, green covered areas, and traffic information to give a general background of the study area for establishing a CFD model. Firstly, this research will not analyse a whole city, but will focus only on mid-scale urban areas. Therefore, a stratified random sampling method (Nowak 1994; McPherson 1998) is used for its advantages in the following areas 1) gains precision over simple random sampling method; 2) estimates each stratum separately; 3) cuts down the sampling cost and time (Yang et al. 2004). In this part, field surveys might be

required to locate the research areas and estimate the area types more accurately. The 'local climate zone' concept, introduced earlier, could help to classify different land use types during the field surveys. Local climate zones contain all classes that emerge from the logical division of the landscape universe, and the classification is based on regional surface cover, structure, material, and human activity (Stewart, Oke 2012). In this research, mid-scale residential areas will be selected from satellite maps on the basis of the field survey results. These areas will then be used to build spaces models using the ENVI-met software. Figure 4-2 shows the spaces model in ENVI-met based on the satellite imagery and information of land types in a study area.



Figure 4-2 A spaces model (downward side) of a mid-scale residential area based on the satellite image (upward side) in Taiyuan by ENVI-met.

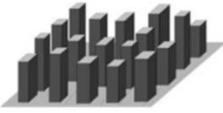
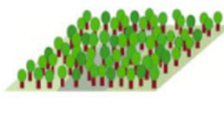


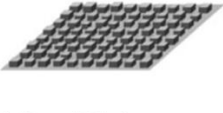
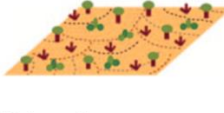
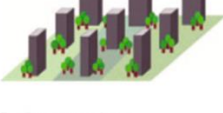

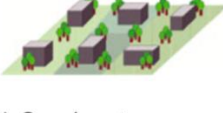

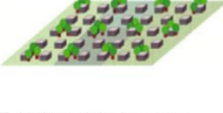

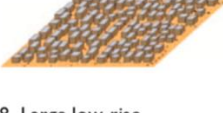




Built types	Definition	Land cover types	Definition
1. Compact high-rise 	Dense mix of tall buildings to tens of stories. Few or no trees. Land cover mostly paved. Concrete, steel, stone, and glass construction materials.	A. Dense trees 	Heavily wooded landscape of deciduous and/or evergreen trees. Land cover mostly pervious (low plants). Zone function is natural forest, tree cultivation, or urban park.
2. Compact midrise 	Dense mix of midrise buildings (3–9 stories). Few or no trees. Land cover mostly paved. Stone, brick, tile, and concrete construction materials.	B. Scattered trees 	Lightly wooded landscape of deciduous and/or evergreen trees. Land cover mostly pervious (low plants). Zone function is natural forest, tree cultivation, or urban park.
3. Compact low-rise 	Dense mix of low-rise buildings (1–3 stories). Few or no trees. Land cover mostly paved. Stone, brick, tile, and concrete construction materials.	C. Bush, scrub 	Open arrangement of bushes, shrubs, and short, woody trees. Land cover mostly pervious (bare soil or sand). Zone function is natural scrubland or agriculture.
4. Open high-rise 	Open arrangement of tall buildings to tens of stories. Abundance of pervious land cover (low plants, scattered trees). Concrete, steel, stone, and glass construction materials.	D. Low plants 	Featureless landscape of grass or herbaceous plants/crops. Few or no trees. Zone function is natural grassland, agriculture, or urban park.
5. Open midrise 	Open arrangement of midrise buildings (3–9 stories). Abundance of pervious land cover (low plants, scattered trees). Concrete, steel, stone, and glass construction materials.	E. Bare rock or paved 	Featureless landscape of rock or paved cover. Few or no trees or plants. Zone function is natural desert (rock) or urban transportation.
6. Open low-rise 	Open arrangement of low-rise buildings (1–3 stories). Abundance of pervious land cover (low plants, scattered trees). Wood, brick, stone, tile, and concrete construction materials.	F. Bare soil or sand 	Featureless landscape of soil or sand cover. Few or no trees or plants. Zone function is natural desert or agriculture.
7. Lightweight low-rise 	Dense mix of single-story buildings. Few or no trees. Land cover mostly hard-packed. Lightweight construction materials (e.g., wood, thatch, corrugated metal).	G. Water 	Large, open water bodies such as seas and lakes, or small bodies such as rivers, reservoirs, and lagoons.
8. Large low-rise 	Open arrangement of large low-rise buildings (1–3 stories). Few or no trees. Land cover mostly paved. Steel, concrete, metal, and stone construction materials.	VARIABLE LAND COVER PROPERTIES	
9. Sparsely built 	Sparse arrangement of small or medium-sized buildings in a natural setting. Abundance of pervious land cover (low plants, scattered trees).	<i>b. bare trees</i>	Leafless deciduous trees (e.g., winter). Increased sky view factor. Reduced albedo.
10. Heavy industry 	Low-rise and midrise industrial structures (towers, tanks, stacks). Few or no trees. Land cover mostly paved or hard-packed. Metal, steel, and concrete construction materials.	<i>s. snow cover</i>	Snow cover >10 cm in depth. Low admittance. High albedo.
		<i>d. dry ground</i>	Parched soil. Low admittance. Large Bowen ratio. Increased albedo.
		<i>w. wet ground</i>	Waterlogged soil. High admittance. Small Bowen ratio. Reduced albedo.

Figure 4-3 Abridged definitions of the local climate zones (Stewart, Oke 2012). LCZs 1–9 correspond to Oke’s (2004) urban climate zones.

4.3.2. Step 2: Collection of meteorological and air quality data

The meteorological data can be provided in two ways. First, a local weather station (AQIcn.org) can be used, as it provides general data in certain districts, such as temperature, relative humidity, wind speed, pressure, and the concentration of PM. Secondly, field surveys can take place to monitor the meteorological data in the study areas to enable a more accurate simulation result. However, due to limitations of the meteorological and air pollution sensors in this study, field surveys might be unable to monitor all of the required data. Hence, it is necessary to combine field survey data with weather station data to create an integrated database. ENVI-met Space models, which are built in step 1 based on the satellite image of study area, can run simulations based on the meteorological data to show hourly variations of wind speed, temperature, and relative humidity. Moreover, due to different building types (building scales, height, density) and tree density, wind speed and direction would change, which could affect the pollutant concentration in the research areas. These simulation results could increase the precision with which the amount of air pollution removal could be calculated. Lastly, plant leaves are a key absorber of air pollutants, so it is important to estimate leaf area. This research will use a direct measurement, which is the area of leaves to ground covered (Ong 2003).

ENVI-met, as mentioned above, is a suitable software for this research method compared to other environmental software, such as ADMS provided by Cambridge Environmental Research Consultants. ENVI-met is designed to simulate the surface-plant-air interactions in an urban environment, with a typical resolution down to 0.5 m in space and 1- 5 seconds in time (Bruse, Fleer 1998). Specifically, modelling research areas in ENVI-met could simplify land cover, thereby increasing the standardization of land analysis. Moreover, ENVI-met could provide hourly data for next system dynamics models, also, it presents the results visually. It is also simple to use and free for general meteorological simulations. ADMS 5 is a dispersion model used to model the air quality impact of the existing and proposed industrial installations. It is good at modelling air quality; however, this research aims to calculate air pollution through system dynamics models. In addition, this software is very expensive and complicated. Hence, ENVI-met is the optimum choice for the current stage in this research.

4.3.3. Step 3: Calculation of air pollution removal

This part is to develop a system dynamic model of dry deposition in order to quantify PM mitigation by trees. First, mathematical equations are needed to quantitatively represent the relationships between the internal factors in dry the deposition system. The amount of PM₁₀ removal at a unit in a certain period could be calculated as (Nowak 1994):

$$Q = F \times L \times T \quad (1)$$

where Q is the amount of a particular air pollutant removed (g) by a certain area of green space, L (m²), in a certain time period, T (s), and F is the pollutant flux (g/m²/s)

The pollutant flux, F , is calculated as (Nowak 1994):

$$F = V_d \times C \times 10^{-8}$$

(2)

where V_d is dry deposition velocity (cm/s) of a particle pollutant with concentration C (µg/m³). This study assumes that particles stick to the surface of vegetation upon contact, the dry deposition velocity is decided by transport properties in the air, and so canopy resistance can be ignored (Lim et al. 2006).

$$V_d = \left(\frac{1}{R_a + R_b + R_a R_b V_g} + V_g \right) \times 10^{-2} \quad (3)$$

where R_a is aerodynamic resistance, R_b is resistance of molecular scale diffusive transport at quasi-laminar boundary layer, and V_g is a gravitational settling velocity (m/s).

R_a is calculated as (Yang et al. 2004):

$$R_a = \frac{u(z)}{u_*^2}$$

(4)

$u(z)$ (m/s) is the wind speed at height z (2m), u_* (m/s) is the frictional velocity, and u_* is expressed as the dimensionless ϕ_m stability function for momentum (Giardina, Buffa 2018).

$$u_* = \frac{k u_{(z-d)}}{\ln \left[\frac{(z-d)}{z_0} \right] - \phi_m \left[\frac{(z-d)}{L} \right] + \phi_m \left(\frac{z_0}{L} \right)}$$

(5)

where k is the von Karman's constant (0.4) (Dyer, Bradley 1982), d the displacement length (1 m), z_0 the roughness length (0.4 m), and L is the Monin–Obukhov stability length. Local meteorological data were classified by Turner classes (Dutton, Panofsky 1984) to stability

classes, while L^{-1} shows the function of the stability classes (Daly, Zannetti 2007; Yang et al. 2004). There are two situations:

Unstable situation ($L < 0$) (Van Ulden, Holtslag 1985):

$$\phi_m = 2 \ln \left[\frac{(1+X)}{2} \right] + \ln \left[\frac{(1+X^2)}{2} \right] - 2 \tan^{-1}(X) + 0.5 \quad (6)$$

where X is a dimensionless factor (Dyer, Bradley 1982).

$$X = (1 - 28 \frac{z}{L})^{0.25} \quad (7)$$

Stable situation ($L > 0$):

$$\phi_m = -17 \left[1 - \exp \left(-0.29 \frac{(z-d)}{L} \right) \right] \quad (8)$$

In the above equations, L would be impacted by wind speed according to the Pasquill stability classes. When the wind speed < 3 m/s in the daytime, it is class A; when the wind speed > 3 m/s, it is class B. Hence, L is -14.3 for class A and -27.5 for class B in this study, which are both unstable situations.

R_b was calculated as (Pederson et al. 1995):

$$R_b = \frac{2s_c^{2/3} \times p_r^{-2/3}}{ku_*}$$

(9)

where k is the von Karman constant, S_c the Schmidt number (0.7), and P_r is the Prandtl number (0.7-0.8) (Yang et al. 2004).

$$V_g = \frac{\rho d_p^2 g C}{18\theta} \quad (10)$$

where ρ is density of particles, which is 1.8×10^3 kg/m³ (Lim et al. 2006) in this study, d_p is the particle diameter (10×10^{-6} m), g (m/s²) is gravitational acceleration, θ is dynamic viscosity coefficient of air, which is 18.37×10^{-6} Pa*s when the air temperature is between 18-30 °C, and C is the rectification of small particles (Zhang et al. 2001).

$$C = 1 + 2\lambda d_p (1.257 + 0.4e^{-0.55d_p/\lambda}) \quad (11)$$

where λ is the mean free path of a moving particle, which is 68 nm under the standard ambient pressure (Jennings 1988).

In this step, a SD dry deposition model is developed in the software Vensim PLE. A simplified schematic of the model is shown in Figure 4-4. The model estimates the amount of particle pollutant removal by the dry deposition equations. The factors of dry deposition process are

entered into Vensim (as a simulation platform) based on the equations. Figure 4-4 shows the graphical interface of Vensim PLE. It can show the representation of variables in the physical dry deposition system through the placement and connection of different graphical elements in the workplace. In Vensim, variables and rates are represented by rectangles, and thick and thin arrows, respectively. Widmark (2012) proposed that both Euler's method and Runge-Kutta-4 method are supported by Vensim, and different methods can be chosen based on the equation types. In Figure 4-4, the variables 'Concentration as zone level' and 'Total PM10 Removal' are combined with rate 'Deposition press' to show a numerical integration. These variables can be setup by using the equation editor (see Figure 4-5). After all variables from deposition process have been setup, Vensim can start to calculate the amount of air pollution removal based on the input data. For example, Table 4-1 shows the contents of variables that is described by the equations and their input data. Graphical results are also provided by Vensim. Figure 4-6 presents the line graphs of one variable together and other variables that causes its results. Different lines in the graphs represent various simulations with their won input data. They can be used to compare the changes of different simulations for result analysis and discussion. But in terms of modelling air pollution mitigation, SD software has not been widely used in the research area of urban planning. In this research, however, the main reason of using SD model is the dry deposition process can be visualized based on the equations. It can present how other factors will change based on different variables. In this part of the simulation process, multiple variables, such as pollution concentration, wind speed and leaf area, may changing at the same time with different scenarios, so visual data graphs are able to clearly show the moving track of each factor. It means that users not only can see the changes of results, but also can understand the change in the process.

Table 4-1 Contents of variables in the dry deposition model described by the equations and their input data.

Variables number	Content	Units
1	Dry deposition velocity of PM10= ((1/ (Aerodynamic resistance Ra+Resistance of quasi laminar boundary layer Rb +Aerodynamic resistance Ra*Resistance of quasi laminar boundary layer Rb*The gravitational settling velocity Vg)) +The gravitational settling velocity Vg) *Adjustment factors	cm/s

2	Adjustment factors=0.0041	
3	Aerodynamic resistance Ra=Wind speed at simulation hight in each zone uz/POWER (Frictional velocity ux, 2)	
4	Concentration at zone level= INTEG (source pollutant concentration time-Deposition process, source pollutant concentration time)	mcg/m ³
5	Density of particles ρ=1.8*POWER (10, 6)	g/m ³
6	Deposition process=Pollutant flux*Total LA	
7	Dimensionless factor X=1	
8	Displacement length d=1	m
9	Displacement length z0=0.4	m
10	Dynamic viscosity coefficient of air θ= 18.37*POWER (10, -6)	Pa s
11	FINAL TIME = 30	Minute
12	Frictional velocity ux= (The von Karman constant k * Wind speed at simulation hight in each zone uz)/LN ((Simulation hight z- Displacement length d)/Displacement length z0)-Stability function for momentum Φm *((Simulation hight z-Displacement length d)/Monin–Obukhov stability length L) +Stability function for momentum Φm*(Displacement length z0/Monin–Obukhov stability length L)	
13	Gravitational acceleration g=9.8	m/s ²
14	INITIAL TIME = 0	Minute
15	Monin–Obukhov stability length L= -14.3	
16	Pollutant flux=Dry deposition velocity of PM10*Concentration at zone level*0.01	mcg/m ² /s
17	Prandtl number Pr=0.75	
18	Rectification of small particles C=1	
19	Resistance of quasi laminar boundary layer Rb=2*POWER (Schmidt number Sc, 2/3) *POWER (Prandtl number Pr, -2/3)/ (The von Karman constant k*Frictional velocity ux)	
20	SAVEPER = TIME STEP	Minute
21	Schmidt number Sc= 0.7	
22	Simulation hight z=2	m
23	source pollutant concentration time = WITH LOOKUP (Time, ((1,200) (30,500)], (1,512.8), (2,500.5), (3,488.3), (4,476), (5,463.8), (6,451.5), (7,439.3), (8,427), (9,423), (10,419), (11,415), (12,511), (13,507), (14,493), (15,479), (16,435), (17,397), (18,399), (19,421), (20,403), (21,445), (22,437), (23 ,437), (24,411), (25,512.8), (26,500.5), (27,488.3), (28,510), (29,499.4), (30,468.8)))	mcg/m ³
24	Stability function for momentum Φm=2*LN ((1+Dimensionless factor X)/2) +LN ((1+POWER (Dimensionless factor X,2))/2)- 2*ARCTAN (Dimensionless factor X) + 0.5	
25	The gravitational settling velocity Vg= (Density of particles ρ*The particle diameter dp*The particle diameter dp*Gravitational acceleration g*Rectification of small particles C)/ (18*Dynamic viscosity coefficient of air θ)	

26	The particle diameter $d_p = 10 * \text{POWER}(10, -6)$	um
27	The von Karman constant $k = 0.4$	
28	TIME STEP = 0.25	Minute
29	Total LA=4644	m ²
30	Total PM10 Removed= INTEG (Deposition process*Adjustment factors, 0)	mcg
31	Wind speed at simulation height in each zone $u_z = 0.4$	

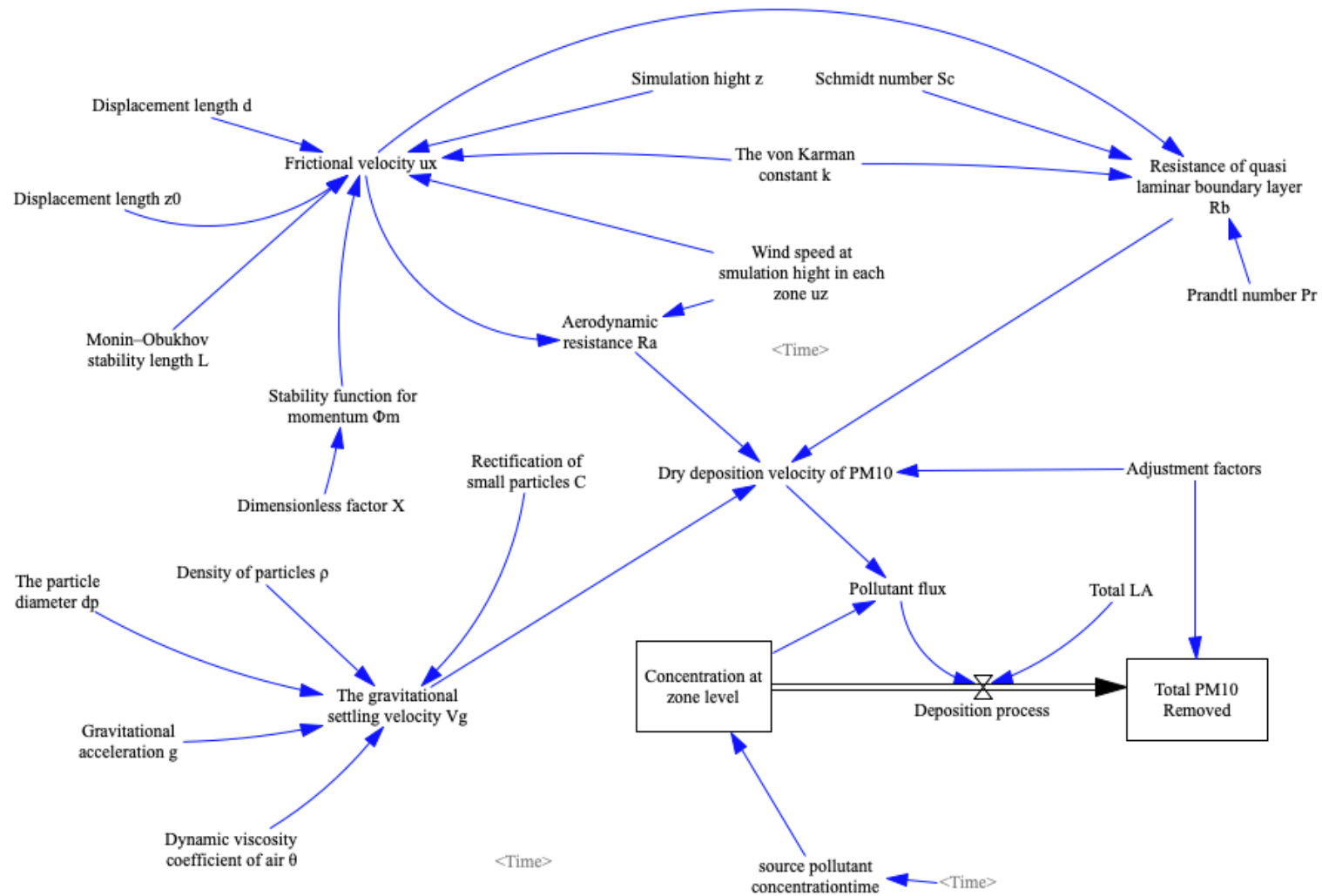


Figure 4-4 Schematic of the dry deposition process based on the differential equations in the Vensim workplace.

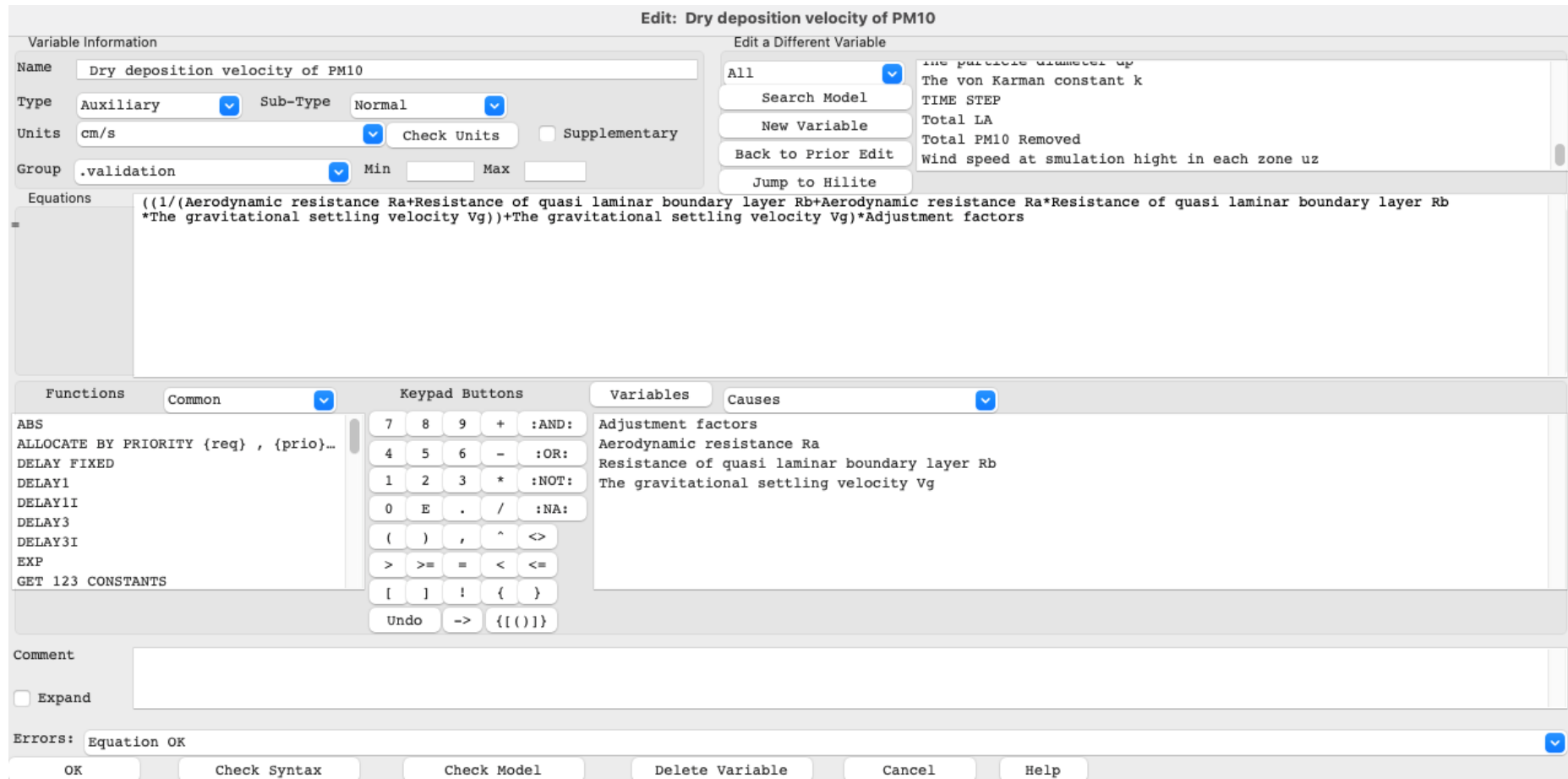


Figure 4-5 Equation editor window shows the variables of the dry deposition velocity equation.

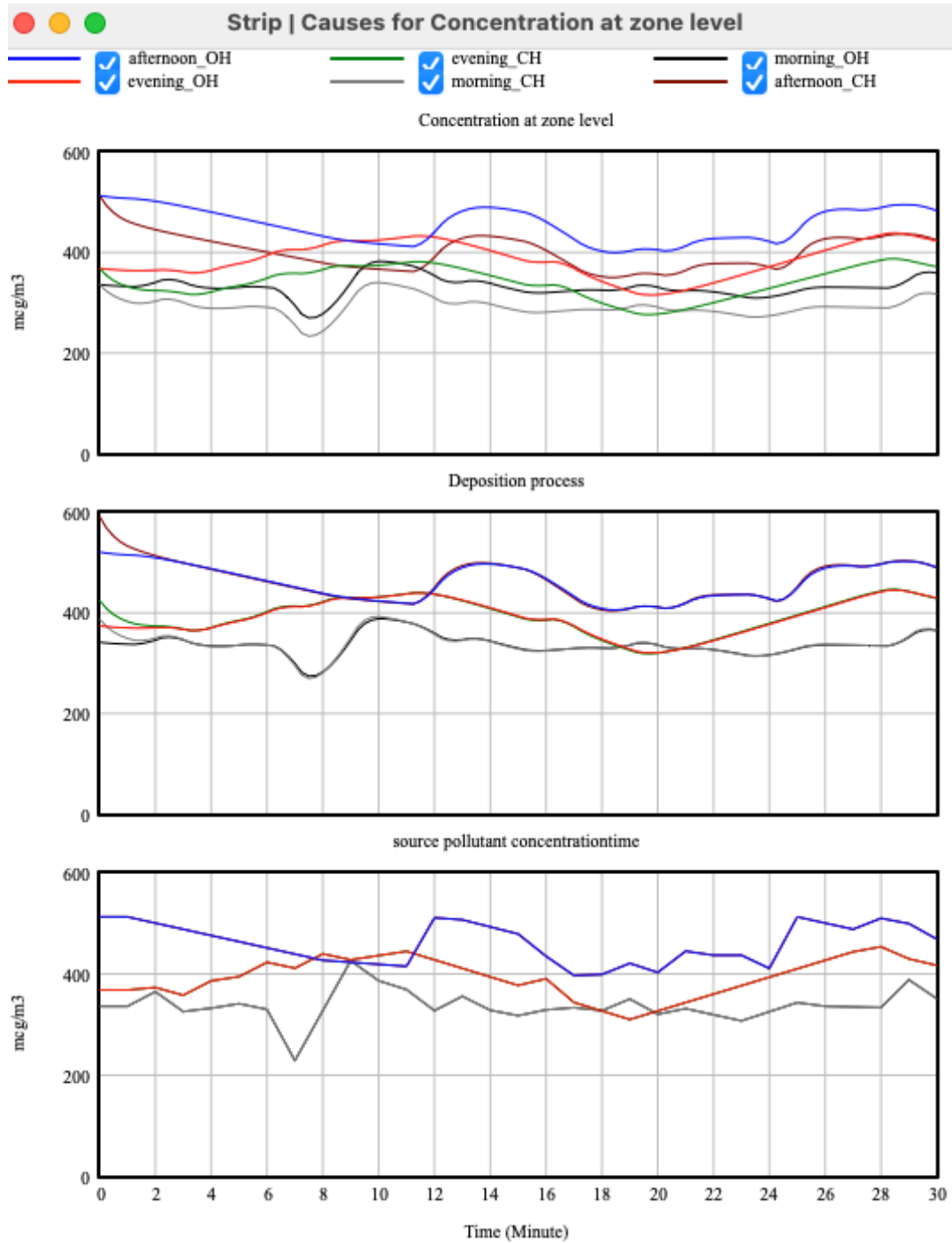


Figure 4-6 Graphs of the box variable 'Concentration at zone level' and its related variables.

4.4. Conclusion

Urban dwellers who live in the near-road residential areas are suffering from high air pollution concentration from road traffic. Absorbing air pollution by dry deposition is one of the environmental benefits of urban green spaces. It is important to understand the efficiency of different green plans on improving air quality. Existing urban planning studies have modelled dry deposition processes to quantify pollutants mitigation. However, most of the research and computer programs focused on national or regional scales, and the considerations of changes to air flow and pollution concentration, and vegetation types, caused by different urban forms were limited. This chapter presented an integrated model as a green planning model to consider the impacts of wind speed, source pollution concentration, and vegetation types more carefully. The model is designed to propose different green plans for different mid-scale residential areas (especially the near-road areas with high levels of pollution) by numerical simulation of dry deposition efficiency. It not only enables the quantification of pollution removal for current green plans, but can also estimate future plans by changing green cover densities, source pollution concentrations, wind speeds, and different locations of trees.

The model framework introduced two parts of the integrated model, which are a CFD model to simulate atmospheric conditions in the chosen areas by ENVI-met, and an SD model to graphically represent the dry deposition process based on the equations input into Vensim PLE. Both ENVI-met and Vensim PLE provide no-cost licences for academic and educational use. Then, three steps of the model setup are discussed to clarify the simulation background, boundaries, and processes. First, to apply this model, study areas need to be chosen and identified based on the local climate zone regulations to provide the general features of building forms, land covers, and green area types. Field surveys or satellite imagery are required to analyse the study areas and build up 3D models in ENVI-met. Second, metrological data and air pollution concentration need to be collected from local weather station or monitored from the study area as model inputs. For simulating current green plans, metrological and pollution data can be monitored in the study areas, in which case the CFD model is not needed as its purpose is provide metrological data (mainly wind speeds) for hypothetical green plans. Hence, for testing different plans, metrological data is taken from the CFD simulation results. Finally, all input data is entered into the dry

deposition SD model in Vensim to calculate the total pollutants removal in the study areas during the investigation period. The results can be used to examine current green plans or guide the improved design of plans for future urban development. However, due to the complex effects of the fluid dynamic process on dry deposition flux, a single dry deposition model cannot represent and simulate the process of particle dry deposition process as accurate as it is in the real world. Moreover, nature ventilation can be impacted by multiple and complex factors, and it is unable to accurately predict in outdoor urban areas by any CFD model (Calautit et al. 2020). Hence, the ENVI-met can only provide simulated outcomes of wind speed based on the meteorological boundary conditions of the study area. The simulated wind speed might be different from the real data. Due to the above reasons, my integrated green planning model aims to suggest possible amount of pollution removal based on different green plans and to calculate pollution mitigation of current green plans based on the monitored wind speed data from the study area.

This integrated model will need to be validated for proposing optimum green plans in mid-scale near-road residential areas. The following chapter will validate this model by comparing the simulation results and real world monitored data to prove its potential in future applications in the urban planning research field.

Chapter 5. Comparison between field measurement and simulation – model validation

5.1. Introduction

In this research, an integrated green planning model (ENVI-met and Vensim) has been developed to explore more appropriate urban green planning for improving outdoor air quality. ENVI-met and Vensim, as independent CFD and SD software, were described in the previous chapter (see chapter 4). The main purpose of this validation process is to determine to what extent the simulations of the dry deposition model correspond to the real situations. In this chapter, a brief overview of the related environmental simulation validation approaches, description of the validation process adopted in this study, and a discussion of the comparison results, are presented.

5.2. Review of environmental model validation methods

For the purpose of using computational models to make environmental simulations with quantified confidence, model verification and validation (V&V) has been widely used in many different fields (Thacker et al. 2004; Sargent, Balci 2018; Kleijnen 1995; Oberkampf, Trucano 2002; Robinson 1997; Chan et al 2004). The definition of V&V is given by Law, Kelton and Kelton, and Sargent, in the 1990s. Verification aims to determine a model implementation that accurately fits the developer's description of the model and its solution. Then, validation is to conclude if a model is able to accurately represent the real world based on the perspective of the intended uses of the model (Kleijnen 1995; Sargent, Balci 2018; Thacker et al. 2004; Law et al. 2000; Sargent 1992). However, even model validation cannot prove that a model is accurate for all types of scenarios, because it only provides evidence of accuracy for certain intended purposes (Thacker et al. 2004; AIAA 1998). The validation process generally includes three general methods, which are

- To obtain real world data: Ideally, the validation process should involve the measurement of detailed inputs and outputs from the real world with the attributes of intermediate variables. In practice, real world data are available in different quantities, so some historical data may be used as a reference, or the scarce data are not critical that provided by analysis.
- To compare simulated and real data: Outputs of real and simulated systems can be plotted, where the X-axis denotes time and the Y-axis denotes the real and simulated values (Barlas 1989).

- Sensitivity analysis: sensitivity analysis is usually used to determine whether a model's behaviour agrees with its purpose, and for locating which inputs dominant (Kleijnen 1995).

For the dry deposition simulation model that was developed in this research, as shown in chapter 4, a validation process (see Figure 5-1) has been developed based on the V&V system to address different validation methods in each stage of the process. Real-world monitoring and comparison of real and simulated data are undertaken to examine to what degree the dry deposition model can represent real world situation.

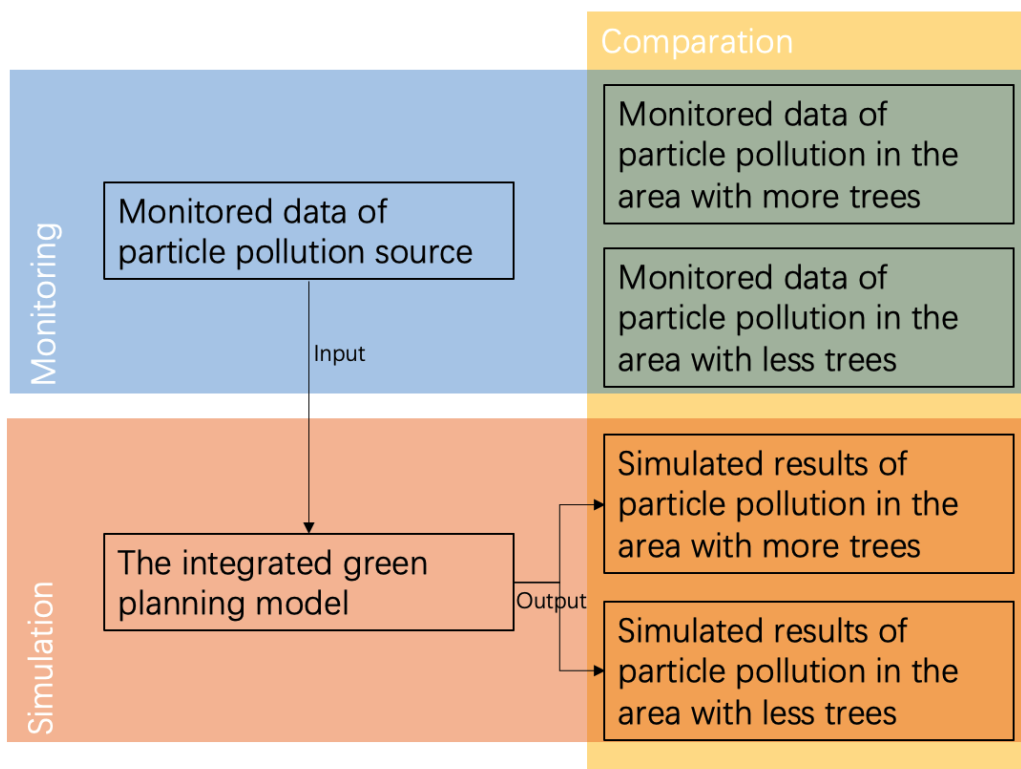


Figure 5-1 Basic process and data flow of the integrated green planning model validation.

A research model framework, as presented in Chapter 3, describes the relationship between different data and elements for guiding the monitoring of real-world data. A number of factors need to be considered when choosing the monitoring sites, including the area with green cover, similar urban forms and function, and whether there is a relatively stable pollution source. The assumptions made for the simulation study, such as meteorological data and PM concentrations, will be discussed in detail in the following section.

5.3. Obtaining real world data — PM2.5 and PM10 concentration monitoring

This part aims to monitor meteorological data and PM2.5 and PM10 air quality data from selected research areas in Taiyuan city. These data will be used for the comparison with the simulation results derived from the integrated model developed in chapter 4.

5.3.1. Zone selection and classification

Taiyuan city can be divided into three strata based on the political and historical development of the city (Figure 5-2): 1) Yingze district (yellow): This is the oldest area of the city and was established in 1945 as a centre for the economy, government, and traffic. 2) Xinghualing and Wanbailing district (red): These were developed since 1998, with a focus on agriculture and several industries, mainly the mining industry, chemical industry, and machine manufacturing. 3) Jiancaoping and Xiaodian district (purple): These areas have been mainly developing from 2007 as a future centre of the government and the economy, and currently hosts many high-tech industry parks.

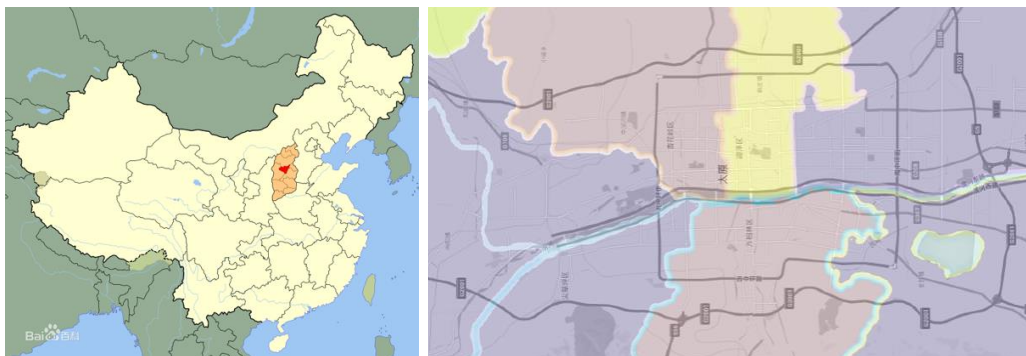


Figure 5-2. Districts in the city of Taiyuan

Based on the local climate zone (Stewart, Oke 2012) and urban texture of Taiyuan City, two zones with similar meteorological situations and different green levels are selected for real world data monitoring (see Figure 5-3), which are:

- **compact high-rise:** mix of building heights (15 – 18m) with dense arrangement, few trees, mostly paved and concrete land cover, and brick, tile, and concrete building materials, and the zone function is residential.

- **open high-rise:** more open arrangement of buildings with the same heights (15 – 18m), more trees and grass, same paved and concrete land cover, and brick, tile, and concrete building materials, and the zone function is mainly residential and partly office.

These two zones are close to each other and have basically the same building types, materials and functions, and tree species, which means the main variable is the different green level. Moreover, both zones are located next to Kang Le Road, which has four lanes for vehicles and two lanes for bicycles. This can ensure that pollutant source of compact-H zone and open-H zone are as similar as possible. The same air pollution source and urban conditions can minimize error between the monitored data and simulated results, as the data cannot be monitored at the same time with one sensor. Four research areas are all located inside of Taiyuan city. The size of the compact-H zone is 136,500sq.m (420 x 325m), and the open-H zone is roughly 150,156sq.m (423 x 355m).

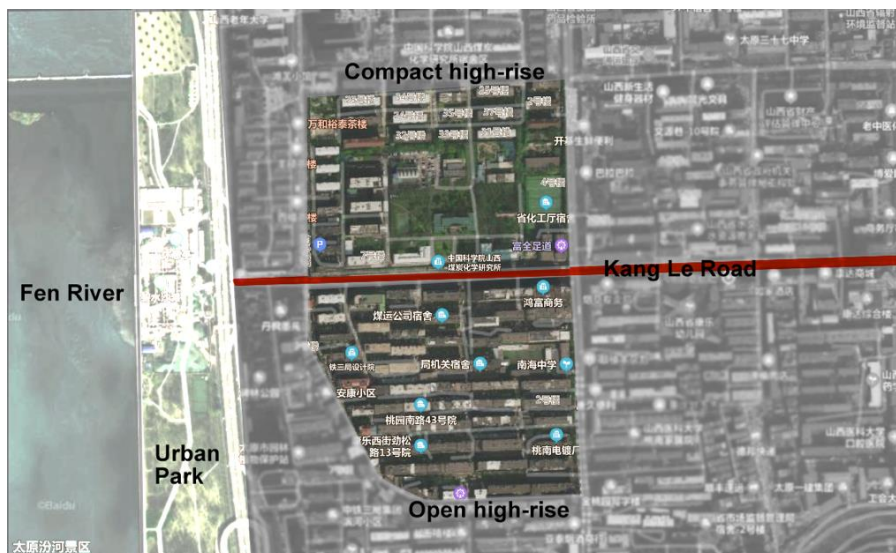


Figure 5-3 Classification of satellite images in Taiyuan City based on building types: compact high-rise (top part of the map) and open high-rise (bottom part of the map) (source: map.baidu.com)

5.3.2. Real-world data monitoring

Meteorological data (wind speed, humidity, and temperature) and PM concentration were monitored from the four research zones in the summer. These data were monitored for half an hour from each zone during three time periods throughout the day, which are T_{morning} (9:00 – 10:10), $T_{\text{afternoon}}$ (12:30 – 13:40), and T_{evening} (17:00 – 18:10). 10 minutes were spent for moving from the open-H to compact-H zones, and a total of 30 minutes was spent in

each zone for monitoring. PM concentration data of Kang Le Road have also been monitored for 30 minutes after finishing the measurement in both zones for use as the initial pollution source for the dry deposition model simulation. Meteorological data (see Table 5-1) were monitored by a Large-Area Vane Anemometer (testo 417, Hampshire). Many studies reviewed in Chapter two reported that the aerodynamic effects are significant compared with tree deposition. Therefore, the monitoring time was specially chosen to be when the wind speed in both zones is stable and relatively low, which ensures the impact of ventilation on the PM concentration was minimized to a low level (see Table 5-1). In other words, wind would not bring much PM pollutants in or out from these zones, so that the PM pollutant concentration would be mainly reduced by tree deposition. PM concentration (see PM10 in

Table 5-2 and PM2.5 in

Table 5-3) was monitored by a Dylos DC1100 (Innovation 2008) device. Two sizes of particles were monitored, which respectively have diameters between 2.5 to 10 μm and 0.5 to 2.5 μm (Williams et al. 2015). Monitored data are recorded by the Dylos every minute, and can be accessed through a PC. The Dylos PM data needed to be converted into micrograms per cubic meter ($\mu\text{g}/\text{m}^3$) for the later calculation using the dry deposition simulation. Particulate Matter mass concentration of micrograms per cubic meter could be calculated from the Dylos monitoring data using Equation 1:

$$C_{\text{PM}} = N \times 3531.5 \times P_{\text{PM}} \times H \times c \quad (5-1)$$

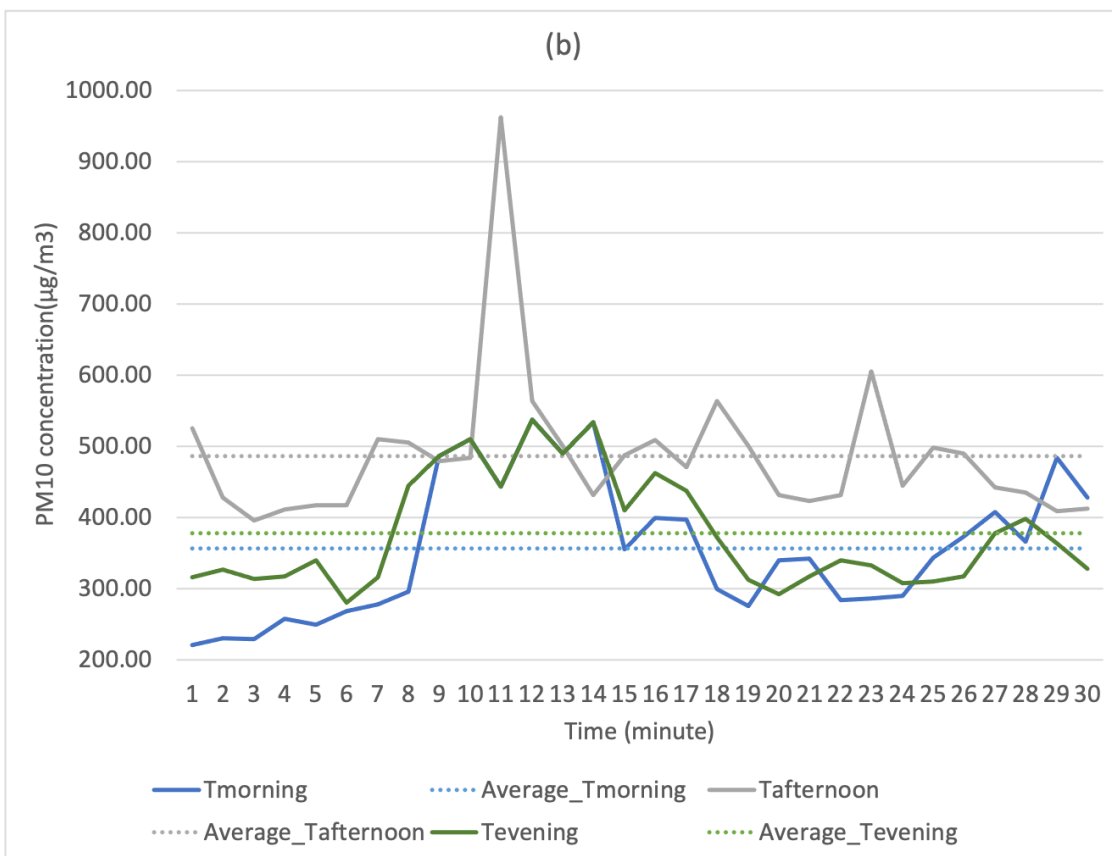
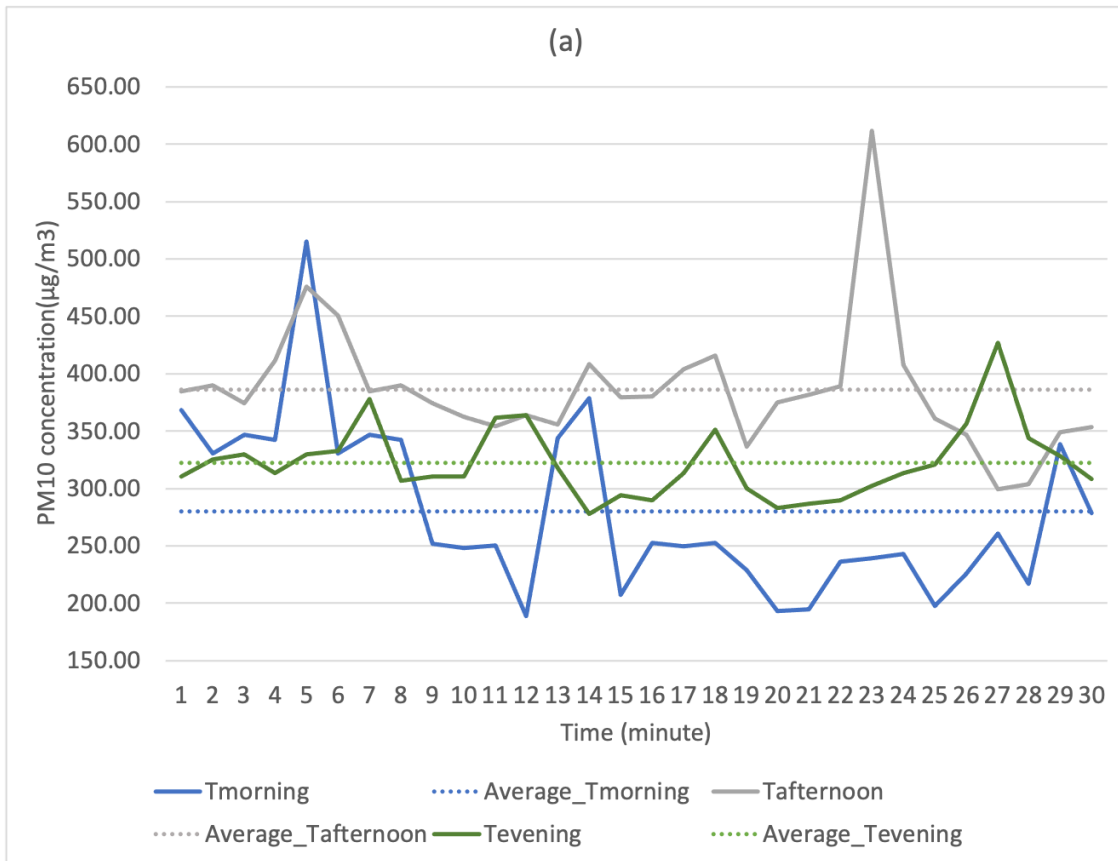
Where the C_{PM} is a certain particle concentration, N is the number of particles, P_{PM} is the mass of a particle, which for $\text{PM}_{2.5}$ is 5.89E^{-7} μg and for PM_{10} is 1.21E^{-4} μg ; H is the relative humidity as a percentage; and c is the correction factor (6.4) (Arling et al. 2010). Figure 5-4 and Figure 5-5 show the ranges of monitored data value, which are 200 to 600 $\mu\text{g}/\text{m}^3$ in the compact-H area, 200 to 1000 $\mu\text{g}/\text{m}^3$ in the open-H area, 200 to 500 $\mu\text{g}/\text{m}^3$ in Kang Le Road for PM_{10} ; and 35 to 70 $\mu\text{g}/\text{m}^3$ in the compact-H area, 45 to 95 $\mu\text{g}/\text{m}^3$ in the open-H area, 55 to 90 $\mu\text{g}/\text{m}^3$ in the Kang Le Road for $\text{PM}_{2.5}$.

Table 5-1 Meteorological data (wind speed, humidity, and temperature) collected from the compact-H zone and open-H zone.

Research Zone	Time	Humidity (%)	Temperature ($^{\circ}\text{C}$)	Wind speed (m/s)		
		Mean	Mean	Mean	Min	Max
Compact-H	T _{morning}	41.5	25.5	1.3	0.3	1.9
	T _{afternoon}	33.3	22.3	0.3	0	1.2
	T _{evening}	32.9	29.7	0.4	0.1	1.7
Open-H	T _{morning}	41.5	25.5	0.9	0	1.7
	T _{afternoon}	33.3	22.3	0.4	0	0.9
	T _{evening}	32.9	29.7	0.7	0.1	1.6

Table 5-2 Dylos monitored data of PM₁₀ concentration($\mu\text{g}/\text{m}^3$) from the compact-H zone, open-H zone, and Kang Le Road over 30 minutes. The table shows the monitored PM₁₀ concentration data per minute.

Time Minute	T _{morning}				T _{afternoon}				T _{evening}
	Comp act-H	Open- H	Kang Le Road	Compa ct-H	Open- H	Kang Le Road	Compa ct-H	Open- H	Kang Le Road
1	368.5	220.7	336.1	384.7	525.5	512.8	310.1	315.5	368.3
2	330.8	229.4	364.9	390.1	427.5	500.5	325.2	326.3	373.2
3	347.0	228.3	325.7	373.9	395.2	488.3	329.5	313.4	358.0
4	342.7	257.4	332.4	411.6	411.3	476.0	313.4	316.6	386.3
5	515.0	248.7	341.2	476.2	416.7	463.8	329.5	339.2	394.7
6	330.8	268.1	330.0	450.4	416.7	451.5	332.7	280.0	423.0
7	347.0	277.8	228.8	384.7	510.4	439.3	378.0	315.5	411.4
8	342.7	295.1	327.5	390.1	505.0	427.0	306.9	444.7	439.7
9	252.2	485.6	426.3	373.9	479.2	423.0	310.1	485.6	428.0
10	247.9	510.4	386.7	362.1	483.5	419.0	310.1	510.4	436.4
11	250.1	443.7	369.1	354.5	962.7	415.0	361.8	443.7	444.7
12	188.7	537.3	327.5	364.2	563.2	511.0	364.0	537.3	427.9
13	344.0	490.0	355.9	355.6	500.7	507.0	317.7	490.0	411.1
14	378.6	534.1	328.3	408.4	431.8	493.0	277.8	534.1	394.2
15	207.3	355.4	317.7	379.3	486.7	479.0	294.0	409.2	377.4
16	252.6	399.5	329.1	380.4	508.3	435.0	289.7	462.0	390.6
17	249.7	396.3	333.5	404.1	470.6	397.0	313.4	437.2	343.8
18	252.4	299.4	327.5	415.9	563.2	399.0	351.0	371.5	326.9
19	228.7	275.7	350.5	336.2	500.7	421.0	300.4	312.3	310.1
20	193.0	339.2	320.5	375.0	431.8	403.0	283.2	291.8	326.8
21	194.4	341.4	331.5	381.4	423.4	445.0	286.4	316.6	343.5
22	236.2	283.2	319.4	389.0	431.5	437.0	289.7	339.2	360.2
23	239.4	286.4	307.4	611.9	604.8	437.0	302.6	332.7	376.9
24	242.7	289.7	325.4	407.3	444.2	411.0	313.4	306.9	393.6
25	197.5	343.5	343.4	361.0	498.4	512.8	320.9	310.1	410.3
26	226.2	372.6	336.1	347.0	490.0	500.5	356.7	316.7	427.0
27	261.0	407.0	334.9	299.6	441.6	488.3	427.1	377.1	443.7
28	216.6	366.1	333.7	304.1	434.5	510.0	343.5	397.4	453.7
29	338.4	483.5	388.4	348.9	408.9	499.4	327.9	363.9	429.8
30	278.3	427.5	351.2	353.8	412.1	468.8	308.3	328.2	416.8
Average	280.0	356.4	337.7	385.8	486.0	459.0	322.5	377.5	394.3



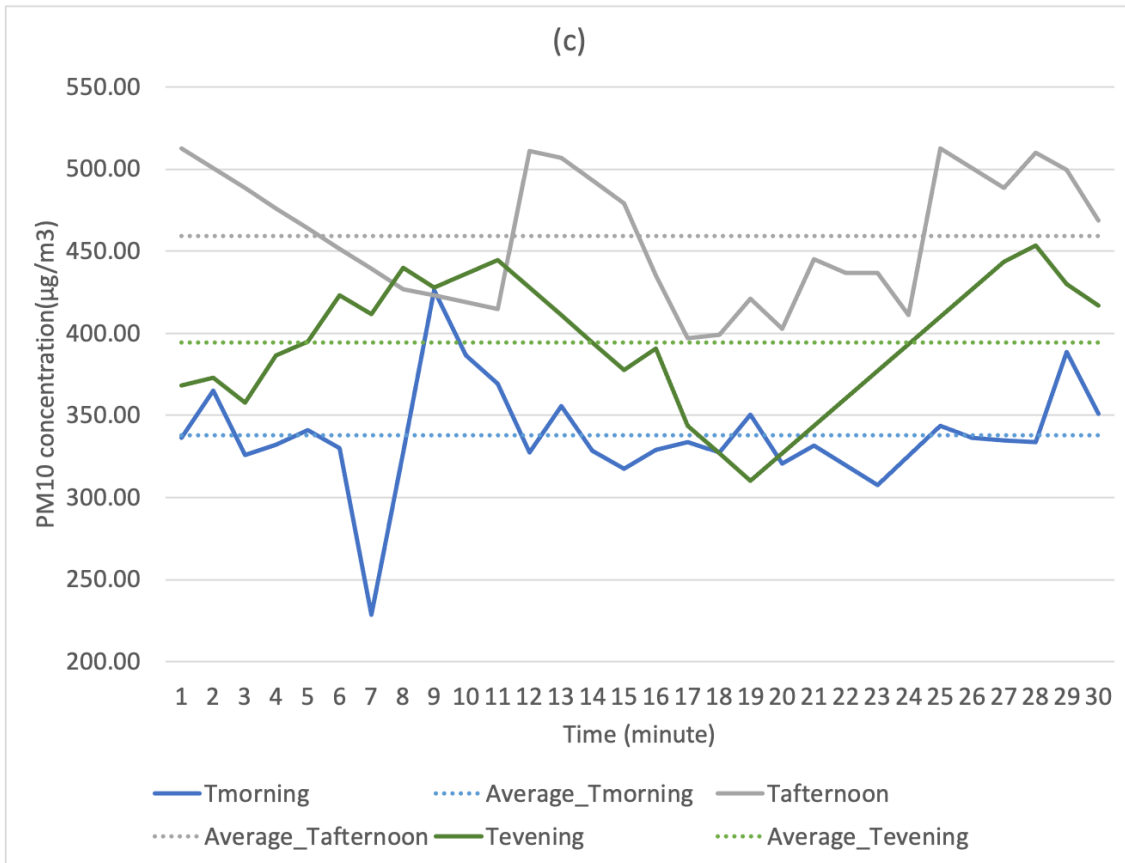
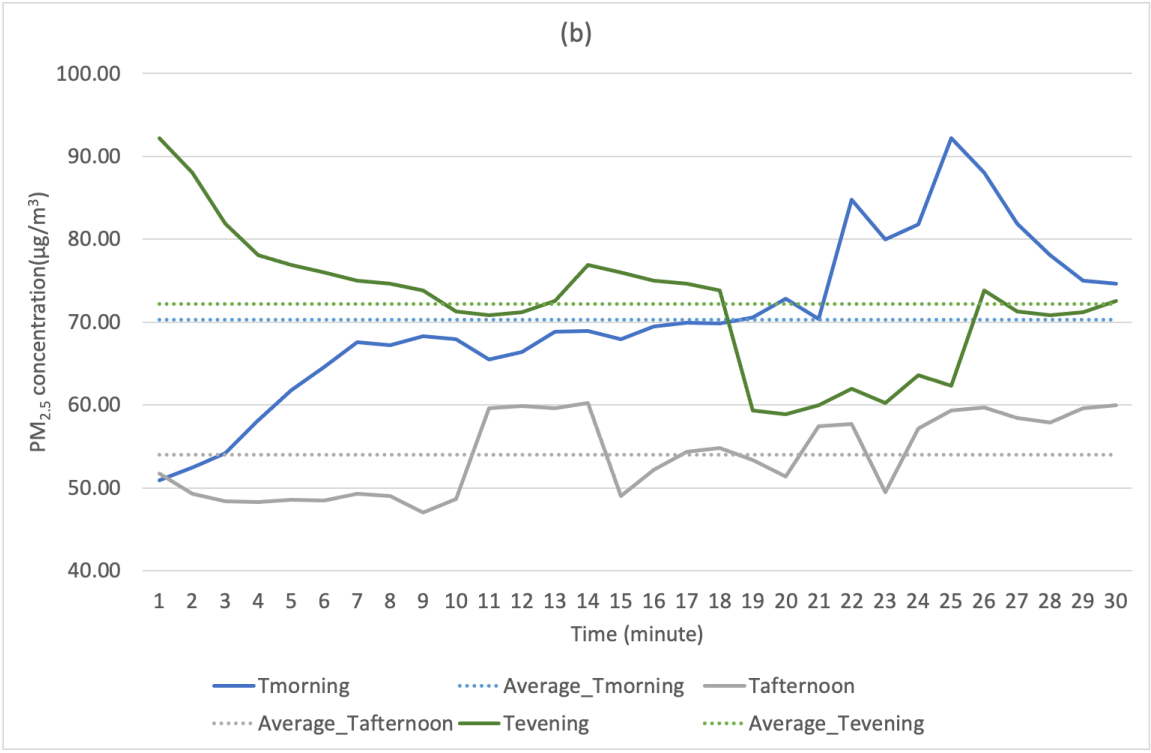
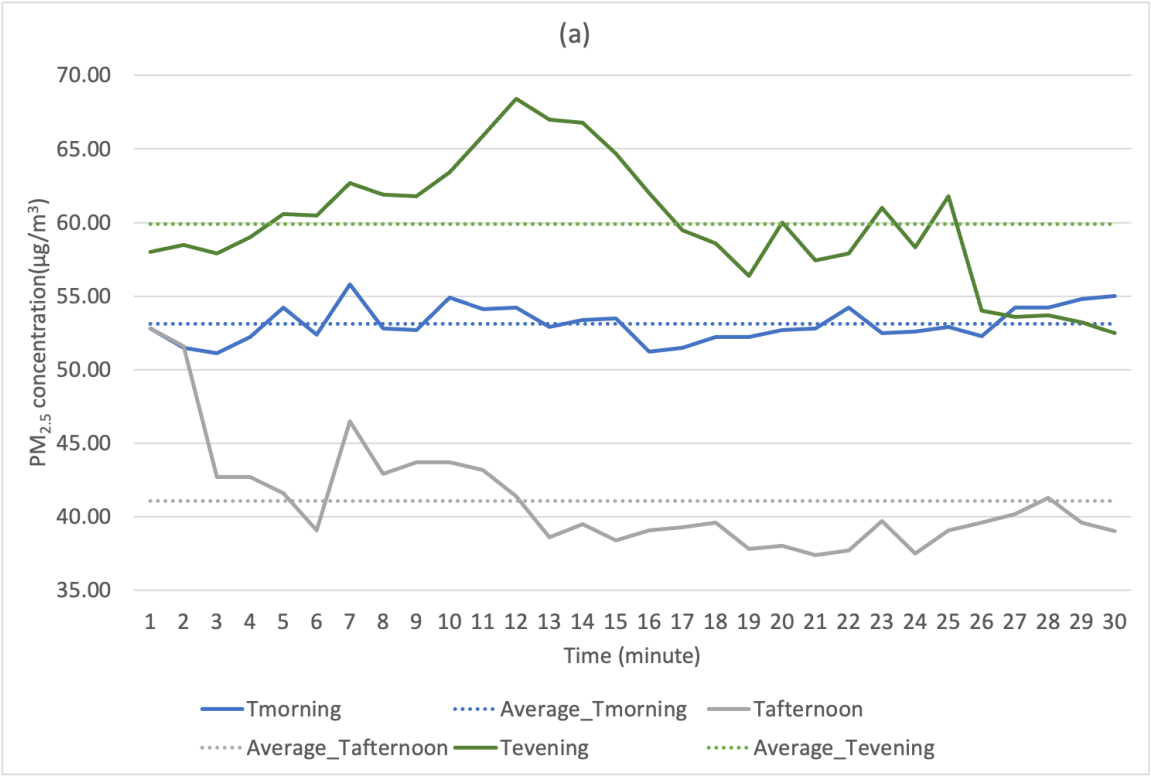


Figure 5-4 Line graphs of monitored data of PM₁₀ concentration(µg/m³) from the (a)compact-H zone, (b) open-H zone, and (c)Kang Le Road over 30 minutes.

Table 5-3 Dylos monitored data of PM_{2.5} concentration($\mu\text{g}/\text{m}^3$) from compact-H zone, open-H zone, and Kang Le Road over 30 minutes. The table shows monitored PM_{2.5} concentration data per minute.

Time Minute	T _{morning}			T _{afternoon}			T _{evening}		
	Com pact- H	Open- H	Kang Le Road	Compa ct-H	Open- H	Kang Le Road	Compa ct-H	Open- H	Kang Le Road
1	52.8	50.9	60.0	52.8	51.7	66.9	58.0	92.2	88.0
2	51.5	52.5	66.4	51.6	49.3	67.0	58.5	88.0	86.8
3	51.1	54.2	72.1	42.7	48.4	67.0	57.9	81.9	84.5
4	52.2	58.2	77.1	42.7	48.3	66.9	59.0	78.1	87.2
5	54.2	61.8	81.6	41.6	48.6	64.8	60.6	76.9	84.7
6	52.4	64.6	85.4	39.1	48.5	60.8	60.5	76.0	80.3
7	55.8	67.6	88.8	46.5	49.3	56.7	62.7	75.0	83.9
8	52.8	67.2	78.7	42.9	49.0	59.8	61.9	74.6	78.6
9	52.7	68.3	74.2	43.7	47.0	64.0	61.8	73.8	74.4
10	54.9	67.9	76.3	43.7	48.7	64.3	63.4	71.3	75.2
11	54.1	65.5	78.2	43.2	59.6	64.7	65.9	70.8	76.1
12	54.2	66.4	79.9	41.4	59.9	68.1	68.4	71.2	74.1
13	52.9	68.8	69.3	38.6	59.6	69.3	67.0	72.6	72.1
14	53.4	68.9	65.7	39.5	60.2	68.5	66.8	76.9	68.1
15	53.5	67.9	74.0	38.4	49.0	65.6	64.7	76.0	70.1
16	51.2	69.5	65.2	39.1	52.2	62.6	62.0	75.0	72.1
17	51.5	69.9	66.3	39.3	54.4	58.7	59.5	74.6	73.1
18	52.2	69.8	67.4	39.6	54.8	57.8	58.6	73.8	72.1
19	52.2	70.6	58.5	37.8	53.4	58.9	56.4	59.3	69.2
20	52.7	72.8	65.7	38.0	51.4	55.9	60.0	58.9	65.3
21	52.8	70.4	60.8	37.4	57.4	54.8	57.4	60.0	67.4
22	54.2	84.8	62.6	37.7	57.7	58.6	57.9	62.0	65.5
23	52.5	80.0	62.3	39.7	49.5	61.4	61.0	60.2	64.6
24	52.6	81.8	67.8	37.5	57.2	64.2	58.3	63.6	61.7
25	52.9	92.2	63.1	39.1	59.3	63.1	61.8	62.3	60.7
26	52.3	88.0	63.6	39.6	59.7	64.0	54.0	73.8	64.9
27	54.2	81.9	64.2	40.2	58.4	60.0	53.6	71.3	66.1
28	54.2	78.1	65.0	41.3	57.9	58.0	53.7	70.8	67.4
29	54.8	75.0	65.9	39.6	59.6	58.0	53.2	71.2	68.8
30	55.0	74.6	66.5	39.0	60.0	58.0	52.5	72.6	67.0
Average	53.1	70.3	69.8	41.1	54.0	62.3	59.9	72.2	73.0



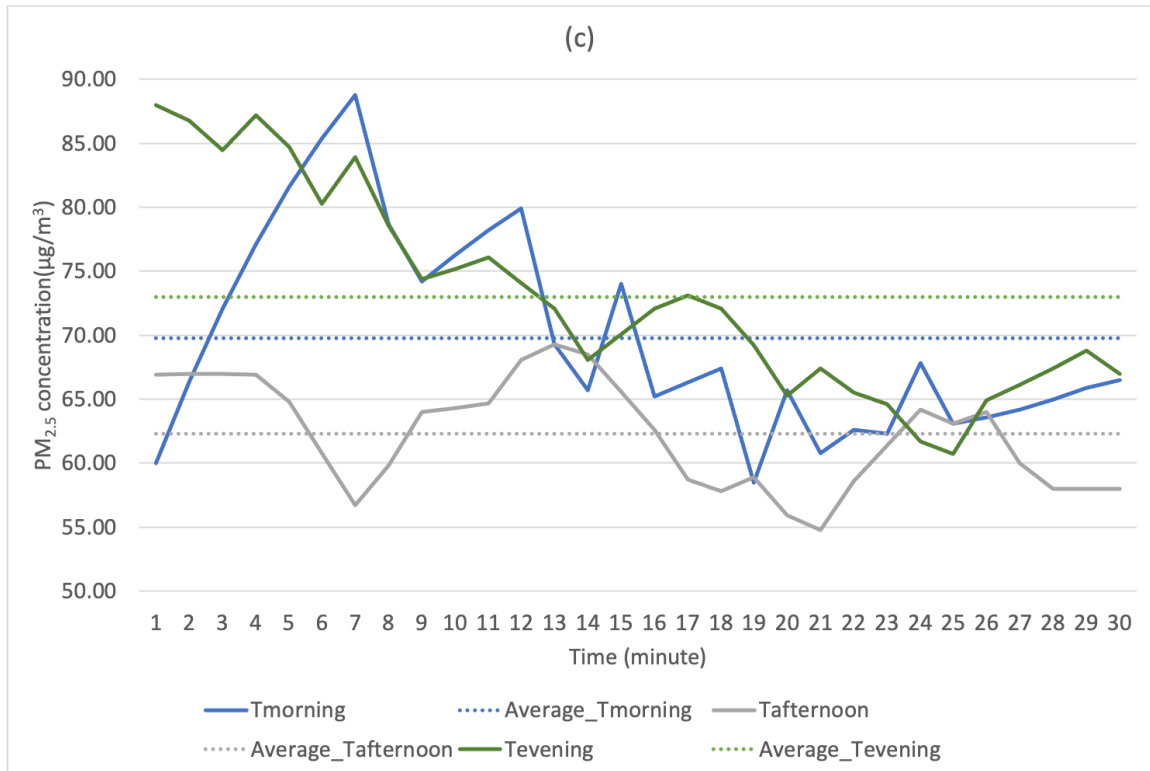


Figure 5-5 Line graphs of monitored data of PM_{2.5} concentration(µg/m³) from the (a)compact-H zone, (b) open-H zone, and (c)Kang Le Road over 30 minutes.

5.4. Comparison of simulated and real data

5.4.1. Simulation

First, satellite images of the compact-H zone and open-H zone are used to calculate size of tree crown area (see in Figure 5-6). The satellite images were printed on a 1:2000 scale, then the tree crown area was measured on the printed maps using rulers by hand (see

Table 5-4). By observation during monitoring process, the selected research zones were mainly covered by deciduous broad leaf trees. Based on the summary of LAI by biomes (see

in Table1 of Chapter 2), a common LAI measurement of deciduous broad leaf trees in the summer is 2.58. The leaf area in each zone can be calculate using:

$$S_c \times LAI_{DBL} = S_t \quad (5-2)$$

where S_c is the tree crown area (m^2); LAI_{DBL} is the mean LAI of the deciduous broad leaf trees, and s_t is total leaf area.



Figure 5-6 Satellite images of compact-H zone (a) and open-H zone (b).

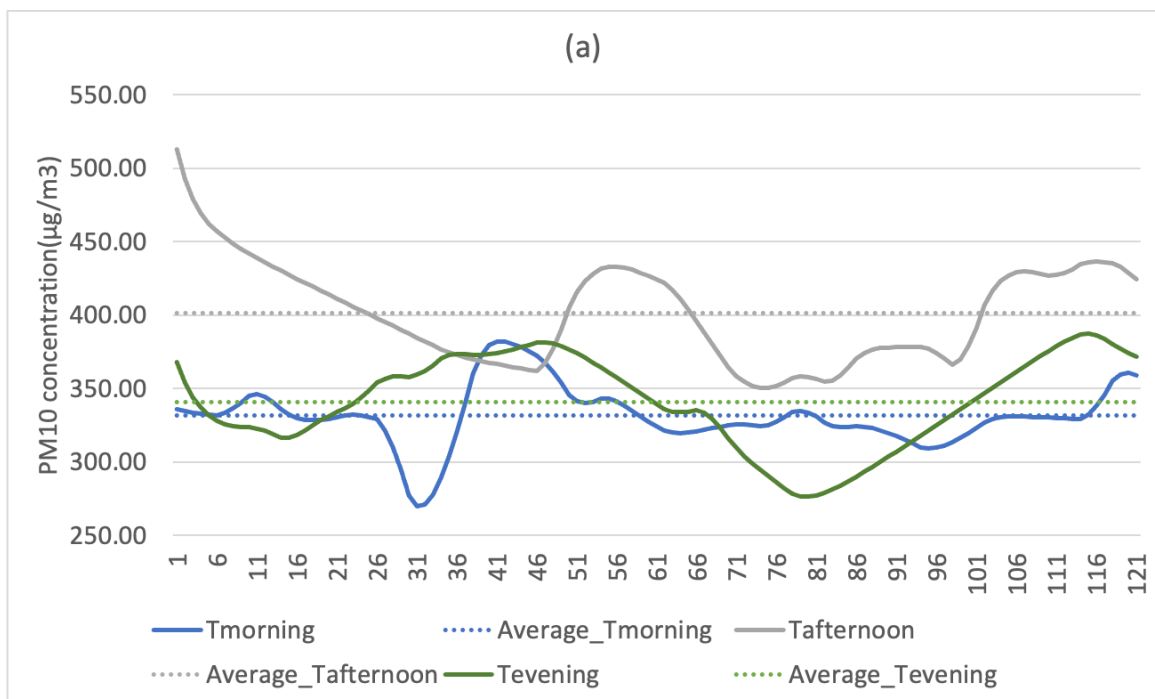
Table 5-4 Input data of leaf areas in compact-H and open-H zones for simulation.

Research Zone	Compact-H	Open-H
Total leaf area in each research zone (m^2)		
Tree Crown area	10,475.0	1,800.0
Total Leaf Area	27,025.5	4,644.0

For the simulation, the wind speed that was monitored locally in each zone was entered into the dry deposition model that described in chapter 4. Wind speed data are recorded at the same time as the PM concentration data. The wind direction was mainly parallel to Kang Le Road during the monitoring period. The average wind speed (see

Table 5-4) from each zone and PM concentration source of Kang Le Road were entered into the dry deposition model (Vensim) to simulate the PM concentration in the compact-H and open-H zones. The concentration monitored from Kang Le Road (see

Table 5-4) is entered every minute as sources pollution. The PM concentration in each zone is simulated every 15 seconds for 30 minutes in total (as shown in APPENDIX 7-5 and APPENDIX 7-1). For the real-world data, PM concentration was monitored every minute, however, for more accurate value, the simulation results were calculated every 15 seconds. Figure 5-7 and Figure 5-8 show the ranges of simulated data value, which are around 300 to 500 $\mu\text{g}/\text{m}^3$ in the compact-H area, 250 to 500 $\mu\text{g}/\text{m}^3$ in the open-H area for PM_{10} ; and 45 to 90 $\mu\text{g}/\text{m}^3$ in the compact-H area, 50 to 90 $\mu\text{g}/\text{m}^3$ in the open-H area $\text{PM}_{2.5}$. Between each input sources pollution, the dry deposition model is calculated three times. So that tries to represent the real situation as deposition is naturally a continuous process, yet the sensor only monitored PM concentration intermittently.



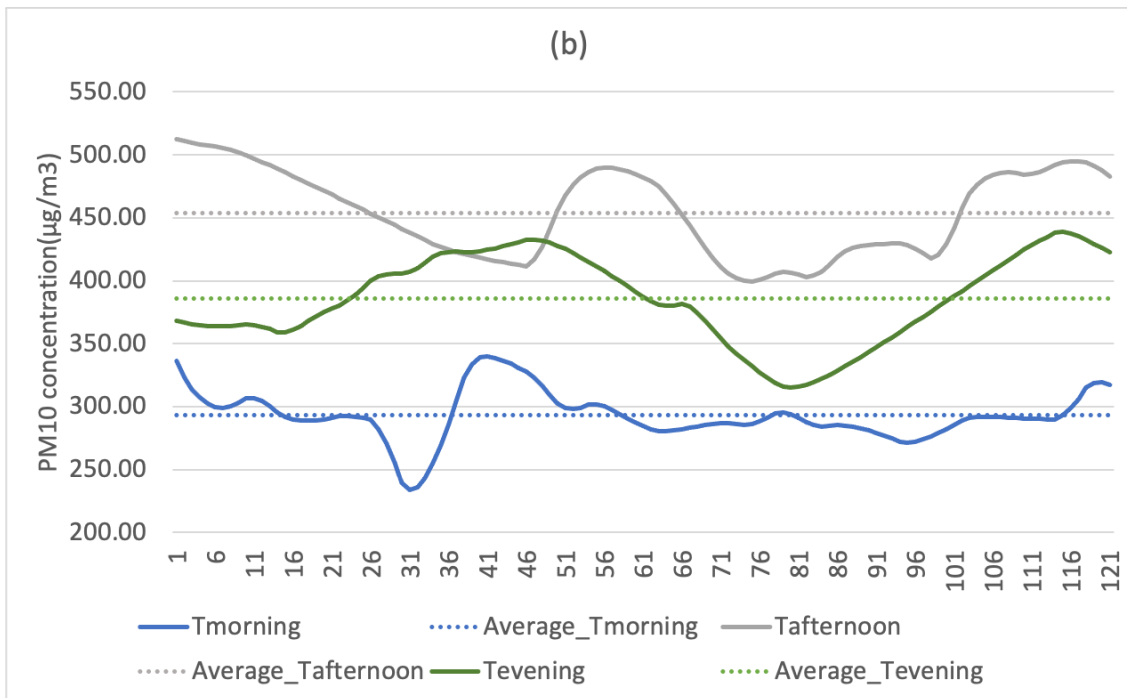
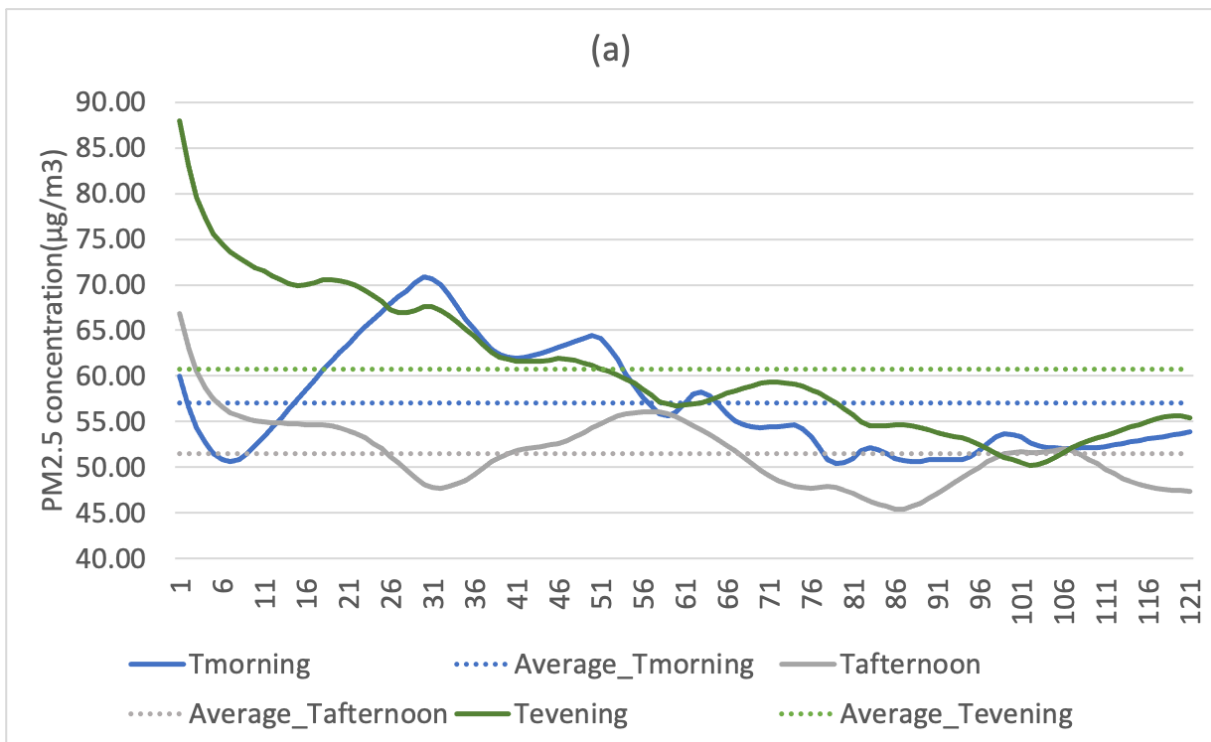


Figure 5-7 Line graphs of simulated PM₁₀ concentration(µg/m³) in (a)compact-H zone and (b)open-H zone over 30 minutes.



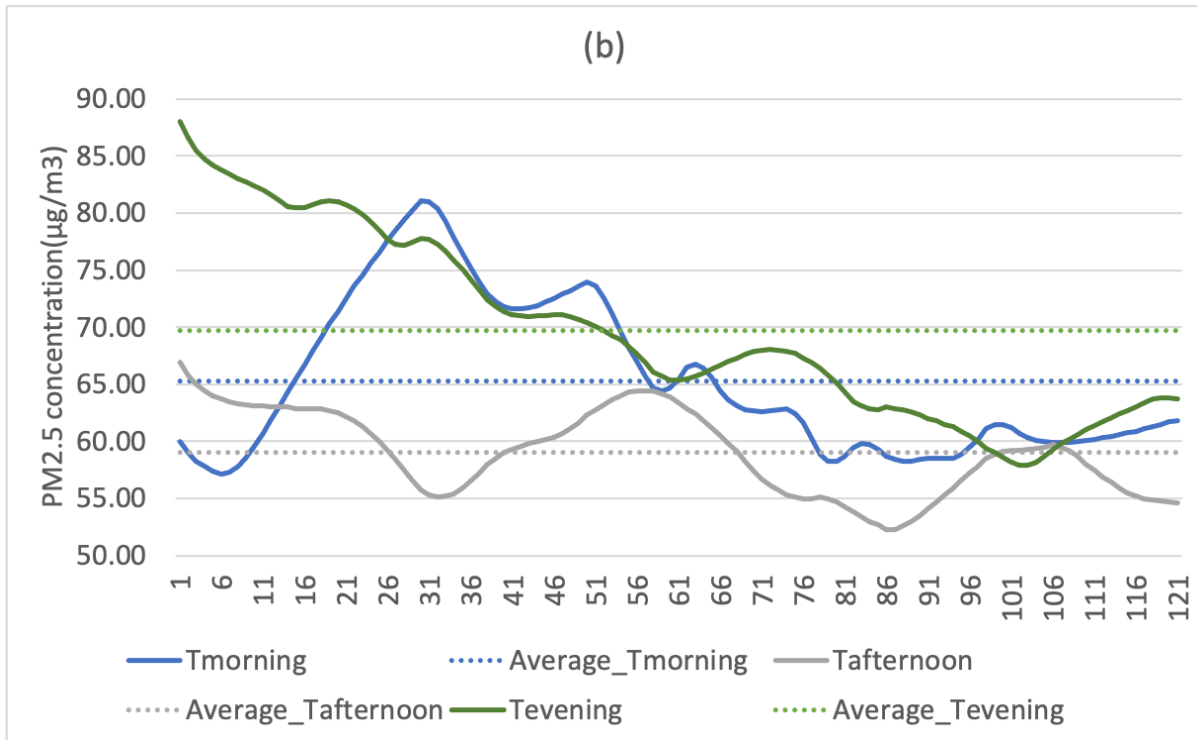


Figure 5-8 Line graphs of simulated PM_{2.5} concentration(µg/m³) in (a)compact-H zone and (b)open-H zone over 30 minutes

5.4.2. Comparison of real-world data and simulated results

Comparing the real-world data and simulation results is an important method of model validation. Analysing the difference between the monitored and simulated PMs concentration would clearly show to what degree the simulation model is able to represent the real situation.

Table 5-5 Monitored and simulated PM₁₀ concentration in compact-H zone and open-H zone over 30 minutes, and the percentage difference between monitored and simulated PM₁₀ concentrations.

Time	Compact-H PM ₁₀ concentration (µg/m ³)			Open-H PM ₁₀ concentration (µg/m ³)		
	Monitored	Simulated	Difference between monitored and simulated	Monitored	Simulated	Difference between monitored and simulated
T _{morning}	280.0	293.0	4.65%	356.4	331.5	-6.99%
T _{afternoon}	385.8	401.5	4.07%	486.0	454.0	-6.58%
T _{evening}	322.5	341.1	5.77%	377.5	385.6	2.15%

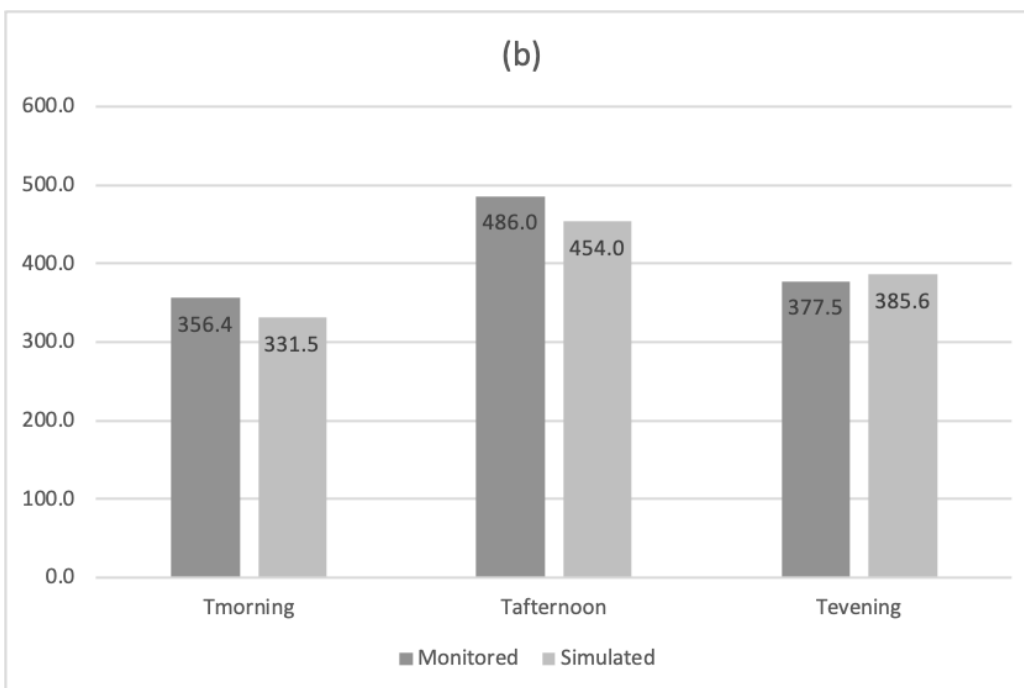
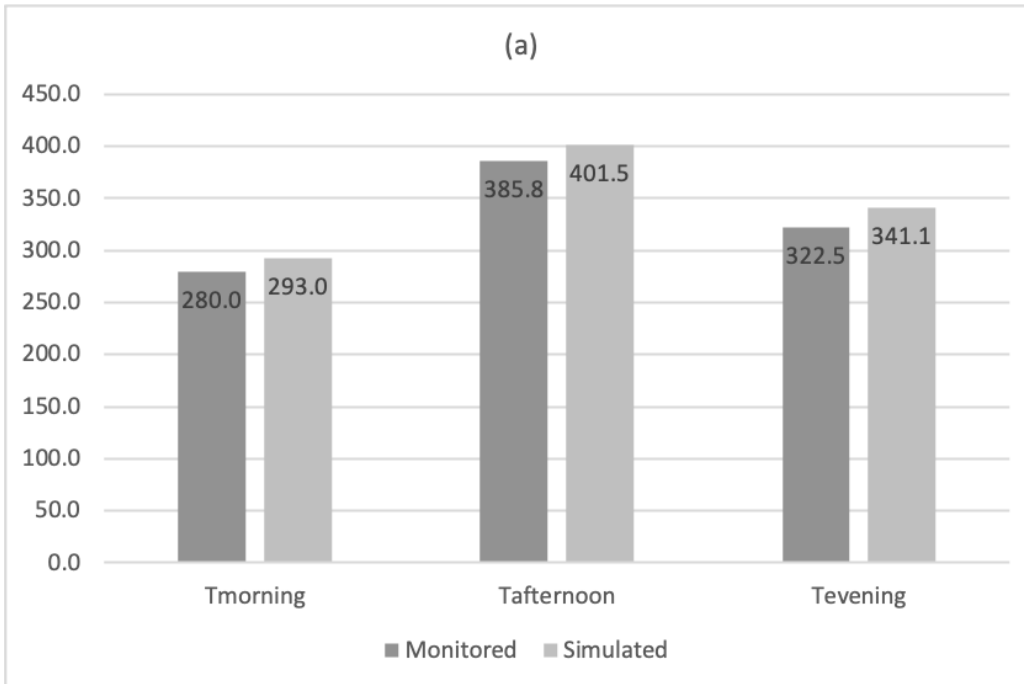


Figure 5-9 Monitored and simulated PM10 concentration in (a) compact-H zone and (b) Open-H zone.

Table 5-5 and Table 5-6 show the average monitored and simulated PM10 and PM2.5 concentrations in the compact-H zone and open-H zone, and the percentage of difference between them. Generally, both the monitored and simulated data show that the PM concentration in the compact-H zone is lower than that of the open-H zone. The highest PM10 concentration in both zones is measured in the afternoon and the lowest is in the morning time, as shown in Figure 5-9. The same results are predicted by the simulation. This is because the PM concentration in Kang Le Road (see in

Table 5-2) is higher, so more pollutants were transported into the two zones. This is also the reason for the 25.3% difference between the simulation and measurement of the PM_{2.5} concentration in compact-H zone in the afternoon. Due to the very limited equipment (one PM sensor and one anemometer) for measuring the real-world data, the PM data was monitored in each location at different time periods. In addition, it is almost impossible to monitor all changes of pollutant sources for each zone at the same time as monitoring the PM concentration in the zones. Therefore, the higher simulation result might be caused by increasing traffic flow during pollutant source monitoring. However, for the rest of time, the road traffic emissions were generally stable and continuous. On the other hand, this shows the dry deposition model is quite sensitive to changes in the source pollution.

Table 5-6 Monitored and simulated PM_{2.5} concentration in compact-H zone and open-H zone over 30 minutes, and the percentage difference between the monitored and simulated PM_{2.5} concentrations.

Time	Compact-H PM _{2.5} concentration (µg/m ³)			Open-H PM _{2.5} concentration (µg/m ³)		
	Monitored	Simulated	Difference between monitored and simulated	Monitored	Simulated	Difference between monitored and simulated
T _{morning}	53.1	57.0	3.9 (7.3%)	70.3	65.3	5.0 (-7.2%)
T _{afternoon}	41.1	51.5	10.4 (25.3%)	54.0	59.0	5.0 (9.2%)
T _{evening}	59.9	60.8	0.9 (1.5%)	72.2	69.7	2.5 (-3.5%)

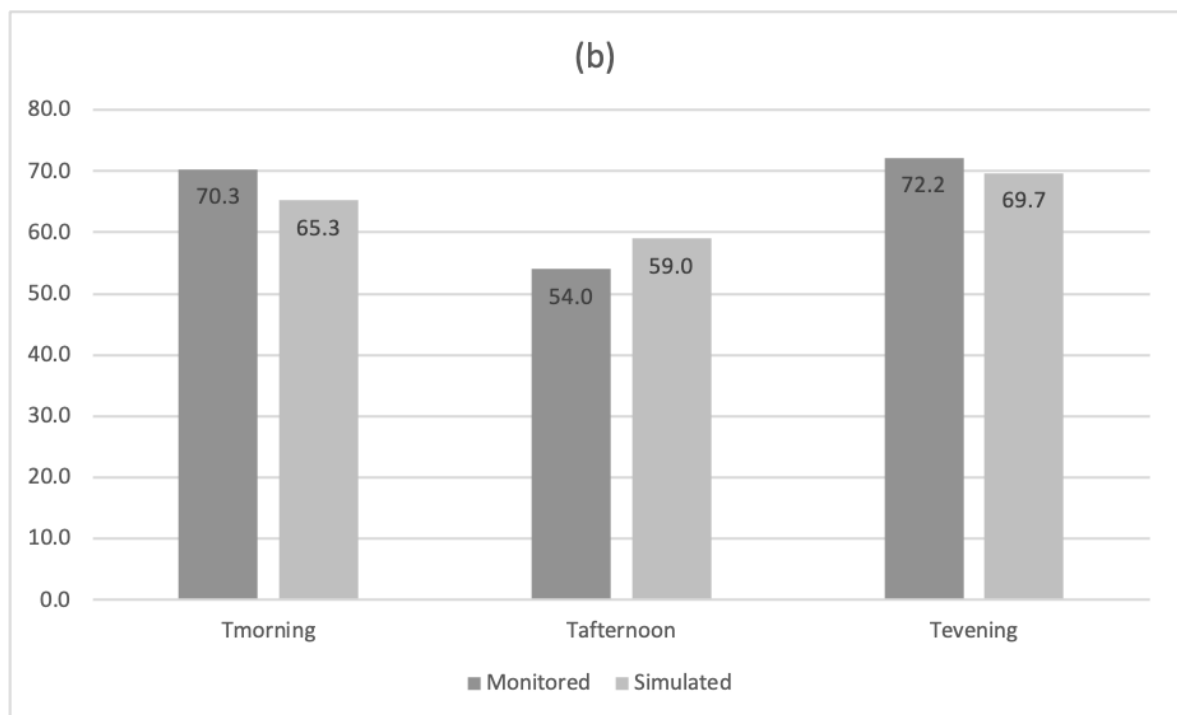
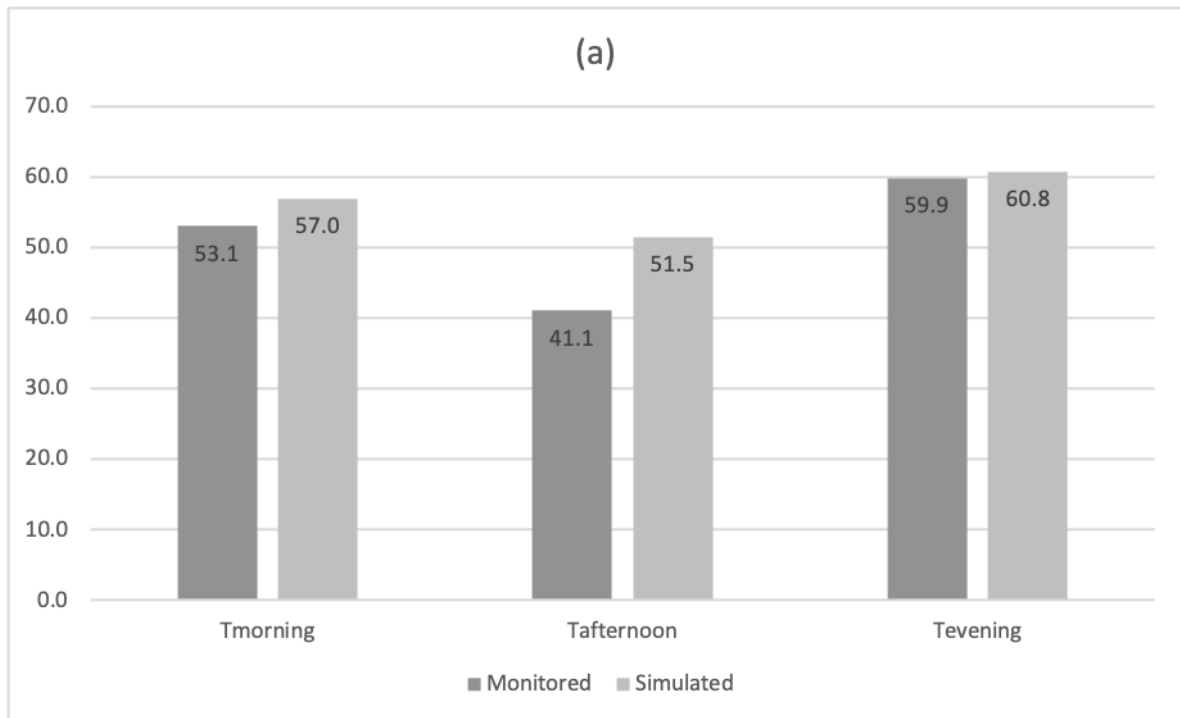


Figure 5-10 Monitored and simulated PM_{2.5} concentration in (a) compact-H zone and (b) Open-H zone.

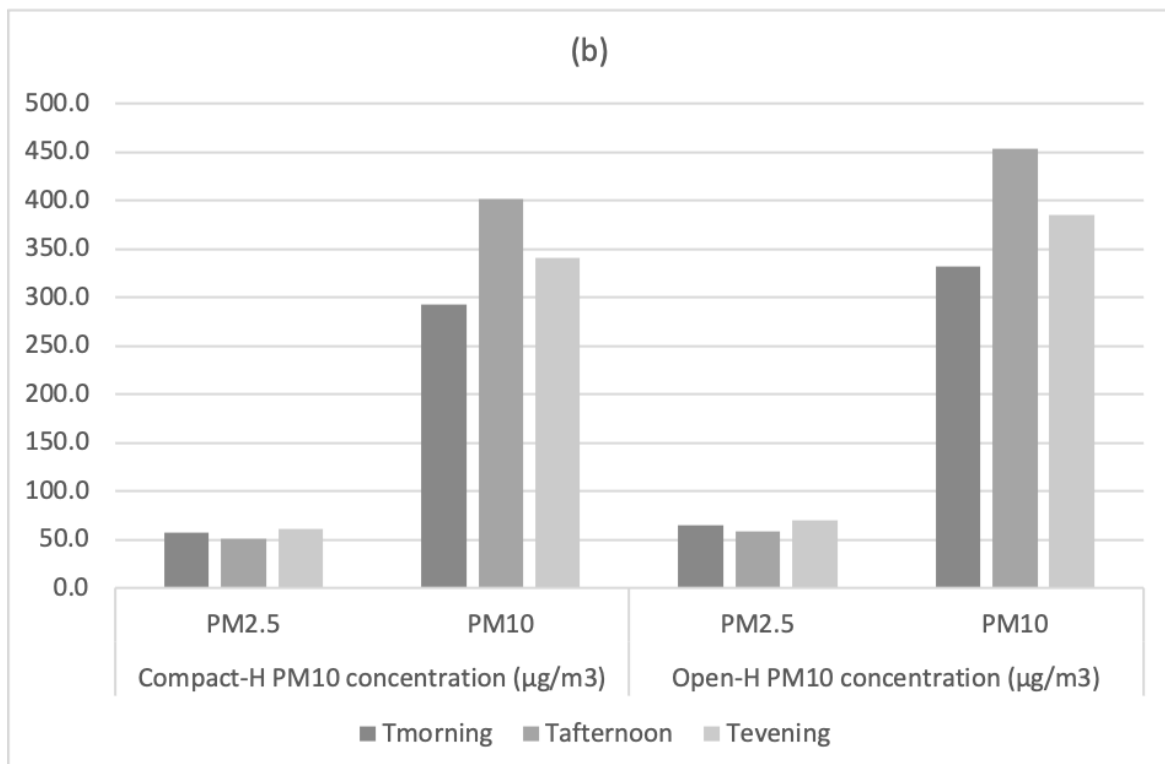
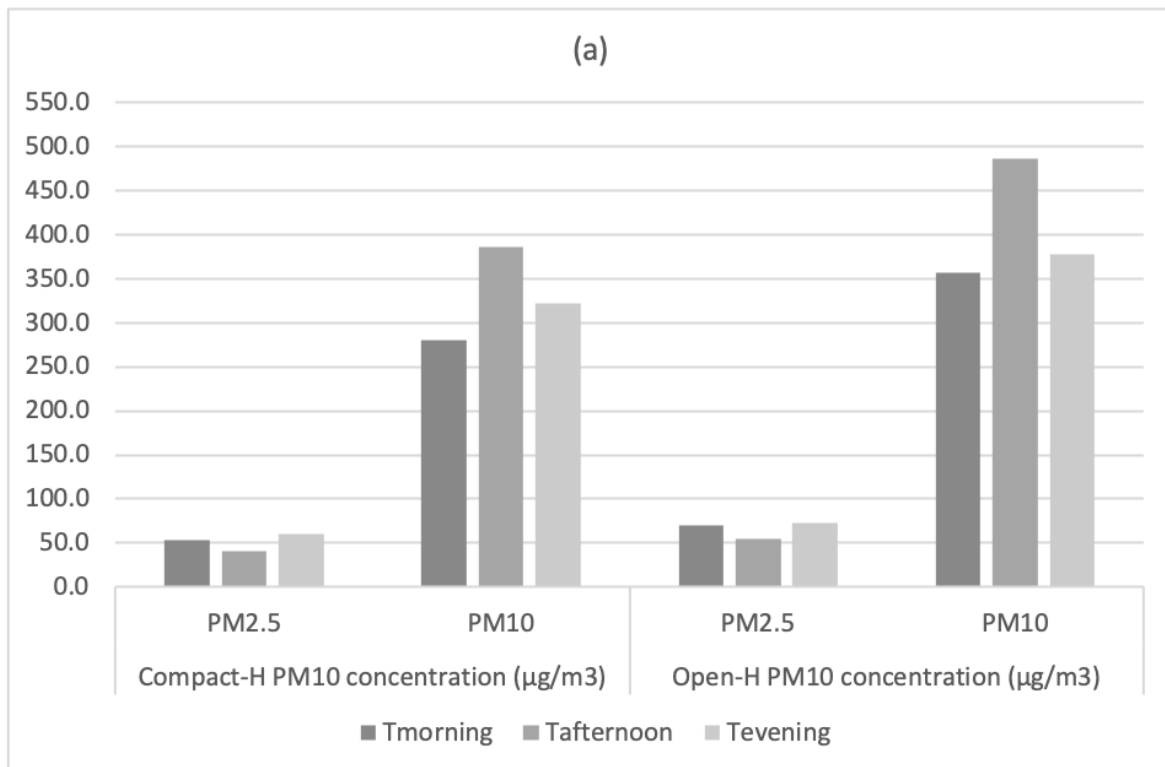


Figure 5-11 Average concentration of PM2.5 and PM10 by (a) monitoring and (b) simulation in compact-H zone and open-H zone

Except for the PM_{2.5} concentration in compact-H zone in the afternoon, the average PM₁₀ and PM_{2.5} concentrations in Table 5-5 and Table 5-6 present a difference of less than 10% between the real-world data and simulation. Moreover, Figure 5-11 shows that the monitored PM_{2.5} concentration is much lower than the PM₁₀ concentration in both zones, which means that PM₁₀ is the main particulate air pollutant in this area. The simulation demonstrates similar results with less than 10% difference. This difference suggests that based on a stable and continuous pollutant source and low aerodynamic effects, this dry deposition model simulation is not only able to represent the real scenario, but also able to work for different PM concentration levels.

In addition, a second monitoring process was planned, which would use more monitoring equipment, but it could not be completed. Due to the global COVID-19 situation, I am unable to get more real-world data. However, the comparison completed during the 2019 period is adequate to verify and validate the simulation model. Nevertheless, future improvement (e.g., the constants used in

Table 5-2,

Table 5-3, APPENDIX 7-5) can be optimised in the future to improve the accuracy of the model.

5.5. Conclusion

The V&V system and various validation methods (Thacker et al. 2004; Sargent, Balci 2018; Kleijnen 1995; Oberkampf, Trucano 2002; Robinson 1997; Chan et al 2004) are reviewed in this chapter to develop a validation method for the dry deposition model. Based on the validation method, two zones were identified for real-world data monitoring. After this, meteorological data (wind speed, humidity, and temperature) and PM concentration data were monitored at the two zones. To remedy the aerodynamic effects, the locations of two zones and time of monitoring were chosen carefully. First, the locations are chosen to be on each side of the same road and have similar surrounding building materials, and heights, and functions. Controlling for these variables means that, first, vehicle exhausts from this road are the main PM source, and second, the similarity between the building and land surface, and human activities in the area, would impact the PM concentration to the same extent. Moreover, monitoring took a place during the day when there was a low wind speed to ensure measurements were taken under stable and continuous pollutant source conditions. The monitored PM concentration data have been compared with the simulation results to validate the dry deposition model. The comparison of the real-world data and simulation results in the compact-H zone and open-H zone shows that the dry deposition model is able to represent the real-world situation with up to 9.2% deviation for most of the time slots. In conclusion, the simulation model can show the particle pollution concentration changes of the mid-scale urban environment based on the tree deposition effect to a certain degree with a stable pollutant source, which will be used as the main part of the green planning model to explore optimum levels of green space and improve local green infrastructures.

However, the equipment (one PM sensor and one anemometer) was limited for the real-world data monitoring, so the pollution concentration from Kang Le road and from compact-H zone and open-H zone were not monitored at the same time. To minimize this impact, I chose the monitored time when there was low wind speed and stable traffic flow.

Moreover, due to the travel restrictions of COVID-19 in China, I couldn't go back to Taiyuan to monitor more data, the real-world data for the modal validation is limited. Hence, a mid-scale area located in the open-H zone will be used as the study area to quantify pollution removal of different green plans by this green planning model.

Chapter 6. Development of optimum
urban green plans for air quality
improvement in mid-scale urban
residential areas — Simulation and
discussion

6.1. Introduction

The question 'how much green space should a city have?' has been asked since the 1920s, but discussions only really started in the 1930s. In fact, the idea of urban green spaces only became more important and popular after World War II. Harnik (2010) defined and classified different kinds of urban green spaces and their size, facilities, and distance from the city, and argued that a standard amount of green spaces, and number of facilities and programs, is what cities wanted. This research aims to develop a new tool for architects and designers to 'meet greenery into their designs' (Ong 2003). The amount of pollution removal could act as a variable in the model to show how different Urban Green Infrastructure plans affect air quality. Dry deposition has been incorporated into this tool to estimate the amount of air pollution removal. This study aims to explore and develop the optimum green plans for air quality improvement in mid-scale residential areas. To achieve this aim, a green planning tool has been developed in this study. This tool integrates together two simulation models, which are a CFD model and a dry deposition model. The deficiencies of current urban environmental models that are based on dry deposition process were discussed in chapter 3. These models do not focus on mid-scale (street or tree level) simulations, and they have limited consideration of the impact of wind speed and tree species. Therefore, the model developed in this study incorporates the effects of cover the wind speed in the mid-scale areas through aerodynamic simulation by an integrated CFD model. Moreover, a dry deposition model has been set up in a systems dynamics software (Vensim PLE) as an open-platform model that allows various tree species as an input variable. Through applying the proposed model in a study area, the question 'what are optimum green plans' would be propose answers. This chapter explores five scenarios of green plans for air quality improvement in mis-scale urban residential areas. The five scenarios are, 1) Green cover levels; 2) Source pollution concentrations; 3) Locations; 4) Monthly particle pollutants removal; and 5) Tree species. The urban green planning will be discussed from the aspects of green cover levels, source pollution concentrations, and tree species.

6.2. The study area

Anthropogenic activities and natural sources can create Particulate matter (PM) (Yang et al. 2017). Particle pollutants mainly affect the health of the respiratory and cardiovascular systems. Currently, PM₁₀ is measured by most routine air quality monitoring systems. Its mass and size is such that it can enter the respiratory tract, so it has been used in many epidemiological studies as the exposure indicator (WHO 2006). The 24-hour and annual average air quality guidelines (AQG) for PM₁₀ are 50µg/m³ (WHO 2006). According to multi-city studies in Europe, mortality will increase by 0.62% if the 24-hour average of PM₁₀ rises by 10 µg/m³ (Katsouyanni et al. 2001). PM₁₀ in most European countries was under 30µg/m³(Agency 2013), but in many cities in northern China, it was above 170 µg/m³ (Zhang et al. 2016). Taiyuan (Figure 5-2) is a northern Chinese city with high air pollution as it is heavily reliant on highly polluting coal for power.

First, a study area is selected from satellite images in Taiyuan city (see Figure 6-1). It is approximately 24,000 m² (120m×200m) and is located in the Yingze district. It is a residential area including 12 buildings, which are all about 18 meters high, and accommodate around 500 residents in total. There is a busy street on the north side with a high concentration of air pollution, making this residential area the desired mid-scale near-road residential area type that was discussed in chapter 4. Between the residential buildings in the study area, there are quiet roads and pavements. This area is substituted into ENVI-met based on its current land use, tree density, and local meteorological data. The simulation provides hourly data for further calculations in Vensim.



Figure 6-1 Satellite image of the study area in Taiyuan City. (Sourced from Baidu Map)

A field study took place to monitor meteorological data and local pollution concentration by anemometers and an air quality sensor. These data can be used to estimate the amount of PM₁₀ removed through dry deposition. Also, they could show current air quality and green plans in the study area. 10 hours of data were collected from the road next to the residential area. The data have been collected every hour for one day. Air quality data are collected by using a Dylos DC1100 (Innovation 2008) device. Two sizes of particles could be counted, which respectively have diameters between 2.5 to 10 micrometres (µm) and 0.5 to 2.5 µm (Williams et al. 2015). The Dylos PM shows particle numbers in .01 cubic foot of air. These data need to be converted to micrograms per cubic meter (µg/m³) for the later calculation using the dry deposition equations.

Particulate Matter mass concentration of micrograms per cubic meter could be calculated from the Dylos results as (Arling et al. 2010):

$$C_{PM} = N \times 3531.5 \times P_{PM} \times H \times c$$

Where CPM is the particle concentration, N is the number of particles, PPM is the mass of a particle, which for PM_{2.5} is 5.89E-7 µg and for PM₁₀ is 1.21E-4 µg, H is the relative humidity as a percentage, and c is the correction factor (6.4) (Arling et al. 2010).

Table 6-1. Meteorological data and PM₁₀ concentrations monitored in the study area.

Time	Humidity	Temperature	Wind speed (m/s)	PM ₁₀ concentration ($\mu\text{g}/\text{m}^3$)
8:00	19.5%	7.2°C	2.4	212.2
9:00	19.6%	14.2°C	2.8	188.5
10:00	12.0%	16.9°C	2.0	215.0
11:00	22.1%	18.3°C	2.6	247.6
12:00	17.9%	18.5°C	2.6	220.8
13:00	18.3%	20.6°C	2.1	339.7
14:00	25.8%	22.2°C	2.2	573.2
15:00	21.7%	19.1°C	2.6	433.5
16:00	23.8%	21.5°C	1.0	226.3
17:00	33.5%	18.4°C	1.2	394.7
18:00	31.8%	17.5°C	1.4	489.0

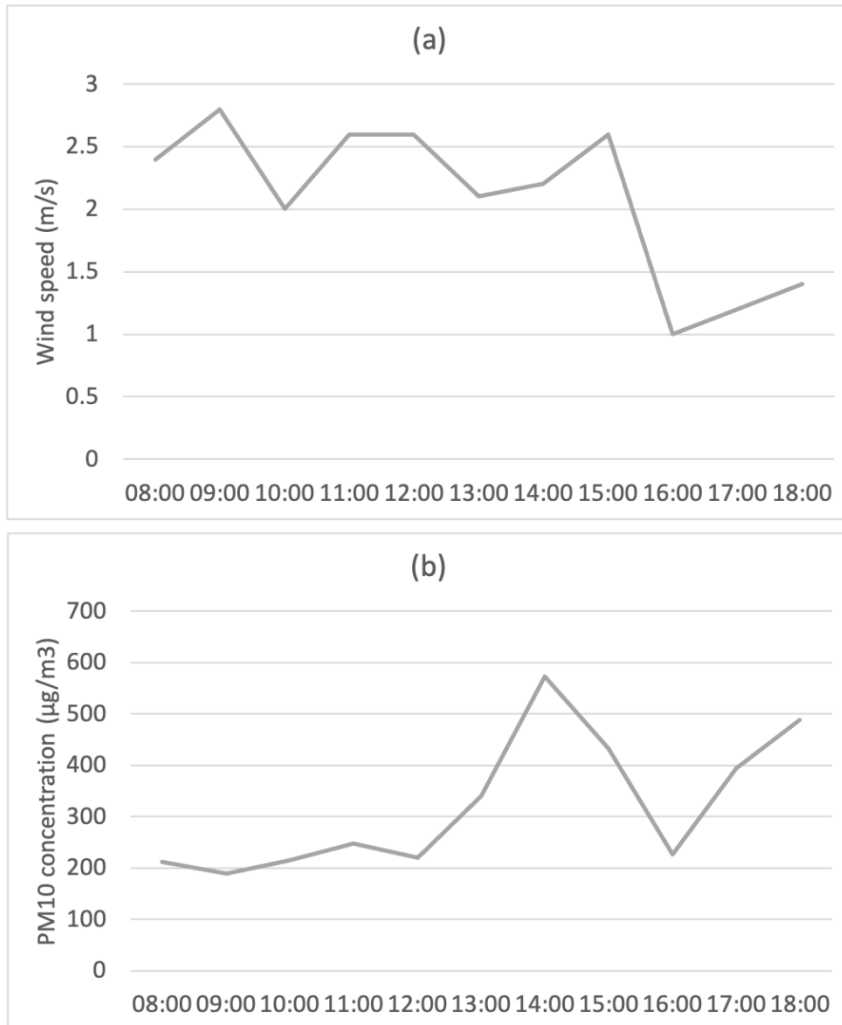


Figure 6-2 Line graphs of (a) monitored wind speeds (m/s) and (b) PM₁₀ concentration (µg/m³) in the study area from 8:00 to 18:00.

The data in Table 6-1 show that the PM₁₀ pollution concentration in the study area is very high, which would have a negative impact on people's respiratory systems. Even the lowest pollution concentration, which is 118.45 µg/m³ at 9am, was much higher than the air quality guidelines, which are 50 µg/m³ (WHO 2006). Figure 6-2 shows the monitored wind speed and PM₁₀ concentration from 8:00 to 18:00 in the study area. The wind speed (see Figure 6-2 (a)) remained steady at around 2.5 m/s until 15:00, then it dropped to 1 m/s in the evening. The PM₁₀ concentration (see Figure 6-2 (b)) rapidly climbed to 573.20 µg/m³ at 14:00, and to 489.04 µg/m³ at 18:00. This could be caused by the increased traffic during the rush hours, which coincides with the time of the peak pollution concentration.

6.3. Scenario development

Five scenarios have been set up to explore the optimum green plans for air quality improvement by dry deposition in the study areas. Various plans, such as different percentages of green cover, source pollution concentrations, locations, and species of trees in the area and monthly average wind speed in Taiyuan, are estimated and discussed. This study monitored both PM₁₀ and PM_{2.5}, but the data of the PM_{2.5} concentration was missing due to technical issues. However, as showed in the validation chapter, the total amount of PM₁₀ and PM_{2.5} removal exhibited similar trends as they have been calculated based on the same dry deposition equations. Therefore, the scenarios will focus on quantifying PM₁₀ removal by the dry deposition model. Different inputs data based on the scenarios are entered into the integrated model to calculate the amounts of PM₁₀ removal for 10 hours through deposition on leaf surfaces. There are two reasons for choosing the 10-hour simulation period, which are, first, the field study in the chosen study area monitored air quality and other meteorological data for 10 hours from 8:00 am to 18:00, and these data are used to setup the model boundary; second, ENVI-met calculates air flow changes based on a CFD simulation model, which requires a length of time for the simulation that is similar to the length of time being simulated. Therefore, simulation of a 10-hour period would take around 8 to 10 hours. Considering the monitored data and time consumption, a 10-hour simulation time has been applied for all scenarios.

Table 6-2 Variables and constants of input data for each scenario.

Green plans	Variables	Constants
Scenario 1 – Green cover levels	LA ¹ ; WS ²	SPC ³
Scenario 2 – Source pollution concentrations	SPC	LA; WS
Scenario 3 – Locations	WS	SPC; LA
Scenario 4 – Monthly particle pollutants removal	SPC; WS	LA
Scenario 5 – Tree species	LA	WS; SPC

¹ Leaf area

² Wind speed

³ Source pollution concentration

6.3.1. Scenario 1 – Green cover levels

One of the common concerns with urban green planning is about how many trees a city needs to achieve better air quality (Richardson et al. 2012). Scenario 1 will estimate PM10 removal for 10 hours based on different numbers of trees in the study area. Table 6-3 shows that the percentages of tree cover increases from 7% to 100%, because the study area currently has 121 trees, which is 7% of the whole area. The percentages have been calculated in ENVI-met using the maps (see Figure 6-4) that were taken from the satellite images (see Figure 6-1). Figure 6-4 (a) is based on the real situation in the area, in which the grey blocks represent the residential buildings, and the green blocks represent the trees and their locations. The satellite image (Figure 6-1) is simplified into a set of 50 X 50 blocks to represent buildings, land, and vegetation in the area. Figure 6-4 (b) – (e) are hypothetical situations to explore optimum green levels.

The average wind speeds in Table 6-3 are simulated using ENVI-met. These wind speeds allow the dry deposition model to quantify particle pollutants removal more precisely as the tree crown densities impact the wind speed in the surrounding areas. The model boundary conditions in ENVI-met are shown in Table 6-4. The simulation takes place in April when tree leaves are in their best conditions.

The total leaf areas in Table 6-3 are calculated by:

$$s_c \times LAI_{DBL} = s_t \quad (6-1)$$

where s_c is the tree crown area (m²), LAI_{DBL} is the mean LAI of the deciduous broad leaf trees, and s_t is total leaf area. The study area is mainly covered by deciduous broad leaf trees (BoDBL). Based on the summary of LAI by biomes in Table 6-13, a common LAI measurement of deciduous broad leaf trees in the summer is found to be 2.6.

Table 6-3 Input data for scenario 1 simulation.

Numbers of trees	Tree Crown area (m ²)	Total leaf area (m ²)	Average wind speed (m/s)	Percentage of land cover by trees (%)	Source pollutant concentration
121	756.3	1951.1	2.9	7 ¹	(1, 212.2), (2, 188.5), (3, 215.0),
246	1537.5	3967.9	2.8	14	(4, 247.6), (5, 220.8),
430	2687.5	6935.9	2.7	25	(6, 339.7), (7, 573.2),
859	5368.8	13855.7	2.7	50	(8, 433.5), (9, 226.3),
1718	10737.5	27711.3	2.5	100	(10, 394.7), (11, 489.0)

¹ 7% of the study area is currently covered by trees

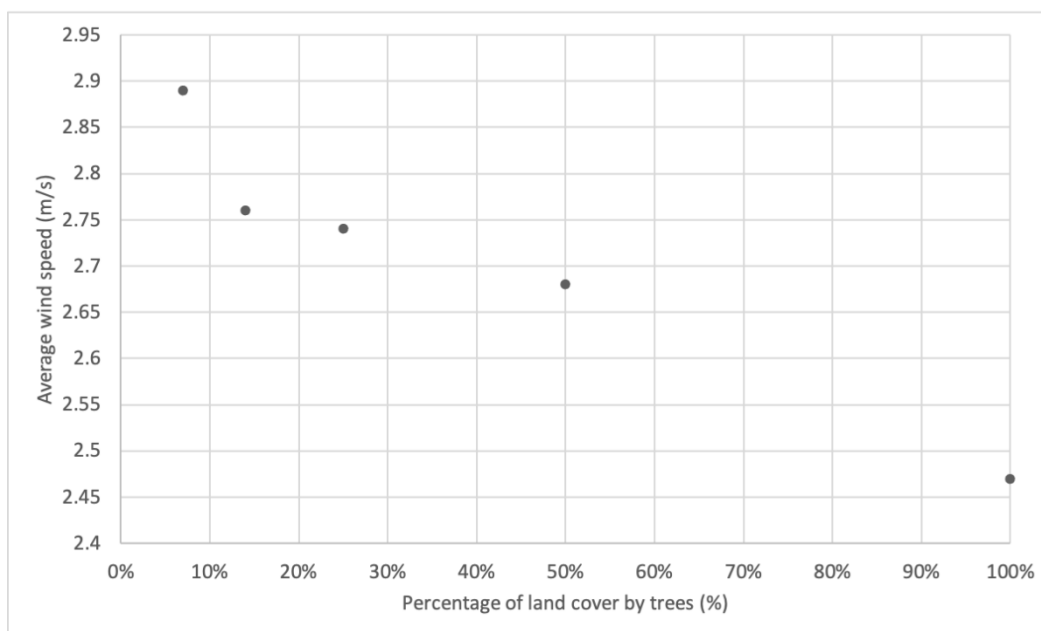


Figure 6-3 Average wind speed simulated by ENVI-met based on different green levels.

Table 6-4 Meteorological boundary conditions for ENVI-met simulation

Air temperature (°C)	10 - 30
Wind speed (m/s)	2.4
Wind direction	East
Roughness length at the site	0.010
Relative humidity (%)	20 to 50
Total simulation time (h)	10
Start time	8:00 am

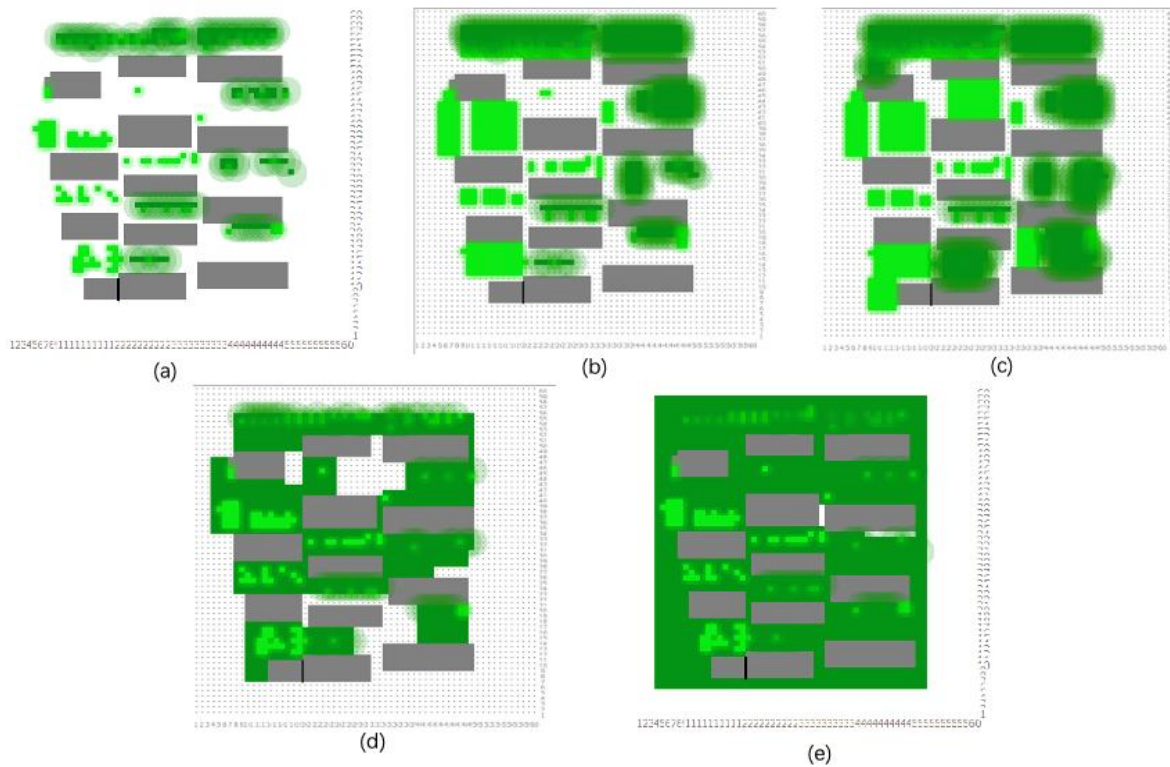


Figure 6-4 Maps of the study area in the ENVI-met interface showing (a) 7%, (b) 14%, (c) 25%, (d) 50%, (e) 100% of land covered by trees.

6.3.1.1. Results and discussion

Table 6-5 Average PM₁₀ concentration (µg/m³) in the study area and Total amount of PM₁₀ removal by different green levels (µg) in 10 hours.

Percentage of land cover by trees (%)	Average PM ₁₀ concentration (µg/m ³)	Total amount of PM ₁₀ removal (µg)
7 ¹	360.0	155.4
14	216.2	187.0
25	131.1	198.9
50	68.2	206.3
100	34.3	210.2

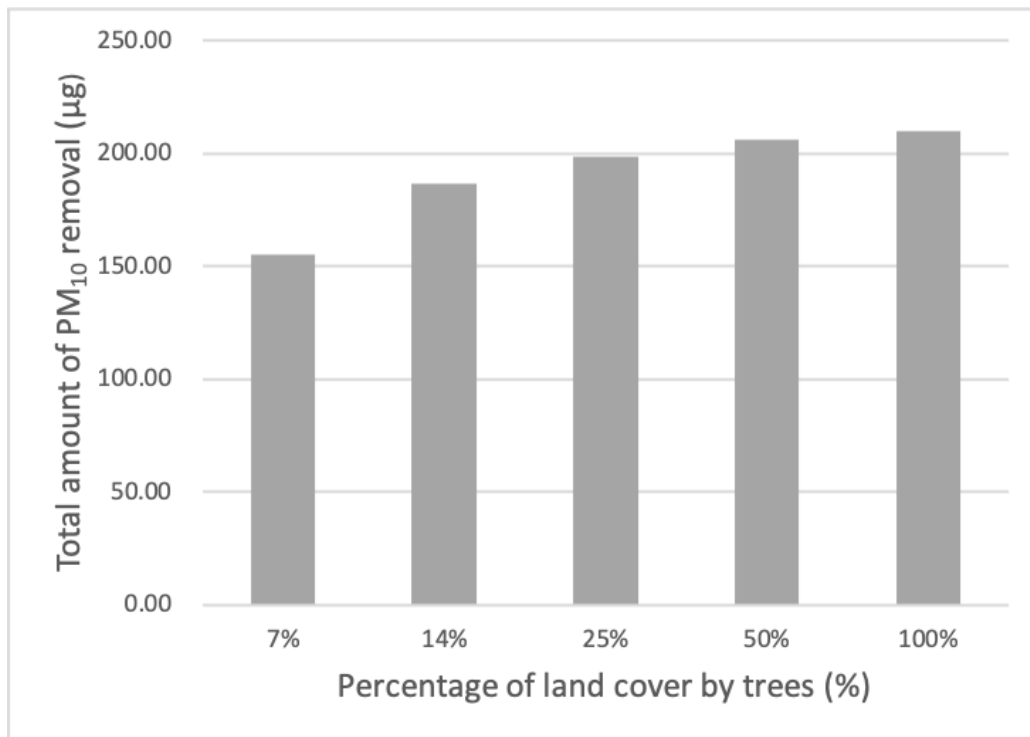


Figure 6-5 Total PM₁₀ removal by different percentages of land covered by trees in a 10-hour simulation.

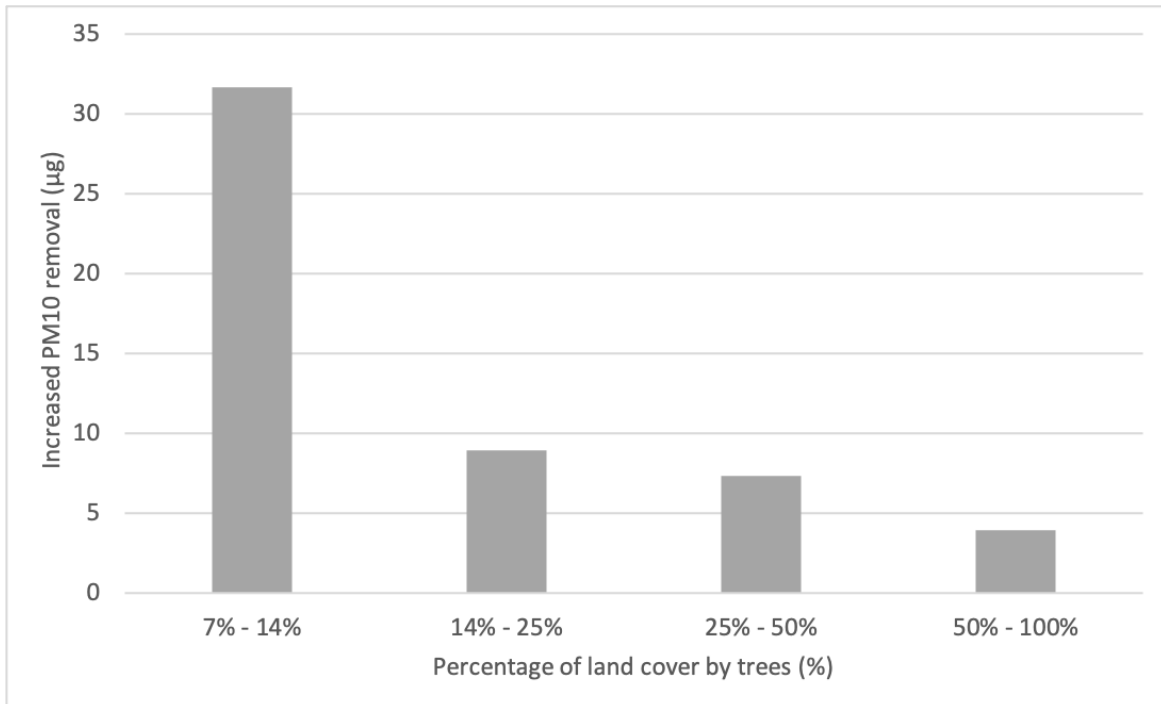


Figure 6-6 Increased PM₁₀ removal between different green cover levels.

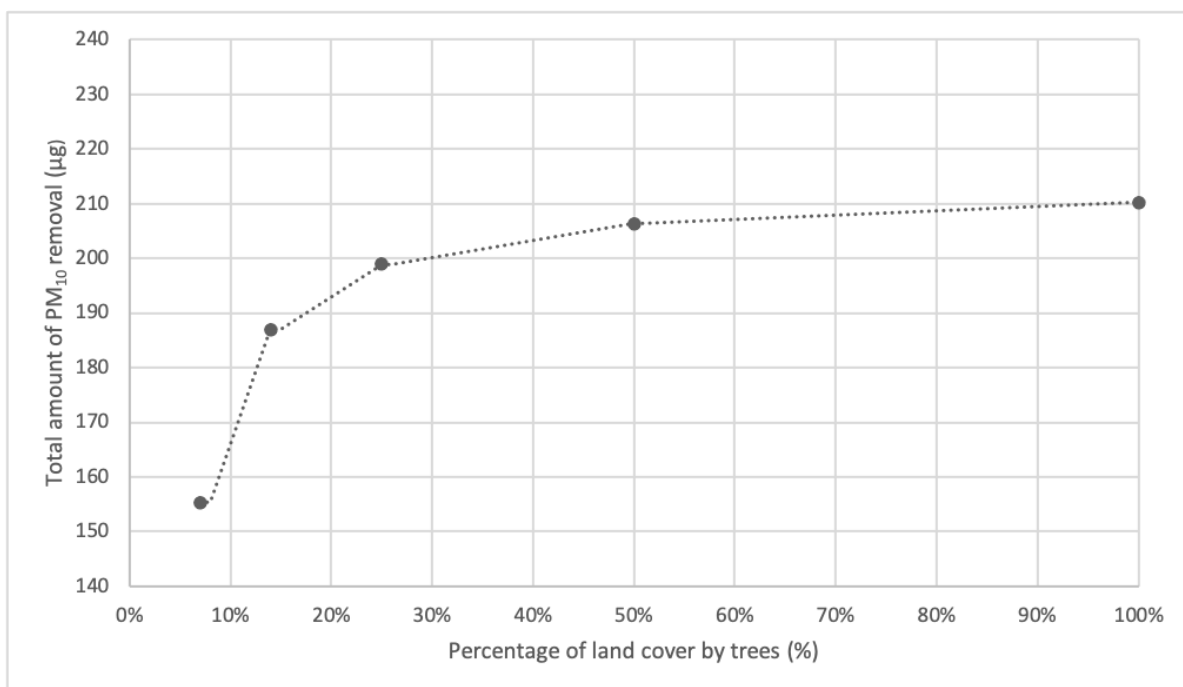


Figure 6-7 The rising rate of PM₁₀ removal by different percentages of land cover by trees.

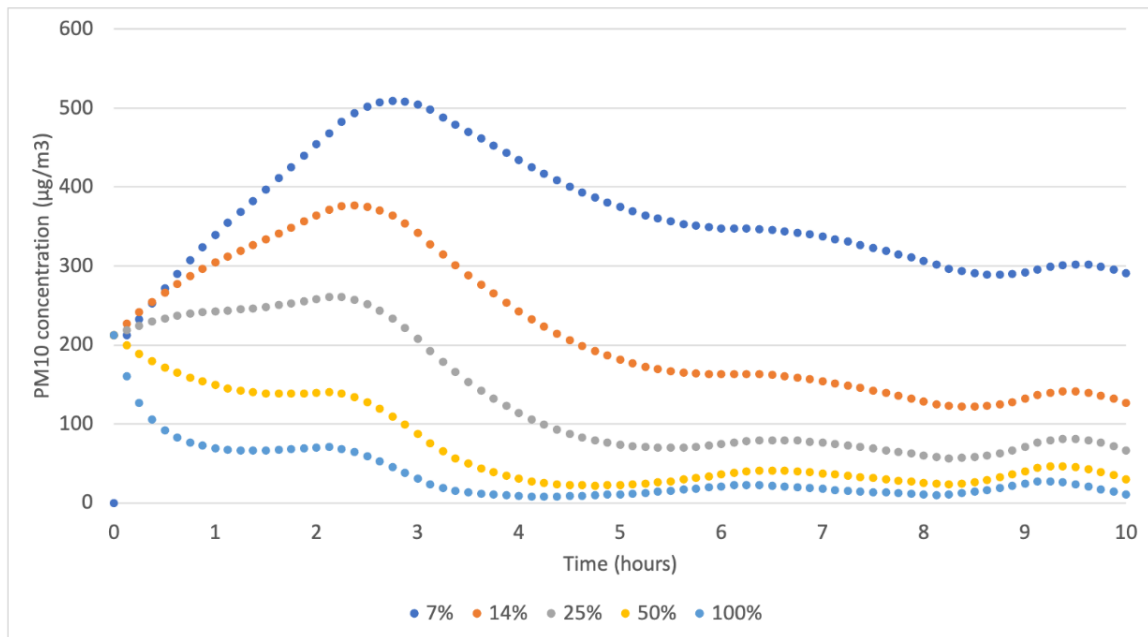


Figure 6-8 PM₁₀ concentrations estimated by the dry deposition model in Vension PLE based on different percentages of green cover for 10 hours.

Simulation results of PM₁₀ dry deposition for different levels of green cover in the study area are shown in Table 6-5. On average, the PM₁₀ removal estimated by the integrated model was 155.3, 187.0, 198.9, 206.3, and 210.2 µg in 10 hours at 7%, 14%, 25%, 50%, 100% green levels, respectively. On the other hand, the average pollution concentration for 10 hours in the study area dropped from 360.0 to 34.3 µg/m³ when the green level was increased from 7% to 100%. Figure 6-8 shows that the average PM₁₀ concentration was estimated by the dry deposition model after pollution mitigation by various green levels. There are a lot of similarities between the trends of average pollution concentration in Figure 6-8, which shows dry deposition process is steady and the differences come from various sizes of green spaces. The pollution removal was generally increasing with larger green spaces (see Figure 6-5). However, the rising trend was uneven. As Figure 6-7 shows, the number sharply went up to 186.99 µg from 155.35 µg when the percentage green cover rose to 14%, which is only a 7% increase. When the green level rose from 50% to 100%, which is a 50% increase, the amount of pollution removal only increased by 3.94 µg. Hence, based on the rising rate of PM₁₀ removal, the green levels between 14% and 25% in the study can provide a relatively high efficiency for air pollution mitigation. Although there was more PM₁₀ removed by larger green spaces, the increased amount seems unworthy considering the expenditure that is

needed to increase the green cover by such huge number of trees in a residential area. The question now is how many trees does this area need to promote the high efficiency of PM₁₀ removal. The simple answer is as much as possible. However, green spaces should not be the only fact to be considered in urban planning development. Moreover, the results from this scenario proved that the highest rising rate of dry deposition efficiency appeared between 14% to 25% of green cover (Figure 6-7). Although 14 % of green cover shows a high efficiency of pollution removal, it was based on the specific urban form and land type in the study area. This green cover level can still be used as a reference for urban green plans, and it also presents a way to use the integrated model proposed in this research for different urban forms and land types. In the following scenarios, 14% of green cover has been used as it is the optimum plan for this study area.

6.3.2. Scenario 2 – Source pollution concentrations

The amount of PM₁₀ removal is also related with source pollution concentrations. More specifically, the question asked in this scenario is whether the dry deposition process is more efficient at high concentration levels. Hence, source pollution concentration is a continuous number for each pollution level when they are entered in the dry deposition model as inputs. The first source pollution level tested was taken from the air quality guidelines, which is 50 µg/m³ (WHO 2006), then 100 µg/m³ was added per level until 450 µg/m³ was reached. The input data for this scenario are listed in Table 6-6. 14% of the green cover level is chosen as it provides high efficiency of particle pollution removal based on the results from scenario 1, which is discussed in the following section.

Table 6-6 Input data for scenario 2 simulation

Source pollution concentration levels	Numbers of trees	Tree Crown area (m ²)	Total leaf area (m ²)	Average wind speed (m/s)	Percentage of land cover by trees (%)
Level_1 (50 µg/m ³)					
Level_2 (150)					
Level_3 (250)	246	1537.5	3968.0	2.8	14
Level_4 (350)					
Level_5 (450)					

6.3.2.1. Results and discussion

Table 6-7 Total amount of PM₁₀ removal in the study area with different source pollution concentrations for 10 hours.

Source pollution concentration levels	PM ₁₀ concentration (µg/m ³)	Total amount of PM ₁₀ removal (µg)
Level_1	50.0	27.8
Level_2	150.0	83.4
Level_3	250.0	139.0
Level_4	350.0	194.6
Level_5	450.0	250.2

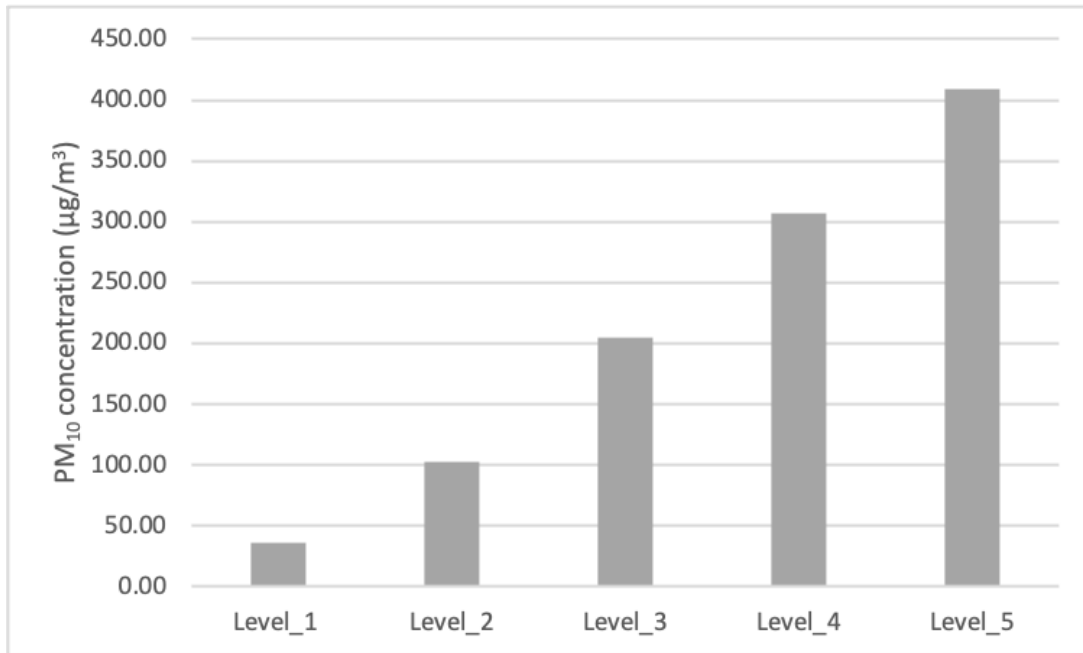


Figure 6-9 Different levels of source PM₁₀ concentration in the study area after 10-hour dry deposition process by trees.

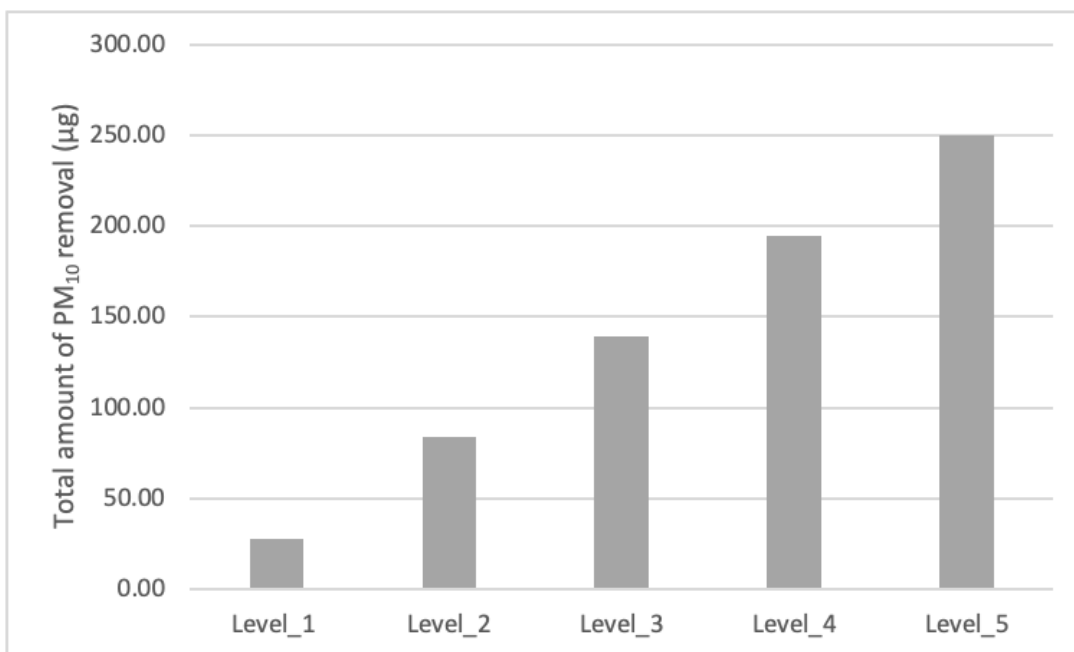


Figure 6-10 Total PM₁₀ removal at different source pollution concentration levels.

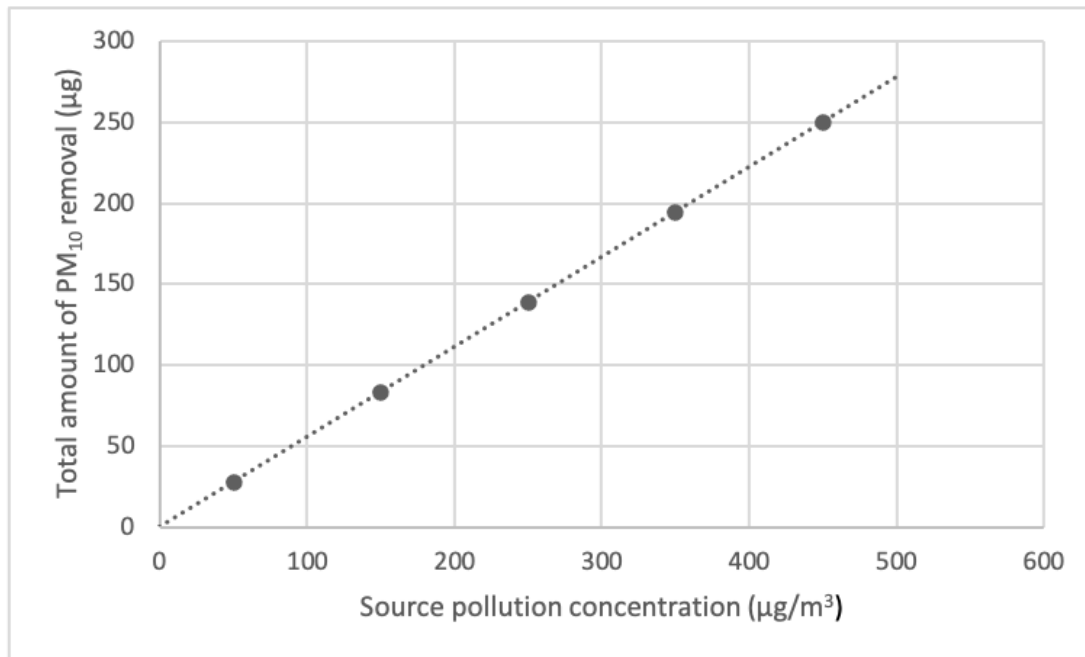


Figure 6-11 The rising rate of PM_{10} removal across different source pollution concentration levels.

Due to the good performance of the 14% green level, this scenario was simulated based on the model boundary of this green level. Total pollution removal estimated in the study are presented in Table 6-7. Dry deposition by trees shows a rising trend with higher pollution concentration (see Figure 6-9 and Figure 6-10). In general, Figure 6-11 showed that more pollutants can be removed by trees in the area with higher pollution concentration. However, the pollution removal was impacted more by the pollution source than by green levels, which means that when pollution concentration in an area is very high, the effect of pollution mitigation by trees would be limited. This can be shown in Figure 6-9, the pollution concentration in the study area after dry deposition process by trees was still high. For example, at source pollution level 5, the source pollution concentration was $450.0 \mu\text{g}/\text{m}^3$, and it decreased to $408.4 \mu\text{g}/\text{m}^3$ after removing by trees. It means that trees can only remove certain amount of pollutants in the study area. Absorbing particle pollutants by urban vegetation is unable to bring a huge improvement of local air quality. In chapter 2, it was discussed that the deposition effects are lower than the aerodynamic effects (Vos et al. 2013). However, this does not mean dry deposition by trees is insignificant. First, the control of the pollution source is an important part in urban planning, but it is not discussed in this study. Second, compared with the aerodynamic effects on air pollution, dry deposition is a

consistent and stable process of pollution mitigation (Petroff et al. 2008). More specifically, green spaces can be designed and planned based on pollutant removal by dry deposition to achieve better air quality. Therefore, it is still good to plant trees in areas that have higher pollution concentrations.

6.3.3. Scenario 3 — Locations

This scenario explores the optimum locations of an individual tree to increase amount of pollutant removal. As shown in Figure 6-1, the special building layout would cause different wind speeds in the study area, which may impact the leave absorbing particles at crown level. Based on the same meteorological boundary conditions as in scenario 1 (see Table 6-4), wind speeds are simulated by ENVI-met in the study area without trees for 10 hours. Figure 6-12 shows the four locations chosen by different wind speeds that are caused by the residential buildings. Table 6-8 presents the simulated wind speeds at each location every 2 hours and the average speeds over 10 hours. By quantifying pollution removal in these locations, it might be possible to determine the optimal location to put trees. The dry deposition model analyses the effects of one tree in each location. The model boundary conditions are listed in Table 6-9.

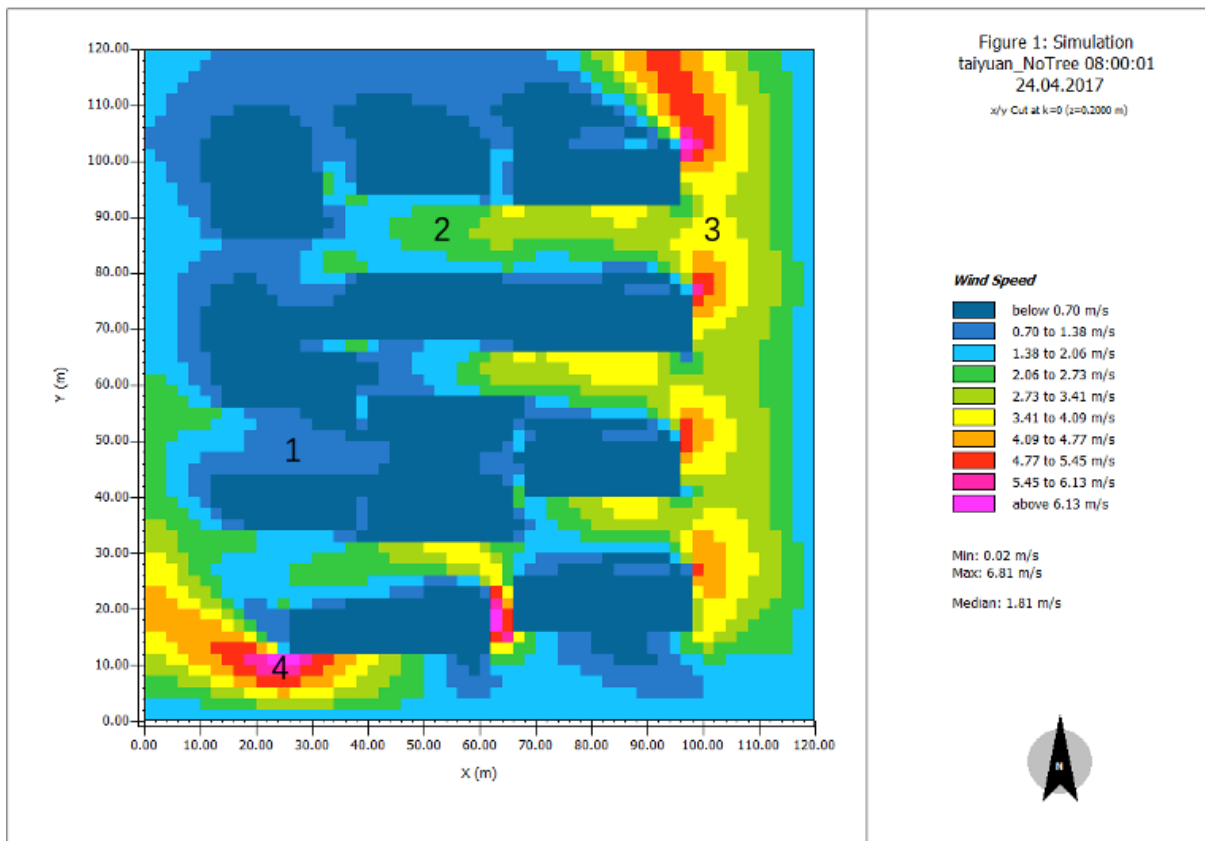


Figure 6-12 Four locations in the study area with different wind speeds.

Table 6-8 Simulated wind speeds (m/s) in the four chosen location.

	Location 1	Location 2	Location 3	Location 4
08:00	0.7	2.5	3.7	6.1
10:00	0.7	2.4	3.7	6.1
12:00	0.7	2.5	3.7	6.1
14:00	0.7	2.5	3.7	6.1
16:00	0.7	2.5	3.7	6.1
18:00	0.7	2.5	3.7	6.1
Average	0.7	2.5	3.7	6.1

Table 6-9 Input data for scenario 3 simulation

	Average wind speed (m/s)	Numbers of trees	Tree Crown area (m ²)	Total leaf area (m ²)	Source pollutant concentration
Location 1	0.7				(1, 212.2), (2, 188.5), (3, 215.0), (4, 247.6), (5, 220.8), (6, 339.7), (7, 573.2), (8, 433.5), (9, 226.3), (10, 394.7), (11, 489.0)
Location 2	2.5	1	6.3	16.1	
Location 3	3.7				
Location 4	6.11				

6.3.3.1. Results and discussion

Table 6-10 Total amount of PM₁₀ removal (10⁻⁵ µg) by a tree that planted in the four chosen locations.

	Average wind speed (m/s)	Total amount of PM ₁₀ removal (µg)
Location 1	0.7	0.3487
Location 2	2.5	0.3496
Location 3	3.7	0.3509
Location 4	6.1	0.3543

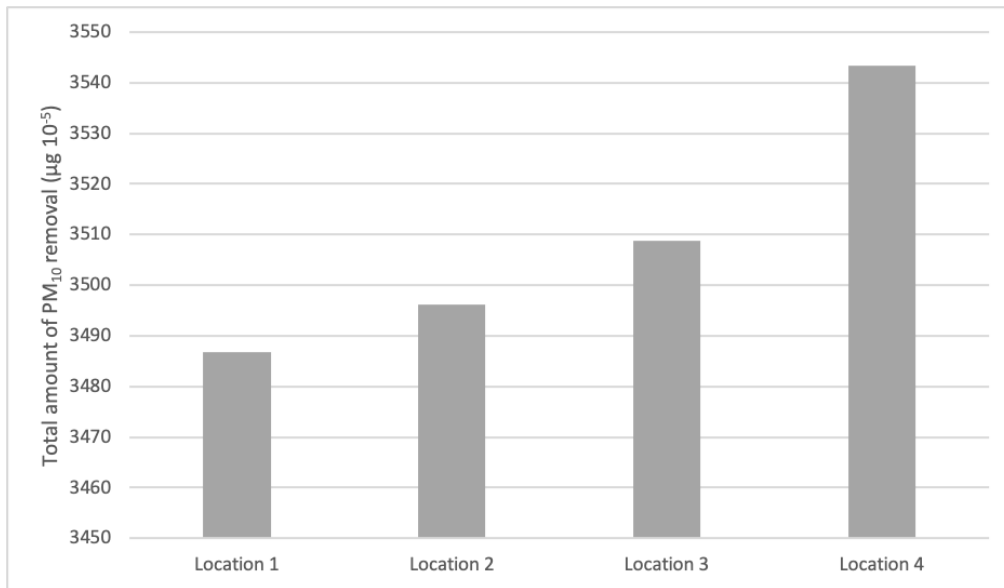


Figure 6-13 Total PM₁₀ removal (10⁻⁵ µg) in the four locations.

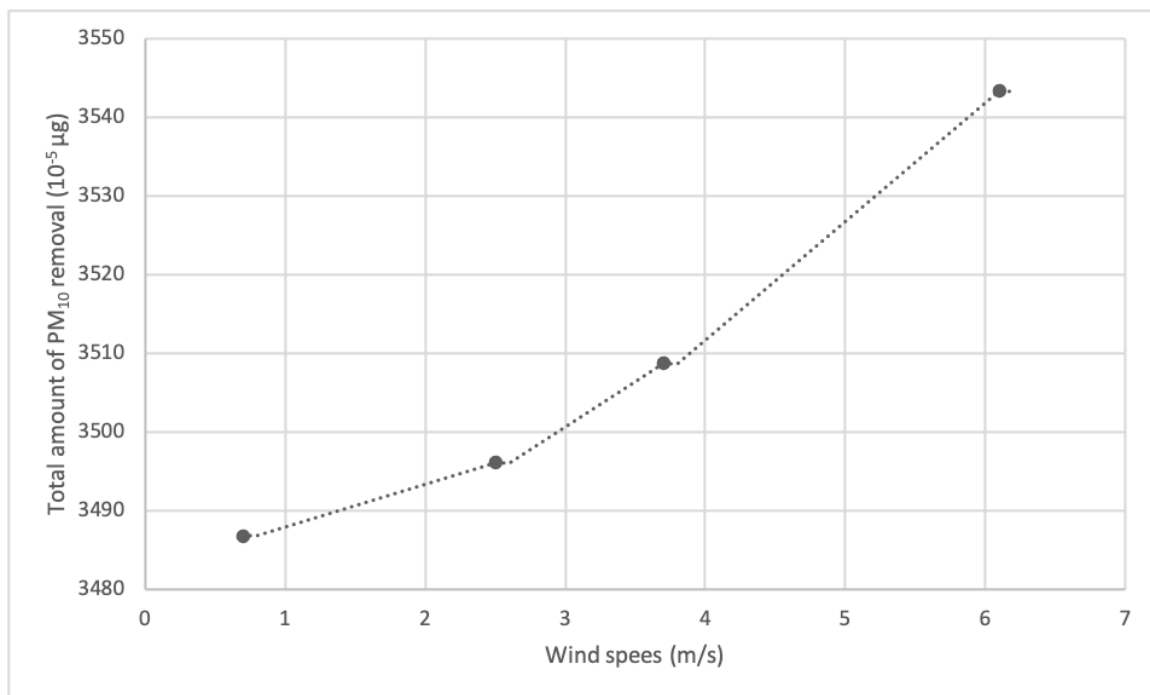


Figure 6-14 Rising rate of PM₁₀ removal (10⁻⁵ µg) under different wind speeds in the study area.

Different tree planting locations were selected according to their wind speeds in the study. This scenario aims to find optimal locations to plant trees for higher efficiency of pollution removal in a residential area. PM₁₀ removal by a single tree in the chosen locations is calculated by the dry deposition model, the results of which are shown in Table 6-10.

Throughout the four locations, wind speed increased from 0.7 to 6.1 m/s, and the total amount of PM₁₀ removal increased from 0.3487 µg to 0.3543 µg. The rates of PM₁₀ removal are magnified by 10⁵ in Figure 6-13 and Figure 6-14 times for clearer presentation, as the numbers of pollution removal in this scenario were based on a single tree. Results show that the tree in location 4 removed the most PM₁₀, which was under the highest wind speed (see Figure 6-13). A gradual climb is illustrated in Figure 6-14, which illustrates that more pollution was absorbed through dry deposition by one tree with a higher wind speed. Although there was more pollution removed with higher wind speeds, the amount absorbed in total is relatively small. Therefore, the impact of wind speed on the dry deposition process is less significant compared with the impacts of leaf area and pollution concentration. To increase the efficiency of pollution removal in the study area, leaf area should be increased in the locations where the wind speed and pollution concentration is high. The leaf area can be increased by planting more trees or planting trees with a bigger leaf area index in those locations. For developing a green plan, first a 14% level of green cover has been shown to achieve high efficiency of dry deposition; second, more pollution can be removed from higher pollution concentrations; then in this scenario, the simulation results show that trees should be planted locations with high wind speeds.

6.3.4. Scenario 4 — Monthly particle pollutants removal

The wind speed in Taiyuan changes over the year, as does the pollution concentration. This scenario calculates the monthly amount of PM₁₀ removal by areas with a 14% level of green cover. This would help to understand which months of the year will have better air quality. Source pollution concentration and wind speed data for each month are acquired from The Shanxi Province Environmental Monitoring Center (Sthjt.shanxi.gov.cn 2017). This scenario assumes that the source pollution and wind speed will be constant based on the monthly average data for the 10-hour simulation period. The input data are listed in Table 6-11. As this scenario simulates the whole year, temperate evergreen broadleaf (TeENL) trees are applied in this area for the simulation, which means that the leaf area does not decrease

during the winter. The leaf area index of evergreen needleleaf trees is 5.5 (see Table 6-13), so the total leaf area is 8456.3 m².

Table 6-11 Input data for scenario 4 simulation.

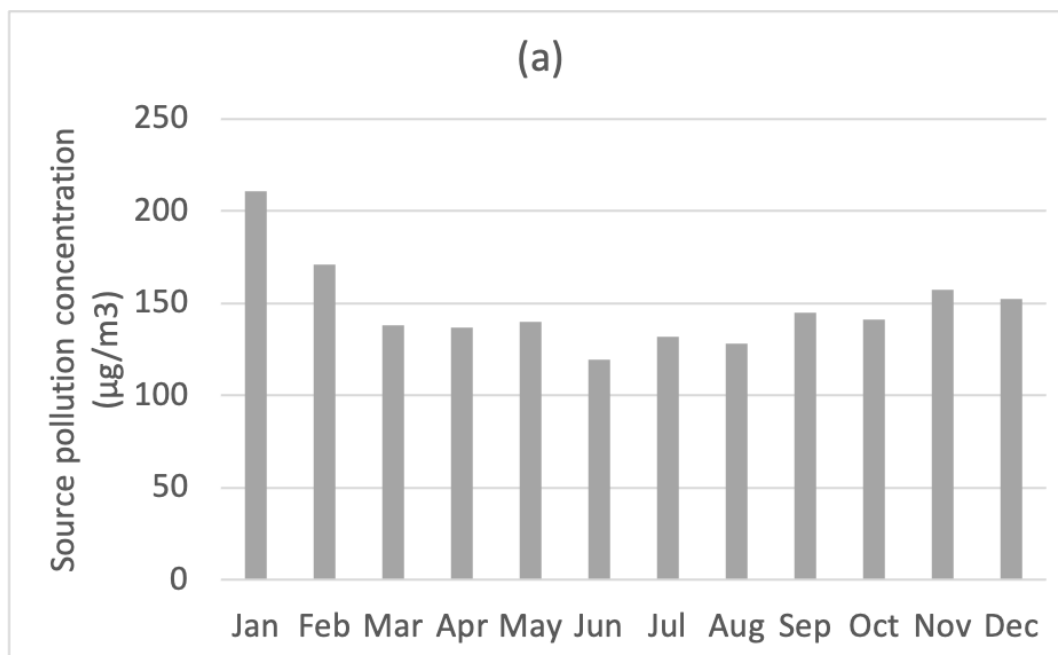
	Source pollution concentration (µg/m ³)	Average wind speed (m/s)	Numbers of trees	Tree Crown area (m ²)	Total leaf area (m ²)	Percentage of land cover by trees (%)
Jan	210.8	3.4				
Feb	170.7	3.6				
Mar	138.2	3.9				
Apr	136.6	4.2				
May	139.9	4.0				
Jun	119.1	3.2	246	1537.5	8456.3	14
Jul	131.8	2.8				
Aug	128.1	2.6				
Sep	144.9	2.7				
Oct	140.8	3.2				
Nov	157.1	3.5				
Dec	152.3	3.6				

6.3.4.1. Results and discussion

Table 6-12 Monthly PM₁₀ concentration (µg/m³) and total amount of PM₁₀ (µg) in Taiyuan city in 2017.

	Source pollution concentration (µg/m ³)	Average wind speed (m/s)	Average PM ₁₀ concentration (µg/m ³)	Total amount of PM ₁₀ removal (µg)
Jan	210.8	3.4	182.8	66.4

Feb	170.7	3.6	156.0	56.7
Mar	138.2	3.9	134.3	48.8
Apr	136.6	4.2	133.1	48.5
May	139.9	4.0	135.4	49.3
Jun	119.1	3.2	121.9	44.2
Jul	131.8	2.8	130.4	47.3
Aug	128.1	2.6	128.1	46.4
Sep	144.9	2.7	139.1	50.5
Oct	140.8	3.2	136.3	49.5
Nov	157.1	3.5	147.1	53.4
Dec	152.3	3.6	143.8	52.3



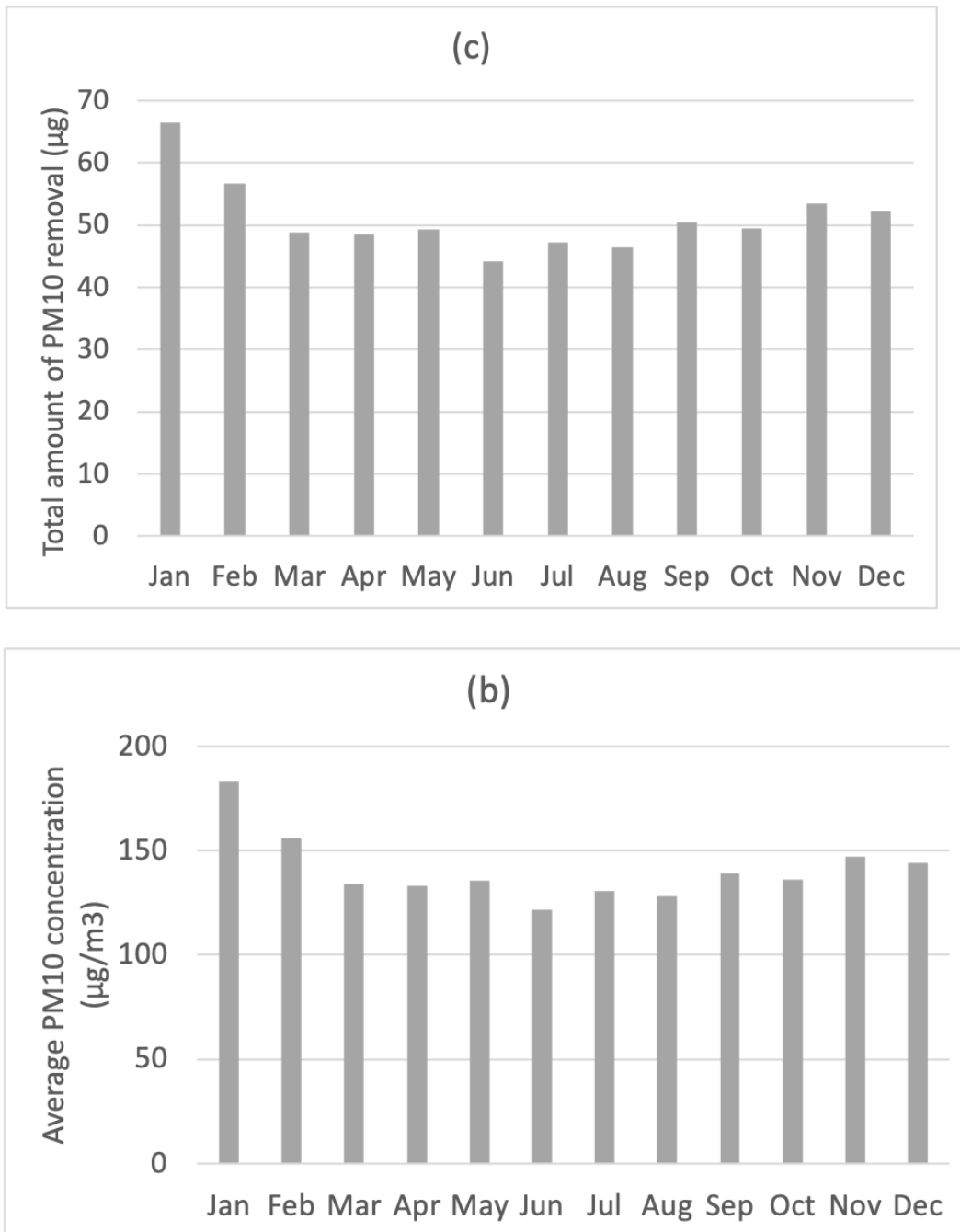


Figure 6-15 Monthly (a) source pollution concentration ($\mu\text{g}/\text{m}^3$), (b) PM_{10} concentration ($\mu\text{g}/\text{m}^3$), and (c) total amount of PM_{10} (μg) in Taiyuan city in 2017.

This scenario describes the efficiency of dry deposition by urban trees at different times of the year. Based on the monthly wind speeds and pollution concentrations in the study area, the total PM_{10} mitigation by the dry deposition process at a 14% level of green cover is listed

in Table 6-12. The table shows the changes in the number of particle pollution concentrations and pollution removal over 2017. From Figure 6-15 (a), we can see that air quality was better in the summer than in winter. This was caused by the high usage of heating systems in Taiyuan in the winter. The data in Figure 6-15 (a) was entered into the dry deposition model as the pollution source to estimate the PM₁₀ concentration with the air purification by trees in the study area for 10 hours. Same as the simulation results in scenario 2, more pollution was removed in the months when the source pollution concentration was higher. Even with the constant leaf area throughout the year, the average PM₁₀ concentration in the winter was still higher than in the summer. This could be an advice for local residents that less outdoor activities should be taken in the winter period in Taiyuan. Although there was more pollution removed by trees in the winter, it still cannot bring the average pollution concentration down to the summer levels.

6.3.5. Scenario 5 – Tree species

Different tree species have different leaf area indexes, which can have different efficiencies for dry deposition by providing various total leaf areas. Asner et al. (2003) summarised leaf area indexes by common urban vegetation types by a global observation method (see Table 6-13). This scenario simulates the efficiency of the particle dry deposition process based on various trees species. The results could suggest the best types of trees for removing air pollution. The simulation runs in the study area with a 14% green cover level, for which the input data are listed in Table 6-14.

Table 6-13 Leaf area index by tree species (Asner et al. 2003) and their acronyms.

Tree species	Leaf area index	Acronyms
Boreal deciduous broadleaf	2.6	BoDBL
Boreal evergreen needleleaf	2.7	BoENL
Boreal/temperate deciduous needleleaf	4.6	BoTeDNL
Temperate deciduous broadleaf	5.1	TeDBL

Temperate evergreen needleleaf	5.7	TeEBL
Temperate evergreen broadleaf	5.5	TeENL
Tropical deciduous broadleaf	3.9	TrDBL
Tropical evergreen broadleaf	4.8	TrEBL

Table 6-14 Input data for scenario 5 simulation.

Tree species	Total leaf area (m ²)	Numbers of trees	Tree Crown area (m ²)	Average wind speed (m/s)	Percentage of land cover by trees (%)	Source pollutant concentration
BoDBL	3968.0					(1, 212.2),
BoENL	4151.3					(2, 188.5),
BoTeDNL	7072.5					(3, 215.0),
TeDBL	7841.3					(4, 247.6),
TeEBL	8763.8	246	1537.5	2.8	14	(5, 220.8), (6, 339.7),
TeENL	8456.3					(7, 573.2), (8, 433.5),
TrDBL	5996.3					(9, 226.3), (10, 394.7),
TrEBL	7380.0					(11, 489.0)

6.3.5.1. Results and discussion

Table 6-15 Average PM₁₀ concentration /in the study and total amount of PM₁₀ estimated based on different tree species.

Tree species	Total leaf area (m ²)	Average PM ₁₀ concentration (µg/m ³)	Total amount of PM ₁₀ removal (µg)
BoDBL	3968.0	216.2	187.0
BoENL	4151.3	211.9	190.4
BoTeDNL	7072.5	131.2	201.2
TeDBL	7841.3	119.2	202.6
TeEBL	8763.8	107.3	204.0
TeENL	8456.3	111.0	203.5
TrDBL	5996.3	152.9	198.6
TrEBL	7380.0	126.1	201.8

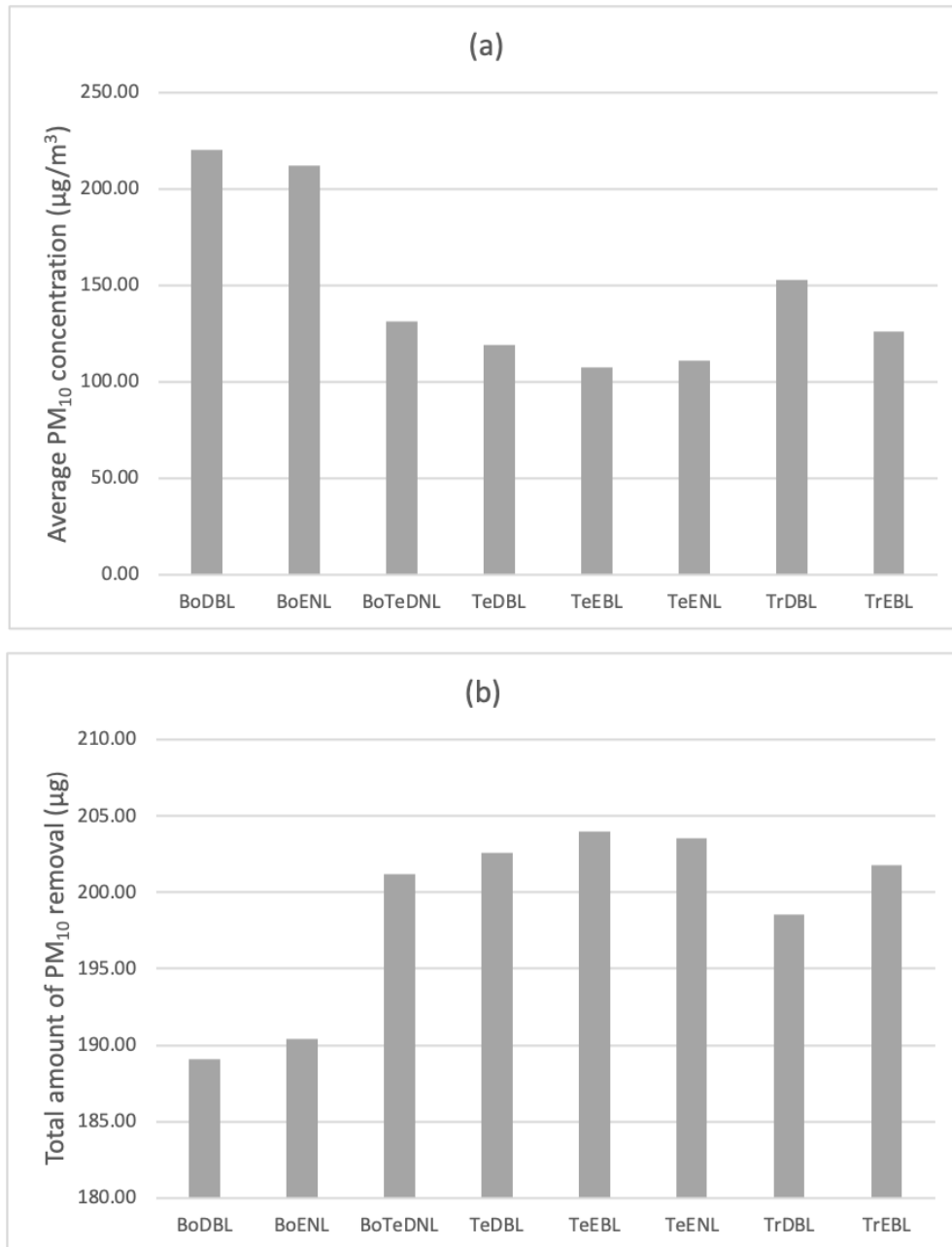


Figure 6-16 (a) PM₁₀ concentration and (b) total amount of PM₁₀ of different tree species.

This part estimated PM₁₀ removal by different tree species when the study area is covered by 14% of green spaces (see Table 6-15). Different tree species lead to different leaf area indexes, which leads to different leaf areas for the same numbers of trees. The total leaf area at the 14% green cover level with various biome types ranges from 3977.0 to 8763.8 square meters. With this rise in leaf area, the amount of PM₁₀ removal rose from 142.9µg to 168.3 µg. Biomes of BoDBL and BoENL showed the least of PM₁₀ removal, whilst TeEBL and

TeENL yielded the highest level of pollution mitigation (see Figure 6-16). Therefore, using trees with a higher leaf area index would significantly increase air pollutant removal with the same numbers of trees. The trees currently planted in the study area are all from the BoDBL biome, so if they can be changed to TeEBL trees, the total amount of PM₁₀ removal can increase from 142.9 µg to 168.3 µg, which represent an improvement of about 15%. If we take into consideration the results from scenario 3, in which the locations with higher wind speed provide more pollution removal, we can achieve the highest efficiency of PM₁₀ mitigation by planting TeEBL trees that can cover 14% of the land in the suggested location.

6.4. Conclusion

Five different scenarios were set up to explore and propose optimal green plans in the study area for better air quality. A field study was undertaken to monitor meteorological data as simulation inputs. The total amount of PM₁₀ removal for 10 hours in the study area was estimated based the setup of each scenario to discuss the factors that can improve air quality by dry deposition. The five scenarios optimise the green plan in the study area for absorbing particle pollutants by trees. Leaf area, wind speed, and source pollution concentration were simulated by the integrated model to explore suggestions to improve the current green plan in the study area.

The first scenario suggested the best percentage of green cover to reach a better air quality in the study area. The results show that 14% to 25% of green cover can increase the efficiency of particle pollutant removal by dry deposition for in the study area. More specifically, when the green spaces doubled from 7% to 14%, 31.6 µg more PM₁₀ was removed, for an increase from 14% to 25%, 8.9 µg was removed, and for an increase 25% to 50%, only 7.4 µg PM₁₀ was removed. Beyond 50% green cover, the pollutant removal only increased by 3.9 µg (see Figure 6-6). The increased in pollution removal dropped significantly after 50% green cover. Hence, for improving air quality in the study area, the green cover should be no more than 50% and no less than 14% to provide a high efficiency of pollution removal.

The next question is whether trees remove larger amounts of pollution when they are in an area with a higher pollution concentration. Scenario 2 set up to evaluate the effects of source pollution concentration levels from 50 to 450 µg/m³ on pollution removal with a 14% level of green cover. Generally, the results show that bigger amounts of PM₁₀ were removed from the area with higher pollution concentration. The rising trend is linear in this scenario, which is different form the logarithmic growth in scenario 1. In addition, as we can see, even in level_5, in which the source pollution concentration is 350 µg/m³, the total pollution removal is slightly higher than the total removal for 14% green cover. A total of 194.6 µg of PM₁₀ was removed when there was a 350 µg/m³ concentration, while 187.0 µg PM₁₀ was removal in scenario 1 (see Table 6-5 and Table 6-7). The reason for this is that the

monitored source pollution concentration is slightly lower than $350 \mu\text{g}/\text{m}^3$, which also followed the trend of larger amounts of pollution being removed in the areas with higher pollution concentrations.

Once the optimum number of trees has been proposed, it is important to discuss the locations of those trees. It has been explained that higher pollution concentrations lead to higher efficiency of particle pollutant mitigation. In the next scenario, different planting locations for the trees were discussed based on the monitored source pollution concentration. PM_{10} removal was calculated based on a single tree instated of a 14% green cover level, as a 14% cover level involves a number of trees that cannot be planted in a single location. The results show that more PM_{10} can be removed in the locations with higher wind speed. The suggestion derived from the results of this scenario is that the locations with higher wind speeds should be prioritized. However, the difference in the level of pollution removal for different wind speeds is relatively small. Hence, if the locations with high wind speed are unsuitable for tree planting, the decline in pollution removal would only have limited impact on the overall air quality in that area.

As the monitored data only covered one day in the study area, the next scenario calculated the total amount of PM_{10} removal in different months of a year. The source pollution concentration and average wind speed in each month were collected from the local weather station. As we can see in Table 6-1 and Table 6-9, monthly pollution concentrations were significantly lower than the monitored concentration. A possible reason is that the pollution concentration from the weather station was averaged based on both daytime and night-time, whilst the monitored data were only from day time. As a result, the weather station provided less data than my field study. Moreover, air quality is better in the summer than in the winter due to the high usage of heating systems in Taiyuan. Hence, the results show that more pollution is removed in the winter, which follows the same trend showed in scenario 2. There is a higher efficiency of pollution mitigation when the pollution concentration is high. Although there was more pollution removed in the winter, the average pollution concentration was still higher than in the summer. Moreover, the tree species applied in this scenario were evergreen needleleaf, which means the leaf area does not decrease in the winter compared to the summer. For areas with deciduous trees, the amount of PM_{10}

removal would drop sharply in the winter. For better air quality in the winter, evergreen trees seem to be a better choice for optimum green plans.

To discuss the effect of different tree species on air pollution removal, various types of trees were simulated by the dry deposition model to quantify the pollution removal in the area. The results show that tree species with a higher leaf area index removed more PM₁₀ from the study area over a 10-hour simulation period. TeEBL and TeEBL trees provided the most pollution removal. However, due to the various weather conditions, it might not be possible to plant those particular trees, with the highest leaf area index, in the locations desired. Therefore, among the suitable tree species in the study area, trees with a high leaf area index should be considered for planting.

To sum up, the optimum green plan for the study area to achieve better air quality is 14% to 25% of green cover with evergreen leaf trees that are planted in locations with higher wind speeds. Through quantifying the pollution removal in the study area for green planning development, the proposed integrated model presents good capability of simulating the effect of green spaces on air pollution mitigation in mid-scale residential areas. With the CFD model, the impact of wind speed on the dry deposition process could be considered in this study. The dry deposition equations that were modelled in the system dynamic software (Vensim) were able to present the impacts of leaf area, wind speed, and source pollution on the efficiency of particle dry deposition.

Chapter 7. Conclusions and Recommendations for future research

7.1. Introduction

This study aimed to explore optimum urban green plans for air quality improvement in mid-scale residential areas in China. A literature review has been done to discuss the effect of dry deposition on air pollution mitigation by green spaces. Then, the deficiencies of current urban green space models (UFORE and EMEP MSC-W model) were identified in chapter 3. An integrated urban planning model has been developed in chapter 4 to be used for quantifying particle pollution removal by vegetation. In chapter 5, this model was validated by comparing simulated results and measured data from Taiyuan, China. Then, a mid-scale study area in Taiyuan was used to estimate pollution removal based on various scenarios. This chapter will conclude the effect of urban green infrastructure on air quality, the applications of the dry deposition process, the urban planning model setup and validation, the findings of simulation results, and finally recommendations for the direction of future study.

7.2. Literature review

7.2.1. Air quality improvement by urban green spaces

Air pollution has become one of the most urgent urban issues not only in China but also in many big cities around the world as it can damage urban residents' well-being and decrease our living environment. Green infrastructures, as Tzoulas et al. (2007) proposed, can help sustainable urban development and public health improvement. They have many environmental benefits such as reducing air pollution, improving health and well-being, reducing noise pollution, and mitigating the urban heat island effect and climate change. To understand the benefits that are received from nature, the concept of ecosystem service was introduced to urban planning studies. Ecosystem service valuation could guide urban development by quantifying the benefits based on an economic and ecological background. However, ecosystem service includes the whole natural world and human society. Green factors help to narrow this broad definition down to the development of green infrastructure in mid-scale residential areas. In this study, the mid-scale residential areas

were defined as being of an area between one hundred and one hundred thousand square metres. By reviewing various green factors, the leaf area index was introduced by the green plot ratio method. The leaf area index is the total one-sided area of photosynthetic tissue per unit area of the ground surface (Watson 1947; Jonckheere et al. 2004), which allows the leaf area to be calculated based on the tree crown size.

In a city, trees, vegetation barriers, green walls, and green roofs can reduce air pollution by aerodynamic effects and the dry deposition process (Escobedo, Nowak 2009; Fantozzi et al. 2015; Janhäll 2015; Nowak et al. 2006; Yin et al. 2011). Many studies (Brantley et al. 2014; Hagler et al. 2012) showed that urban trees can act as a vegetation barrier to block the diffusion of air pollution from streets to the surrounding areas. On the other hand, this would also cause a high pollution concentration in the street areas by decreasing natural ventilation. Air pollution can also be absorbed by leaf surface through dry deposition, but Jeanjean et al. (2017) presented that the amount of pollution removal by deposition is much less than that removed by vegetation barriers. Therefore, there has been less attention paid to improving air quality by dry deposition compared to aerodynamic effects. However, dry deposition is a consistent and stable process with different wind speeds and directions. Moreover, this process can remove pollutants from the atmosphere without causing a high pollution concentration in another certain area.

The conclusion of this literature review can be summarised as:

- Many studies of green factors clarified the relationship between built environment and green infrastructures, which means the benefits that are brought by green infrastructures were identified and used to develop our living environment. However, they primarily focused on the configurations of land and buildings. To study green spaces in greater detail, this study reviewed the green plot ratio. This method introduced leaf area index as a biological parameter of greenery to quantify the benefits of different green types. Although these methods linked the green spaces and mid-scale built environment, they still had less focus on the effect of air particle pollution mitigation by green infrastructures.

- To explore the effect of urban vegetation on air pollution mitigation, studies of green spaces improving air quality have been reviewed in this thesis. Some of them claimed that urban trees can increase the pollution concentration at street level, but most of them showed that trees can improve air quality. In general, more studies believed that green spaces lead to a positive effect of air quality improvement. Hence, it is worth studying air pollution removal by trees.
- Trees can reduce air pollution by the filtration of polluted air and the dilution of pollution concentration. Filtration by vegetation barriers are commonly studied, but the dilution by dry deposition is less discussed. Moreover, many studies of dry deposition were focused on large-scale areas, such as urban forest and wetland. Therefore, this part of literature review highlighted the lack of studies that concentrate on the dilution of particulate pollutant concentration by dry deposition in mid-scale areas.

7.2.2. Particle pollution mitigation by dry deposition

Particle pollution that is usually emitted from industry and road traffic is a critical issue in many Chinese cities. However, it can be absorbed by trees through the dry deposition process. As Abhijith (2017) described, there are three paths after particle pollutants have been captured by leaf surfaces. They may be resuspended to the atmosphere, washed off by rain, or drop to the ground with the leaves. Hence, dry deposition can remove particles from the atmosphere to prevent them from being moved by winds to pollute other areas. The amount of pollution removal can be calculated based on the dry deposition velocity and leaf area. The leaf area of different tree species is depended on the leaf area index that was discussed in chapter 2. The other important factor required when setting up a dry deposition model is the deposition velocity. One of the first theoretical frameworks that described the dry deposition velocity on the vegetation canopy was contributed by Slinn (1982). The aerodynamic resistance and surface resistance of vegetation were used to

express the deposition process. Through development over several decades, Giardina and Buffa (2018) contributed a new approach to describe the parallel relation between turbulent diffusion and Brownian motion of particles at the sublayer of the vegetation canopy. This has been adopted by my model to improve the accuracy of quantifying pollution removal. While the deposition velocity was developing, the dry deposition equations were used in many urban planning studies (Sehmel 1980a; Slinn 1982; Baldocchi et al. 1987; Wesely et al. 1985; Cabaraban et al. 2013; Yang et al. 2004; Nowak 1994; Currie, Bass 2008; Hirabayashi et al. 2011; Zhang et al. 2016; Liu, Zhu, et al. 2016; Huang et al. 2016; Han et al. 2017) to analyze urban forests, green walls, and green roofs. Dry deposition was also applied in atmospheric simulation models to evaluate green spaces at a city or global level based on various weather conditions. Two commonly used computer programs that were based on dry deposition for urban green planning are UFORE and EMEP MSC-W. They have been developed and applied internationally for analysis of regional green spaces and urban forests.

To sum up, the deficiencies of current models are,

- The UFORE model has a limited air flow effect on calculating dry deposition process. Wind speed that can affect dry deposition is not considered in this model when it calculates the particle pollutant removal. The flexibility of the UFORE model on different land and tree types is limited, as the dry deposition velocity in the UFORE model is pre-set according to only a limited range of tree species.
- The EMEP MSC-W model is only able to accurately estimate the pollution removal of large-scale green spaces based on the average leaf area index in the simulation area. Hence, a green planning model was developed in this study to address the deficiencies of current models.

7.3. The integrated green planning model

This study developed a green planning model to quantify the urban green spaces effect on particle pollution mitigation. This model aimed to propose the optimum number of trees, locations for planting the trees, and tree species, in a mid-scale residential area to achieve a high efficiency of particle pollution mitigation. The green planning model integrated a CFD model and an SD model together. The CFD model (ENVI-met) was used to simulate wind speeds based on different land types and green spaces in the selected study area. The inputs of the CFD model are meteorological data such as temperature, relative humidity, wind speed, and land types, such as building height, tree type, and land cover. The SD model was used to simulate the dry deposition process based on the equations for quantifying pollution removal. The input data for the SD model are: 1) simulated wind speed from ENVI-met or monitored wind speed from the study area for current green plans; 2) monitored pollution concentration in the study area or pollution concentration data from the location weather station; 3) vegetation data in the study area, such as numbers and locations of trees and their species. This model is validated in the study by comparing the measurements from real world and the model outcomes. This demonstrated that it is able to predict particle pollution mitigation by trees in a mid-scale residential area. Then, it has been applied in the study area in Taiyuan to develop the local green spaces by calculating the pollution reduction. The model validation and application will be concluded in the following sections.

7.3.1. Model validation

In this study, real-world data was monitored in Taiyuan, China. Two residential zones were chosen as they are located on the two sides of the same busy road, which means they share a common pollution source. The data of wind speed and PM_{2.5} and PM₁₀ were monitored from the two zones and the road. The separate 30-minute periods of data were monitored, which were the morning, afternoon and evening period. The simulated results were compared with the monitored data from the zones to analyse the difference between them. The comparison of the real-world data and simulation results in the zones showed that the dry deposition SD model is able to represent the real-world situation with up to 9.2%

deviation for most of the time slots. In conclusion, this model can show the particle pollution concentration changes of the mid-scale residential areas based on the effect of dry deposition. Therefore, this validated model is able to predict the amount of particle pollution mitigation by trees. Moreover, this model is able to predict accurate results of PM₁₀ and PM_{2.5} mitigation with the precise inputs in specific urban environmental conditions.

7.3.2. Application of the green planning model

The question 'what are the optimum green plans to improving air pollution mitigation in mid-scale residential areas?' was asked. A green planning model was developed in this study to quantify the effect of pollution removal. To answer this question, five scenarios, each with a variation of different green planning factors, were simulated by the model in a mid-scale study area in Taiyuan, China. Taiyuan is northern Chinese city with long industrial history and serious air pollution issues. The five factors, one investigated in each scenario, were: 1) Green cover levels; 2) Source pollution concentrations; 3) Locations; 4) Monthly particle pollutants removal; and 5) Tree species. The total amount of particle pollution removal was calculated based on each scenario. The results of these five scenarios can be compared with the results from previous dry deposition studies and concluded as,

- The results of scenario 1 show that larger green spaces in the study can remove more particle pollution, which has also been supported by Escobedo and Nowak's (2009) study. However, my results showed that 14% - 25% of the green cover in the study area provided a high efficiency of pollution removal. After the green cover rose to 50%, the amount of pollution removal only increased slightly.
- Scenario 3 presented that higher wind speeds can lead to more pollution removal. The effect of wind speed has been often studied with the filtration by tree barrier, but less discussed with its effect on dry deposition in current studies and models. Although the wind speed has less of an impact on dry deposition efficiency in a large-scale urban area compared with the pollution concentration and leaf area, it still can lead to improvements to pollution removal in a mid-scale area.

- Beckett (2000) also concluded that trees with lower leaf density, larger size, and bigger leaf area can capture more PM pollution. Similar outcomes were presented by scenario 5's results, in which temperate evergreen needleleaf trees and temperate evergreen broadleaf trees removed the most particle pollution from the study area. Moreover, evergreen leaf trees also lead to a high amount of pollution removal during the winter as they can maintain the same amount of leaf area throughout the year. In the study area, an optimum green plan could be proposed as having 14% - 25% green cover with evergreen leaf trees that are planted in the locations with higher wind speeds.

Moreover, the wide application range of this model can be described by the following questions:

- **How:** The model estimates the amount of particle pollutants removal by three steps, which are: step 1 is identification of land types and local microclimate zones. In this step, satellite imagery and field surveys are needed. In addition, field surveys might be required in the study area for more accurate information of the current land types; Step 2 is collection of meteorological and air quality data. In this step, the meteorological data and pollution concentration data can be collected in two ways, which are local weather stations and field surveys. They can be combined as an integrated database, if there a limited number meteorological and air pollution sensors that also have only limited functions; Step 3 is calculation of air pollution removal. In this step, different green planning scenarios can be set up in this step to evaluate the efficiency of particle pollution mitigation. The results can be discussed to propose optimum green plans for the study area.
- **Where:** This model is focused on quantifying particle pollutant mitigation in the mid-scale residential areas. In addition, this model can be used at street level or in the mid-scale urban parks. For instance, it can be used to estimate the amount of pollution removal by street trees. It is also able to predict pollutant reduction based

on mixed tree species in the parks. To achieve this, users will need to collect data regarding each tree type and its crown area, so the total leaf area can be calculated. In conclusion, this model can be applied on the mid-scale areas in which there is high particle pollution concentration and there are (or will be) trees. More specifically, it not only can estimate the particle pollution mitigation by current green spaces but also can predict the pollution removal based on future green plans in the area.

- **When:** This model can be used in the different stages of an urban plan for different purposes. For example, in the beginning of an urban plan, it can suggest the optimum numbers and species of trees that will reduce a high amount of particle pollutants. In the middle stage, this model can be used to regulate where to plant the trees. With the developing of an urban plan, the locations of gray infrastructures, such as buildings and roads, will be decided. Hence, based on the land form, this model can estimate particle pollution removal with different locations of trees to find the optimum locations of the high efficiency of dry deposition. At the end of an urban plan, this model can calculate the amount of particle pollution removal based on the developed plan, which can evaluate the effect of the green spaces on improving air quality.
- **Who:** The simple design and easy operation of the model allow various groups of users to apply it in their interested mid-scale study areas. For instance, researchers can use it to study the effect of urban trees on particle pollution mitigation in mid-scale residential areas, as it doesn't require high programming skills to be used. Urban planners are able to use this model to develop urban green spaces for air quality improvement, because it can predict accurate results of particle pollutant mitigation by trees with the precise inputs in an urban environment. Moreover, due to the low-cost software used in this model, students can use it for research and training purposes.

7.4. Contribution

The contribute of this study to the existing body of knowledge can be concluded as,

- Due to the lack of research on the particle pollutant removal by dry deposition in mid-scale areas, this study developed a green planning model to quantify the amount of particle pollution mitigation in mid-scale residential area.
- The deficiencies of the current models led to the development of the model in this study. First, the current models didn't consider the effect of wind speed and different tree species on particle pollution removal. Therefore, in this model, wind speeds and tree species are able to be entered as variables to estimate particle pollution removal. Second, the EMEP MSC-W model can only apply on large-scale areas, so my model focuses on mid-scale residential areas.
- This green planning model is able to predict the amount of particle pollution removal based on various pollution concentration, wind speeds and leaf areas. Therefore, it not only can estimate the particle pollution mitigation of current green plans, but also can predict the pollution removal of future green plans to develop optimum green plans of high dry deposition efficiency. More specifically, it is able to propose the optimum numbers of trees, better locations of planting the trees, and suitable trees species in a mid-scale study area to achieve high efficiency of particle pollution mitigation.
- The estimated amount of particle pollutant removal has been compared with field measurement. The results of the comparing showed generally good agreement between estimated and monitored PM_{10} and $PM_{2.5}$ concentration in the study area in Taiyuan. Hence, this model can effectively predict the particle pollution removal in the real world.
- Both the ENVI-met and Vensim PLE provide low-cost licences. Hence, this green planning model is suitable for low-budget urban planning research. Moreover, dry

deposition equations are described as a SD system in Vensiom PLE, which presented an open-source model that first, allows changes to be applied in different study areas; second, each factor and each step can be adjusted and followed for various pollution types and vegetation surfaces. All the data that was required for this model to calculate the particle pollution removal can be easily accessed. Therefore, it can be used not only by researchers and urban planners, but also by anyone who is interested in investigating the effect of green spaces on air quality improvement.

7.5. Limitation of the green planning model

Despite the detailed research of dry deposition equations, a single model cannot represent and simulate the process of particle dry deposition process as perfectly in line with the real-world situation. This is caused by the complex effects of the fluid dynamics processes on dry deposition. Moreover, natural wind speed can be impacted by multiple and complex factors, and hence cannot be accurately predicted in outdoor urban areas by any CFD model (Calautit et al. 2020). Hence, the ENVI-met can only provide simulated outcomes of wind speed based on the meteorological boundary conditions of the study area. The simulated wind speed might be different from the real data. Hence, the limitations of the green planning model and the application are:

- Limited modelling of particle pollutants resuspension, which means all the particle pollutants that are captured by leaf surface will not return back to the atmosphere in this model.
- Limited number of meteorological and pollution sensors. For instance, the real-world data that was monitored in Taiyuan was from different time slots. The inputs of monthly pollution concentrations and windspeeds in scenario 4 from the local weather station were not monitored in the study area, but the average data from pollution monitors around Taiyuan were used.

- Uncertainties of estimating tree cover and leaf area in the study. The tree crown area was calculated based on the satellite image of the study area, so the image might not accurately present the actual tree area. Also, the angle of the satellite imagery could affect the size of the tree crowns.
- The results of the model were only focused on particle pollution removal by trees and did not include other types of pollutions and vegetations.

7.6. Future research

The potential recommendations of future research are proposed based on this study. The green planning model can be used as a starting point. Moreover, although the aims and objective in this study have been achieved, more research areas can be investigated to improve this model by broadening its applicability. The future study can be as follows:

- Bring the dry deposition of gaseous pollution removal into the green planning model to include more pollutant types for evaluating green space. Moreover, various types of UGI can be estimated by the model to explore appropriate green types in a mid-scale urban area.
- Indoor air quality improvement can be investigated based on various types of indoor plants and building ventilation. More specifically, a CFD model can be used to simulate the ventilation to suggest the best location to put the plants. Moreover, the model can also be used to calculate the pollution removal by dry deposition and compare this with other methods of air purification, such as ionisation and photocatalysis, which can help to discover the most efficient combination of different air pollution mitigation strategies.

- Different CFD and SD software can be used to replace ENVI-met and Vensim PLE. For instance, ANSYS is a powerful dynamic simulation software that allows both CFD and SD systems to be simulated in the same interface. However, there is no low-cost licence in ANSYS that comes with full accessibility.

Reference

- Abadi, L.S.K., Shamsai, A., Goharnejad, H., 2015. An analysis of the sustainability of basin water resources using Vensim model. *KSCE Journal of Civil Engineering*. 10.1007/s12205-014-0570-7.
- Abhijith, K. V. et al., 2017. 10.1016/j.atmosenv.2017.05.014.
- Agency, E.E., 2013. *Particulate Matter (PM10): annual mean concentrations in Europe*.
- Agyemang, C. et al., 2007. The association of neighbourhood psychosocial stressors and self-rated health in Amsterdam, the Netherlands. *Journal of Epidemiology and Community Health*. 10.1136/jech.2006.052548.
- Ahmed Memon, R., Leung, D.Y., Chunho, L., 2008. A review on the generation, determination and mitigation of Urban Heat Island. *Journal of Environmental Sciences*.
- AIAA, 1998. Guide for the verification and validation of computational fluid dynamics simulations. *American Institute of Aeronautics and Astronautics*.
- Akbari, H., Pomerantz, M., Taha, H., 2001. Cool surfaces and shade trees to reduce energy use and improve air quality in urban areas. *Solar Energy*. 10.1016/S0038-092X(00)00089-X.
- Alexandri, E., Jones, P., 2008. Temperature decreases in an urban canyon due to green walls and green roofs in diverse climates. *Building and Environment*. 10.1016/j.buildenv.2006.10.055.
- Alonso, R. et al., 2011. Modelling the influence of peri-urban trees in the air quality of Madrid region (Spain). *Environmental Pollution*. 10.1016/j.envpol.2010.12.005.
- Amorim, J.H. et al., 2013. CFD modelling of the aerodynamic effect of trees on urban air pollution dispersion. *Science of the Total Environment*, 461–462, pp.541–551. 10.1016/j.scitotenv.2013.05.031.
- Arling, J., O'Connor, K., Mercieca, M., 2010. *Air Quality Sensor Network for Philadelphia*.
- Ash, N. et al., 2010. *Ecosystems and human well-being: a manual for assessment practitioners*.
- Asner, G.P., Scurlock, J.M.O., Hicke, J. a, 2003. Global synthesis of leaf area index observations : *Global Ecology & Biogeography*, 12(2003), pp.191–205. 10.1046/j.1466-822X.2003.00026.x.

- Attwell, K., 2000. Urban land resources and urban planting - Case studies from Denmark. *Landscape and Urban Planning*. 10.1016/S0169-2046(00)00129-8.
- Baldocchi, D.D., Hicks, B.B., Camara, P., 1987. A canopy stomatal resistance model for gaseous deposition to vegetated surfaces. *Atmospheric Environment (1967)*, 21(1), pp.91–101. 10.1016/0004-6981(87)90274-5.
- Barlas, Y., 1989. Multiple tests for validation of system dynamics type of simulation models. *European Journal of Operational Research*. 10.1016/0377-2217(89)90059-3.
- Baró, F. et al., 2014. Contribution of ecosystem services to air quality and climate change mitigation policies: The case of urban forests in Barcelona, Spain. *Ambio*. 10.1007/s13280-014-0507-x.
- Beckett, K.P., Freer-Smith, P.H., Taylor, Gail, 2000. Particulate pollution capture by urban trees: Effect of species and windspeed. *Global Change Biology*, 6(8), pp.995–1003. 10.1046/j.1365-2486.2000.00376.x.
- Beckett, K.P., Freer-Smith, P.H., Taylor, G., 2000. The capture of particulate pollution by trees at five contrasting urban sites. *Arboricultural Journal*. 10.1080/03071375.2000.9747273.
- Beckett, P.K., Freer-smith, P., Taylor, G., 1995. EFFECTIVE TREE SPECIES FOR LOCAL AIR-QUALITY MANAGEMENT. *J. Arboriculture*.
- Benedict, M.A., MacMahon, E.T., 2002. Green infrastructure: Smart conservation for the 21st century. *Renewable Resources Journal*.
- Bharadwaj, P. et al., 2016. Early-life exposure to the Great Smog of 1952 and the development of asthma. *American Journal of Respiratory and Critical Care Medicine*. 10.1164/rccm.201603-0451OC.
- Binkowski, F.S., Shankar, U., 1995. The Regional Particulate Matter Model. 1. Model description and preliminary results. *Journal of Geophysical Research*. 10.1029/95jd02093.
- Bowler, D.E. et al., 2010. 10.1016/j.landurbplan.2010.05.006.
- Brandt, J., Christensen, J.H., Frohn, L.M., 2002. Modelling transport and deposition of caesium and iodine from the Chernobyl accident using the DREAM model. *Atmospheric Chemistry and Physics*, 2(5), pp.397–417.
- Brantley, H.L. et al., 2014. Field assessment of the effects of roadside vegetation on near-road black carbon and particulate matter. *Science of the Total Environment*.

- 10.1016/j.scitotenv.2013.08.001.
- Brunekreef, B., Forsberg, B., 2005. 10.1183/09031936.05.00001805.
- Bruse, M., Fleer, H., 1998. Simulating surface-plant-air interactions inside urban environments with a three dimensional numerical model. *Environmental Modelling and Software*, 13(3–4), pp.373–384. 10.1016/S1364-8152(98)00042-5.
- Buccolieri, R. et al., 2011. Analysis of local scale tree-atmosphere interaction on pollutant concentration in idealized street canyons and application to a real urban junction. *Atmospheric Environment*, 45(9), pp.1702–1713. 10.1016/j.atmosenv.2010.12.058.
- Bucur, V., 2006. *Urban forest acoustics*. 10.1007/3-540-30789-3.
- Cabaraban, M.T.I. et al., 2013. Modeling of air pollutant removal by dry deposition to urban trees using a WRF/CMAQ/i-Tree Eco coupled system. *Environmental Pollution*, 176, pp.123–133. 10.1016/j.envpol.2013.01.006.
- Calautit, J.K. et al., 2020. Development of a natural ventilation windcatcher with passive heat recovery wheel for mild-cold climates: CFD and experimental analysis. *Renewable Energy*. 10.1016/j.renene.2020.05.177.
- Carter, W.P.L., 1999. Documentation of the SAPRC-99 Chemical Mechanism for VOC Reactivity Assessment. *Assessment*.
- Chamberlain, A.C., 1953. Deposition of airborne radioiodine vapor. *Nucleonics*, 8, pp.22–25.
- Chameides, W.L. et al., 1988. The role of biogenic hydrocarbons in urban photochemical smog: Atlanta as a case study. *Science*. 10.1126/science.3420404.
- Chan et al, 2004. *Analytical Method Validation and Instrument Performance Verification*. 10.1016/j.patrec.2005.01.006.
- Charles, M. et al., 2020. Connecting air quality regulating ecosystem services with beneficiaries through quantitative serviceshed analysis. *Ecosystem Services*. 10.1016/j.ecoser.2019.101057.
- Charron, A., Harrison, R.M., 2005. Fine (PM_{2.5}) and coarse (PM_{2.5-10}) particulate matter on a heavily trafficked London highway: Sources and processes. *Environmental Science and Technology*. 10.1021/es050462i.
- Chate, D.M. et al., 2003. Scavenging of aerosols and their chemical species by rain. *Atmospheric Environment*. 10.1016/S1352-2310(03)00162-6.
- Chen, A., Gao, J., 2011. Urbanization in China and the coordinated development model-the case of chengdu. *Social Science Journal*, 48(3), pp.500–513.

10.1016/j.soscij.2011.05.005.

Chen, D. et al., 2014. Urban vegetation for reducing heat related mortality. *Environmental Pollution*, 192, pp.275–284. 10.1016/j.envpol.2014.05.002.

CHEN, J.M., BLACK, T.A., 1992. Defining leaf area index for non-flat leaves. *Plant, Cell & Environment*. 10.1111/j.1365-3040.1992.tb00992.x.

Chen, Y. et al., 2007. Gaseous and particulate polycyclic aromatic hydrocarbons (PAHs) emissions from commercial restaurants in Hong Kong. *Journal of Environmental Monitoring*. 10.1039/b710259c.

China CSR Map, 2015. State Environmental Protection Administration (SEPA). *China CSR Map*.

China, N.B. of S. of the P.R. of, 2015. *National Bureau of Statistics of the People's Republic of China*.

Communities, P.S., 2005. A Green Infrastructure Guide for Milton Keynes & the South Midlands; River Nene Regional Park, Environment Agency, Countryside Agency, English Nature. *English Heritage et al.*

Costanza, R., 2012a. Ecosystem health and ecological engineering. *Ecological Engineering*, 45, pp.24–29. 10.1016/j.ecoleng.2012.03.023.

Costanza, R., 2012b. Ecosystem health and ecological engineering. *Ecological Engineering*, 45, pp.24–29. 10.1016/j.ecoleng.2012.03.023.

Cotton, W.R. et al., 2003. RAMS 2001: Current status and future directions. *Meteorology and Atmospheric Physics*. 10.1007/s00703-001-0584-9.

Coutts, C., Horner, M., Chapin, T., 2010. Using geographical information system to model the effects of green space accessibility on mortality in Florida. *Geocarto International*. 10.1080/10106049.2010.505302.

Crosby, T.S., Hackett, B., 1972. Landscape Planning-An Introduction to Theory and Practice. *The Journal of Applied Ecology*. 10.2307/2402070.

CSANADY, G.T., 1973. TURBULENT DIFFUSION IN THE ENVIRONMENT. *BOOK: PUBL. BY D. REIDEL PUBLISHING COMPANY, DORDRECHT-HOLLAND/BOSTON-U.S.A.* 10.1007/978-94-010-2527-0.

Currie, B.A., Bass, B., 2008. Estimates of air pollution mitigation with green plants and green roofs using the UFORE model. *Urban Ecosystems*, 11(4), pp.409–422. 10.1007/s11252-008-0054-y.

- Daly, A., Zannetti, P., 2007. Air Pollution Modeling – An Overview. *Ambient Air Pollution*, I(2003), pp.15–28.
- Darley, E.F., 1971. Vegetation damage from air pollution. In: *Combustion-Generated Air Pollution*. Springer, 1971, pp. 245–255.
- Davidson, C.I., Miller, J.M., Pleskow, M.A., 1982. The influence of surface structure on predicted particle dry deposition to natural grass canopies. *Water, Air, and Soil Pollution*. 10.1007/BF02419401.
- Dean, J., van Dooren, K., Weinstein, P., 2011. Does biodiversity improve mental health in urban settings? *Medical Hypotheses*. 10.1016/j.mehy.2011.02.040.
- Dengel, D.R. et al., 2009. Does the built environment relate to the metabolic syndrome in adolescents? *Health and Place*. 10.1016/j.healthplace.2009.03.001.
- van Dillen, S.M.E. et al., 2012. Greenspace in urban neighbourhoods and residents' health: Adding quality to quantity. *Journal of Epidemiology and Community Health*. 10.1136/jech.2009.104695.
- Donaldson, K. et al., 2001. Ambient particle inhalation and the cardiovascular system: Potential mechanisms. *Environmental Health Perspectives*, 109(SUPPL. 4), pp.523–527. 10.2307/3454663.
- Donateo, A., Contini, D., 2014. Correlation of dry deposition velocity and friction velocity over different surfaces for PM_{2.5} and particle number concentrations. *Advances in Meteorology*. 10.1155/2014/760393.
- Dore, C., Vidič, S., 2012. *Considerations of changing the EMEP grid*. note 3, www.unece.org.
- Dutton, J.A., Panofsky, H.A., 1984. Atmospheric Turbulence. *Wiley, New York*.
- Dyer, A.J., Bradley, E.F., 1982. An alternative analysis of flux-gradient relationships at the 1976 ITCE. *Boundary-Layer Meteorology*, 22(1), pp.3–19. 10.1007/BF00128053.
- Ehrlich, P.R., Raven, P.H., 1964. Butterflies and Plants: A Study in Coevolution [online]. *Evolution; international journal of organic evolution*, 18, pp.586–608. Available at: <http://www.jstor.org/stable/2406212%5Cnpapers2://publication/uuid/4C33E495-513D-4FF5-A066-54D53AE5EE99>.
- Escobedo, F.J., Nowak, D.J., 2009. Spatial heterogeneity and air pollution removal by an urban forest. *Landscape and Urban Planning*, 90(3–4), pp.102–110. 10.1016/j.landurbplan.2008.10.021.
- Fantozzi, F. et al., 2015. Spatio-temporal variations of ozone and nitrogen dioxide

- concentrations under urban trees and in a nearby open area. *Urban Climate*.
10.1016/j.uclim.2015.02.001.
- Farber, S.C., Costanza, R., Wilson, M.A., 2002. Economic and ecological concepts for valuing ecosystem services [online]. *Ecol. Econ.*, 41(3), pp.375–392. Available at:
<http://www.sciencedirect.com/science/article/B6VDY-45R7NTR-5/2/f17ccd95dacd2c01ad070676807ba9b1>.
- Fenger, J., 2009. Air pollution in the last 50 years - From local to global. *Atmospheric Environment*. 10.1016/j.atmosenv.2008.09.061.
- Folke, C. et al., 2011. Reconnecting to the biosphere. In: *Ambio*. pp. 719–738.
10.1007/s13280-011-0184-y.
- Forrester, J.W., 1968. Industrial Dynamics—After the First Decade. *Management Science*.
10.1287/mnsc.14.7.398.
- Freer-Smith, P.H., El-Khatib, A.A., Taylor, G., 2004. Capture of particulate pollution by trees: A comparison of species typical of semi-arid areas (*Ficus nitida* and *Eucalyptus globulus*) with European and North American species. *Water, Air, and Soil Pollution*, 155(1–4), pp.173–187. 10.1023/B:WATE.0000026521.99552.fd.
- Gallagher, M.W. et al., 1997. Measurements of aerosol fluxes to speulderforest using a micrometeorological technique. *Atmospheric Environment*. 10.1016/S1352-2310(96)00057-X.
- Garrigues, S. et al., 2008. Validation and intercomparison of global Leaf Area Index products derived from remote sensing data. *Journal of Geophysical Research: Biogeosciences*. 10.1029/2007JG000635.
- Giardina, M., Buffa, P., 2018. 10.1016/j.atmosenv.2018.02.038.
- Gromke, C., Ruck, B., 2007. Influence of trees on the dispersion of pollutants in an urban street canyon-Experimental investigation of the flow and concentration field. *Atmospheric Environment*. 10.1016/j.atmosenv.2006.12.043.
- Guidolotti, G., Salviato, M., Calfapietra, C., 2016. Comparing estimates of EMEP MSC-W and UFORE models in air pollutant reduction by urban trees. *Environmental Science and Pollution Research*. 10.1007/s11356-016-7135-x.
- Guo, L. et al., 2012. Particulate matter (PM 10) exposure induces endothelial dysfunction and inflammation in rat brain. *Journal of Hazardous Materials*.
10.1016/j.jhazmat.2012.01.034.

- Hagler, G.S.W. et al., 2012. Field investigation of roadside vegetative and structural barrier impact on near-road ultrafine particle concentrations under a variety of wind conditions. *Science of the Total Environment*. 10.1016/j.scitotenv.2011.12.002.
- Han, X. et al., 2017. Modeling dry deposition of reactive nitrogen in China with RAMS-CMAQ. *Atmospheric Environment*, 166, pp.47–61.
- Hanemann, W.M., 1991. Willingness to pay and willingness to accept: How much can they differ? *The American Economic Review*, 81(3), pp.635–647.
10.1257/000282803321455430.
- Hanna, S.R., Gifford, F.A., Yamartino, R.J., 1991. Long range radioactive plume transport simulation model/code–phase I. *USNRC Division of Contracts and Property Management, Contract Administration Branch, P-902, Washington, DC, 20555*.
- Harnik, P., 2010. *Urban green : innovative parks for resurgent cities*. Washington, DC : Island Press.
- Harrison, R.M. et al., 2001. Studies of the coarse particle (2.5-10 μ m) component in UK urban atmospheres. *Atmospheric Environment*. 10.1016/S1352-2310(00)00526-4.
- Harrison, R.M., Hester, R.E., 2010. *Ecosystem services*. Royal Society of Chemistry.
- Häyhä, T., Franzese, P.P., 2014. Ecosystem services assessment: A review under an ecological-economic and systems perspective [online]. *Ecological Modelling*, 289, pp.124–132. Available at: <http://dx.doi.org/10.1016/j.ecolmodel.2014.07.002>.
- He, L.Y. et al., 2004. Characterization of fine organic particulate matter from Chinese cooking. *Journal of Environmental Sciences*.
- Hicks, B.B. et al., 1987. A preliminary multiple resistance routine for deriving dry deposition velocities from measured quantities. *Water, Air, and Soil Pollution*.
10.1007/BF00229675.
- Hinds, W.C., 1999. *Aerosol Technology Properties, Behavior, and Measurement of Airborne Particles Second Edition*. *Journal of Aerosol Science*.
- Hirabayashi, S., Kroll, C.N., Nowak, D.J., 2011. Component-based development and sensitivity analyses of an air pollutant dry deposition model. *Environmental Modelling and Software*, 26(6), pp.804–816. 10.1016/j.envsoft.2010.11.007.
- Hirabayashi, S., Kroll, C.N., Nowak, D.J., 2012. Development of a distributed air pollutant dry deposition modeling framework. *Environmental Pollution*.
10.1016/j.envpol.2012.07.002.

- Hirabayashi, S., Kroll, C.N., Nowak, D.J., 2015. I-Tree Eco Dry Deposition Model Descriptions.
- Hoek, G. et al., 2002. Association between mortality and indicators of traffic-related air pollution in the Netherlands: A cohort study. *Lancet*. 10.1016/S0140-6736(02)11280-3.
- Hoek, G. et al., 2013. 10.1186/1476-069X-12-43.
- Hofman, J. et al., 2016. Influence of tree crown characteristics on the local PM10 distribution inside an urban street canyon in Antwerp (Belgium): A model and experimental approach. *Urban Forestry and Urban Greening*. 10.1016/j.ufug.2016.09.013.
- Hou, X. et al., 2018. Seasonal statistical analysis of the impact of meteorological factors on fine particle pollution in China in 2013–2017. *Natural Hazards*. 10.1007/s11069-018-3315-y.
- van Houdt, F., Suvarierol, S., Schinkel, W., 2011. Neoliberal communitarian citizenship: Current trends towards 'earned citizenship' in the United Kingdom, France and the Netherlands. *International Sociology*. 10.1177/0268580910393041.
- Huang, L. et al., 2016. The impact of drought on ozone dry deposition over eastern Texas. *Atmospheric Environment*. 10.1016/j.atmosenv.2015.12.022.
- Huang, R.J. et al., 2015. High secondary aerosol contribution to particulate pollution during haze events in China. *Nature*. 10.1038/nature13774.
- Hung, H.S. et al., 2007. Association of cooking oil fumes exposure with lung cancer: Involvement of inhibitor of apoptosis proteins in cell survival and proliferation in vitro. *Mutation Research - Genetic Toxicology and Environmental Mutagenesis*. 10.1016/j.mrgentox.2006.12.005.
- Innovation, L.T., 2008. DC1100 Air Quality Monitor User manual. , 134113. 10.1007/SpringerReference_28001.
- Janhäll, S., 2015. 10.1016/j.atmosenv.2015.01.052.
- Jarup, L. et al., 2008. Hypertension and exposure to noise near airports: The HYENA study. *Environmental Health Perspectives*. 10.1289/ehp.10775.
- Jeanjean, A. et al., 2017. Air quality affected by trees in real street canyons: The case of Marylebone neighbourhood in central London. *Urban Forestry and Urban Greening*, 22, pp.41–53. 10.1016/j.ufug.2017.01.009.
- Jennings, S., 1988. The mean free path in air. *Journal of Aerosol Science*, 19(2), pp.159–166. 10.1016/0021-8502(88)90219-4.

- Ji, W., Zhao, B., 2014. Numerical study of the effects of trees on outdoor particle concentration distributions. *Building Simulation*. 10.1007/s12273-014-0180-9.
- Jim, C.Y., Chen, W.Y., 2008. Assessing the ecosystem service of air pollutant removal by urban trees in Guangzhou (China). *J Environ Manage*, 88(4), pp.665–676.
- Jonckheere, I. et al., 2004. Review of methods for in situ leaf area index determination Part I. Theories, sensors and hemispherical photography. *Agricultural and Forest Meteorology*. 10.1016/j.agrformet.2003.08.027.
- Kalácska, M. et al., 2004. Leaf area index measurements in a tropical moist forest: A case study from Costa Rica. *Remote Sensing of Environment*. 10.1016/j.rse.2004.02.011.
- Karttunen, S. et al., 2020. Large-eddy simulation of the optimal street-tree layout for pedestrian-level aerosol particle concentrations – A case study from a city-boulevard. *Atmospheric Environment: X*. 10.1016/j.aeaoa.2020.100073.
- Kassomenos, P. et al., 2012. Levels, sources and seasonality of coarse particles (PM 10-PM 2.5) in three European capitals - Implications for particulate pollution control. *Atmospheric Environment*. 10.1016/j.atmosenv.2012.02.051.
- Katsouyanni, K. et al., 2001. Confounding and Effect Modification in the Short-Term Effects of Ambient Particles on Total Mortality: Results from 29 European Cities within the APHEA2 Project [online]. *Epidemiology*, 12(5), pp.521–531. Available at: <http://content.wkhealth.com/linkback/openurl?sid=WKPTLP:landingpage&an=00001648-200109000-00011>.
- Kim, H.K. et al., 2014. Impacts of different plant functional types on ambient ozone predictions in the Seoul Metropolitan Areas (SMAs), Korea. *Atmospheric Chemistry and Physics*. 10.5194/acp-14-7461-2014.
- Kleijnen, J.P.C., 1995. Verification and validation of simulation models. *European Journal of Operational Research*. 10.1016/0377-2217(94)00016-6.
- Kumar, P. et al., 2016. 10.1016/j.atmosenv.2016.05.059.
- Lam, K.C. et al., 2005. Environmental quality of urban parks and open spaces in Hong Kong. *Environmental Monitoring and Assessment*. 10.1016/j.cccn.2005.02.014.
- Lane, J., 2019. Yong-Chan Kim, Matthew D. Matsaganis, Holley A. Wilkin, and Joo-Young Jung (Eds.), *The Communication Ecology of 21st Century Urban Communities*. *International Journal of Communication*, 13, p.4.
- Law, A.M., Kelton, W.D., Kelton, W.D., 2000. *Simulation modeling and analysis*. McGraw-Hill

New York.

- Legg, B.J., Powell, F.A., 1979. Spore dispersal in a barley crop: A mathematical model. *Agricultural Meteorology*. 10.1016/0002-1571(79)90050-5.
- Leonenko, G., Los, S.O., North, P.R.J., 2013. Retrieval of leaf area index from MODIS surface reflectance by model inversion using different minimization criteria. *Remote Sensing of Environment*. 10.1016/j.rse.2013.07.012.
- Li, L., Hao, T., Chi, T., 2015. Evaluation on China's forestry resources efficiency based on big data. *Journal of Cleaner Production*. 10.1016/j.jclepro.2016.02.078.
- Lim, J.H. et al., 2006. Concentration, size distribution, and dry deposition rate of particle-associated metals in the Los Angeles region. *Atmospheric Environment*, 40(40), pp.7810–7823. 10.1016/j.atmosenv.2006.07.025.
- Lin, M.Y. et al., 2016. The effects of vegetation barriers on near-road ultrafine particle number and carbon monoxide concentrations. *Science of the Total Environment*. 10.1016/j.scitotenv.2016.02.035.
- Lipfert, F. et al., 2006. PM_{2.5} constituents and related air quality variables as predictors of survival in a cohort of U.S. military veterans. *Inhalation Toxicology*. 10.1080/08958370600742946.
- Litschike, T., Kuttler, W., 2008. On the reduction of urban particle concentration by vegetation - A review. In: *Meteorologische Zeitschrift*. 10.1127/0941-2948/2008/0284.
- Liu, Jiakai, Zhu, L., et al., 2016. Dry deposition of particulate matter at an urban forest, wetland and lake surface in Beijing. *Atmospheric Environment*, 125, pp.178–187. 10.1016/j.atmosenv.2015.11.023.
- Liu, Jiakai et al., 2017. Particle removal by vegetation: comparison in a forest and a wetland [online]. *Environmental Science and Pollution Research International; Heidelberg*, 24(2), pp.1597–1607. Available at:
<http://abc.cardiff.ac.uk/login?url=https://search.proquest.com/docview/1956471721?accountid=9883>.
- Liu, Jiakai, Mo, L., et al., 2016. Removal efficiency of particulate matters at different underlying surfaces in Beijing. *Environmental Science and Pollution Research*. 10.1007/s11356-015-5252-6.
- Liu, S. et al., 2020. Revealing the impacts of transboundary pollution on PM_{2.5}-related deaths in China. *Environment International*. 10.1016/j.envint.2019.105323.

- Liu, Y., Liu, R., Chen, J.M., 2012. 10.1029/2012JG002084.
- Lovett, G.M., 1994. Atmospheric deposition of nutrients and pollutants in North America: An ecological perspective. *Ecological Applications*, 4(4), pp.629–650. 10.2307/1941997.
- Luber, G., McGeehin, M., 2008. 10.1016/j.amepre.2008.08.021.
- Maas, J. et al., 2009. Morbidity is related to a green living environment. *Journal of Epidemiology and Community Health*. 10.1136/jech.2008.079038.
- le Maire, G. et al., 2008. Calibration and validation of hyperspectral indices for the estimation of broadleaved forest leaf chlorophyll content, leaf mass per area, leaf area index and leaf canopy biomass. *Remote Sensing of Environment*. 10.1016/j.rse.2008.06.005.
- Maleki, K., Hosseini, S., 2011. Investigation of the effect of leaves, branches and canopies of trees on noise pollution reduction. *Annals of Environmental Science*.
- Mammarella, I. et al., 2011. Long-term aerosol particle flux observations. Part II: Particle size statistics and deposition velocities. *Atmospheric Environment*. 10.1016/j.atmosenv.2011.04.022.
- Maryon, R.H. et al., 1996. *An intercomparison of three long range dispersion models developed for the UK meteorological office, DNMI and EMEP, UK Met Office Turbulence and Diffusion*. Note 234, ISBN 82-7144-026-08, 44 pp.
- Matos, P. et al., 2019. Modeling the provision of air-quality regulation ecosystem service provided by urban green spaces using lichens as ecological indicators. *Science of the Total Environment*. 10.1016/j.scitotenv.2019.02.023.
- McHarg, I.L., 1969. *Design with nature*. American Museum of Natural History New York.
- McPherson, E.G., 1998. Structure and sustainability of Sacramento's urban forest. *Journal of Arboriculture*, 24(4), pp.174–189.
- McPherson, G.E. et al., 1994. *Chicago's urban forest ecosystem: Results of the Chicago Urban Forest Climate Project*. 10.1111/pace.12264.
- Medina-Ramón, M. et al., 2008. Residential exposure to traffic-related air pollution and survival after heart failure. *Environmental Health Perspectives*. 10.1289/ehp.10918.
- Mitchell, R., Astell-Burt, T., Richardson, E.A., 2011. A comparison of green space indicators for epidemiological research. *Journal of Epidemiology and Community Health*. 10.1136/jech.2010.119172.
- Mitchell, R., Popham, F., 2008. Effect of exposure to natural environment on health

- inequalities: an observational population study. *The Lancet*. 10.1016/S0140-6736(08)61689-X.
- Morani, A. et al., 2014. Comparing i-Tree modeled ozone deposition with field measurements in a periurban Mediterranean forest. *Environmental Pollution*. 10.1016/j.envpol.2014.08.031.
- Nenes, A., Pandis, S.N., Pilinis, C., 1999. Continued development and testing of a new thermodynamic aerosol module for urban and regional air quality models. *Atmospheric Environment*. 10.1016/S1352-2310(98)00352-5.
- Nguyen1310, 2006. *Map of Qin Empire*.
- Northern Research Station, 2009. *Urban Forest Effects Model - UFORE. Northern Research Station*.
- Nowak, D., Crane, D., 1998. The urban forest effects (UFORE) model: quantifying urban forest structure and function. *Integrated Tools Proceedings*, pp.714–720.
- Nowak, D.J. et al., 2008. A ground-based method of assessing urban forest structure and ecosystem services. In: *Arboriculture and Urban Forestry*.
- Nowak, D.J. et al., 2000. A modeling study of the impact of urban trees on ozone. *Atmospheric Environment*. 10.1016/S1352-2310(99)00394-5.
- Nowak, D.J., 1994. Air Pollution Removal by Chicago's Urban Forest. In: *Chicago's Urban Forest Ecosystem: Results of the Chicago Urban Forest Climate Project*. , 1994, pp. 63–81.
- Nowak, D.J. et al., 2002. Brooklyn's Urban Forest. *United States Department of Agriculture*.
- Nowak, D.J., 2006. Institutionalizing urban forestry as a 'biotechnology' to improve environmental quality. *Urban Forestry and Urban Greening*. 10.1016/j.ufug.2006.04.002.
- Nowak, D.J. et al., 2014. Tree and forest effects on air quality and human health in the United States. *Environmental Pollution*, 193, pp.119–129. 10.1016/j.envpol.2014.05.028.
- Nowak, D.J., Crane, D.E., Stevens, J.C., 2006. Air pollution removal by urban trees and shrubs in the United States. *Urban Forestry and Urban Greening*, 4(3–4), pp.115–123. 10.1016/j.ufug.2006.01.007.
- Oberkampf, W.L., Trucano, T.G., 2002. Verification and validation in computational fluid dynamics. *Progress in Aerospace Sciences*. 10.1016/S0376-0421(02)00005-2.

- Oke, T.R., 2004. Initial guidance to obtain representative meteorological observations at urban sites. *World Meteorological Organization*.
- Olivas, P.C. et al., 2013. Comparison of direct and indirect methods for assessing leaf area index across a tropical rain forest landscape. *Agricultural and Forest Meteorology*. 10.1016/j.agrformet.2013.04.010.
- Ong, B.L., 2003. Green plot ratio: An ecological measure for architecture and urban planning. *Landscape and Urban Planning*, 63(4), pp.197–211. 10.1016/S0169-2046(02)00191-3.
- Papafotiou, M. et al., 2004. The impact of design on traffic noise control in an urban park. *Acta Horticulturae*, pp.277–280.
- Pathak, V., Tripathi, B.D., Mishra, V.K., 2011. Evaluation of Anticipated Performance Index of some tree species for green belt development to mitigate traffic generated noise. *Urban Forestry and Urban Greening*. 10.1016/j.ufug.2010.06.008.
- Pederson, J.R. et al., 1995. California ozone deposition experiment: Methods, results, and opportunities. *Atmospheric Environment*, 29(21), pp.3115–3132. 10.1016/1352-2310(95)00136-M.
- Petroff, A. et al., 2008. 10.1016/j.atmosenv.2007.09.043.
- Pollution, H.E.I.P. on the H.E. of T.-R.A., 2010. Traffic-related air pollution: a critical review of the literature on emissions, exposure, and health effects.
- Powe, N.A., Willis, K.G., 2004. Mortality and morbidity benefits of air pollution (SO₂ and PM₁₀) absorption attributable to woodland in Britain. *Journal of Environmental Management*. 10.1016/j.jenvman.2003.11.003.
- Pullman, M.R., 2009. *Conifer PM_{2.5} Deposition and Re-suspension in Wind and Rain Events*. Cornell University.
- Putrik, P. et al., 2015. Living Environment Matters: Relationships Between Neighborhood Characteristics and Health of the Residents in a Dutch Municipality. *Journal of Community Health*. 10.1007/s10900-014-9894-y.
- Querol, X. et al., 2004. Speciation and origin of PM₁₀ and PM_{2.5} in selected European cities. *Atmospheric Environment*. 10.1016/j.atmosenv.2004.08.037.
- Rice, M.B. et al., 2015. Long-term exposure to traffic emissions and fine particulate matter and lung function decline in the Framingham Heart Study. *American Journal of Respiratory and Critical Care Medicine*. 10.1164/rccm.201410-1875OC.

- Richardson, E.A. et al., 2012. Green cities and health: A question of scale? *Journal of Epidemiology and Community Health*. 10.1136/jech.2011.137240.
- Robinson, S., 1997. Simulation model verification and validation. In: *Proceedings of the 29th conference on Winter simulation - WSC '97*. 10.1016/S0363-5023(03)00249-1.
- Rolstad Denby, B. et al., 2020. Description of the uEMEP_v5 downscaling approach for the EMEP MSC-W chemistry transport model. *Geoscientific Model Development Discussions*. 10.5194/gmd-2020-119.
- Roupsard, P. et al., 2013. Measurement in a wind tunnel of dry deposition velocities of submicron aerosol with associated turbulence onto rough and smooth urban surfaces. *Journal of Aerosol Science*. 10.1016/j.jaerosci.2012.07.006.
- Rudlin, D., Falk, N., 1999. *Building the 21st century home: the sustainable urban neighbourhood*. Butterworth-Heinemann.
- Salmond, J.A. et al., 2016. 10.1186/s12940-016-0103-6.
- Sandström, U.G., 2002. Green infrastructure planning in urban Sweden. *Planning Practice and Research*. 10.1080/02697450216356.
- Sargent, R.G., 1992. Validation and verification of simulation models. In: *Proceedings - Winter Simulation Conference*. 10.1145/167293.167311.
- Sargent, R.G., Balci, O., 2018. History of verification and validation of simulation models. In: *Proceedings - Winter Simulation Conference*. 10.1109/WSC.2017.8247794.
- Schirpke, U. et al., 2014. Mapping beneficiaries of ecosystem services flows from Natura 2000 sites. *Ecosystem Services*. 10.1016/j.ecoser.2014.06.003.
- Scire, J.S., Strimaitis, D.G., Yamartino, R.J., 2000. A User's Guide for the CALPUFF Dispersion Model. *Earth Tech. Inc*.
- Scurlock, J. M. O., Asner, G.P., Gower, S.T., 2001. Global Leaf Area Index from Field Measurements, 1932-2000 [online]. *Oak Ridge National Laboratory Distributed Active Archive Center, Oak Ridge, Tennessee, U.S.A*, p.DOI:10.3334/ORNLDAAC/584. Available at: doi:10.3334/ORNLDAAC/584.
- Scurlock, J M O, Asner, G.P., Gower, S.T., 2001. *Worldwide Historical Estimates and Bibliography of Leaf Area Index, 1932-2000*.
- Sehmel, G.A., 1980a. Particle and gas dry deposition: A review. *Atmospheric Environment (1967)*, 14(9), pp.983–1011. 10.1016/0004-6981(80)90031-1.
- Sehmel, G.A., 1980b. Particle and gas dry deposition: A review. *Atmospheric Environment*

- (1967). 10.1016/0004-6981(80)90031-1.
- Seinfeld, J.H., Pandis, S.N., 2006. Atmospheric Chemistry and Physics. *Atmospheric Chemistry and Physics*.
- Sgrigna, G. et al., 2015. Particulate Matter deposition on Quercus ilex leaves in an industrial city of central Italy. *Environmental Pollution*. 10.1016/j.envpol.2014.11.030.
- Shafik, N., 1994. Economic development and environmental quality: An econometric analysis. *Oxford Economic Papers*. 10.1093/oep/46.Supplement_1.757.
- Simpson, D. et al., 2012. The EMEP MSC-W chemical transport model – Technical description. *Atmospheric Chemistry and Physics*. 10.5194/acp-12-7825-2012.
- Slinn, S.A., Slinn, W.G.N., 1980. Predictions for particle deposition on natural waters. *Atmospheric Environment (1967)*, 14(9), pp.1013–1016. 10.1016/0004-6981(80)90032-3.
- Slinn, W.G.N., 1982. Predictions for particle deposition to vegetative canopies. *Atmospheric Environment*. 10.1016/0004-6981(82)90271-2.
- Slinn, W.G.N. et al., 1978. 10.1016/0004-6981(78)90163-4.
- Smith, G.B. et al., 2012. Multi-parameter sensitivity analysis: A design methodology applied to energy efficiency in temperate climate houses. *Energy and Buildings*. 10.1016/j.enbuild.2012.09.007.
- Solazzo, E., Vardoulakis, S., Cai, X., 2007. Evaluation of traffic-producing turbulence schemes within Operational Street Pollution Models using roadside measurements. *Atmospheric Environment*. 10.1016/j.atmosenv.2007.02.017.
- Stathopoulos, T., 2002. The numerical wind tunnel for industrial aerodynamics: Real or virtual in the new millennium? In: *Wind and Structures, An International Journal*. pp. 193–208.
- Sternam, J.D., 2002.
- Stewart, I.D., 2011. *Redefining the Urban Heat Island*.
- Stewart, I.D., Oke, T.R., 2012. Local climate zones for urban temperature studies. *Bulletin of the American Meteorological Society*, 93(12), pp.1879–1900. 10.1175/BAMS-D-11-00019.1.
- Sthjt.shanxi.gov.cn, 2017. *Shanxi Province Environmental Monitoring Center*.
- Stigsdotter, U.K. et al., 2010. Health promoting outdoor environments - Associations between green space, and health, health-related quality of life and stress based on a

- Danish national representative survey. *Scandinavian Journal of Public Health*.
10.1177/1403494810367468.
- Sturm, R., Cohen, D., 2014. Proximity to urban parks and mental health. *Journal of Mental Health Policy and Economics*.
- Sullivan, T.J. et al., 2018. Air pollution success stories in the United States: The value of long-term observations. *Environmental Science and Policy*. 10.1016/j.envsci.2018.02.016.
- Sun, X. et al., 2016. The associations between birth weight and exposure to fine particulate matter (PM_{2.5}) and its chemical constituents during pregnancy: A meta-analysis. *Environmental Pollution*. 10.1016/j.envpol.2015.12.022.
- Susca, T., Gaffin, S.R., Dell’Osso, G.R., 2011. Positive effects of vegetation: Urban heat island and green roofs. *Environmental Pollution*. 10.1016/j.envpol.2011.03.007.
- Tai, A.Y.C. et al., 2017. Atmospheric deposition of particles at a sensitive alpine lake: Size-segregated daily and annual fluxes from passive sampling techniques. *Science of the Total Environment*. 10.1016/j.scitotenv.2016.11.117.
- Takano, T., Nakamura, K., Watanabe, M., 2002. Urban residential environments and senior citizens’ longevity in megacity areas: The importance of walkable green spaces. *Journal of Epidemiology and Community Health*. 10.1136/jech.56.12.913.
- Tanaka, A. et al., 1996. Health Levels Influenced by Urban Residential Conditions in a Megacity—Tokyo. *Urban Studies*. 10.1080/00420989650011645.
- Thacker, B.H. et al., 2004. *Concepts of model verification and validation*. Los Alamos National Lab.
- Thorpe, A.J. et al., 2007. Estimation of particle resuspension source strength on a major London Road. *Atmospheric Environment*. 10.1016/j.atmosenv.2007.07.006.
- Tominaga, Y., Stathopoulos, T., 2013. 10.1016/j.atmosenv.2013.07.028.
- Tong, Z. et al., 2016. Roadside vegetation barrier designs to mitigate near-road air pollution impacts. *Science of the Total Environment*. 10.1016/j.scitotenv.2015.09.067.
- Tremback, C.J., Kessler, R., 1985. A surface temperature and moisture parameterization for use in mesoscale numerical models.
- Tzoulas, K. et al., 2007. 10.1016/j.landurbplan.2007.02.001.
- Van Ulden, a. P., Holtslag, a. a. M., 1985. 10.1175/1520-0450(1985)024<1196:EOABLP>2.0.CO;2.
- United Nations, 2014. *World Urbanization Prospects 2014*. (ST/ESA/SER.A/366).

- Vardoulakis, S. et al., 2003. Modelling air quality in street canyons: A review. *Atmospheric Environment*, 37(2), pp.155–182. 10.1016/S1352-2310(02)00857-9.
- Venkatram, A., Pleim, J., 1999. The electrical analogy does not apply to modeling dry deposition of particles. *Atmospheric Environment*. 10.1016/S1352-2310(99)00094-1.
- Vet, R. et al., 2014. A global assessment of precipitation chemistry and deposition of sulfur, nitrogen, sea salt, base cations, organic acids, acidity and pH, and phosphorus. *Atmospheric Environment*. 10.1016/j.atmosenv.2013.10.060.
- Viecco, M. et al., 2018. Potential of particle matter dry deposition on green roofs and living walls vegetation for mitigating urban atmospheric pollution in semiarid climates. *Sustainability (Switzerland)*. 10.3390/su10072431.
- Villeneuve, P.J. et al., 2012. A cohort study relating urban green space with mortality in Ontario, Canada. *Environmental Research*. 10.1016/j.envres.2012.03.003.
- Voldner, E.C., Barrie, L.A., Sirois, A., 1986. 10.1016/0004-6981(86)90305-7.
- Vong, R.J. et al., 2010. Size-dependent aerosol deposition velocities during BEARPEX'07. *Atmospheric Chemistry and Physics*. 10.5194/acp-10-5749-2010.
- Vos, P.E.J. et al., 2013. Improving local air quality in cities: To tree or not to tree? *Environmental Pollution*. 10.1016/j.envpol.2012.10.021.
- de Vries, S. et al., 2003. Natural environments - Healthy environments? An exploratory analysis of the relationship between greenspace and health. *Environment and Planning A*. 10.1068/a35111.
- Walmsley, A., 2006. Greenways: multiplying and diversifying in the 21st century. *Landscape and Urban Planning*. 10.1016/j.landurbplan.2004.09.036.
- Wan, L. et al., 2015. A study of regional sustainable development based on GIS/RS and SD model - Case of Hadaqi industrial corridor [online]. *Journal of Cleaner Production*, 142, pp.654–662. Available at: <http://dx.doi.org/10.1016/j.jclepro.2016.09.086>.
- Wang, W. et al., 2019. Characteristics of individual particles emitted from an experimental burning chamber with coal from the lung cancer area of Xuanwei, China. *Aerosol and Air Quality Research*. 10.4209/aaqr.2018.05.0187.
- Wang, W. xing et al., 2008. Study on ambient air quality in beijing for the summer 2008 olympic games. *Air Quality, Atmosphere and Health*. 10.1007/s11869-008-0003-1.
- Wang, X., Zhang, Y., Cheng, X., 2014. Lung cancer risk assessment of cooking oil fume for Chinese nonsmoking women. In: *WIT Transactions on the Built Environment*.

10.2495/ICBEEE20130311.

- Wania, A. et al., 2012. Analysing the influence of different street vegetation on traffic-induced particle dispersion using microscale simulations. *Journal of Environmental Management*. 10.1016/j.jenvman.2011.06.036.
- Watson, D.J., 1947. Comparative Physiological Studies on the Growth of Field Crops. In: *Annals of Applied Biology*. , 1947.
- Wesely, M.L., 1989. Parameterization of surface resistances to gaseous dry deposition in regional-scale numerical models. *Atmospheric Environment (1967)*. 10.1016/0004-6981(89)90153-4.
- Wesely, M.L., Cook, D.R., Hart, R.L., 1985. Measurements and parameterization of particulate sulfur dry deposition over grass. *Journal of Geophysical Research*. 10.1029/jd090id01p02131.
- Wesely, M.L., Hicks, B.B., 1977. Some factors that affect the deposition rates of sulfur dioxide and similar gases on vegetation. *Journal of the Air Pollution Control Association*. 10.1080/00022470.1977.10470534.
- WHO, 2006. Air Quality Guidelines: Global Update 2005 [online]. *Who*, (October). Available at: http://www.who.int/phe/health_topics/outdoorair/outdoorair_aqg/en/.
- Widmark, S., 2012. Modeling Physical Systems Using Vensim PLE Systems Dynamics Software. *The Physics Teacher*. 10.1119/1.3677287.
- Williams, R., Kaufman, A., Garvey, S., 2015. Dylos DC1100 Citizen Science Operating Procedure. *Citizen Science Operating Procedure*, EPA/600(R-15/116 |).
- Wong, J.K.W., Lau, L.S.K., 2013. From the 'urban heat island' to the 'green island'? A preliminary investigation into the potential of retrofitting green roofs in Mongkok district of Hong Kong. *Habitat International*. 10.1016/j.habitatint.2012.10.005.
- Xianfeng, L. et al., 2010. Influence of land cover data on regional forest leaf area index inversion. *Journal of remote sensing*.
- Xing, Y. et al., 2018. Exploring design principles of biological and living building envelopes: what can we learn from plant cell walls? *Intelligent Buildings International*, 10(2), pp.78–102. 10.1080/17508975.2017.1394808.
- Xing, Y., Jones, P., Donnison, I., 2017. Characterisation of nature-based solutions for the built environment. *Sustainability*, 9(1), p.149.
- Xu, T. et al., 2012. Quantifying the direct benefits of cool roofs in an urban setting: Reduced

- cooling energy use and lowered greenhouse gas emissions. *Building and Environment*. 10.1016/j.buildenv.2011.08.011.
- Xu, X., Zhang, T., 2020. Spatial-temporal variability of PM_{2.5} air quality in Beijing, China during 2013–2018. *Journal of Environmental Management*. 10.1016/j.jenvman.2020.110263.
- Yan, H. et al., 2014. Dry deposition of PM₁₀ over the Yellow Sea during Asian dust events from 2001 to 2007. *Journal of Environmental Sciences (China)*, 26(1), pp.54–64. 10.1016/S1001-0742(13)60380-0.
- Yang, J. et al., 2004. The urban forest in Beijing and its role in air pollution reduction. *Urban Forestry and Urban Greening*, 3(2), pp.65–78. 10.1016/j.ufug.2004.09.001.
- Yang, J., Yu, Q., Gong, P., 2008. Quantifying air pollution removal by green roofs in Chicago. *Atmospheric Environment*, 42(31), pp.7266–7273. 10.1016/j.atmosenv.2008.07.003.
- Yang, L. et al., 2017. Biomarkers of the health outcomes associated with ambient particulate matter exposure [online]. *Science of The Total Environment*, 579, pp.1446–1459. Available at: <http://linkinghub.elsevier.com/retrieve/pii/S0048969716326006>.
- Yang, L., Xing, Y., Jones, P., 2019. Exploring the potential for air pollution mitigation by urban green infrastructure for high density urban environment. In: *IOP Conference Series: Earth and Environmental Science*. 10.1088/1755-1315/227/5/052001.
- Yin, S. et al., 2011. Quantifying air pollution attenuation within urban parks: An experimental approach in Shanghai, China. *Environmental Pollution*, 159(8–9), pp.2155–2163. 10.1016/j.envpol.2011.03.009.
- Zhang, D., Liu, J., Li, B., 2014. Tackling air pollution in China-What do we learn from the great smog of 1950s in London. *Sustainability (Switzerland)*. 10.3390/su6085322.
- Zhang, L. et al., 2001. A size-segregated particle dry deposition scheme for an atmospheric aerosol module. *Atmospheric Environment*, 35(3), pp.549–560. 10.1016/S1352-2310(00)00326-5.
- Zhang, L. et al., 2012. Nitrogen deposition to the United States: Distribution, sources, and processes. *Atmospheric Chemistry and Physics*. 10.5194/acp-12-4539-2012.
- Zhang, T. et al., 2016. Semi-Physical Estimates of National-Scale PM₁₀ Concentrations in China Using a Satellite-Based Geographically Weighted Regression Model. *Atmosphere*, 7(7), p.88. 10.3390/www.mdpi.com/journal/atmosphere.
- Zhang, Y., 2019. Dynamic effect analysis of meteorological conditions on air pollution: A case

- study from Beijing. *Science of the Total Environment*. 10.1016/j.scitotenv.2019.05.360.
- Zhang, Z. et al., 2014. Development tendency analysis and evaluation of the water ecological carrying capacity in the Siping area of Jilin Province in China based on system dynamics and analytic hierarchy process. *Ecological Modelling*, 275, pp.9–21.
10.1016/j.ecolmodel.2013.11.031.
- Zhang, Z. et al., 2017. Multi-scale comparison of the fine particle removal capacity of urban forests and wetlands. *Scientific Reports*, 7. 10.1038/srep46214.
- Zhao, Y., Chen, C., Zhao, B., 2019. Emission characteristics of PM 2.5 -bound chemicals from residential Chinese cooking. *Building and Environment*.
10.1016/j.buildenv.2018.12.060.
- Zhu, L. et al., 2009. Pollution level, phase distribution and source analysis of polycyclic aromatic hydrocarbons in residential air in Hangzhou, China. *Journal of Hazardous Materials*. 10.1016/j.jhazmat.2008.05.150.
- Zhu, L. et al., 2016. Spatiotemporal characteristics of particulate matter and dry deposition flux in the Cuihu Wetland of Beijing. *PLoS ONE*, 11(7). 10.1371/journal.pone.0158616.

**APPENDIX 7-5 Simulated PM10 concentration($\mu\text{g}/\text{m}^3$) in compact-H zone
and open-H zone over 30 minutes. The table shows the simulated
PM10 concentration data at a 15 second frequency.**

Time Minute	T _{morning}		T _{afternoon}		T _{evening}	
	Compact- H	Open-H	Compact- H	Open-H	Compact- H	Open-H
0	336.1	336.1	512.8	512.8	368.3	368.3
0.25	334.7	323.1	493.1	510.8	354.2	366.8
0.5	333.7	313.9	479.1	509.3	344.1	365.7
0.75	333.0	307.4	469.2	508.1	337.0	364.9
1	332.4	302.7	462.1	507.3	331.9	364.3
1.25	332.0	299.4	457.0	506.7	328.2	363.9
1.5	333.5	298.8	452.7	505.4	326.0	363.8
1.75	336.4	300.2	448.8	503.7	324.7	364.1
2	340.4	303.0	445.3	501.7	324.0	364.6
2.25	345.1	306.8	442.0	499.4	323.9	365.3
2.5	346.2	307.0	438.9	497.0	322.8	364.9
2.75	344.6	304.8	436.0	494.4	321.2	363.6
3	340.9	300.7	433.1	491.6	319.0	361.7
3.25	335.8	295.3	430.3	488.9	316.5	359.3
3.5	332.3	292.0	427.5	486.0	316.5	359.3
3.75	330.2	290.0	424.8	483.1	318.3	361.1
4	329.0	289.0	422.1	480.2	321.3	364.2
4.25	328.5	288.7	419.4	477.3	325.2	368.3
4.5	328.7	289.0	416.7	474.3	328.5	371.8
4.75	329.4	289.8	414.0	471.3	331.4	375.0
5	330.5	290.9	411.3	468.3	334.0	377.9
5.25	331.8	292.3	408.7	465.4	336.4	380.6
5.5	332.1	292.5	406.0	462.4	339.8	384.4
5.75	331.7	292.0	403.3	459.4	344.0	389.0
6	330.6	291.0	400.7	456.3	348.8	394.2
6.25	329.1	289.5	398.0	453.3	354.0	399.8
6.5	321.7	282.1	395.4	450.3	356.9	403.3
6.75	309.8	270.6	392.7	447.3	358.3	405.2
7	294.6	256.0	390.1	444.3	358.6	405.8
7.25	277.0	239.3	387.4	441.3	358.0	405.6
7.5	270.0	233.6	384.8	438.3	359.4	407.2
7.75	271.0	235.8	382.1	435.3	362.1	410.2
8	277.8	243.4	379.4	432.3	365.9	414.1
8.25	289.1	255.1	376.8	429.2	370.3	418.9
8.5	303.7	269.5	374.6	426.7	372.7	421.7

8.75	320.8	286.0	372.9	424.6	373.7	423.0
9	339.7	303.8	371.3	422.8	373.7	423.3
9.25	360.0	322.7	370.0	421.2	372.9	422.8
9.5	372.6	333.7	368.8	419.7	372.9	422.9
9.75	379.6	339.0	367.7	418.4	373.4	423.6
10	382.3	340.3	366.7	417.1	374.3	424.6
10.25	381.9	338.8	365.7	415.9	375.5	425.8
10.5	380.4	336.6	364.7	414.8	376.8	427.3
10.75	378.3	334.0	363.8	413.7	378.3	428.9
11	375.6	331.0	362.9	412.7	379.9	430.6
11.25	372.4	327.7	362.0	411.6	381.5	432.4
11.5	367.5	322.8	367.4	416.8	381.6	432.7
11.75	361.2	316.7	377.2	426.7	380.6	431.9
12	353.9	309.8	390.2	440.1	378.9	430.2
12.25	345.9	302.3	405.4	456.1	376.6	427.9
12.5	341.7	298.7	416.0	467.8	373.9	425.2
12.75	340.3	297.9	423.3	476.2	371.0	422.1
13	341.1	299.2	428.2	482.3	367.8	418.7
13.25	343.4	301.8	431.5	486.6	364.5	415.1
13.5	343.4	302.0	433.0	488.9	361.1	411.4
13.75	341.7	300.4	433.1	489.7	357.7	407.6
14	338.7	297.5	432.3	489.5	354.1	403.7
14.25	334.7	293.7	430.9	488.4	350.6	399.7
14.5	331.1	290.4	429.0	486.8	347.0	395.7
14.75	327.8	287.3	426.8	484.7	343.4	391.6
15	324.6	284.5	424.4	482.2	339.8	387.6
15.25	321.6	281.8	421.8	479.5	336.1	383.5
15.5	320.0	280.6	417.1	474.7	334.4	381.3
15.75	319.6	280.5	411.1	468.4	334.0	380.4
16	320.0	281.1	404.1	461.0	334.5	380.6
16.25	321.0	282.3	396.3	452.7	335.7	381.6
16.5	322.0	283.4	388.4	444.1	333.6	379.4
16.75	323.0	284.4	380.4	435.3	329.2	374.8
17	324.1	285.4	372.3	426.4	323.2	368.5
17.25	325.1	286.4	364.2	417.4	315.9	360.9
17.5	325.5	286.8	358.6	410.7	309.7	354.1
17.75	325.5	286.7	354.7	405.9	304.2	348.0
18	325.0	286.2	352.0	402.5	299.3	342.4
18.25	324.3	285.5	350.3	400.0	294.7	337.2
18.5	325.3	286.4	350.4	399.6	290.4	332.2
18.75	327.4	288.5	351.9	400.6	286.3	327.4
19	330.4	291.4	354.3	402.7	282.3	322.9
19.25	334.1	295.0	357.4	405.7	278.4	318.4

19.5	335.0	295.6	358.4	406.8	276.7	316.1
19.75	333.8	294.2	358.1	406.5	276.5	315.4
20	331.0	291.3	356.7	405.1	277.4	316.0
20.25	327.0	287.4	354.6	403.0	279.1	317.4
20.5	324.8	285.2	355.7	404.0	281.4	319.5
20.75	323.8	284.4	359.1	407.4	284.0	322.2
21	323.7	284.5	364.2	412.6	287.0	325.2
21.25	324.4	285.3	370.4	419.1	290.1	328.5
21.5	324.1	285.1	374.4	423.4	293.4	332.0
21.75	323.1	284.2	376.7	426.1	296.7	335.6
22	321.6	282.8	377.8	427.7	300.2	339.4
22.25	319.8	281.0	378.1	428.3	303.7	343.2
22.5	317.7	279.0	378.3	428.8	307.2	347.1
22.75	315.3	276.9	378.5	429.1	310.7	351.1
23	312.8	274.6	378.6	429.4	314.3	355.1
23.25	310.2	272.2	378.7	429.6	317.9	359.1
23.5	309.4	271.6	377.1	428.1	321.5	363.2
23.75	309.9	272.3	374.4	425.4	325.1	367.3
24	311.4	274.0	370.8	421.8	328.7	371.3
24.25	313.6	276.3	366.6	417.4	332.3	375.4
24.5	316.4	279.0	370.0	420.5	335.9	379.5
24.75	319.7	282.1	378.8	429.2	339.6	383.6
25	323.2	285.4	391.4	442.0	343.2	387.7
25.25	326.9	288.9	406.7	458.0	346.8	391.8
25.5	329.3	290.9	416.9	469.1	350.4	395.9
25.75	330.6	291.9	423.3	476.6	354.0	400.0
26	331.1	292.2	427.2	481.5	357.6	404.1
26.25	331.0	291.9	429.1	484.3	361.3	408.2
26.5	330.9	291.6	429.7	485.7	364.9	412.3
26.75	330.7	291.3	429.4	486.0	368.5	416.4
27	330.5	291.1	428.4	485.4	372.1	420.6
27.25	330.3	290.8	427.0	484.2	375.7	424.7
27.5	330.0	290.5	427.3	484.7	378.9	428.4
27.75	329.8	290.3	428.9	486.4	381.8	431.7
28	329.5	290.0	431.3	489.0	384.5	434.9
28.25	329.2	289.7	434.5	492.3	387.1	437.9
28.5	332.4	293.0	436.0	494.1	387.4	438.6
28.75	338.2	298.7	436.5	494.8	386.1	437.6
29	346.0	306.2	436.1	494.7	383.7	435.4
29.25	355.2	314.9	435.2	493.9	380.5	432.3
29.5	359.8	318.8	432.7	491.4	377.4	429.1
29.75	360.8	319.3	428.9	487.6	374.4	426.0
30	359.3	317.3	424.4	482.9	371.5	422.8

Average	331.5	293.0	401.5	454.0	341.1	385.6
----------------	--------------	--------------	--------------	--------------	--------------	--------------

**APPENDIX 7-1 Simulated PM2.5 concentration($\mu\text{g}/\text{m}^3$) in compact-H zone
and open-H zone over 30 minutes. The shows the simulated PM10
concentration data at a 15 second frequency.**

Time Minute	T _{morning}		T _{afternoon}		T _{evening}	
	Compact-H	Open-H	Compact-H	Open-H	Compact-H	Open-H
0	60.0	60.0	66.9	66.9	88.0	88.0
0.25	56.6	59.0	63.1	65.8	83.1	86.6
0.5	54.3	58.3	60.5	65.0	79.6	85.5
0.75	52.7	57.8	58.7	64.4	77.3	84.7
1	51.5	57.4	57.5	64.0	75.6	84.2
1.25	50.8	57.1	56.6	63.7	74.5	83.8
1.5	50.6	57.3	56.0	63.5	73.6	83.4
1.75	50.9	57.8	55.6	63.3	72.9	83.0
2	51.5	58.6	55.3	63.2	72.4	82.7
2.25	52.4	59.6	55.1	63.1	71.9	82.4
2.5	53.3	60.7	55.0	63.1	71.5	82.0
2.75	54.3	61.9	54.9	63.0	71.0	81.6
3	55.3	63.1	54.9	63.0	70.5	81.1
3.25	56.4	64.3	54.8	63.0	70.1	80.6
3.5	57.5	65.5	54.8	62.9	69.9	80.5
3.75	58.5	66.7	54.7	62.9	70.0	80.5
4	59.6	67.9	54.7	62.9	70.2	80.7
4.25	60.6	69.1	54.7	62.9	70.5	81.0
4.5	61.6	70.3	54.5	62.7	70.6	81.1
4.75	62.6	71.4	54.3	62.5	70.4	81.0
5	63.5	72.5	54.0	62.2	70.2	80.7
5.25	64.5	73.6	53.7	61.8	69.9	80.4
5.5	65.4	74.6	53.2	61.3	69.4	79.9
5.75	66.2	75.6	52.6	60.7	68.8	79.3
6	67.1	76.6	52.0	60.0	68.1	78.5
6.25	67.9	77.6	51.2	59.2	67.3	77.7
6.5	68.7	78.5	50.5	58.4	67.0	77.3
6.75	69.4	79.4	49.7	57.5	67.0	77.2
7	70.2	80.2	48.9	56.6	67.2	77.4
7.25	70.9	81.1	48.1	55.7	67.6	77.8
7.5	70.7	81.0	47.8	55.3	67.6	77.7
7.75	70.0	80.4	47.7	55.1	67.2	77.3
8	68.9	79.3	47.9	55.2	66.6	76.7
8.25	67.5	77.9	48.2	55.4	65.9	75.9
8.5	66.2	76.5	48.6	55.9	65.1	75.1

8.75	65.1	75.3	49.2	56.5	64.3	74.2
9	64.0	74.0	49.9	57.2	63.5	73.3
9.25	62.9	72.9	50.6	58.0	62.6	72.4
9.5	62.4	72.2	51.1	58.5	62.1	71.8
9.75	62.1	71.8	51.5	59.0	61.8	71.4
10	62.0	71.6	51.8	59.3	61.6	71.1
10.25	62.1	71.6	52.0	59.6	61.6	71.0
10.5	62.3	71.7	52.2	59.8	61.6	70.9
10.75	62.5	71.9	52.3	60.0	61.6	71.0
11	62.8	72.2	52.5	60.2	61.7	71.0
11.25	63.1	72.5	52.6	60.3	61.9	71.1
11.5	63.5	72.9	52.9	60.7	61.8	71.1
11.75	63.8	73.2	53.3	61.1	61.7	70.9
12	64.1	73.6	53.8	61.6	61.4	70.7
12.25	64.5	74.0	54.3	62.3	61.2	70.4
12.5	64.1	73.6	54.8	62.8	60.8	70.1
12.75	63.1	72.6	55.2	63.2	60.5	69.7
13	61.8	71.3	55.6	63.6	60.1	69.3
13.25	60.2	69.6	55.9	64.0	59.7	68.9
13.5	58.9	68.2	56.0	64.3	59.2	68.3
13.75	57.7	66.9	56.1	64.4	58.6	67.6
14	56.7	65.7	56.1	64.4	57.9	66.9
14.25	55.8	64.7	56.1	64.4	57.2	66.1
14.5	55.6	64.4	55.8	64.2	56.9	65.7
14.75	56.1	64.7	55.5	63.9	56.7	65.4
15	56.9	65.5	55.1	63.4	56.8	65.4
15.25	58.0	66.5	54.6	62.9	56.9	65.5
15.5	58.2	66.8	54.1	62.4	57.1	65.7
15.75	57.8	66.4	53.6	61.8	57.4	66.0
16	56.9	65.6	53.0	61.2	57.7	66.3
16.25	55.8	64.4	52.4	60.5	58.1	66.7
16.5	55.1	63.6	51.8	59.8	58.4	67.0
16.75	54.7	63.1	51.1	59.1	58.7	67.3
17	54.4	62.8	50.4	58.3	58.9	67.6
17.25	54.3	62.7	49.6	57.4	59.2	67.9
17.5	54.4	62.6	49.1	56.7	59.3	68.0
17.75	54.4	62.7	48.6	56.2	59.3	68.1
18	54.5	62.8	48.2	55.7	59.2	68.0
18.25	54.7	62.9	47.9	55.3	59.1	67.9
18.5	54.2	62.4	47.8	55.1	58.9	67.7
18.75	53.4	61.6	47.7	55.0	58.5	67.3
19	52.2	60.3	47.8	55.0	58.1	66.9
19.25	50.9	58.9	47.9	55.1	57.6	66.4

19.5	50.4	58.3	47.8	55.0	57.0	65.8
19.75	50.5	58.3	47.5	54.7	56.4	65.1
20	51.0	58.7	47.1	54.3	55.7	64.3
20.25	51.8	59.5	46.7	53.8	55.0	63.5
20.5	52.1	59.8	46.3	53.4	54.6	63.1
20.75	51.9	59.7	46.0	53.0	54.5	62.9
21	51.5	59.3	45.7	52.7	54.5	62.8
21.25	51.0	58.7	45.4	52.3	54.7	63.0
21.5	50.7	58.4	45.4	52.3	54.7	62.9
21.75	50.6	58.3	45.7	52.6	54.5	62.8
22	50.6	58.3	46.1	53.0	54.3	62.6
22.25	50.8	58.4	46.6	53.5	54.1	62.3
22.5	50.9	58.5	47.2	54.1	53.8	62.0
22.75	50.9	58.5	47.7	54.7	53.6	61.8
23	50.9	58.5	48.3	55.3	53.4	61.5
23.25	50.9	58.5	48.9	55.9	53.2	61.3
23.5	51.2	58.9	49.4	56.6	52.9	60.9
23.75	51.8	59.5	50.0	57.2	52.5	60.5
24	52.6	60.2	50.6	57.8	52.0	60.0
24.25	53.4	61.1	51.1	58.5	51.5	59.4
24.5	53.7	61.5	51.5	58.9	51.1	59.0
24.75	53.6	61.5	51.6	59.1	50.8	58.6
25	53.3	61.2	51.7	59.2	50.5	58.2
25.25	52.7	60.7	51.6	59.2	50.2	57.9
25.5	52.4	60.3	51.6	59.3	50.3	57.9
25.75	52.2	60.1	51.7	59.4	50.6	58.2
26	52.1	60.0	51.8	59.5	51.1	58.7
26.25	52.0	59.9	52.0	59.7	51.6	59.3
26.5	52.0	59.9	51.8	59.5	52.1	59.8
26.75	52.1	59.9	51.4	59.2	52.6	60.2
27	52.2	60.0	50.9	58.7	52.9	60.6
27.25	52.2	60.1	50.4	58.0	53.2	61.0
27.5	52.3	60.2	49.8	57.5	53.5	61.4
27.75	52.5	60.3	49.3	56.9	53.8	61.7
28	52.6	60.4	48.8	56.4	54.1	62.1
28.25	52.8	60.6	48.4	55.9	54.4	62.4
28.5	52.9	60.8	48.1	55.5	54.7	62.7
28.75	53.1	60.9	47.9	55.2	55.0	63.0
29	53.2	61.1	47.7	55.0	55.3	63.4
29.25	53.4	61.3	47.6	54.9	55.5	63.7
29.5	53.6	61.5	47.5	54.8	55.6	63.8
29.75	53.7	61.7	47.5	54.7	55.6	63.8
30	53.9	61.8	47.4	54.6	55.4	63.7

Average	57.0	65.3	51.5	59.0	60.8	69.7
----------------	-------------	-------------	-------------	-------------	-------------	-------------

APPENDIX 1 – Scenario 1 output data of PM₁₀ concentration in the study area

Time (Hour)	PM ₁₀ concentration with the percentages of land cover by trees				
	7%	14%	25%	50%	100%
0.000	212.00	212.00	212.00	212.00	212.00
0.125	232.87	227.24	218.77	199.19	159.92
0.250	252.81	241.30	224.53	188.38	126.77
0.375	271.84	254.23	229.38	179.20	105.53
0.500	289.99	266.10	233.41	171.34	91.79
0.625	307.29	276.97	236.68	164.57	82.76
0.750	323.75	286.88	239.28	158.68	76.71
0.875	339.40	295.89	241.25	153.51	72.53
1.000	354.26	304.05	242.67	148.92	69.52
1.125	368.35	311.40	243.59	144.80	67.25
1.250	382.48	318.78	244.84	141.87	66.24
1.375	396.67	326.20	246.39	139.91	66.03
1.500	410.89	333.64	248.22	138.73	66.32
1.625	425.17	341.10	250.31	138.19	66.93
1.750	439.48	348.59	252.62	138.18	67.73
1.875	453.84	356.11	255.14	138.59	68.65
2.000	468.23	363.65	257.84	139.34	69.66
2.125	482.67	371.21	260.72	140.38	70.71
2.250	493.86	375.51	260.47	138.36	68.52
2.375	501.90	376.72	257.38	133.86	64.28
2.500	506.86	375.01	251.72	127.34	58.75
2.625	508.83	370.53	243.73	119.16	52.41
2.750	507.89	363.42	233.62	109.65	45.56
2.875	504.12	353.84	221.59	99.03	38.39
3.000	497.58	341.91	207.83	87.53	31.02
3.125	488.37	327.75	192.48	75.30	23.52
3.250	479.20	314.15	178.38	65.15	18.62
3.375	470.10	301.09	165.40	56.69	15.34
3.500	461.05	288.53	153.44	49.62	13.09
3.625	452.05	276.46	142.41	43.67	11.49
3.750	443.10	264.84	132.22	38.63	10.29
3.875	434.20	253.65	122.79	34.34	9.35
4.000	425.36	242.86	114.05	30.66	8.57
4.125	416.56	232.46	105.93	27.48	7.90
4.250	408.29	222.91	98.87	25.18	7.77

4.375	400.53	214.17	92.76	23.60	7.98
4.500	393.28	206.18	87.52	22.62	8.41
4.625	386.52	198.92	83.06	22.11	8.98
4.750	380.24	192.34	79.31	22.00	9.64
4.875	374.42	186.40	76.21	22.20	10.35
5.000	369.05	181.08	73.69	22.66	11.09
5.125	364.12	176.34	71.71	23.33	11.85
5.250	359.85	172.38	70.44	24.41	12.87
5.375	356.23	169.16	69.82	25.82	14.03
5.500	353.24	166.64	69.79	27.50	15.30
5.625	350.85	164.79	70.30	29.40	16.63
5.750	349.06	163.57	71.28	31.48	18.00
5.875	347.85	162.94	72.71	33.71	19.39
6.000	347.20	162.88	74.54	36.05	20.80
6.125	347.10	163.36	76.72	38.49	22.21
6.250	346.54	163.34	78.24	40.01	22.64
6.375	345.52	162.85	79.14	40.78	22.43
6.500	344.06	161.92	79.50	40.94	21.84
6.625	342.17	160.57	79.35	40.59	20.99
6.750	339.86	158.82	78.74	39.85	19.99
6.875	337.14	156.70	77.73	38.77	18.89
7.000	334.03	154.22	76.34	37.43	17.73
7.125	330.53	151.40	74.61	35.86	16.54
7.250	326.86	148.47	72.77	34.32	15.52
7.375	323.02	145.43	70.84	32.80	14.61
7.500	319.02	142.28	68.83	31.30	13.77
7.625	314.86	139.04	66.73	29.81	12.98
7.750	310.54	135.70	64.57	28.33	12.22
7.875	306.07	132.27	62.34	26.85	11.47
8.000	301.45	128.76	60.05	25.39	10.73
8.125	296.69	125.17	57.71	23.93	10.00
8.250	293.13	122.84	56.65	23.81	10.61
8.375	290.71	121.69	56.75	24.77	12.05
8.500	289.43	121.66	57.91	26.61	14.02
8.625	289.24	122.70	60.02	29.18	16.32
8.750	290.12	124.75	63.00	32.33	18.84
8.875	292.03	127.74	66.76	35.96	21.48
9.000	294.96	131.65	71.23	39.98	24.21
9.125	298.88	136.40	76.35	44.32	26.98
9.250	301.22	139.44	79.53	46.38	27.26
9.375	302.03	140.85	80.94	46.59	25.97
9.500	301.35	140.71	80.75	45.30	23.69

9.625	299.22	139.11	79.11	42.77	20.78
9.750	295.67	136.13	76.15	39.25	17.49
9.875	290.76	131.84	72.00	34.91	13.94
10.000	284.50	126.30	66.77	29.90	10.24
Average	360.03	216.21	131.11	68.20	34.72

APPENDIX 2 – Scenario 2 output data of PM₁₀ removal in the study area

Time (Hour)	Level_50	Level_150	Level_250	Level_350	Level_450
0.00	0.00	0.00	0.00	0.00	0.00
0.25	0.38	1.15	1.91	2.68	3.44
0.50	0.84	2.51	4.18	5.85	7.53
0.75	1.36	4.07	6.78	9.50	12.21
1.00	1.94	5.82	9.70	13.58	17.46
1.25	2.58	7.74	12.91	18.07	23.23
1.50	3.28	9.83	16.39	22.94	29.50
1.75	4.00	12.00	20.00	28.01	36.01
2.00	4.73	14.18	23.63	33.08	42.54
2.25	5.42904	16.2871	27.1452	38.0032	48.8613
2.50	6.09	18.26	30.44	42.61	54.78
2.75	6.73	20.18	33.64	47.09	60.54
3.00	7.37	22.12	36.87	51.62	66.37
3.25	8.05	24.15	40.26	56.36	72.46
3.50	8.78	26.34	43.91	61.47	79.03
3.75	9.54	28.61	47.68	66.76	85.83
4.00	10.29	30.87	51.46	72.04	92.62
4.25	11.02	33.07	55.11	77.15	99.20
4.50	11.71	35.12	58.53	81.94	105.36
4.75	12.3704	37.1112	61.8521	86.5929	111.334
5	13.0402	39.1205	65.2009	91.2813	117.362
5.25	13.739	41.2169	68.6949	96.1728	123.651
5.5	14.4889	43.4666	72.4443	101.422	130.4
5.75	15.2626	45.7879	76.3132	106.839	137.364
6	16.0349	48.1048	80.1746	112.244	144.314
6.25	16.7819	50.3456	83.9094	117.473	151.037
6.5	17.4812	52.4436	87.406	122.368	157.331
6.75	18.1598	54.4795	90.7992	127.119	163.439
7	18.843	56.5291	94.2152	131.901	169.587
7.25	19.5544	58.6632	97.772	136.881	175.99
7.5	20.316	60.9481	101.58	142.212	182.844
7.75	21.1009	63.3026	105.504	147.706	189.908
8	21.8835	65.6504	109.417	153.184	196.951
8.25	22.6401	67.9202	113.2	158.48	203.761
8.5	23.3484	70.0453	116.742	163.439	210.136
8.75	24.0355	72.1066	120.178	168.249	216.32
9	24.7267	74.18	123.633	173.087	222.54

9.25	25.4454	76.3363	127.227	178.118	229.009
9.5	26.214	78.6421	131.07	183.498	235.926
9.75	27.0053	81.016	135.027	189.037	243.048
10	27.794	83.3821	138.97	194.558	250.146

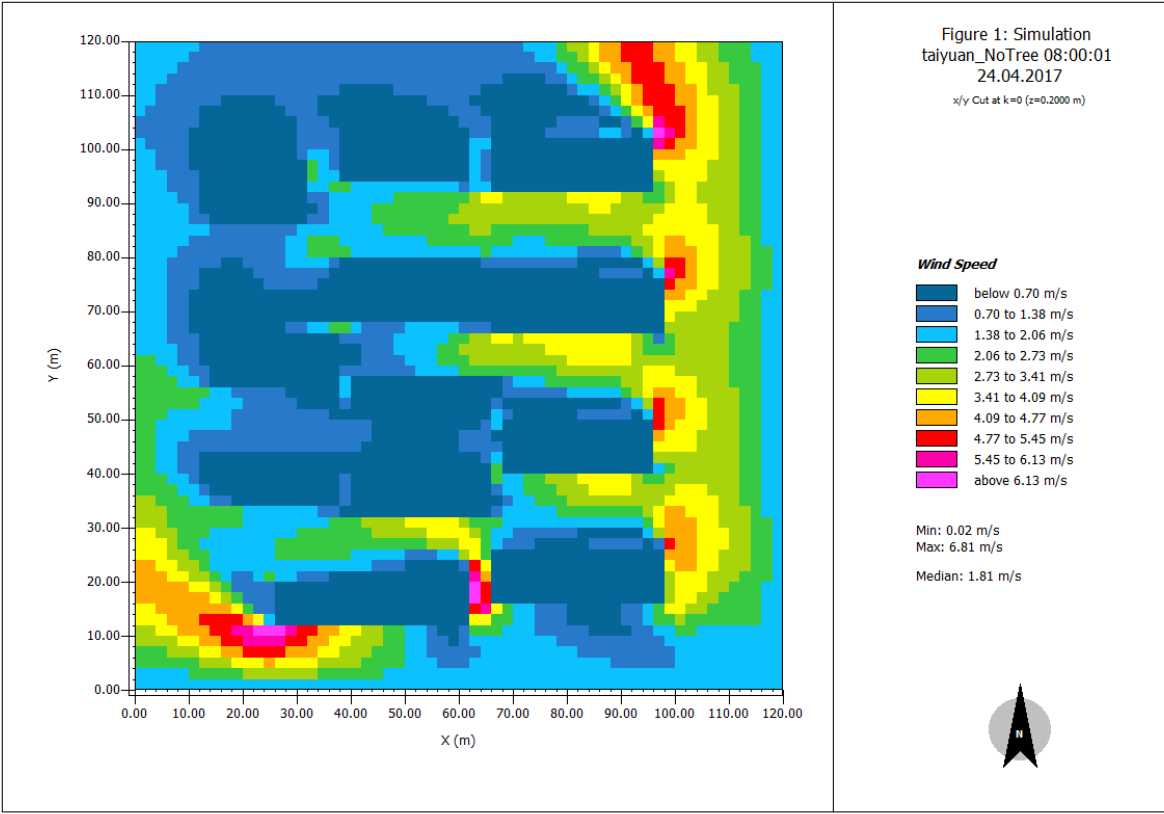
APPENDIX 3.1 – Scenario 3 output data of PM₁₀ removal in the study area

Time (Hour)	Location1	Location2	Location3	Location4
0	0	0	0	0
0.25	0.00021235	0.00021292	0.00021369	0.00021582
0.5	0.00047773	0.00047902	0.00048076	0.00048554
0.75	0.00079615	0.0007983	0.0008012	0.00080916
1	0.00116758	0.00117073	0.00117498	0.00118666
1.25	0.00159202	0.00159632	0.00160211	0.00161803
1.5	0.00206945	0.00207504	0.00208257	0.00210326
1.75	0.00258953	0.00259652	0.00260594	0.00263183
2	0.00314189	0.00315037	0.0031618	0.00319321
2.25	0.00371619	0.00372622	0.00373973	0.00377688
2.5	0.00430207	0.00431368	0.00432933	0.00437233
2.75	0.00490374	0.00491698	0.00493481	0.00498382
3	0.0055254	0.00554031	0.0055604	0.00561562
3.25	0.00617125	0.0061879	0.00621034	0.00627201
3.5	0.00684548	0.00686395	0.00688884	0.00695724
3.75	0.00755144	0.00757182	0.00759927	0.00767471
4	0.00829248	0.00831485	0.00834499	0.00842783
4.25	0.00907192	0.00909639	0.00912937	0.00921999
4.5	0.00989312	0.0099198	0.00995576	0.0100546
4.75	0.0107522	0.0107812	0.0108203	0.0109277
5	0.0116454	0.0116768	0.0117191	0.0118354
5.25	0.0125688	0.0126027	0.0126484	0.0127739
5.5	0.0135187	0.0135551	0.0136042	0.0137392
5.75	0.0144963	0.0145354	0.014588	0.0147328
6	0.015503	0.0155448	0.0156011	0.0157559
6.25	0.0165403	0.0165849	0.016645	0.0168101
6.5	0.0176094	0.0176569	0.0177208	0.0178966
6.75	0.0187325	0.018783	0.018851	0.019038
7	0.0199316	0.0199853	0.0200577	0.0202566
7.25	0.0212287	0.021286	0.021363	0.0215749
7.5	0.0226461	0.0227071	0.0227893	0.0230153
7.75	0.0241632	0.0242283	0.024316	0.0245571
8	0.0257596	0.025829	0.0259225	0.0261796
8.25	0.027415	0.0274888	0.0275884	0.0278619
8.5	0.0291089	0.0291873	0.029293	0.0295834
8.75	0.0308439	0.030927	0.031039	0.0313467
9	0.0326228	0.0327107	0.0328291	0.0331546
9.25	0.0344482	0.034541	0.034666	0.0350097
9.5	0.0363227	0.0364205	0.0365524	0.0369147

9.75	0.0382442	0.0383473	0.038486	0.0388675
10	0.0402108	0.0403191	0.040465	0.040866
10.25	0.0422202	0.0423339	0.0424871	0.0429082
10.5	0.0442705	0.0443897	0.0445504	0.0449918
10.75	0.0463633	0.0464881	0.0466563	0.0471186
11	0.0485002	0.0486308	0.0488067	0.0492903
11.25	0.0506828	0.0508193	0.0510031	0.0515084
11.5	0.0529128	0.0530553	0.0532472	0.0537747
11.75	0.0551902	0.0553388	0.0555389	0.0560891
12	0.0575149	0.0576697	0.0578783	0.0584516
12.25	0.059887	0.0600482	0.0602653	0.0608623
12.5	0.0623063	0.0624741	0.0627	0.063321
12.75	0.0647731	0.0649474	0.0651823	0.0658278
13	0.0672871	0.0674682	0.0677121	0.0683827
13.25	0.0698484	0.0700364	0.0702896	0.0709856
13.5	0.072457	0.072652	0.0729147	0.0736366
13.75	0.0751129	0.075315	0.0755873	0.0763357
14	0.0778161	0.0780255	0.0783075	0.0790827
14.25	0.0805665	0.0807833	0.0810753	0.0818778
14.5	0.0833642	0.0835885	0.0838906	0.084721
14.75	0.0862091	0.086441	0.0867534	0.0876121
15	0.0891012	0.0893409	0.0896638	0.0905512
15.25	0.0920406	0.0922882	0.0926217	0.0935383
15.5	0.0950272	0.0952828	0.0956271	0.0965733
15.75	0.098061	0.0983247	0.0986799	0.0996564
16	0.101142	0.101414	0.10178	0.102787
16.25	0.10427	0.10455	0.104928	0.105966
16.5	0.107445	0.107734	0.108123	0.109193
16.75	0.110668	0.110965	0.111366	0.112468
17	0.113937	0.114244	0.114656	0.115791
17.25	0.117254	0.117569	0.117994	0.119161
17.5	0.120618	0.120942	0.121379	0.12258
17.75	0.124029	0.124362	0.124812	0.126046
18	0.127487	0.12783	0.128291	0.12956
18.25	0.130992	0.131344	0.131819	0.133122
18.5	0.134545	0.134906	0.135393	0.136732
18.75	0.138144	0.138515	0.139015	0.14039
19	0.141791	0.142171	0.142685	0.144095
19.25	0.145484	0.145875	0.146401	0.147849
19.5	0.149225	0.149625	0.150165	0.15165
19.75	0.153012	0.153423	0.153977	0.155499
20	0.156847	0.157268	0.157836	0.159395

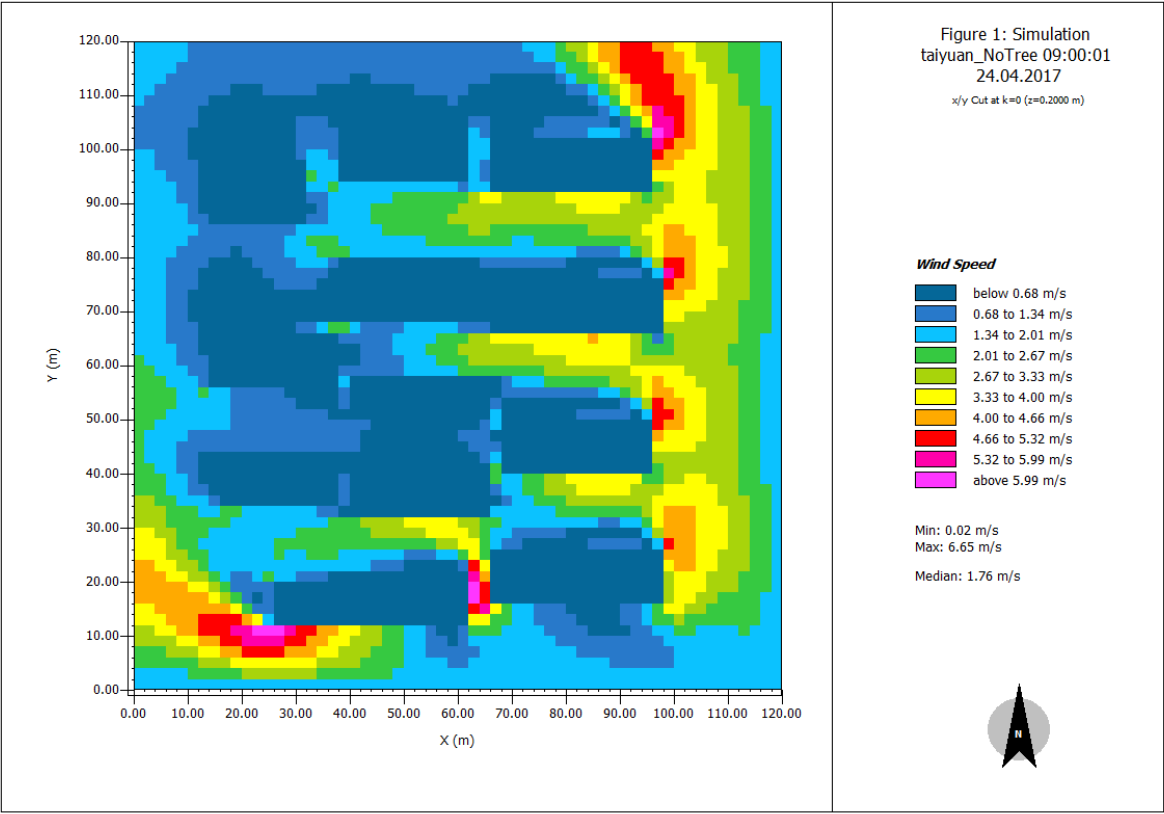
20.25	0.160728	0.16116	0.161742	0.16334
20.5	0.164657	0.165099	0.165695	0.167332
20.75	0.168633	0.169085	0.169696	0.171372
21	0.172655	0.173119	0.173743	0.17546
21.25	0.176725	0.177199	0.177839	0.179596
21.5	0.180841	0.181327	0.181981	0.183779
21.75	0.185005	0.185502	0.186171	0.18801
22	0.189215	0.189723	0.190408	0.192288
22.25	0.193473	0.193992	0.194692	0.196615
22.5	0.197777	0.198308	0.199023	0.200989
22.75	0.202128	0.202671	0.203402	0.20541
23	0.206526	0.207081	0.207827	0.20988
23.25	0.210971	0.211538	0.2123	0.214396
23.5	0.215463	0.216042	0.21682	0.218961
23.75	0.220002	0.220592	0.221388	0.223573
24	0.224588	0.22519	0.226002	0.228233
24.25	0.22922	0.229835	0.230664	0.232941
24.5	0.2339	0.234527	0.235372	0.237696
24.75	0.238626	0.239266	0.240128	0.242498
25	0.243399	0.244052	0.244931	0.247348
25.25	0.248219	0.248884	0.249781	0.252246
25.5	0.253085	0.253764	0.254679	0.257191
25.75	0.257999	0.258691	0.259623	0.262184
26	0.262959	0.263664	0.264614	0.267225
26.25	0.267966	0.268685	0.269652	0.272313
26.5	0.27302	0.273752	0.274738	0.277448
26.75	0.27812	0.278866	0.27987	0.282631
27	0.283268	0.284027	0.28505	0.287861
27.25	0.288462	0.289235	0.290276	0.293139
27.5	0.293702	0.29449	0.29555	0.298465
27.75	0.29899	0.299791	0.300871	0.303837
28	0.304324	0.305139	0.306238	0.309258
28.25	0.309705	0.310535	0.311653	0.314725
28.5	0.315132	0.315977	0.317114	0.32024
28.75	0.320606	0.321465	0.322623	0.325803
29	0.326127	0.327001	0.328178	0.331413
29.25	0.331695	0.332583	0.33378	0.33707
29.5	0.337309	0.338212	0.33943	0.342775
29.75	0.34297	0.343888	0.345126	0.348527
30	0.348677	0.349611	0.350869	0.354327

**APPENDIX 3.2 – Scenario 3 output data of wind speeds in the study area
from 8:00 to 18:00**



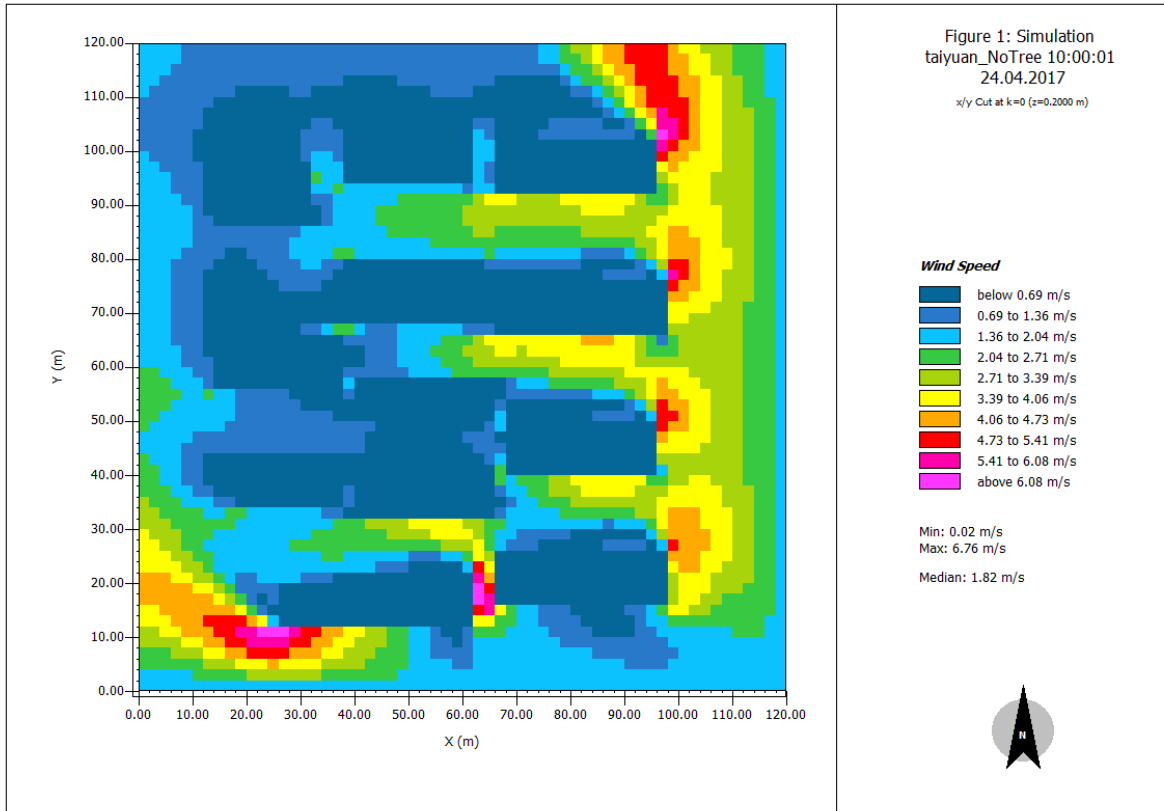
ENVI_met

<Right foot>

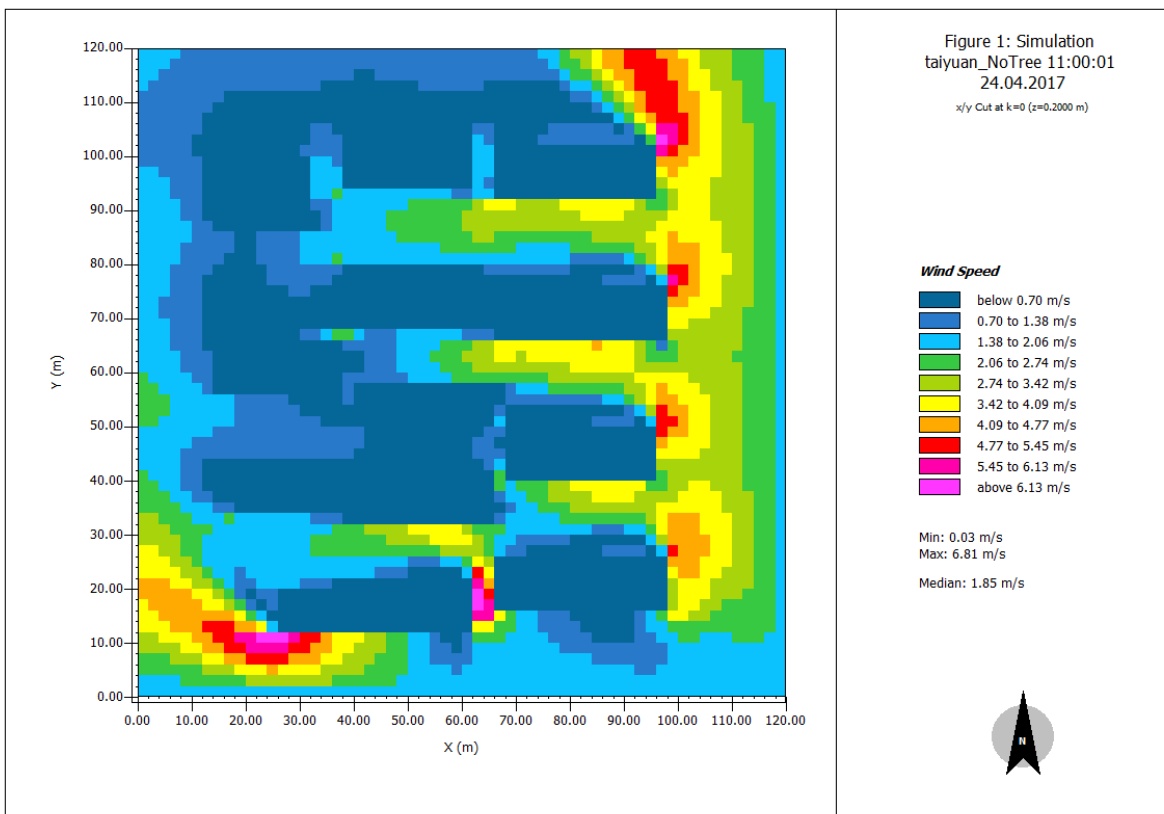


ENVI_met

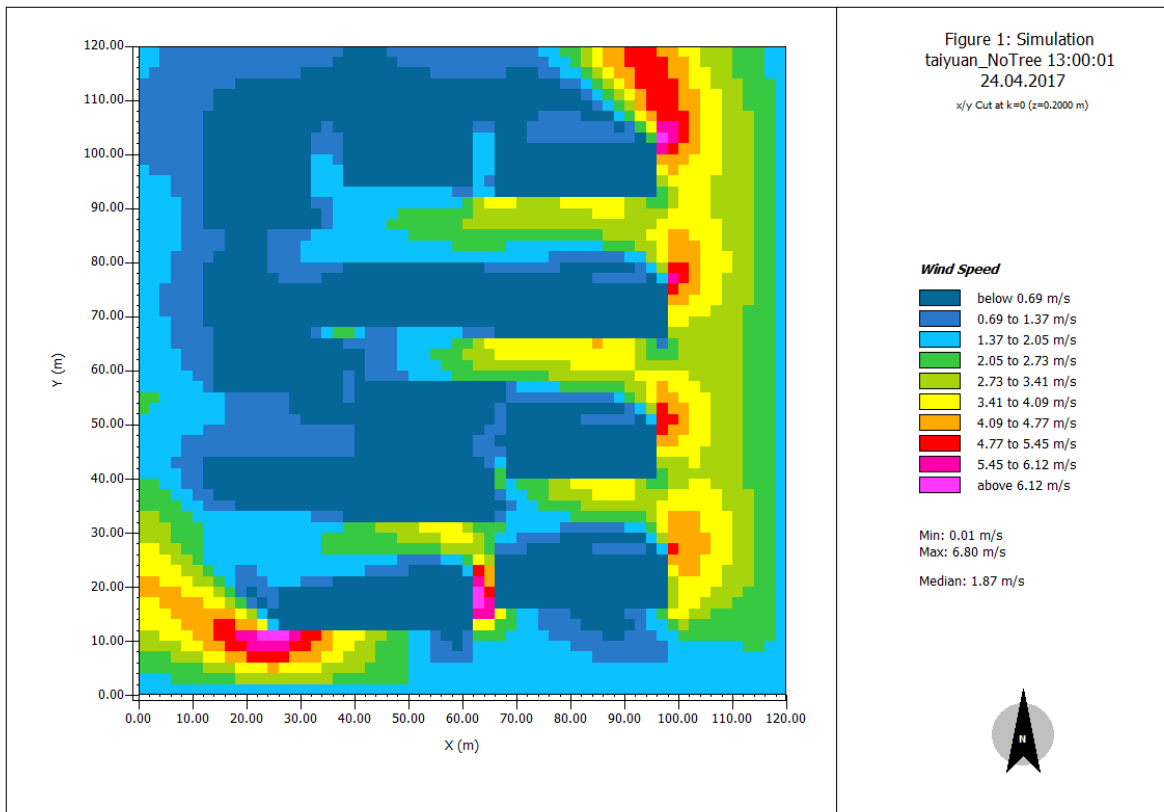
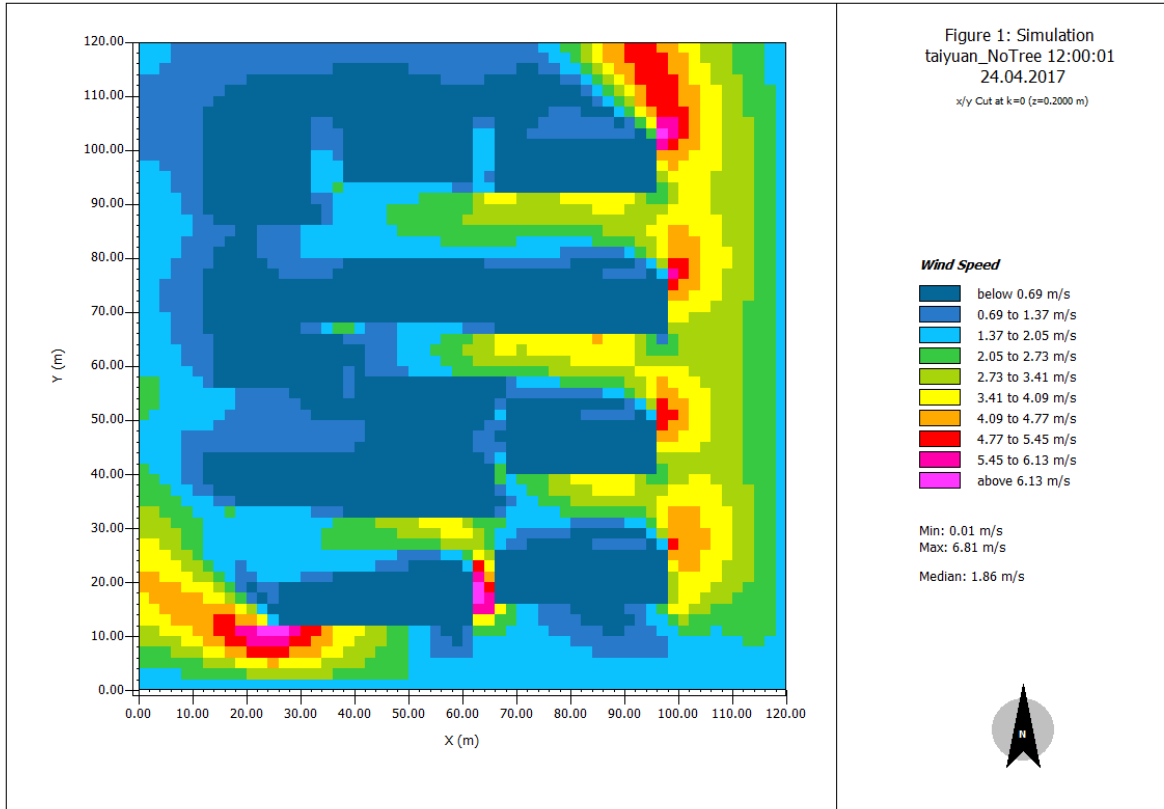
<Right foot>

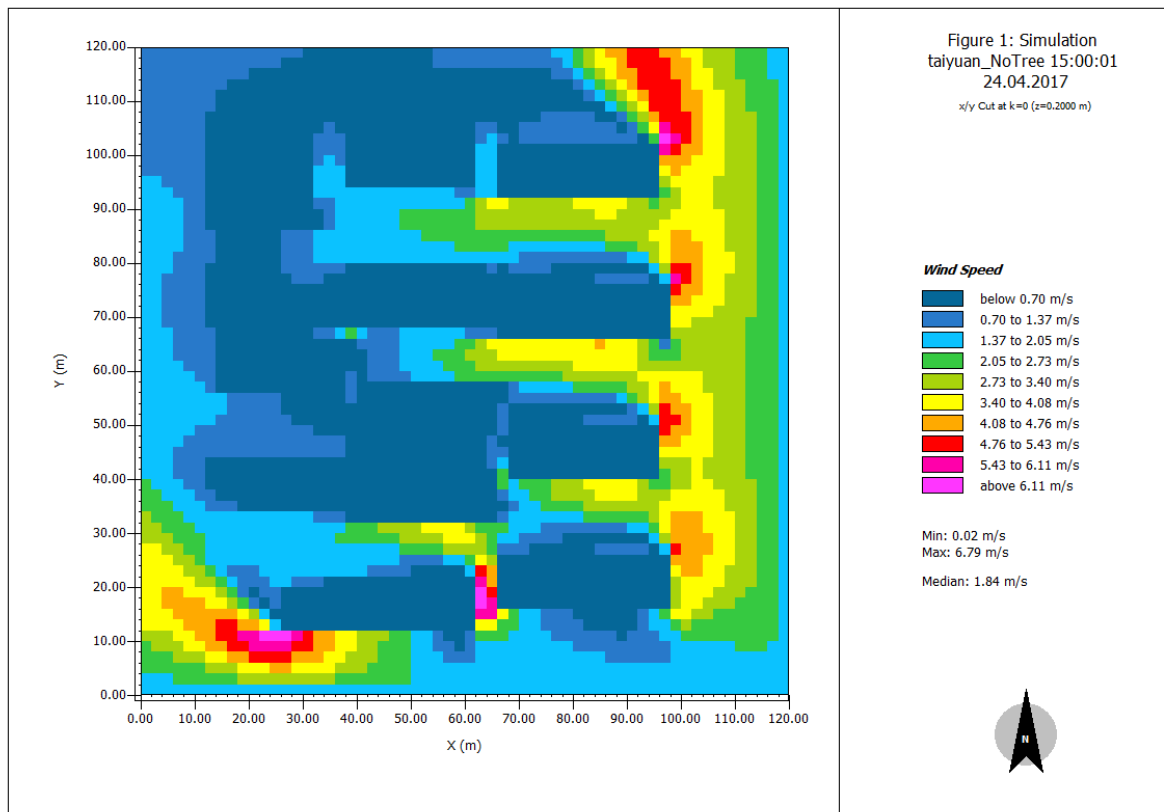
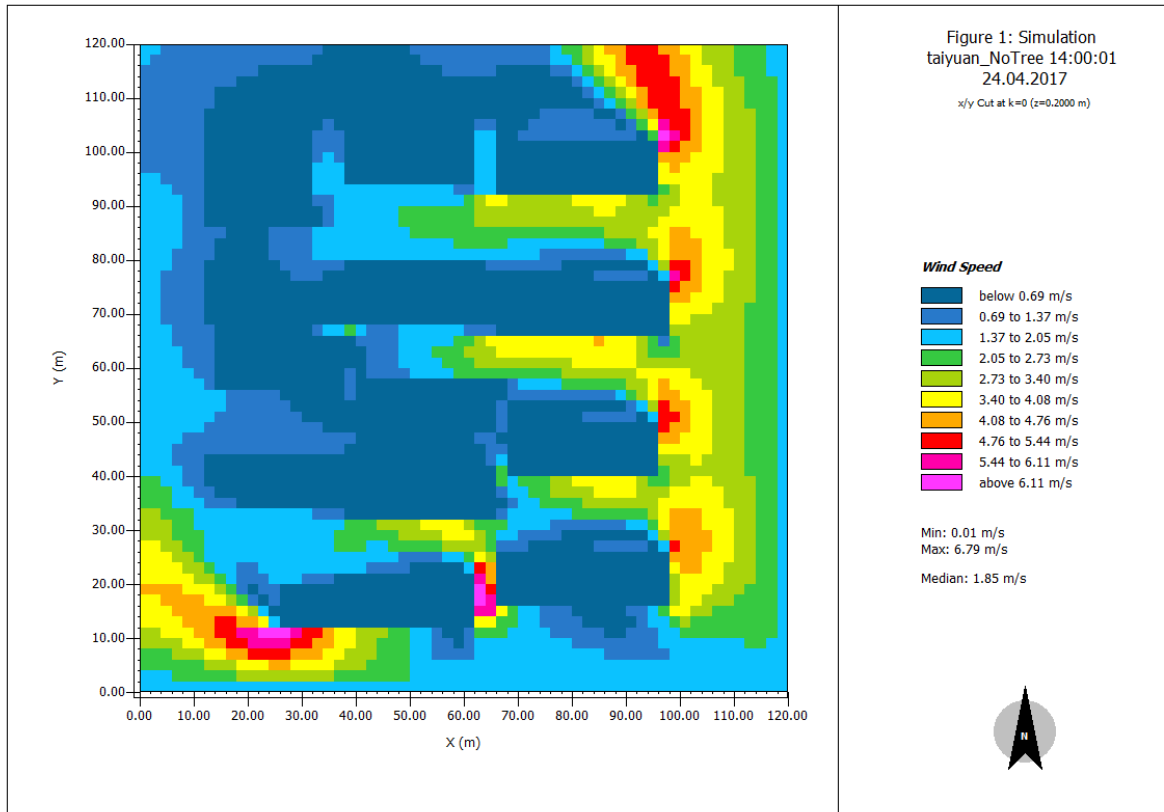


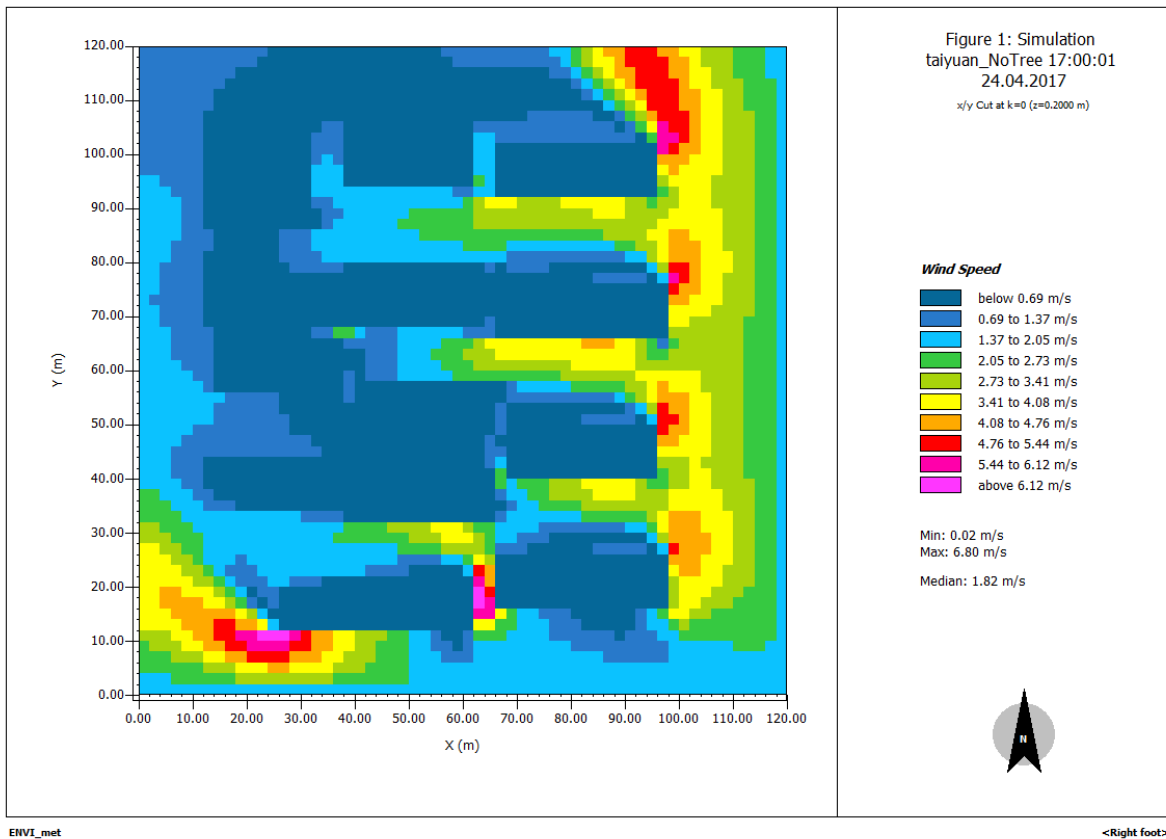
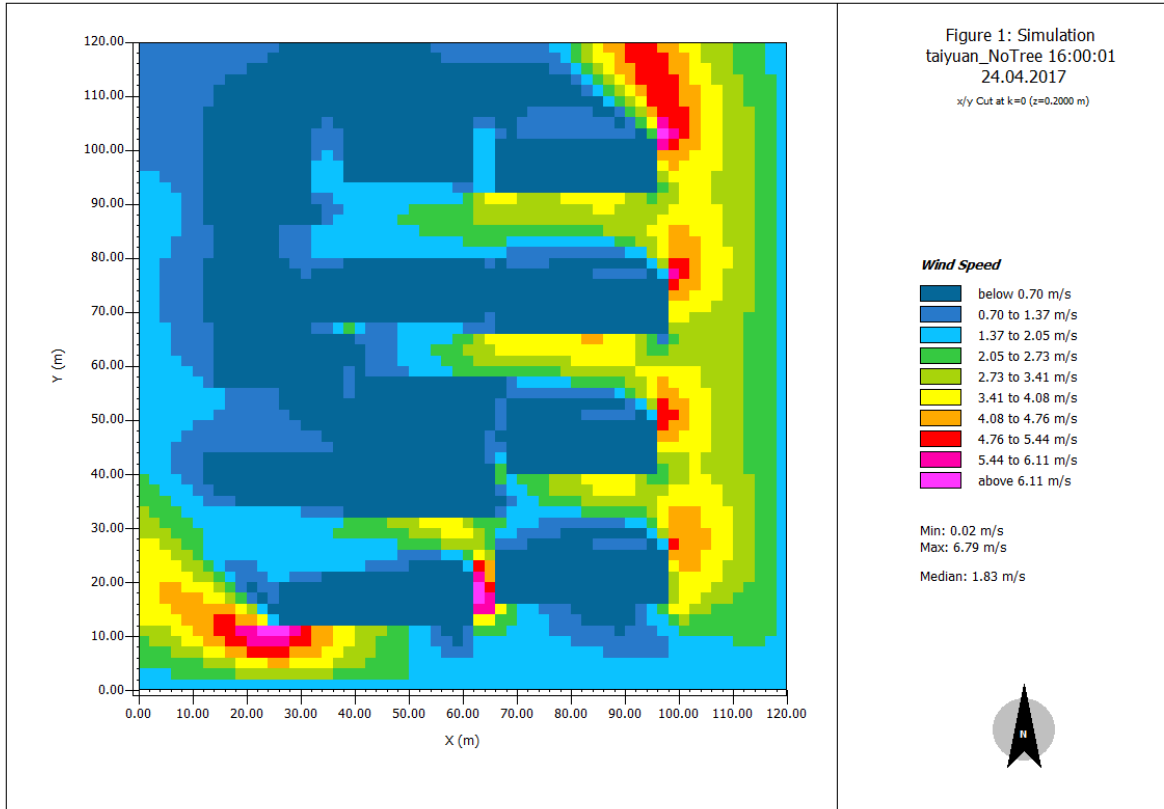
ENV1_met

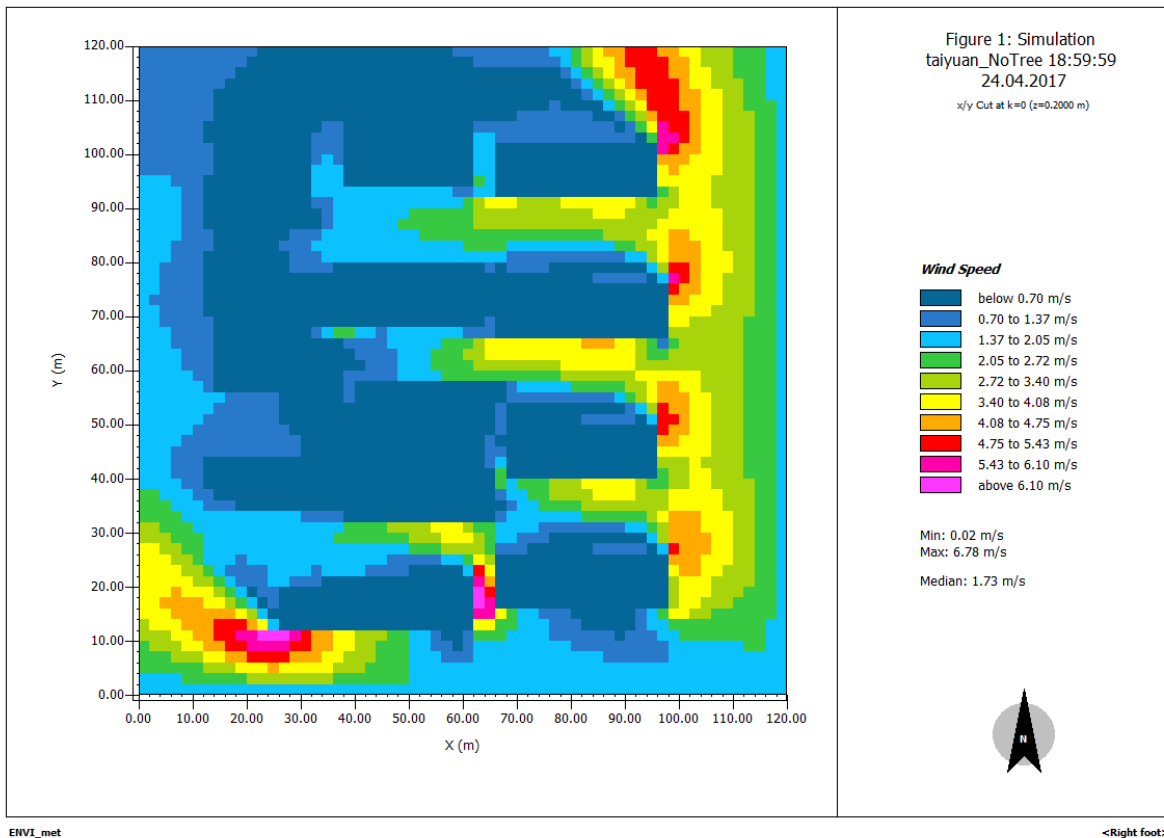
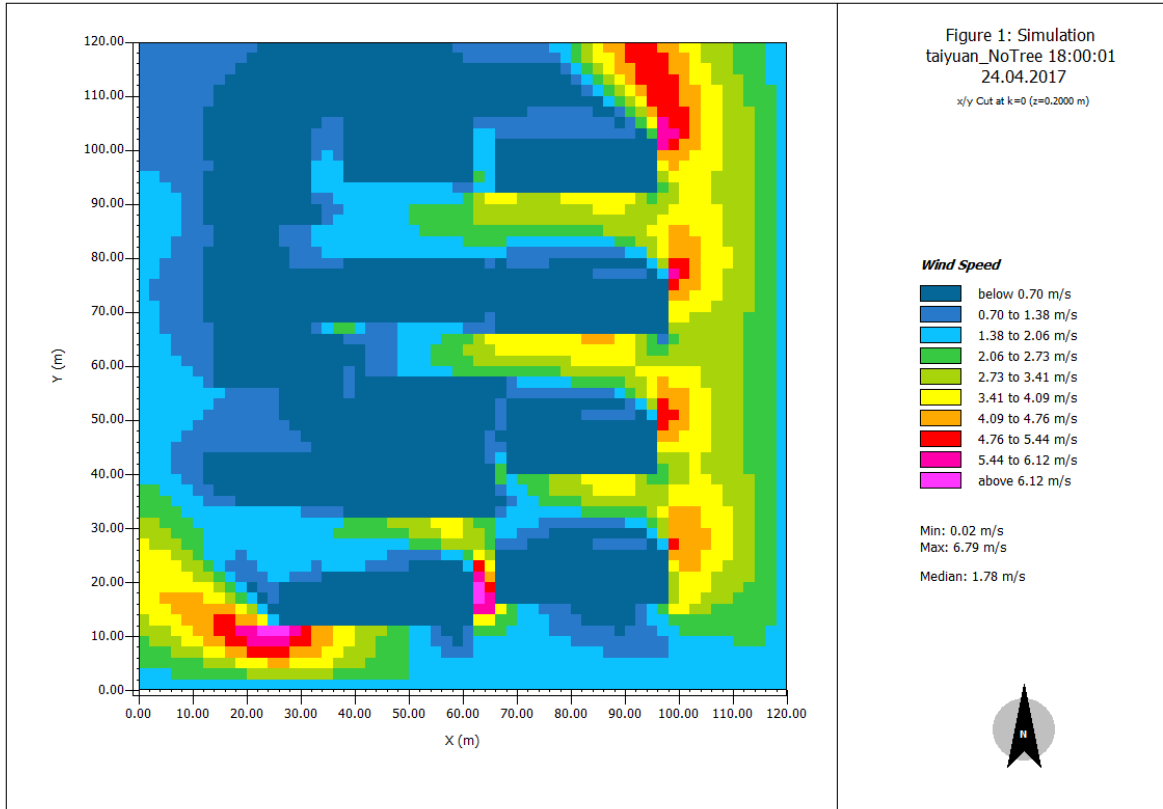


ENV1_met









**APPENDIX 4.1 – Scenario 4 Input data of PM₁₀ concentration in Taiyuan in
2017 from the local weather station**

Jan	Feb	Mar	Apr	May	Jun	Jul	Aug	Sep	Oct	Nov	Dec
373	190	143	71	164	116	142	149	153	165	211	145
-	166	75	97	174	132	152	155	147	171	285	157
445	224	137	116	164	151	158	142	156	134	236	198
412	286	177	149	125	137	161	134	123	70	93	148
198	298	165	132	279	110	149	105	169	92	141	83
176	165	90	155	244	97	160	117	171	144	214	92
242	199	63	166	153	81	208	139	174	187	250	143
361	178	64	193	139	123	137	94	-	165	104	114
171	127	91	125	145	104	149	148	-	72	135	101
161	71	121	77	156	142	128	123	-	50	169	173
144	104	164	148	115	158	105	148	-	53	89	84
116	164	166	136	121	134	119	157	127	88	142	160
99	164	78	120	138	144	120	136	154	124	228	185
138	162	115	144	99	144	163	117	155	151	154	197
151	207	148	146	91	118	139	142	159	170	92	286
322	245	149	141	118	124	101	150	159	182	118	262
352	202	180	147	135	148	105	125	177	188	191	67
161	130	216	169	134	161	130	173	148	141	153	119
156	170	169	116	136	150	140	149	121	120	121	118
130	204	224	143	120	94	153	106	113	161	174	113
98	87	172	149	125	100	165	136	106	181	186	81
130	116	184	79	132	127	151	158	140	179	144	163
137	207	183	146	118	111	128	159	129	159	76	172
175	118	156	167	88	76	138	91	157	138	69	155
208	142	143	146	82	76	86	87	162	166	131	99
344	143	81	130	114	79	73	102	164	177	163	166
280	151	76	134	123	76	114	87	130	210	120	187
126	159	124	128	140	107	104	60	138	172	216	195
276		156	161	160	133	60	109	104	132	167	231
149		159	166	158	119	85	128	131	79	141	233
93		115		147		162	146		145		95
210.80	170.68	138.19	136.57	139.90	119.07	131.77	128.13	144.88	140.84	157.10	152.32

APPENDIX 4.2 – Scenario 4 output data of PM₁₀ concentration in the study

area

Time (Hour)	Jan	Feb	Mar	Apr	May	Jun	Jul	Aug	Sep	Oct	Nov	Dec
0	210.8	170.68	138.19	136.57	139.9	119.07	131.77	128.13	144.88	140.84	157.1	152.32
0.25	215.694	174.618	141.343	139.653	143.085	121.848	134.878	131.165	148.261	144.126	160.736	155.837
0.5	219.478	177.662	143.78	142.035	145.546	123.997	137.283	133.514	150.875	146.668	163.547	158.555
0.75	222.404	180.016	145.664	143.875	147.447	125.659	139.143	135.33	152.897	148.633	165.721	160.657
1	224.667	181.835	147.119	145.297	148.917	126.943	140.582	136.736	154.46	150.153	167.401	162.282
1.25	226.416	183.242	148.244	146.395	150.053	127.937	141.695	137.824	155.669	151.328	168.701	163.538
1.5	220.844	179.912	146.727	144.958	148.436	127.514	140.571	136.907	153.799	149.685	166.136	161.239
1.75	209.61	172.92	143.167	141.562	144.694	125.994	137.715	134.44	149.548	145.861	160.585	156.192
2	193.999	163.097	138.029	136.653	139.308	123.628	133.521	130.773	143.456	140.352	152.724	149.02
2.25	175.003	151.086	131.672	130.575	132.652	120.605	128.29	126.177	135.939	133.539	143.078	140.205
2.5	167.24	146.218	129.145	128.164	130.002	119.46	126.23	124.38	132.931	130.823	139.189	136.661
2.75	168.163	146.872	129.58	128.588	130.449	119.766	126.621	124.748	133.41	131.275	139.751	137.191
3	175.801	151.795	132.302	131.213	133.287	121.195	128.91	126.79	136.586	134.177	143.754	140.87
3.25	188.633	160.019	136.793	135.505	137.975	123.492	132.666	130.129	141.846	138.973	150.418	146.985
3.5	191.629	161.958	137.877	136.544	139.103	124.076	133.586	130.954	143.11	140.13	152.001	148.442
3.75	187.021	159.041	136.328	135.062	137.481	123.336	132.312	129.834	141.281	138.472	149.656	146.299
4	176.532	152.367	132.744	131.631	133.734	121.572	129.34	127.209	137.063	134.638	144.275	141.372
4.25	161.498	142.791	127.587	126.695	128.345	119.015	125.056	123.42	130.995	129.12	136.545	134.293
4.5	156.798	139.805	125.989	125.167	126.674	118.231	123.728	122.247	129.108	127.405	134.138	132.09
4.75	160.089	141.915	127.14	126.272	127.877	118.815	124.686	123.097	130.454	128.632	135.846	133.657
5	169.558	147.963	130.417	129.411	131.3	120.46	127.412	125.513	134.299	132.133	140.735	138.138
5.25	183.805	157.056	135.336	134.122	136.439	122.923	131.507	129.141	140.078	137.393	148.083	144.873
5.5	187.896	159.668	136.751	135.477	137.916	123.636	132.69	130.189	141.742	138.908	150.196	146.809
5.75	184.134	157.27	135.458	134.237	136.564	122.996	131.618	129.242	140.224	137.527	148.261	145.036
6	174.301	150.999	132.071	130.994	133.025	121.309	128.804	126.751	136.245	133.907	143.196	140.396
6.25	159.772	141.733	127.067	126.202	127.797	118.812	124.642	123.066	130.363	128.555	135.711	133.538
6.5	155.464	138.987	125.587	124.786	126.251	118.073	123.407	121.973	128.619	126.968	133.493	131.507

6.75	159.0 57	141.2 82	126.8 3	125.9 78	127.5 5	118.6 94	124.4 38	122.8 85	130.0 75	128.2 94	135.3 47	133.2 06
7	168.7 6	147.4 74	130.1 77	129.1 84	131.0 47	120.3 66	127.2 2	125.3 49	134.0 07	131.8 71	140.3 49	137.7 9
7.25	183.1 88	156.6 78	135.1 51	133.9 47	136.2 43	122.8 5	131.3 59	129.0 14	139.8 52	137.1 91	147.7 85	144.6 04
7.5	187.4 19	159.3 76	136.6 08	135.3 41	137.7 65	123.5 8	132.5 75	130.0 91	141.5 67	138.7 52	149.9 66	146.6 01
7.75	183.7 66	157.0 44	135.3 47	134.1 32	136.4 47	122.9 52	131.5 3	129.1 66	140.0 89	137.4 06	148.0 83	144.8 75
8	174.0 16	150.8 24	131.9 86	130.9 13	132.9 35	121.2 75	128.7 36	126.6 93	136.1 4	133.8 13	143.0 58	140.2 71
8.25	159.5 52	141.5 98	127.0 01	126.1 4	127.7 28	118.7 86	124.5 88	123.0 21	130.2 82	128.4 82	135.6 05	133.4 42
8.5	155.2 93	138.8 83	125.5 36	124.7 38	126.1 97	118.0 53	123.3 66	121.9 38	128.5 56	126.9 12	133.4 11	131.4 32
8.75	158.9 25	141.2 01	126.7 9	125.9 41	127.5 08	118.6 78	124.4 06	122.8 58	130.0 27	128.2 51	135.2 84	133.1 49
9	168.6 59	147.4 11	130.1 47	129.1 56	131.0 15	120.3 54	127.1 96	125.3 28	133.9 69	131.8 38	140.3	137.7 45
9.25	183.1 1	156.6 3	135.1 27	133.9 25	136.2 18	122.8 41	131.3 4	128.9 98	139.8 23	137.1 65	147.7 47	144.5 69
9.5	187.3 58	159.3 39	136.5 9	135.3 24	137.7 46	123.5 73	132.5 6	130.0 78	141.5 45	138.7 32	149.9 36	146.5 75
9.75	183.7 19	157.0 15	135.3 33	134.1 19	136.4 33	122.9 47	131.5 18	129.1 56	140.0 71	137.3 91	148.0 6	144.8 55
10	173.9 79	150.8 02	131.9 75	130.9 03	132.9 24	121.2 71	128.7 27	126.6 85	136.1 27	133.8 01	143.0 41	140.2 55
Average	182.7 8	156.0 3	134.3 1	133.1 1	135.4 1	121.8 7	130.4 4	128.0 7	139.0 3	136.3 4	147.0 5	143.8 4

**APPENDIX 5 – Scenario 5 output data of PM₁₀ concentration in the study
area**

Time (Hour)	BoDBL	BoENL	BoTeDNL	TeDBL	TeEBL	TeENL	TrDBL	TrEBL
0	212	212	212	212	212	212	212	212
0.25	242.479	241.439	224.86	220.496	215.261	217.006	230.968	223.114
0.5	268.221	266.107	233.784	225.709	216.256	219.379	245.391	230.533
0.75	289.728	286.533	239.519	228.328	215.519	219.714	255.999	234.985
1	307.451	303.189	242.668	228.897	213.454	218.474	263.403	237.058
1.25	321.791	316.494	243.721	227.846	210.373	216.014	268.12	237.222
1.5	336.295	330.008	246.262	228.704	209.703	215.799	273.766	239.041
1.75	350.945	343.707	250.009	231.069	210.878	217.32	280.194	242.187
2	365.727	357.572	254.735	234.625	213.464	220.184	287.277	246.4
2.25	380.627	371.583	260.253	239.122	217.132	224.087	294.911	251.468
2.5	382.505	372.599	253.289	231.237	208.501	215.669	289.882	244.097
2.75	372.747	362.065	236.205	213.57	190.458	197.72	274.222	226.745
3	352.588	341.265	210.919	188.175	165.21	172.396	249.639	201.383
3.25	323.133	311.338	178.984	156.673	134.449	141.368	217.565	169.595
3.5	296.057	283.987	152.344	131.034	110.154	116.614	189.889	143.338
3.75	271.107	258.926	129.999	110.027	90.8101	96.7141	165.907	121.518
4	248.058	235.901	111.135	92.6796	75.2543	80.5693	145.024	103.259
4.25	226.707	214.684	95.0925	78.2241	62.5982	67.3295	126.743	87.8577
4.5	208.812	197.012	83.2751	67.9906	54.099	58.2745	112.585	76.6868
4.75	194.005	182.492	74.8826	61.0929	48.7813	52.4569	101.887	68.9105
5	181.958	170.773	69.2667	56.8306	45.8988	49.1439	94.0935	63.8581
5.25	172.379	161.544	65.9016	54.6506	44.8801	47.7683	88.7388	60.9914
5.5	165.942	155.466	65.2987	55.0532	46.2253	48.8292	86.3687	60.8161
5.75	162.315	152.188	66.9349	57.4963	49.38	51.7749	86.504	62.8004
6	161.197	151.4	70.3864	61.5516	53.9195	56.1788	88.7426	66.5177
6.25	162.323	152.824	75.3093	66.8805	59.519	61.7106	92.7469	71.6255
6.5	161.455	152.215	77.4251	69.2158	61.9297	64.1152	94.2333	73.8492
6.75	158.804	149.798	77.2653	69.1859	61.8998	64.1003	93.6062	73.7585
7	154.559	145.775	75.2607	67.2872	60.0019	62.2139	91.2047	71.8107
7.25	148.89	140.325	71.7607	63.9121	56.6743	58.8795	87.3137	68.3728
7.5	142.761	134.417	67.8609	60.183	53.0649	55.2374	82.9848	64.5516
7.75	136.221	128.104	63.637	56.1743	49.2399	51.3574	78.2884	60.4229
8	129.313	121.429	59.1504	51.9445	45.2498	47.2933	73.2833	56.0474
8.25	122.076	114.434	54.4508	47.5402	41.1333	43.0867	68.0192	51.4739
8.5	119.858	112.467	54.891	48.3105	42.2327	44.0824	67.8502	52.054
8.75	122.126	114.968	59.4978	53.169	47.3241	49.1027	71.9583	56.7695

9	128.402	121.441	67.4824	61.2577	55.4709	57.2365	79.6569	64.8033
9.25	138.262	131.444	78.2052	71.8983	65.9564	67.7789	90.3697	75.4999
9.5	141.2	134.461	81.0227	74.4302	68.1068	70.0597	93.4877	78.2081
9.75	137.95	131.268	77.4317	70.5557	63.8776	65.9491	90.2303	74.5062
10	129.171	122.554	68.6456	61.6195	54.7657	56.8941	81.6207	65.6607
	220.20	211.91	131.24	119.19	107.34	111.02	152.85	126.14